

Enzymology of the periplasmic pyoverdine maturation

Von der Naturwissenschaftlichen Fakultät der
Gottfried Wilhelm Leibniz Universität Hannover

zur Erlangung des Grades

Doktor der Naturwissenschaften (Dr. rer. nat.)

genehmigte Dissertation

von

Michael Thomas Ringel, M. Sc.

2018

Referent: Prof. Dr. rer. nat. Thomas Brüser

Korreferent: Prof. Dr. rer. nat. Hans-Peter Braun

Korreferent: Prof. Dr. R. Gary Sawers

Tag der Promotion: 18.12.2017

„A new scientific truth does not triumph by convincing its opponents and making them see the light, but rather because its opponents eventually die, and a new generation grows up that is familiar with it“

-Max Planck

Abstract

Keywords: Iron, siderophores, pyoverdine, periplasm, pyridoxal phosphate, *Pseudomonas*

Iron is of prominent importance for most living organisms, involved in many central processes, such as respiration or photosynthesis. To circumvent iron limitation, many organisms have developed strategies to keep ferric iron soluble, for instance by production of siderophores, which are small high-affinity iron-chelators. A remarkable example in this context are pyoverdines, being produced by the fluorescent pseudomonads, a very diverse group of organisms. Pyoverdine research has a long and illustrious history and was first described in 1892. From this time on, scientists were faced with elementary questions of chemistry and biology that could only be unraveled by a rewarding interplay of disciplines.

However, a number of questions remained unresolved that are now addressed in this thesis. Specifically, the acylated ferribactin precursor, generated by non-ribosomal synthesis in the cytoplasm, is exported to the periplasm and there subject to a number of tailoring reactions performed by PvdMNOPQ to form the mature siderophore. However, only the functions of PvdP and PvdQ were known. In this thesis, it was discovered that PvdN is an unusual pyridoxal phosphate-containing enzyme, catalyzing a novel oxidative decarboxylation under retention of the amine involved in the side-chain modification of pyoverdine. Furthermore, the enzyme PtaA was determined to catalyze a transamination-reaction converting a glutamic acid- into an α -ketoglutaric acid side-chain. The relevance of these side-chain modifications remains obscure although further investigations indicate a role in pyoverdine export by PvdRT-OpmQ. Moreover, PvdO is required for the completion of the oxidative cyclization reactions in conjunction with PvdP, forming the characteristic chromophore of pyoverdine. Finally, PvdM could be postulated to function as a membrane-associated peptidase involved in the pyoverdine signaling-pathway.

Zusammenfassung

Schlagworte: Eisen, Siderophore, Pyoverdin, Periplasma, Pyridoxalphosphat, *Pseudomonas*

Eisen ist von herausragender Bedeutung für die meisten lebenden Organismen und ist an vielen zentralen Prozessen, wie Atmung und Photosynthese, beteiligt. Um Eisenlimitation zu verhindern haben viele Organismen Strategien entwickelt um Fe(III) in Lösung zu halten z.B. durch die Produktion von Siderophoren, kleinen hochaffinen Eisenchelatoren. Ein in diesem Kontext bemerkenswertes Beispiel sind die Pyoverdine, welche durch fluoreszierende Pseudomonaden, einer heterogenen Gruppe an Organismen, gebildet werden. Pyoverdinforschung hat eine lange und illustre Geschichte, beginnend im Jahr 1892 mit der Erstbeschreibung. Pyoverdine haben seitdem Wissenschaftler vor elementare Fragen der Chemie sowie der Biologie gestellt, die nur durch die außergewöhnliche Zusammenarbeit von verschiedenen Disziplinen enträtselt werden konnten.

Viele Fragen blieben allerdings unbeantwortet, welche Thema dieser Arbeit sind. Insbesondere wird der akylierte Ferribactin-Vorläufer, welcher im Zytoplasma durch nicht-ribosomale Peptidsynthese generiert wird, in das Periplasma exportiert, wo er durch eine Reihe von Modifikationen – ausgeführt von PvdMNO PQ – in das fertige Siderophor umgewandelt wird. Bislang waren nur die Funktionen von PvdP und PvdQ bekannt. Im Rahmen dieser Arbeit wurde entdeckt, dass PvdN ein ungewöhnliches Pyridoxalphosphat enthaltendes Enzym ist, welches eine neuartige oxidative Decarboxylierung unter Retention des Amins katalysiert, die an einer Seitenkettenmodifikation beteiligt ist. Des Weiteren wurde festgestellt, dass das Enzym PtaA eine Transaminierung katalysiert und dadurch einen Glutaminsäure- in einen α -Ketoglutarsäurerest überführt. Die Relevanz der Seitenkettenmodifikationen bleibt obskur, jedoch zeigten weitere Untersuchungen eine mögliche Rolle im Export durch PvdRT-OpmQ auf. Ferner konnte gezeigt werden, dass PvdO in Verbindung mit PvdP für die Vervollständigung der oxidativen Zyklisierung zur Bildung des charakteristischen Chromophors vonnöten ist. Schlussendlich konnte für PvdM eine Funktion als membranassoziierte Peptidase, welche an der Pyoverdin-Signalkaskade beteiligt sein könnte, vorhergesagt werden.

List of abbreviations

a.m.u.	atomic mass units
ABC	adenosine triphosphate binding cassette
AHLs	<i>N</i> -acyl homoserine lactones
ATP	adenosine triphosphate
Bicine	<i>N,N</i> -bis(2-hydroxyethyl)glycine
CAA	casaminoacid
CAS	chrome azurol S
c-di-GMP	3',5'-cyclic diguanylic acid
CF	cystic fibrosis
CHES	<i>N</i> -cyclohexyl-2-aminoethanesulfonic acid
CP	cytoplasmic fraction
cRNAP	core RNA-polymerase
DH-PVD	dihydropyoverdine
DSC	differential scanning calorimetry
ECF	extracytoplasmic-function sigma factors
EDDHA	ethylenediamine di(<i>o</i> -hydroxy)phenylacetic acid
EDTA	ethylenediaminetetraacetic acid
FGE	formylglycine-generating enzyme
Fur	ferric uptake regulator
HA	human influenza hemagglutinin
HEPES	4-(2-hydroxyethyl)-1-piperazineethanesulfonic acid
hrDP	human renal dipeptidase
HR-MS	high-resolution mass-spectrometry
ICP-MS	inductively coupled plasma mass spectrometry
IEF	isoelectric focusing
IM	inner membrane
IPTG	isopropyl β -D-1-thiogalactopyranoside
ISR	induced systemic resistance
L-ASA	L-aspartate β -semialdehyde
L-Dab	L-2,4-diaminobutyrate

L-fOHOrn	L- <i>N</i> ₅ -formyl- <i>N</i> ₅ -hydroxy ornithine
L-OHOrn	L- <i>N</i> ₅ -hydroxy ornithine
MALS-RI	multiangle light scattering/refractive index
MB	membrane fraction
mRNA	messenger ribonucleic acid
MS	mass-spectrometry
OD	optical density
oePCR	overlap extension polymerase chain reaction
OM	outer membrane
ONC	overnight culture
PAGE	polyacrylamide gel electrophoresis
PCR	polymerase chain reaction
PDB	protein data bank
PGPR	plant growth-promoting rhizobacteria
pI	isoelectric point
PLP	pyridoxal phosphate
PMF	protonmotive force
PP	periplasmic fraction
PQS	2-heptyl-3-hydroxy-4(1 <i>H</i>)-quinolone
PVD	pyoverdine
rRNA	ribosomal ribonucleic acid
SDS	sodium dodecyl sulfate
SEC	size-exclusion chromatography
sRNA	small non-coding ribonucleic acid
Tat	twin-arginine translocation
UPLC	ultra-performance liquid chromatography

Numbering of figures: Please note that, when the text refers to figures contained in the original publications in sections 3.1 to 3.3, the corresponding section is mentioned explicitly (e.g. section 3.2; Figure 4). The numbering of all other figures in the text is continuous and figures are referenced without mentioning the section.

Table of contents

Abstract.....	I
Zusammenfassung.....	II
List of abbreviations	III
1. Introduction.....	1
1.1. A brief history of pyoverdine research.....	1
1.2. Siderophores – structure and function.....	2
1.3. Fluorescent pseudomonads – Pyoverdines and their biosignificance	4
1.4. Recycling and uptake of pyoverdine.....	6
1.5. Regulation of pyoverdine production	9
1.6. Pyoverdine biogenesis.....	14
1.7. Pyoverdine as target for antibiotic treatments.....	18
2. Aims of this study.....	20
3. Results.....	21
3.1. PvdN Enzyme Catalyzes a Periplasmic Pyoverdine Modification	21
3.2. The periplasmic transaminase PtaA of <i>Pseudomonas fluorescens</i> converts the glutamic acid residue at the pyoverdine fluorophore to α -ketoglutaric acid	32
3.3. PvdO is required for the oxidation of dihydropyoverdine as the last step of fluorophore formation in <i>Pseudomonas fluorescens</i>	48
3.4. Additional data – Studies on the functional role of PvdN, PtaA and PvdM.....	62
3.4.1. Pyoverdine side-chain modifications and their implication in export	62
3.4.2. Towards understanding the function of PvdM.....	64
3.4.3. Experimental procedures	68

4. Concluding discussion and outlook	73
4.1. Pyoverdine side-chain modifications	74
4.2. Chromophore maturation	83
4.3. Putative role of PvdM in pyoverdine biogenesis, recycling and signaling	86
5. References	89
Acknowledgements	126
Curriculum vitae	127

1. Introduction

1.1. A brief history of pyoverdine research

The discovery of pyoverdines reaches back to 1892 when Gessard described yellow-green fluorescent pigments and named them fluorescins (1). However, sometimes the first described observation of this phenomenon is attributed to Schroeter, who vaguely described green pigments that might be produced by bacteria in 1872 (2), but no further experimental evidence is provided therein. Gessard on the other hand observed that the green pigmentation could be bleached by acidification but reobtained the color after neutralization with bases (1). Based on the ability of some bacteria to produce this green pigment, it was later proposed by Turfitt to exploit the observed phenotype for classification purposes (3, 4). Nowadays, these early observations have led to the naming-convention of the *Pseudomonas* subgroup commonly referred to as “fluorescent pseudomonads” being eponymous for the species *Pseudomonas fluorescens*. The term “pyoverdine” itself has been introduced by Turfreijs in 1941 (5) but until now, there exists no final consensus regarding the terminal letter “e” in this spelling. In this document, we adopt the original Dutch spelling, including the terminal “e”, since it was also the first to be cited in literature (6) and not as proposed by Cox & Adams in 1985 (7) without it. Furthermore, another term was introduced by Kloepper *et al.* in 1980 (8) terming the green fluorescent substance “pseudobactin”, but this designation is now considered obsolete (9). The next step towards unraveling the function of pyoverdine was the observation that the production of pyoverdine was inversely correlated with the iron concentration in cultivation media in 1953 by Totter & Moseley (10). The causality implied by this observation, specifically that pyoverdine had to be involved in iron uptake, only ensued in 1978 and was deduced by Meyer & Hornsperger (11), who observed that by adding a pyoverdine-⁵⁹Fe³⁺ complex to iron depleted media, iron is actively imported into the cell. Together with data obtained by Meyer & Abdallah in 1978 (12), who showed that pyoverdine has a high iron-affinity (with a stability constant of $\sim 10^{32}$), it was concluded that pyoverdine belonged to the class of bacterial siderophores (11). The term “siderophore” had been introduced by Lankford in 1973 (13), describing (small) iron-binding chelators involved in iron-transport into the cell. Still,

the chemical nature of pyoverdine remained a mystery until 1981, when the first structure of pyoverdine could be solved by Teintze *et al.* (14). For a more detailed summary on the discovery of pyoverdines the reader is referred to the excellent review by Budzikiewicz (15).

1.2. Siderophores – structure and function

Although iron is recognized to be the fourth most abundant element in the earth's crust (16), it may become growth limiting due to its physicochemical properties. This may seem paradox, but under neutral pH conditions, in the presence of oxygen, iron forms nearly insoluble Fe^{III} oxide hydrates, which limits the amount of readily available iron. Therefore, many organisms produce siderophores that keep ferric iron soluble. Since Fe³⁺-ions are hard Lewis acids, they thus preferentially bind to hard Lewis bases such as oxide anions. Consequently, common ligands encountered in siderophores are hydroxamates, catecholates and carboxylates, which may act as bidentate ligands. Furthermore, Fe³⁺-ions provide six coordination sites and thereby strong siderophores usually form octahedral d⁵ high spin complexes as hexadentate ligands, typically provided by three bidentate ligands. Sometimes, siderophores are grouped according to the functional groups that are involved in coordinating the metal, e.g. hydroxamate-, catecholate-, carboxylate- and also mixed-type siderophores (reviewed in 17–19). Enterobactin, the siderophore produced by some gram-negative bacteria e.g. *Escherichia coli* (20), *Salmonella typhimurium* (21) and *Klebsiella pneumoniae* (formerly known as *Aerobacter aerogenes*; 20) only provide catechol-ligands, and have very high iron binding affinities under near-neutral conditions (for enterobactin 10⁵² M⁻¹; 22). The catechol ligands lose their iron-chelation capacity upon protonation in acidic media. On the other hand, siderophores like deferoxamine, which is produced by the actinobacterium *Streptomyces pilosus*, provide three hydroxamate moieties for iron-chelation (23). Pyoverdines usually contain two hydroxamate ligands (sometimes also β-hydroxy-carboxylates instead of hydroxamates) located in the peptide backbone and one catechol ligand (15). Further, less common chelating groups are *inter alia* hydroxyphenyloxazoline groups as found in mycobactin from *Mycobacterium johnei* (24) and in parabactin from *Micrococcus denitrificans* (25) or α-hydroxy-carboxylate groups as found in aerobactin from *Aerobacter*

aerogenes (*Klebsiella pneumoniae*; 26), in rhizobactin from *Rhizobium meliloti* (27) or in the phytosiderophore mugineic acid produced by e.g. barley (28). By arranging all coordinating groups in one molecule, an entropic advantage is achieved over distributed groups in distinct

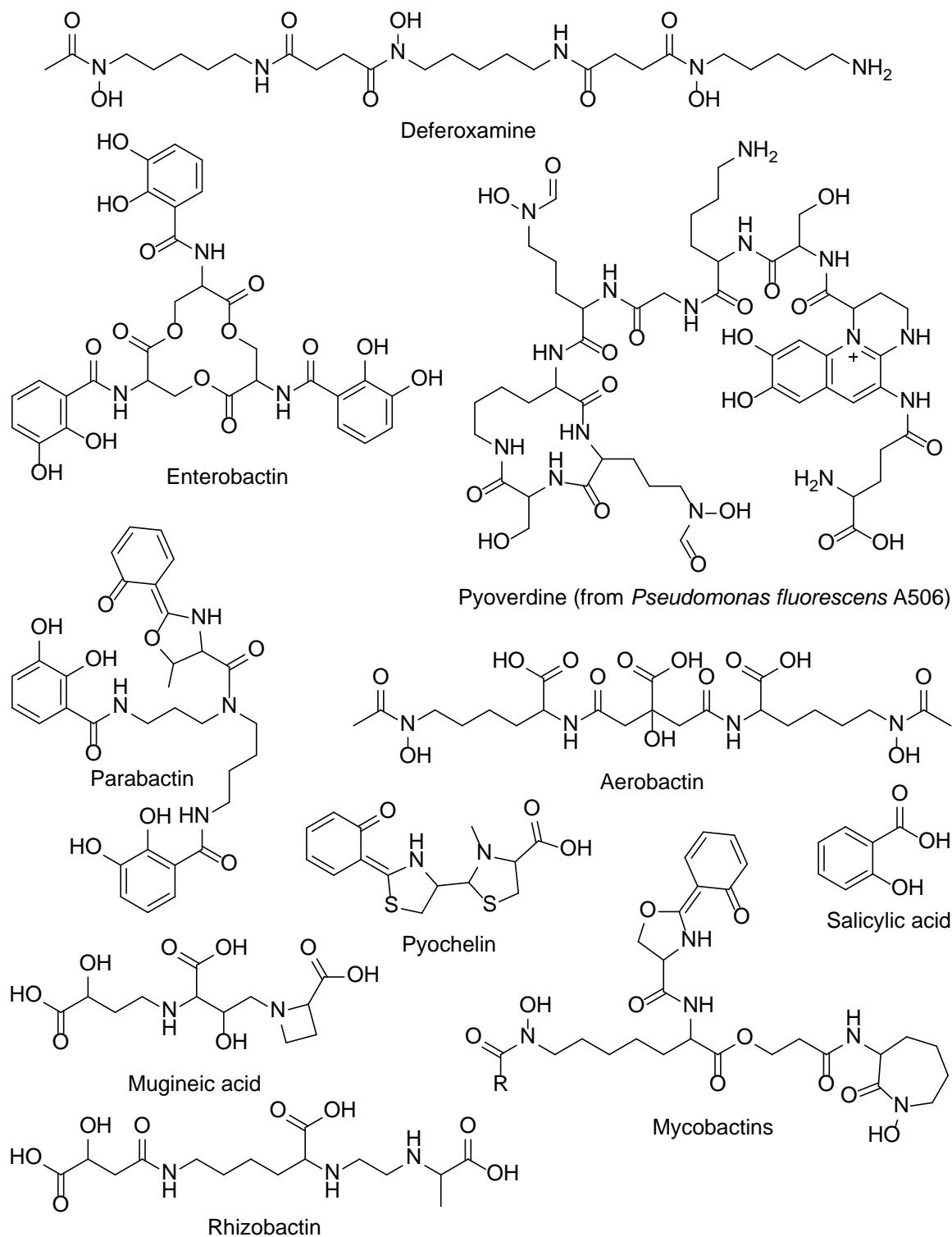


Figure 1: Representative siderophore structures. Structures of catechol- (e.g. enterobactin), hydroxamate- (e.g. deferoxamine), carboxylate- (e.g. rhizobactin) and mixed-type (e.g. pyoverdine structure of *P. fluorescens* A506), as well as some non-conventional siderophores (e.g. parabactin, pyochelin, mycobactins, etc.).

molecules, such as salicylic acid, which was first isolated from *Burkholderia cepacia* (previously known as *Pseudomonas cepacia*; 29) and later also found in some *Pseudomonas* strains (30–32) or pyochelin, a small siderophore first described in *Pseudomonas aeruginosa* (33–35) which only comprises a tetradentate ligand (36). However, the function of salicylic acid as a siderophore has been questioned (37). For structures of the discussed compounds please refer to Figure 1.

1.3. Fluorescent pseudomonads – Pyoverdines and their biosignificance

Fluorescent pseudomonads all belong to the family of pseudomonadaceae, as first introduced in 1917 by Winslow *et al.* (38), based on the previously described genus *Pseudomonas* as introduced by Migula in 1894 (39). The family constitutes a rather large group of Gram-negative bacteria, members of which are found in soil, fresh water and in the marine environment, or in association with plants and animals (40). Pseudomonadaceae belong to the order of pseudomonadales in the class of γ -proteobacteria within the phylum of proteobacteria. They are rod-shaped cells that can be either straight or slightly curved, usually have one or more polar flagella, thus being motile, do not produce spores, do not ferment or possess the ability to perform photosynthesis, cannot fix N_2 and can use a large variety of organic substrates for their chemoorganotrophic growth (40). The genus of *Pseudomonas* was later subgrouped into five rRNA homology groups in 1973 by Palleroni *et al.*, which also obviated the large heterogeneity of the genus (41). All fluorescent pseudomonads belong to the rRNA homology group I (e.g. *P. aeruginosa*, *P. fluorescens*, *P. chlororaphis*, *P. putida*, *P. syringae*, *P. cichorii*, etc.), however, this group also includes non-fluorescent species such as *P. stutzeri*, *P. mendocina* or *P. alcaligenes* (40). The roles of fluorescent pseudomonads within the environment are diverse, as for instance *P. aeruginosa* and *P. putida* are well known opportunistic human pathogens (42–45), whereas *P. syringae* and *P. cichorii* are important plant pathogens (46–49) and many *P. fluorescens* and *P. chlororaphis* species belong to the group of plant growth-promoting rhizobacteria (50–53).

In this regard, pyoverdines have been proven to contribute to the environmental fitness in all of the diverse lifestyles of fluorescent pseudomonads. For instance, pyoverdine is able to remove iron bound by transferrin (54–57) or lactoferrin (57), thereby enabling *P. aeruginosa* to grow in

human serum or plasma (7). Consequently, *P. aeruginosa* mutants impaired in pyoverdine formation are also impaired in virulence as demonstrated in various animal models (58, 59). Furthermore, pyoverdine has been found in sputum samples of cystic fibrosis (CF) patients (60, 61). Unexpectedly, it could be demonstrated, that in *P. aeruginosa* strains isolated from CF patients with prolonged infection times, pyoverdine-negative mutants accumulated, which retained the capacity to take up pyoverdine (62). This aspect of social behavior, involving extracellular products referred to as “public goods”, which are subject to “cheating”, consequentially leading to mixed bacterial populations, has generated considerable interest, adding to the complexity of bacterial interactions (63–66). In addition to the direct involvement of pyoverdine in pathogenicity, the genetic regulation of other genes that contribute to virulence of *P. aeruginosa* are under the control of the PvdS-regulon (as detailed in section 1.5). However, in a recent meta-analysis it could be demonstrated that although pyoverdine is consistently involved in infections, it is not indispensable for virulence (67), which argues for a more complex relationship between individual virulence traits and the context of pathogenic potential. Pyoverdine may also be important for plant pathogenicity, as it is required for full virulence of *P. syringae* pv. *tabaci* 6605 (68) , although it is unclear whether this is a direct or an indirect effect. However, alternative studies have found that pyoverdine is dispensable for plant pathogenicity of other *P. syringae* strains using different host systems (69, 70). Therefore, the situation is comparable to the one outlined above for human pathogenicity, where the implied correlation between pathogenicity and pyoverdine production must be viewed in context of the complexity of pathogen-host interactions. On the other hand, many *P. fluorescence* species belong to the group of plant growth-promoting rhizobacteria (PGPR), as introduced by Kloepper & Schroth in 1978 (71). The term rhizobacteria refers to the compartment comprising the soil-root-interface, as designated by Hiltner in 1904 (72, 73). PGPR can stimulate plant growth by a wide variety of mechanisms which can be grouped according to their mode of action into: 1.) Biocontrol, i.e. the suppression of plant diseases; 2.) Biofertilization, i.e. the mobilization of plant-nutrients; 3.) Phytostimulation, i.e. the modification of plant-hormone levels; 4.) (Rhizo-)remediation (74). In this context, pyoverdine

has been demonstrated by *in vitro* and *in vivo* experiments to be directly involved in biocontrol, probably by depriving the detrimental organisms of their iron-supply (8, 75–83). An indirect mechanism by which pyoverdine can contribute to biocontrol is the elicitation of induced systemic resistance (ISR; as defined by Kloepper *et al.* in 1992; 84), which could be demonstrated for a number of plants (85–89), although the interactions seem to be rather specific. Furthermore, the ferripyoverdine chelate can enhance iron-supply in plants, thus contributing to biofertilization (90–93), although the exact mechanism by which this process proceeds remains to be elucidated. Finally, pyoverdines can aid in the detoxification of heavy-metal polluted soils by facilitating phytoextraction of e.g. copper (94), thus also playing a potential role in rhizoremediation.

Besides the presented versatility of pyoverdine implications in environmental function, it could be shown, that the iron status of *P. aeruginosa* cells is very important for biofilm development. Specifically, iron starvation abrogates biofilm formation and a functional pyoverdine system is important for the development of a mature biofilm (95–97). It should be noted however, that it has also been demonstrated that abundant iron may perturb biofilm formation (98). Nevertheless, as discussed in (99), the data suggest a model, where, under extreme iron starvation, cells may favor motility to exploit new iron supplies elsewhere, under moderate iron starvation, the pyoverdine dependent iron supply may suffice to acquire adequate amounts of iron to form biofilms and an excess of iron may cause iron toxicity, thus promoting biofilm breakup to escape toxic iron-levels. Furthermore, pyoverdine has been shown to alleviate heavy-metal toxicity by hampering uptake of the toxic metal-ions into the cytoplasm (100–102).

1.4. Recycling and uptake of pyoverdine

There exist many structurally diverse siderophores (17), which exemplifies how organisms have adapted to the lack of soluble iron whilst staying competitive, since the siderophore-uptake systems are usually specific for the siderophore used by the organism. This is especially obvious in case of pyoverdines (103, 104), since the peptide moiety attached to the fluorophore is highly variable in-between strains of *Pseudomonas* (15). Nonetheless, pyoverdine uptake is not unambiguous as it has been shown that some pyoverdines can be taken up by strains other than

the producer (103). The variation in the peptide-backbone attached to the fluorophore of pyoverdines allows the outer membrane ferripyoverdine receptor FpvA to distinguish between pyoverdines produced by itself and other strains. FpvA has first been proven to be the outer-membrane receptor for pyoverdine in *P. aeruginosa* in 1990 by Meyer *et al.* (105) and later identified again by Poole *et al.* in 1991 (106), which is due to the discrepancy in the described molecular weight determined to be ~80 kDa or ~90 kDa respectively, but probably both research groups described the same protein, whose coding sequence was sequenced in 1993 by Poole *et al.* (107). In 2005, the structure of FpvA was elucidated by Cobessi *et al.* (36) and later structures of FpvA bound to the cognate ferripyoverdine (108) and the full length FpvA structure (109) were solved. Furthermore, FpvA was subject to a number of mutational studies trying to elucidate which residues were implicated in pyoverdine binding, signaling and transport (110–112). In 2009 it could be demonstrated by Greenwald *et al.* (113), that the first amino acid residues in the peptide backbone of pyoverdine determine the binding affinity of pyoverdines to their cognate or non-cognate Fpv's. The uptake is probably energized by the direct interaction of FpvA with the TonB-ExbBD complex, that is located in the inner membrane, thereby being able to transduce sufficient energy for transport obtained from the electrochemical gradient inherent to the inner membrane of living bacteria (114, 115). However, *P. aeruginosa* has two TonB homologs and although TonB1 seems to be more important for iron uptake, TonB2 can partially fulfill the function of TonB1 (116).

Interestingly, FpvA allegedly not only binds to ferripyoverdine but also to the iron-free apo-pyoverdine, which is not imported but exchanged with ferripyoverdine during the course of import, where the exchange is supposedly accelerated by TonB in conjunction with the protonmotive force (PMF) (117–121). However, it has been suggested by another study, that the observation regarding binding of apo-pyoverdine by FpvA is *de facto* an artifact and that the observed binding is actually due to trace-contaminations of aluminum chelates (122, 123). Moreover, FpvA can bind to other pyoverdine-metal complexes (Ag^+ , Al^{3+} , Cd^{2+} , Co^{2+} , Ga^{3+} , Hg^{2+} , Mn^{2+} , Zn^{2+}), that may even be imported (in case of Cu^{2+} , Ga^{3+} , Mn^{2+} , Ni^{2+}), although with reduced

efficiency (124). Intriguingly, the presence of Ga³⁺-, Mn²⁺-, Cd²⁺-, Co²⁺- and Hg²⁺ pyoverdine chelates inhibit the uptake of ferripyoverdine, although it is not known by which mechanism (124). Furthermore, some strains carry more than one homolog of FpvA, each with differential affinities for specific pyoverdines, or overlapping specificities. Probably one of the most extensive investigations in this matter was performed by Hartney *et al.* in 2013 (125), who carried out mutational analysis and cross-feeding experiments, which demonstrated the specificity of a multitude of Fpv's and their pyoverdine-scavenging potential in *P. protegens* Pf-5. Since efficient iron uptake is advantageous in regard to the competition in the environment it is not surprising, that it could be demonstrated for *P. aeruginosa* that it could take up many other xenosiderophores, such as, but not limited to, aerobactin (126), enterobactin and derivatives thereof (126–128), cepabactin (129), deferrioxamines (129), deferrichrysin (129), deferrirubin (129), coprogen (129), nitrilotriacetic acid (130), citrate (34, 131) and *myo*-inositol hexakisphosphate (132).

The fate of siderophores after uptake into the respective organism varies according to the strategy employed for iron liberation from the chelate (133). Enterobactin for example is imported into the cytoplasm, where it is partially hydrolyzed to liberate bound iron (134, 135). On the contrary, pyoverdine is not degraded or modified and not imported into the cytoplasm. Instead, after import of the iron-chelated form of pyoverdine into the periplasm by FpvA, Fe³⁺ is probably reduced to Fe²⁺ (136, 137) and consequently dechelated by FpvC and FpvF in conjunction with the iron-reductase FpvG requiring FpvHJK, concluded by the import of the Fe²⁺ via an FpvD₂E₂ complex (138, 139). Subsequently, pyoverdine is reexported into the extracellular compartment by OpmQ-PvdRT (140, 141), which is also involved in exporting *de novo* synthesized pyoverdine, although it cannot be the only export route (137). However, recently it was suggested that the type VI secretion system may be involved in pyoverdine export and that the OpmQ-PvdRT system might not be involved at all (142). Furthermore, pyoverdine can be stored in the periplasmic compartment (143) before translocation into the extracellular compartment. Yet, it is not understood how storage of pyoverdines in the periplasm is achieved or how adverse effects on metal-bearing enzymes due to the strong chelating function of pyoverdine in the periplasm are

avoided, although several models have been proposed, such as periplasmic pyoverdine chaperones or competition models (144). The intricate mechanisms underlying import, recycling and storage not only clearly illustrate the complexity involved in such a simple task as to acquire sufficient iron but also that still many questions remain to be solved.

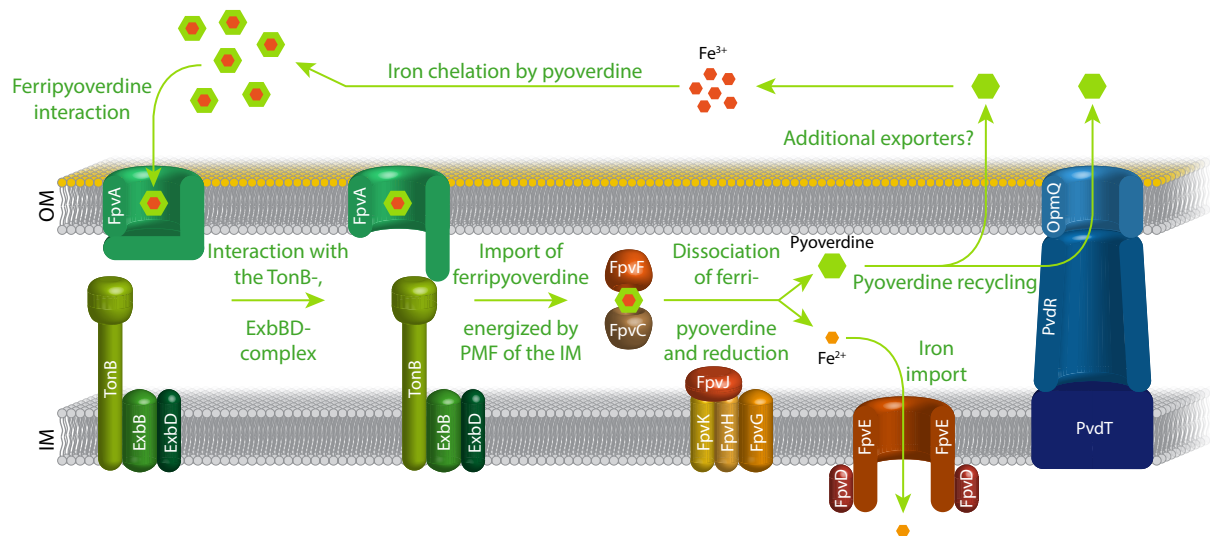


Figure 2: Import and recycling of pyoverdine. In a first step, ferripyoverdine binds to the outer membrane receptor-protein FpvA, which triggers a conformational change therein that allows the interaction with the TonB-ExbBD-complex. Subsequently, the TonB-ExbBD-complex facilitates the import of the ferripyoverdine energized by coupling the PMF of the inner membrane to FpvA. The imported ferripyoverdine is bound by FpvC and FpvF, which, in conjunction with the reductase FpvG, requiring FpvHJK, liberates the reduced Fe^{2+} from ferripyoverdine. Successively, unmodified pyoverdine is reexported by PvdRT-OpmQ or the type VI secretion system or other yet unidentified exporters and Fe^{2+} is imported into the cytoplasm via the FpvD₂E₂ importer. PMF, protonmotive force; IM, inner membrane; OM, outer membrane.

1.5. Regulation of pyoverdine production

For *Pseudomonas* the production of pyoverdine only makes sense when available iron is limiting. Furthermore, a high accumulation of iron should be avoided, since it may lead to iron toxicity by forming hydroxyl radicals through the Fenton reaction (145). Therefore, it is coherent that biosynthesis is tightly regulated. The master regulator in many Gram-negative bacteria in regard to iron is the Ferric uptake regulator (Fur) (146), which was first identified in *S. typhimurium* (147)¹ and later also in *E. coli* (148), where it was also initially characterized (148–152). The identification of a Fur-homolog in *P. aeruginosa* was achieved in 1991 by Prince *et al.*

¹ The first description of Fur in *S. typhimurium* did not identify the respective gene but rather described a mutant strain, whose phenotype was named “Fur”. The true identification of the *fur*-gene was later performed in *E. coli*.

(153). This homolog was subsequently shown to be involved in the regulation of siderophore production shortly thereafter in 1993 (154). However, investigations in this matter were complicated by the fact that no Fur null mutant could be obtained by standard genetic techniques, thus Fur was suggested to be essential in *P. aeruginosa* (154). Only recently, utilizing a conditional mutant, it could be demonstrated that this is not the case (155). Fur acts as a repressor of transcription for genes carrying a “Fur-box” sequence motif in their promoter/operator region when it binds to the co-repressor Fe²⁺ (156–159, 146). Nevertheless, Fur can also indirectly act as an activator, for instance, by repressing the transcription of the small non-coding RNA (sRNA) *ryhB*, which in turn is a repressor of e.g. *sodB* by binding to its target mRNA, which is subsequently degraded (160, 161). For a more extensive discussion on Fur-regulation, please refer to the excellent review by Troxell *et al.* (162). The Fur-regulon in *P. aeruginosa* includes many diverse genes as evidenced by cycle selection- and GeneChip® experiments (163–165), as well as bioinformatic analysis (166). Most notably, in regard to pyoverdine production, Fur regulates the expression of the extracytoplasmic-function sigma factors (ECFs) *pvdS* and *fpvI*, as well as the anti-sigma factor *fpvR* (163), which are important regulators of pyoverdine-related genes as detailed below (Figure 3).

FpvA, which is the already introduced outer membrane pyoverdine receptor involved in import, has a dual function, also being involved in the signal-cascade, triggering pyoverdine production by inhibiting the anti-sigma activity of FpvR (167, 168). Although it could be shown by mutational studies that FpvA signaling does not necessarily require pyoverdine transport (110), it has been concluded from further structural and biochemical analysis that signaling and transport are tightly coupled in FpvA (169). Furthermore, it has been demonstrated, that the presence of a functional TonB1 protein is mandatory for triggering the signaling cascade (170). The mechanism proposed by Schalk *et al.* in 2009 (169) begins by FpvA-ferripyoverdine recognition, which leads to a conformational change, that allows TonB to interact with the TonB-box and the signaling-domain to interact with FpvR. Interestingly, other metal complexes of

pyoverdine can also trigger this signaling cascade, specifically Al^{3+} , Cu^{2+} , Ga^{3+} , Mn^{2+} , Ni^{2+} and Zn^{2+} (124).

The anti-sigma factor FpvR binds to the ECFs PvdS and FpvI, which sequesters them to the cytoplasmic face of the inner membrane and furthermore renders PvdS sensitive to peptidases (167, 168, 171–173). However, in an earlier study it had been demonstrated that PvdS and FpvI bound to FpvR are more stable than their free forms (171), which argues for a strict regulation by reducing the life-time of active PvdS and FpvI. As outlined above, FpvA can quench the anti-sigma activity of FpvR (167, 168) and the mechanism by which FpvR liberates PvdS and

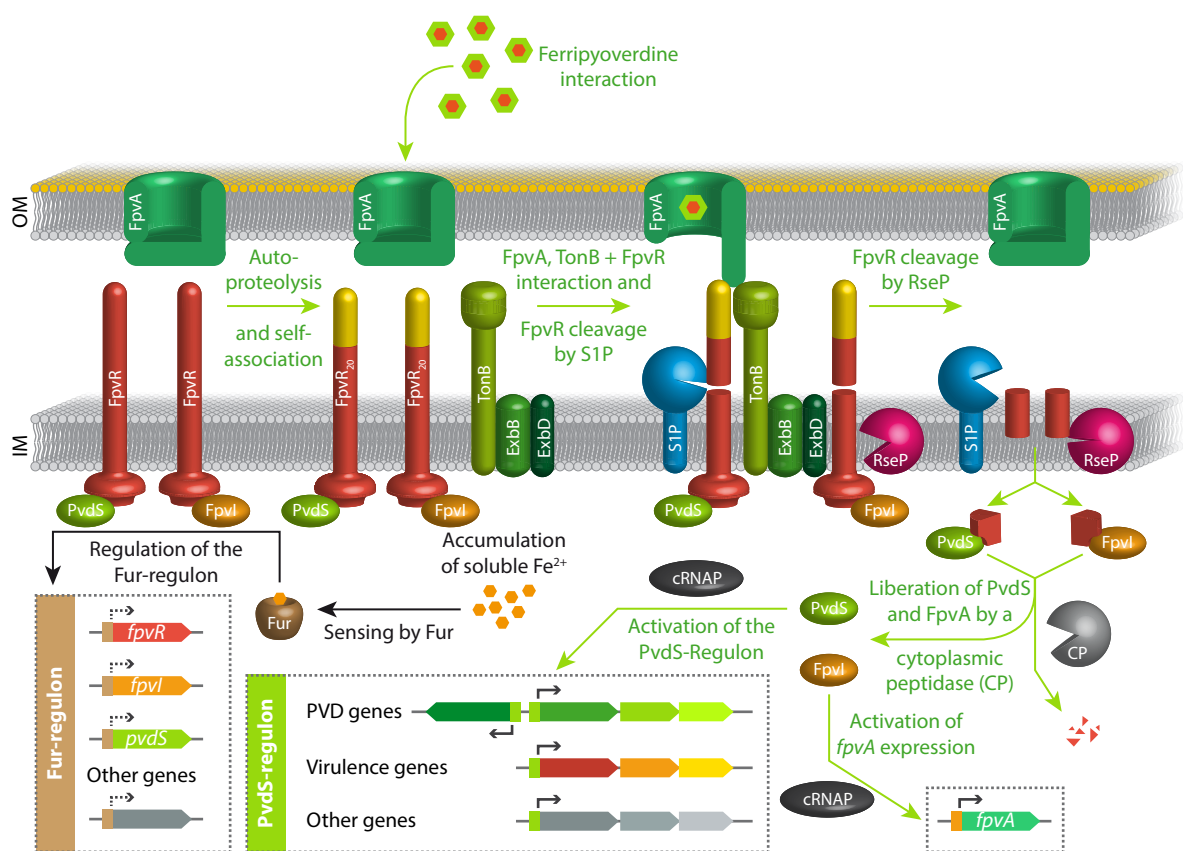


Figure 3: Regulation of pyoverdine related genes. FpvR acts as an anti-sigma factor, inactivating both PvdS and FpvI. In a first step, FpvR autoproteolytically cleaves itself but the cleaved C-terminal fragment reassociates with the membrane bound N-terminal FpvR₂₀ fragment. The interaction of ferripyoverdine (or other metal-chelates of pyoverdine: Al^{3+} , Cu^{2+} , Ga^{3+} , Mn^{2+} , Ni^{2+} , Zn^{2+}) with FpvA triggers a signal-cascade, ultimately resulting in the upregulation of the PvdS-regulon. FpvR and TonB from the TonB-ExbBD complex interact with FpvA after it has bound to ferripyoverdine. In response to this interaction, FpvR undergoes a structural reorganization, making it susceptible to cleavage by the “site-1-like peptidase” (S1P, unidentified component). Thereafter, RseP cleaves the resulting membrane-bound subfragment of FpvR, releasing PvdS and FpvI from the membrane. Probably, a cytoplasmic peptidase (CP, unidentified component) degrades the residual FpvR fragments, liberating PvdS and FpvI. Whilst FpvI upregulates the expression of *fpvA*, PvdS enhances the transcription of numerous genes collectively shown as the PvdS-regulon. Once enough iron has accumulated in the cytoplasm, the Fur-repressor binds to its co-repressor Fe^{2+} , which downregulates the expression of *fpvR*, *fpvI*, *pvdS* and many other genes contained in the Fur-regulon. See text for details. Dotted arrows indicate suppression of transcription, while filled arrows indicate enhanced transcription. IM, inner membrane; OM, outer membrane; cRNAP, core RNA-polymerase.

FpvI will be explained hereafter. It was observed that the predominant form of FpvR, detected in cells either lacking FpvA or pyoverdine (production), is not the approx. 37 kDa full length protein, but rather a 20 kDa N-terminal subfragment, which disappears upon FpvA dependent signaling (174). This initial cleavage was later proven to proceed autoproteolytically, although it was not essential for functionality in the homolog FoxR (175). However, the autoproteolytically cleaved periplasmically localized C-terminal fragment interacts with the membrane bound N-terminal fragment and is required for functionality (175). Once the signal is perceived by FpvA and is transduced to FpvR, the FpvR₂₀ subfragment is further cleaved into an approx. 14 kDa membrane bound fragment by an unknown site-1-like peptidase (174). This makes the subfragment vulnerable to cleavage by the site-2 intramembrane peptidase RseP (174). Probably, a residual fragment bound to the respective ECF is degraded by an yet unidentified cytoplasmic peptidase (174). The liberated PvdS and FpvI then bind to the core RNA-polymerase (cRNAP), which is thereby targeted to specifically recognized promotor-regions that have been characterized accordingly (176–178, 171).

FpvI was discovered in 2003 by Rédly & Poole (179), who could show that the expression of *fpvA* is under the control of FpvI. Later they could also prove that both PvdS and FpvI are bound by the anti-sigma factor FpvR (171). The ECF PvdS had been discovered in 1995 by Cunliffe *et al.* (180) and is the master regulator for pyoverdine biosynthesis related genes (164, 181). However, the PvdS-regulon is not limited to pyoverdine-related genes but also positively acts on the production of virulence factors such as exotoxin A (ToxA or ETA), although it is unclear whether this is a direct or indirect regulation via RegA (ToxR) and/or PtxR (182–184), the PrpL endopeptidase (185) and possibly also the alkaline protease AprA (186–188). Consequently, PvdS deletion mutants exhibit a compromised pathogenicity *in vivo* (189, 190). In *P. syringae* pv. *tomato* DC3000, it could be proven that a number of additional genes, e.g. an OprD family porin, an azurin and a tannase/feruloyl esterase, are under the control of the PvdS-regulon (191). Interestingly, mutants defective in pyoverdine production cannot upregulate the PvdS-regulon even under iron-limiting conditions (167, 168), suggesting an auto-induction pathway. However, this would result

in a hen-egg problem, since no pyoverdine could be produced without pyoverdine already being present. This apparent paradox could be resolved recently by Edgar *et al.* in 2017 (192), who could show that, in the absence of ferripyoverdine, less FpvR is present in the cell than PvdS and Fpvl, allowing for a basal expression, save in the presence of iron, when Fur binds Fe²⁺ and inhibits the transcription of *pvdS* altogether.

However, the complexity of pyoverdine regulation goes beyond the iron-status of the cell. For instance, oxygen has a positive influence on the expression of *pvdS*, although the signal-transduction pathway is unclear (182, 193, 184). Furthermore, it could be demonstrated that oxidative stress also positively influences *pvdS* transcription *via* OxyR and PA2206 (194, 195). On the other hand, low phosphate concentrations enhance, whilst high phosphate concentrations inhibit pyoverdine production through an unknown mechanism (196, 197). Interestingly, copper starvation leads to a reduced expression of pyoverdine-related genes (198). CysB, a transcriptional activator for the cysteine-regulon, also enhances transcription of *pvdS*, tentatively linking iron-sulfur biogenesis with the iron-status (199). Additionally, quorum sensing has been implicated in regulating pyoverdine production, although it is unclear how the regulation occurs (200). For the quorum signaling substance 2-heptyl-3-hydroxy-4(1*H*)-quinolone (PQS; 201) of *P. aeruginosa*, it has been proposed that it can chelate iron but does not function as a siderophore, thus inducing the iron-starvation response (202, 203). Moreover, AmpR, a regulator involved in β -lactam stress, seems to indirectly upregulate pyoverdine production, possibly *via* the sRNA asPrrF1 (204). The Gac/Rsm system, composed of the two-component system GacS (sensor kinase) and GacA (response regulator) and the sRNA's *rsmXYZ* (reviewed in 205), which is interwoven with the cyclic-di-GMP (c-di-GMP) pathway (206), regulate pyoverdine production probably by modifying *pvdS* expression (207–213). The putative cytoplasmic membrane sensor PA2663, involved in biofilm formation, also positively influences *pvdS* expression (214). The extracellular lipase LipA upregulates *pvdS* expression by an unknown mechanism (215). On the contrary, the exoprotease SprP reduces pyoverdine formation, albeit also by an unknown mechanism (216). For more details on pyoverdine regulation, the reader is referred to the

extensive review by Llamas *et al.* (217). The complex regulatory network of pyoverdine production, which integrates many different environmental signals, is still far from understood, but illustrates how vigilantly fluorescent pseudomonads adapt to prevail in specific environmental settings.

1.6. Pyoverdine biogenesis

The elucidation of the structure of pyoverdine (14) led to a new era in pyoverdine research. The general structure of pyoverdine [1-6] is composed of: 1) the characteristic 2,3-diamino-6,7-dihydroxyquinoline fluorophore, 2) a variable acyl side chain attached to the 3-amino group of the chromophore and 3) a strain-specific peptide backbone, usually bound to the C₁-carboxy group of the ring system (reviewed in 218, 219), although so called isopyoverdines [7-12] (Figure 4A) have also been observed, where the peptide backbone is attached to the C₃-carboxy group (220, 221). The biosynthetic precursor of pyoverdine is ferribactin [14], which is probably converted to pyoverdine via the intermediate dihydropyoverdine [15] (previously termed pseudobactin A) (222-224, 220, 225-227) by an oxidative cyclization cascade as proposed by Dorrestein *et al.* (Figure 4E; 228, 229). Nevertheless, an alternative mechanism has been postulated, based on the observation of the trihydroxylated "pseudoverdin" intermediate [13] (Figure 4C), which is produced by a strain impaired in pyoverdine biogenesis (230). This alternative mechanism is a variant of the intramolecular Bucherer reaction, possibly involving the observed dihydropyoverdine-7-sulfonic acids [16] (Figure 4F; 230, 225, 231, 226, 232, 233). A third pathway for chromophore biogenesis, starting at dihydroorotic acid and phenylalanine, has been postulated (234, 235), although it was not widely recognized and labeling experiments argued against this pathway (226). The variable acyl side chain attached to the 3-amino group of the chromophore can be one of the following residues (Figure 4B): [R₁] glutamic acid (236), [R₂] α-ketoglutaric acid (237), [R₃] succinamide (14), [R₄] succinic acid (238) or the intramolecular cyclized succinate (239), [R₅] malamide (240) and [R₆] malic acid (238). However, these side-chain modifications could not be explained, although it was concluded from cultivation experiments that [R₂] and [R₃] are genuine products and that [R₄] is a hydrolysis product of [R₃],

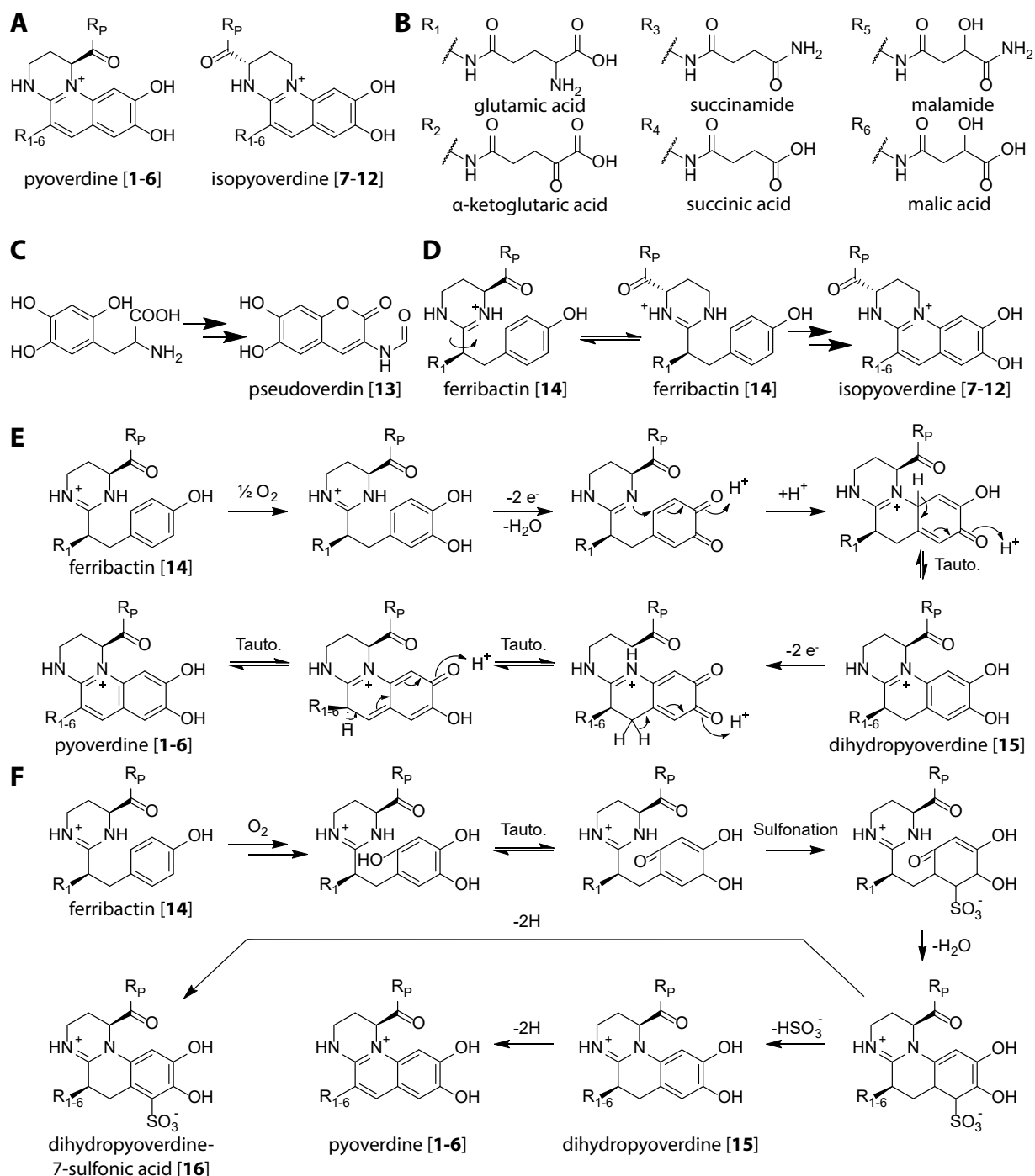


Figure 4: Pyoverdine and its precursors/derivatives, as well as possible routes towards chromophore formation. (A) General structure of pyoverdines and isopyoverdines; (B) acyl side chains attached to the 3-amino group of the chromophore; (C) possible formation of pseudoverdin from the 2,4,5-trihydroxy phenylalanine; (D) possible pathway of isopyoverdine biogenesis from ferribactin, implying ferribactin to be a precursor of pyoverdine; (E) oxidative chromophore cyclization as proposed by Dorrestein *et al.* (F) chromophore formation formulated as modified intramolecular Bucherer reaction as suggested by Schröder *et al.*. Please refer to the text for details. A range of assigned numbers in square brackets correspond to the six distinct side-chains as depicted in (B). Tauto., tautomerization; R_p, Peptide backbone.

whilst [R₁] is the product of reductive transamination of [R₂] (241). Furthermore, it was noted that all observed modifications are intermediates of the citric acid cycle, implying a correlation (241). Although the biosignificance of these side-chain modifications still remain a

mystery, the physicochemical properties thereof have been employed for siderotyping *via* isoelectric focusing (IEF), which was developed to a widely used method (242).

The strain-specific peptide backbone varies according to the strain used for production and can either be linear or (partially) intramolecularly cyclized. Furthermore, it can contain a number of unusual amino acids, such as β -hydroxy aspartic acid, β -hydroxy histidine, ornithine, cyclo- N_5 -hydroxy ornithine, N_5 -formyl- N_5 -hydroxy ornithine, N_5 -acetyl- N_5 -hydroxy ornithine and N_5 -hydroxybutyryl- N_5 -hydroxy ornithine, of which the hydroxamates or β -hydroxy carboxylates contribute to iron-chelation. Additionally, the amino acids in the peptide backbone may also be isomerized to the D-enantiomeric form (reviewed in 15, 219).

The pyoverdine biosynthesis occurs in many steps, involving the cytoplasmic generation of the acylated ferribactin precursor by non-ribosomal peptide synthesis, export and consecutive maturation by tailoring enzymes in the periplasm, as detailed hereafter (Figure 5). Pyoverdine biogenesis starts in the cytoplasm, where the non-ribosomal peptide synthases (NRPSs) PvdL (243), PvdI (244) and PvdD (245, 246) (depending on the strain considered, further NRPSs can be involved in synthesis) assemble the acylated ferribactin precursor. Module 1 of PvdL incorporates either a myristic- or myristoleic acid side-chain instead of an amino acid as first building block (247), thus ferribactin is acylated on the free amino group of the glutamic acid residue (248). The NRPS PvdL is conserved in all known fluorescent pseudomonads, thus the first building block consisting of the acylated L-glutamic acid, coupled *via* its γ -carboxylic acid to D-tyrosine and L-2,4-diaminobutyrate (L-Dab) is conserved, which is coherent, since it is later cyclized to the characteristic chromophore. L-Dab, required by PvdL, is produced by PvdH from L-aspartate β -semialdehyde (L-ASA) (249). L- N_5 -formyl- N_5 -hydroxy ornithine (L-fOHOrn) is produced in two steps, first, the monooxygenase PvdA hydroxylates L-ornithine to L- N_5 -hydroxy ornithine (250–253), which is then formylated by PvdF to L- N_5 -formyl- N_5 -hydroxy ornithine (254). All these enzymes have been implicated in forming membrane associated complexes called “siderosomes”, possibly to circumvent cytoplasmic toxicity (255, 256). Furthermore, a small MbtH like protein may be involved in pyoverdine synthesis (257). MbtH proteins have been implied in

enhancing adenylation domain activity (258, 259). Also, a soluble thioesterase PvdG may be involved in pyoverdine production (181), although it does not seem to be essential in *P. aeruginosa*, possibly due to the functional redundancy of PA2411 (260). Additionally, further auxiliary enzymes, such as the *N*₅-hydroxy ornithine acetylase PvdY_{II}, are involved in the cytoplasmic pyoverdine synthesis in some strains (261). After the cytoplasmic steps in biogenesis of the acylated precursor are completed, the acylated ferribactin is translocated into the periplasm by the ABC transporter PvdE (262, 143).

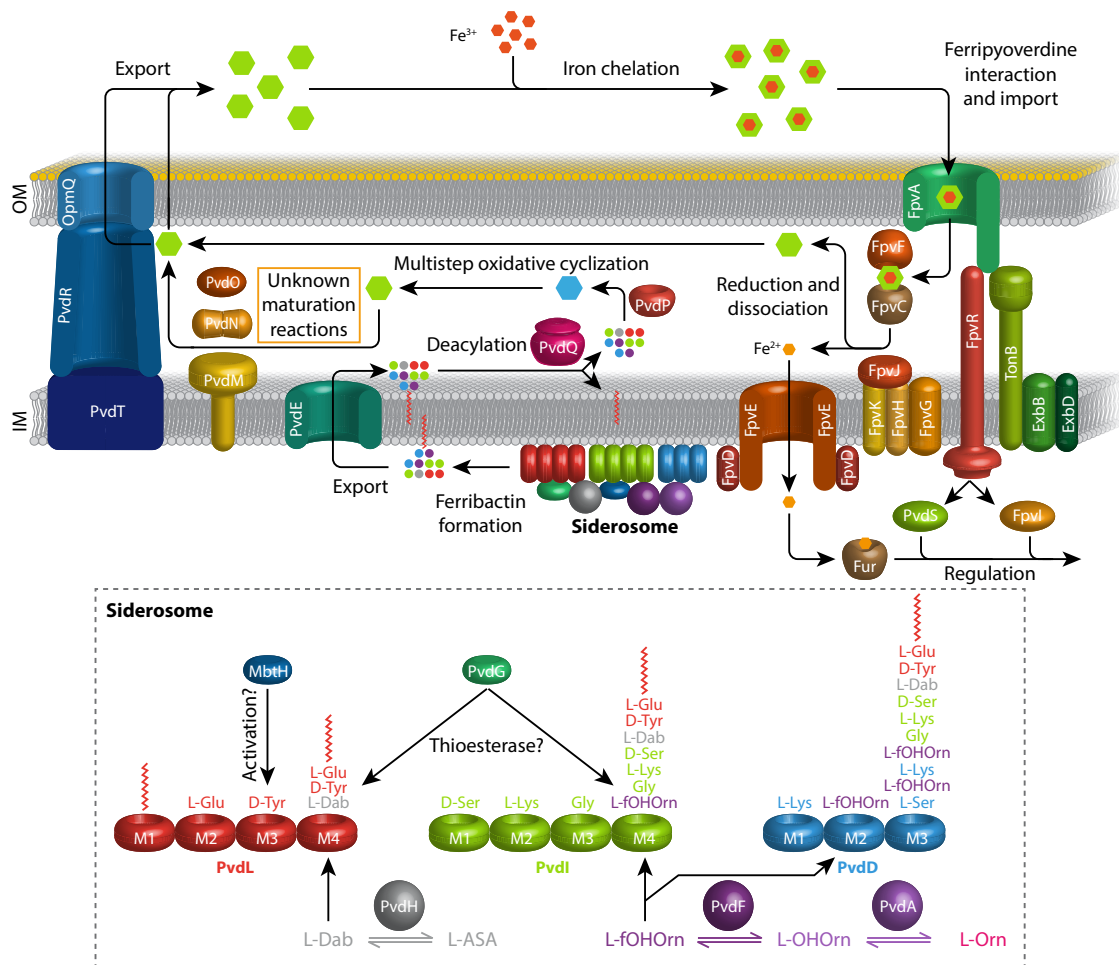


Figure 5: Overview over pyoverdine biosynthesis, export, recycling and signaling in *P. fluorescens* A506. The acylated ferribactin precursor is synthesized in the periplasm by the non-ribosomal peptide synthetases PvdL, PvdI and PvdD, involving the enzymes PvdH, PvdF and PvdA, which generate the non-proteinogenic amino acids L-Dab and L-fOHOrn, organized as membrane bound complex referred to as “siderosome”. The adenylation-domain activating protein Mbth and the soluble thioesterase PvdG may also be involved. The acylated precursor is then exported into the periplasm *via* PvdE, where it is deacylated by PvdQ. Thereafter, PvdP catalyzes the chromophore formation. Further unknown maturation steps may be carried out by the putative but required enzymes PvdM, PvdN and PvdO. Subsequently, the matured pyoverdine is exported *via* PvdRT-OpmQ or the type VI secretion system and other yet unidentified export pathways. After binding iron, ferripyoverdine is imported by FpvA in conjunction with TonB-ExbBD (see section 1.4 for details) and simultaneously triggers the regulation cascade involving FpvR, FpvI and PvdS (see section 1.5 for details). Iron is liberated from pyoverdine, facilitated by FpvF, FpvC, and FpvGHJK. The liberated Fe²⁺ is imported into the cytoplasm *via* FpvD₂E₂, where it can trigger the Fur-regulon and the deferrated pyoverdine is recycled (see previous sections for details). Please refer to the text for further details. L-Dab, L-2,4-diaminobutyrate; L-ASA, L-aspartate β semialdehyde; L-fOHOrn, L-*N*₅-formyl-*N*₅-hydroxy ornithine; L-OHOrn, L-*N*₅-hydroxy ornithine; IM, inner membrane; OM, outer membrane.

In the periplasm, the acylation of ferribactin is removed by the NTN-type hydrolase PvdQ (247, 143, 248). PvdQ was first discovered as quorum-quenching enzyme, which acts by deacylating 3-oxo-dodecanoic homoserine lactone that belongs to the autoinducers *N*-acyl homoserine lactones (AHLs) (263–265). PvdQ is produced as a proenzyme that autoproteolytically cleaves itself in the periplasm by excising a 23-residue spacer forming an 18 kDa α -chain and a 60 kDa β -chain, which reassociate to form a functional heterodimer (263). Thereafter, the copper-dependent tyrosinase like enzyme PvdP catalyzes the formation of the pyoverdine chromophore starting from ferribactin (266), probably via the oxidative cyclization cascade proposed by Dorrestein *et al.* (Figure 4E; 228, 229). Interposon studies revealed that the putative periplasmic enzymes PvdM, PvdN and PvdO are required for pyoverdine biosynthesis but their function is unknown (164, 181, 267, 143, 260, 268). For the enzyme PvdN it could be demonstrated that it is exported *via* the twin-arginine translocation (Tat) pathway (267). After periplasmic maturation, pyoverdine is exported *via* the PvdRT-OpmQ pathway, although it cannot be the only export route (137). Furthermore, the type VI secretion system was implied in pyoverdine export (142). The complex biosynthesis and maturation of pyoverdines is obviously demanded by the chemical complexity of the siderophore, which in turn is apparently a tribute to the intricate interplay of environmental and biological factors implicated in something seemingly simple as the competition for iron.

1.7. Pyoverdine as target for antibiotic treatments

Due to the importance of pyoverdine for virulence (see section 1.3 for details), it has been regarded as potential target for novel antibiotics, although the approaches vary according to their specific target within the pathways involved in biosynthesis, uptake, recycling and regulation. An elegant approach referred to as “trojan horse” strategy, exploits the pyoverdine import pathway to shuttle covalently attached antibiotics into the cell (269–271). In this regard, a number of pyoverdine derivatives have been synthesized and tested for enhanced antibacterial activity, either consisting of pyoverdines conjugated to β -lactam- (272, 273) or quinolone antibiotics (274), establishing the feasibility of this approach. Furthermore, it could be demonstrated that a

hydrolysable linker is preferable for activity (274) and that the sterical hindrance of the uptake of pyoverdine by conjugation is minimal at the variable acyl side chain attached to the 3-amino group of the chromophore (275). This approach has the advantage of being strain specific, since pyoverdines are taken up only if the respective bacterium is in possession of a compatible outer membrane receptor FpvA (as discussed in section 1.4), also established experimentally (274). These findings suggest that it may be worthwhile to explore the possibilities of the “trojan horse” strategy by further experiments. A second approach, also targeting uptake but also the signaling pathway has been investigated using “Gallium-mediated siderophore quenching” (276, 277), which supposedly acts by interfering with iron uptake by gallium-pyoverdine chelates that are known not to be dissociatable by reduction (136), thus also highjacking the signaling pathway for iron-starvation, thereby possibly increasing the metabolic burden (276). In a previous study gallium-chelates were shown to downregulate *pvdS* expression (277). Interestingly, it could be demonstrated, that this strategy seems to be evolutionary robust, since, in comparison to classical antibiotics, resistance development was retarded (276).

Another promising approach interferes with the biosynthesis of siderophores, specifically by inhibiting the deacylating NTN-type hydrolase PvdQ (247, 278, 279). Previously, it could be shown, that a PvdQ deletion mutant is impaired in virulence against *Caenorhabditis elegans* and *Solanum tuberosum* (280). Furthermore, since PvdQ also plays a role in quorum quenching by AHL deacylation (263), it is interesting to note that the observed reduced virulence is attributable to the lack in pyoverdine maturation and not to the disturbance of the AHL quorum-sensing circuit (280).

Moreover, in a screening for antivirulence activity against *P. aeruginosa* of already marketed drugs, the antimycotic drug flucytosine was found to inhibit *pvdS* expression, thereby reducing virulence in a mouse model lung infection (190). Although the exact mode of action for flucytosine has not been elucidated yet, it could be demonstrated that the conversion of the prodrug flucytosine to 5-fluorouracil is required for activity (190).

The promising results obtained by the presented approaches demand to invest more time and effort into understanding the exact processes involved in biosynthesis, uptake, recycling and regulation of pyoverdine.

2. Aims of this study

Although investigations into the biosynthesis of pyoverdine have elucidated most of the cytoplasmic biosynthesis pathway, the periplasmic maturation of pyoverdine is generally not well understood. Even though the functions of the periplasmic enzymes PvdP and PvdQ could be revealed, the functions of the proposedly essential periplasmic enzymes PvdM, PvdN and PvdO have not been exposed. Additionally, although PvdRT-OpmQ and the type VI secretion system are implied to be involved in pyoverdine export and recycling, an open question remains as to which other export routes are engaged therein. Furthermore, a number of enzymes involved in the signaling pathway, for instance the site-1-like protease that obviously is of importance for the whole signaling cascade, remain to be identified. Another unresolved puzzle is the production of different side-chain variants of pyoverdines, which have been recognized for many years, although neither their biosynthetic origin nor their biological function have yet been unraveled. In light of the biosignificance of pyoverdines that are important in a multitude of environmental settings, especially pathogenicity and plant-growth promotion, it is unsatisfactory not to understand the intricate details involved in pyoverdine biosynthesis, uptake, recycling and regulation.

Therefore, in this thesis, we sought to shed some light on the complex periplasmic maturation pathway. As a starting point, we focused on the investigation of the functions of PvdM, PvdN and PvdO. To examine the potential roles of these enzymes, knock-out mutants of the genes encoding the respective proteins were to be constructed. In combination with pyoverdine extraction and intermediate analysis, as well as complementation of the deletion mutants, we aimed to obtain insights into the steps these putative enzymes catalyze. By this approach we hoped to gain an understanding of how the remaining unsolved steps of pyoverdine biosynthesis, uptake, recycling and regulation can be explained and how PvdM, PvdN and PvdO are involved.

3. Results

3.1. PvdN Enzyme Catalyzes a Periplasmic Pyoverdine Modification

Authors: Michael T. Ringel¹, Gerald Dräger², and Thomas Brüser¹

Affiliations: ¹Institute of Microbiology, Leibniz Universität Hannover, Herrenhäuser Straße 2, 30419 Hannover
²Institute of Organic Chemistry, Leibniz Universität Hannover, Schneiderberg 1 B, 30167 Hannover, Germany

Type of authorship: First author

Type of article: Original research article

Share of work: 90 %

Contribution: MTR performed the experiments, prepared the figures, and analyzed the data together with TB. GD performed the MS analyses. TB conceived and coordinated the study and TB and MTR wrote the paper.

Journal: Journal of Biological Chemistry

Impact factor (2016): 4.125

Date of publication: October 4th, 2016

Number of citations (05.04.2018): 6

DOI: 10.1074/jbc.M116.755611

PMID: 27703013

PvdN Enzyme Catalyzes a Periplasmic Pyoverdine Modification*

Received for publication, August 26, 2016, and in revised form, September 30, 2016. Published, JBC Papers in Press, October 4, 2016, DOI 10.1074/jbc.M116.755611

Michael T. Ringel[‡], Gerald Dräger[§], and Thomas Brüser^{‡1}

From the [‡]Institute of Microbiology, Leibniz Universität Hannover, Herrenhäuser Straße 2, 30419 Hannover and the [§]Institute of Organic Chemistry, Leibniz Universität Hannover, Schneiderberg 1 B, 30167 Hannover, Germany

Edited by F. Peter Guengerich

Pyoverdines are high affinity siderophores produced by a broad range of pseudomonads to enhance growth under iron deficiency. They are especially relevant for pathogenic and mutualistic strains that inhabit iron-limited environments. Pyoverdines are generated from non-ribosomally synthesized highly modified peptides. They all contain an aromatic chromophore that is formed in the periplasm by intramolecular cyclization steps. Although the cytoplasmic peptide synthesis and side-chain modifications are well characterized, the periplasmic maturation steps are far from understood. Out of five periplasmic enzymes, PvdM, PvdN, PvdO, PvdP, and PvdQ, functions have been attributed only to PvdP and PvdQ. The other three enzymes are also regarded as essential for siderophore biosynthesis. The structure of PvdN has been solved recently, but no function could be assigned. Here we present the first in-frame deletion of the PvdN-encoding gene. Unexpectedly, PvdN turned out to be required for a specific modification of pyoverdine, whereas the overall amount of fluorescent pyoverdines was not altered by the mutation. The mutant strain grew normally under iron-limiting conditions. Mass spectrometry identified the PvdN-dependent modification as a transformation of the N-terminal glutamic acid to a succinamide. We postulate a pathway for this transformation catalyzed by the enzyme PvdN, which is most likely functional in the case of all pyoverdines.

Under aerobic conditions in the neutral pH range, iron can form insoluble Fe^{III} oxide hydrates, limiting the amount of readily available iron. Therefore, many organisms produce siderophores that bind and thereby solubilize iron in their surroundings. A special group of these siderophores are the pyoverdines, yellow-green pigments that were first described in 1892 by Gessard (1). Turfitt (2, 3) used the production of pyoverdines for taxonomic classification of “fluorescent pseudomonads,” which include many important pathogenic as well as beneficial pseudomonads. Today it is known that pyoverdines are non-ribosomally synthesized, highly modified peptides whose biosynthesis and regulation involve more than 20

proteins (4). The cytoplasmic biosynthesis reactions are well established, but recently, the periplasmic maturation has gained interest. Of the five periplasmic enzymes, PvdM, PvdN, PvdO, PvdP, and PvdQ, which are found in all known pyoverdine-producing species, functions have been assigned so far only to PvdQ and PvdP, which are involved in a precursor deacylation step and the chromophore cyclization, respectively (5–8). PvdQ has been identified as a potential novel drug target (5). Based on interposon mutagenesis studies, PvdM, PvdN, and PvdO are all considered to be essential for the formation of functional pyoverdines (6, 9–11).

PvdN is translocated via the Tat² system (11). As heterologously produced PvdN contains as prosthetic group a pyridoxal phosphate cofactor (PLP (12)), the Tat system may transport PvdN together with a bound PLP or a derivative thereof. However, no specific function in pyoverdine biogenesis could be attributed to PvdN.

Here we demonstrate that the enzyme PvdN specifically introduces a side-chain modification into the produced pyoverdine. The side-chain modification did not influence growth under iron-limiting conditions at different pH settings. Fluorescent pseudomonads usually produce more than one isoform of pyoverdine, which is exploited by a method known as siderotyping (13). This method utilizes the different pI values of siderophores, which include modified pyoverdine isoforms. Most of the modifications influencing the pI can be attributed to variations of a side chain at the 3-amino group of the chromophore (4, 14, 15). PvdN is responsible for such a modification. In contrast to results from earlier interposon mutagenesis studies that could not exclude polar effects (9, 10), a scar-less in-frame deletion of *pvdN* selectively abolished this modification without affecting the formation of functional pyoverdine. A mechanism for the catalyzed reaction of PvdN is proposed that attributes a key function to the bound cofactor. Lys-261 in the cofactor-binding pocket was essential for activity and translocation into the periplasm, suggesting that the Tat system has to translocate PvdN in an active, cofactor-containing conformation.

* This work was supported by the German Research Foundation (DFG) as a project of the GRK1798 “Signaling at the Plant-Soil Interface.” The authors declare that they have no conflicts of interest with the contents of this article.

¹ To whom correspondence should be addressed. Tel.: 49-511-762-5945; Fax: 49-511-762-5287; E-mail: brueser@ifmb.uni-hannover.de.

² The abbreviations used are: Tat, twin-arginine translocation; oePCR, overlap extension polymerase chain reaction; EDDHA, ethylenediamine di(*o*-hydroxy)phenylacetic acid; PLP, pyridoxal phosphate; IEF, isoelectric focusing; CAS, chrome azurol S; CAA, casaminoacid; UPLC, ultra-performance liquid chromatography; Bicine, *N,N*-bis(2-hydroxyethyl)glycine.

Functional Role of PvdN

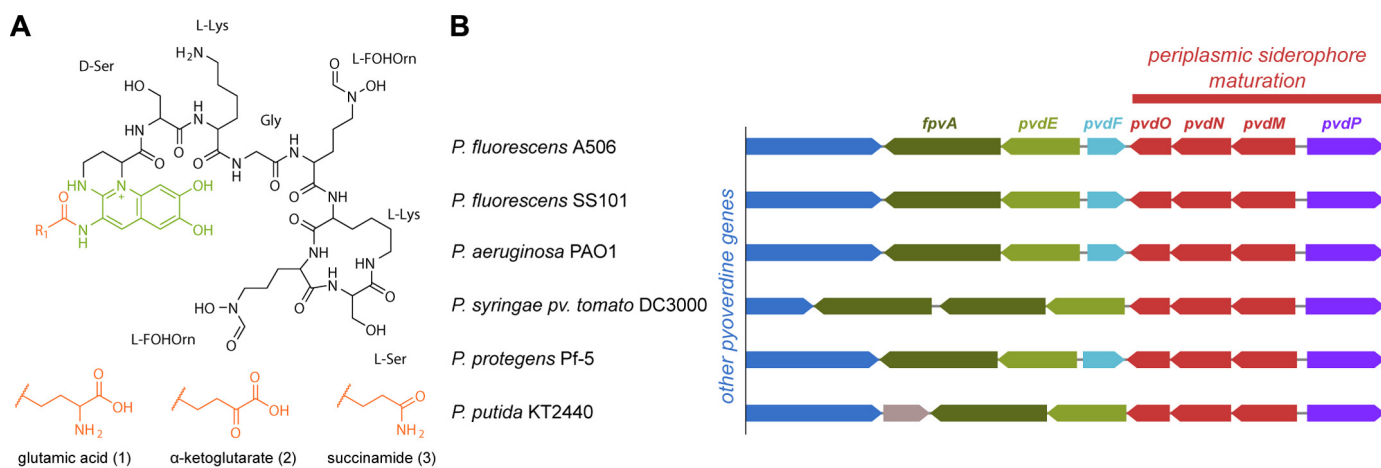


FIGURE 1. **Pyoverdine maturation by periplasmic enzymes and their genetic relatedness.** *A*, postulated structure of PVD_{A506} (24), showing the fluorophore and the position of the modified N-terminal residue (R₁), which are the regions where periplasmic maturation occurs. The three shown R₁ side chains represent the three structures that are relevant in this study. *B*, conserved clustered organization of the *pvdMNO* operon and the *pvdP* gene, which encode the periplasmic pyoverdine maturation enzymes. PvdQ, which has also functions in other pathways, is not encoded in this cluster.

Results

Pseudomonas fluorescens A506 Produces a Typical Pyoverdine—Based on genetic analyses, it was recently proposed that *P. fluorescens* strain A506 produces a typical pyoverdine, which is expected to bind Fe^{III} via six ligands provided by two hydroxamates of the peptide moiety and two oxo groups of the catechol fluorophore (Fig. 1A) (4). While the cytoplasmically generated peptide moiety varies in sequence, length, and cyclic/linear structure among the many known pyoverdines, the enzymes involved in the periplasmic maturation of this siderophore are highly conserved in all pyoverdine-producing species and strains, indicating that their activities are required for all known pyoverdines (Fig. 1B). We chose to study these aspects in the fully genome sequenced *P. fluorescens* strain A506, for which we have established versatile genetic tools such as genomic in-frame knock-outs and complementation vectors, as well as phenotypic assays such as pyoverdine formation analyses. For an initial chemical characterization of the pyoverdine produced by *P. fluorescens* A506 (referred to as PVD_{A506} throughout), we carried out the Csáky assay for the detection of hydroxamates (16), the Arnow reaction for the identification of the catechol functionality (17), and a ferric perchlorate assay to detect binding of iron at low pH values (18). Furthermore, we evaluated the expected influence of iron chelation by PVD_{A506} on spectral properties (19).

The fluorescence emission spectrum changed upon chelation of iron by PVD_{A506} (Fig. 2, A and B). Specifically, the maximum at ~500 nm was quenched and the intensity of the major emission peak at ~440 nm was reduced. The electronic absorption spectrum (Fig. 2C) showed a shift of a 405 nm maximum to 400 nm and the formation of a shoulder at 460 nm. PVD_{A506} reacted positively in the Csáky assay (16) that hydrolyzes the δ -N-formyl- δ -N-hydroxyornithines and thereby forms hydroxylamine that is detectable by a sensitive colorimetric assay (Fig. 2D), indicative for the presence of hydroxamates. This was expected for the δ -N-formyl- δ -N-hydroxyornithines of the siderophore. The Arnow assay (17) is based on the formation of a colored compound with a nitrite-molybdate reagent. As characteristic for pyoverdines (20), PVD_{A506} did not react positively

in this assay despite the presence of a catechol group. As expected, PVD_{A506} did not show binding of iron in the ferric perchlorate assay (18), as the protonatable catechol is required for efficient binding (PVD_{A506} is not a Tris(hydroxamate) type siderophore that would react positively).

The Gene Encoding PvdN Is Not Essential for Pyoverdine Formation—In previous mutagenesis studies, it was already noted that the observed essential phenotype of a *pvdN* interposon mutation could have been caused by polar effects within the *pvdMNO* operon (10). To examine the role of PvdN in PVD_{A506} biosynthesis, we therefore first needed to establish a scar- and marker-less in-frame deletion method for *P. fluorescens* A506. This was achieved by combining two methods (Fig. 3A) (21, 22). First, a deletion plasmid derived from the suicide plasmid pK18*mobsacB* (23) was constructed, containing ~1 kbp of the left and right flanking regions of the target gene. Then, instead of conjugative transfer of the plasmid, we employed electroporation (22), which worked efficiently for *P. fluorescens* A506. Single crossover integrands were selected on the appropriate antibiotic. Double crossover mutants were selected by successive counter-selection on sucrose-containing medium, and scar- and marker-less deletions were identified and confirmed by PCR and sequencing. We included a deletion of monocistronic *pvdP* as control, as PvdP has been biochemically confirmed to be essential for the fluorophore formation (8).

The resulting Δ *pvdN* and Δ *pvdP* deletion strains were tested for growth and pyoverdine production on *casamino acid* (CAA) medium plates with or without the iron-depleting chelator ethylenediamine di(*o*-hydroxy)phenylacetic acid (EDDHA) (Fig. 3, B–E). As expected, the Δ *pvdP* control strain could not produce fluorescent pyoverdine and did not grow on EDDHA-containing medium. However, unlike what was expected from the earlier interposon mutagenesis studies that could not exclude polar effects in the operon (6, 10, 11), the scar-less Δ *pvdN* mutant strain was not impaired in pyoverdine formation, nor did the deletion affect growth on iron-depleted medium. In fact, the Δ *pvdN* strain showed the same phenotype as the WT strain on both media, producing approximately equivalent

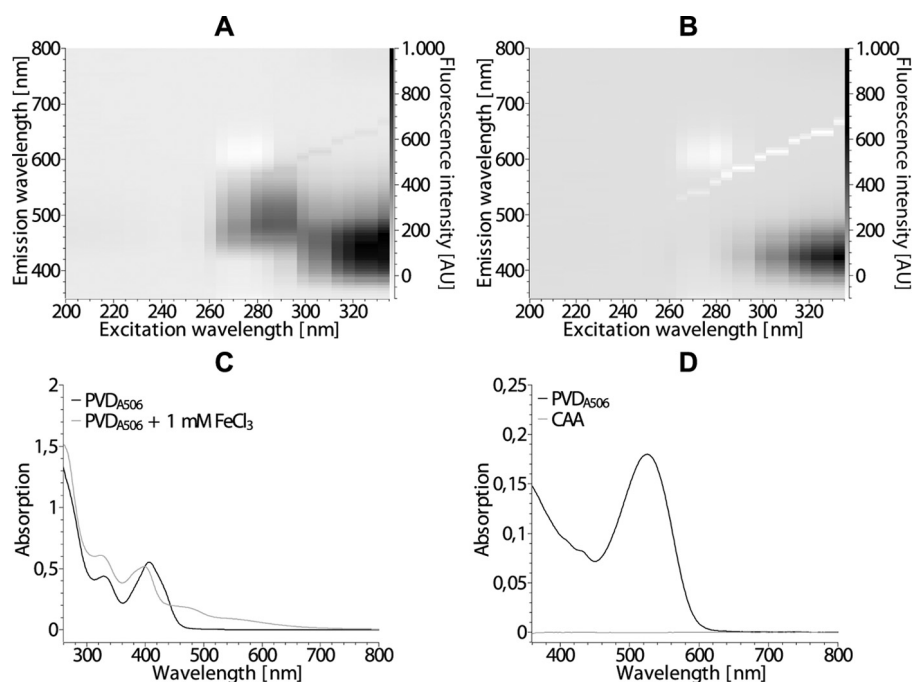


FIGURE 2. **Initial characterization of the pyoverdine PVD_{A506}.** A and B, fluorescence in the range of 350–800 nm of PVD_{A506} in culture supernatant from *P. fluorescens* A506, excited at 200–340 nm in the absence (A) or presence (B) of 1 mM FeCl₃. AU, arbitrary units. C, electronic absorption spectra of the samples from A and B. D, electronic absorption spectrum of the Csáky assay (16), indicating the presence of hydroxamates. Fresh medium (CAA) was treated in the same manner as the culture supernatant (PVD_{A506}).

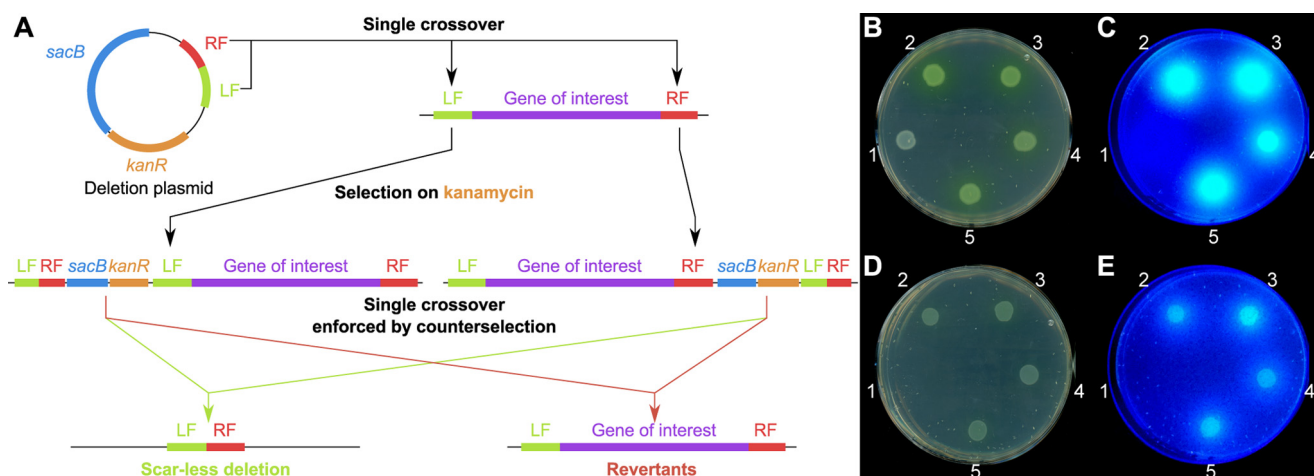


FIGURE 3. **A scar- and marker-less in-frame deletion of *pvdN* in *P. fluorescens* A506 does not abolish formation of fluorescent pyoverdines.** A, scheme for the scar- and marker-less in-frame gene deletion in *P. fluorescens* A506 (see “Results” for details). LF, left fragment; RF, right fragment; left fragment and right fragment are derived from the upstream or downstream sequences of the region to be deleted. B–E, droplet assays of 1) *P. fluorescens* A506 Δ *pvdN*, 2) *P. fluorescens* A506, 3) *P. fluorescens* A506 Δ *pvdN*, 4) *P. fluorescens* A506 Δ *pvdN* + pME6010-*pvdN*-*strep*, and 5) *P. fluorescens* A506 Δ *pvdN* + pME6010-*pvdN*_{K261A}-*strep*. Strains were incubated either in the absence (B and C) or in the presence of EDDHA (D and E). The plates were imaged (B and D), and fluorescence was detected on a UV table (C and E).

amounts of pyoverdine. Complementation vectors did not further increase the amount of pyoverdine released into the medium. We therefore further investigated the role of PvdN in pyoverdine formation.

PvdN Is Responsible for a Specific Modification of Pyoverdine—To initially assess the impact of the Δ *pvdN* mutation on pyoverdine formation, we utilized isoelectric focusing (IEF) gels in combination with a chrome azurol S (CAS) overlay assay (Fig. 4A) (13), which detects iron chelators that liberate iron from chrome azurol S, resulting in color reduction. The results revealed that PvdN is involved in the formation of a pyoverdine derivative that can be separated based on its specific pI. As it is

known that multiple pyoverdine isoforms with varied side chains attached to the 3-amino group of the chromophore are generally produced in parallel (15), we could clearly attribute such a variation to the enzyme activity of PvdN.

It was now important to exactly determine the nature of the chemical modification introduced by PvdN. We approached this aspect by UPLC mass spectrometry. Two components were identified in the wild type strain (Fig. 4B). Confirming the postulated structures (24), high resolution mass spectrometry revealed that one component had the mass of 1160.53 Da, which is the exact mass of the succinamide form of the pyoverdine, and the other had the mass of 1189.51 Da, which corre-

Functional Role of PvdN

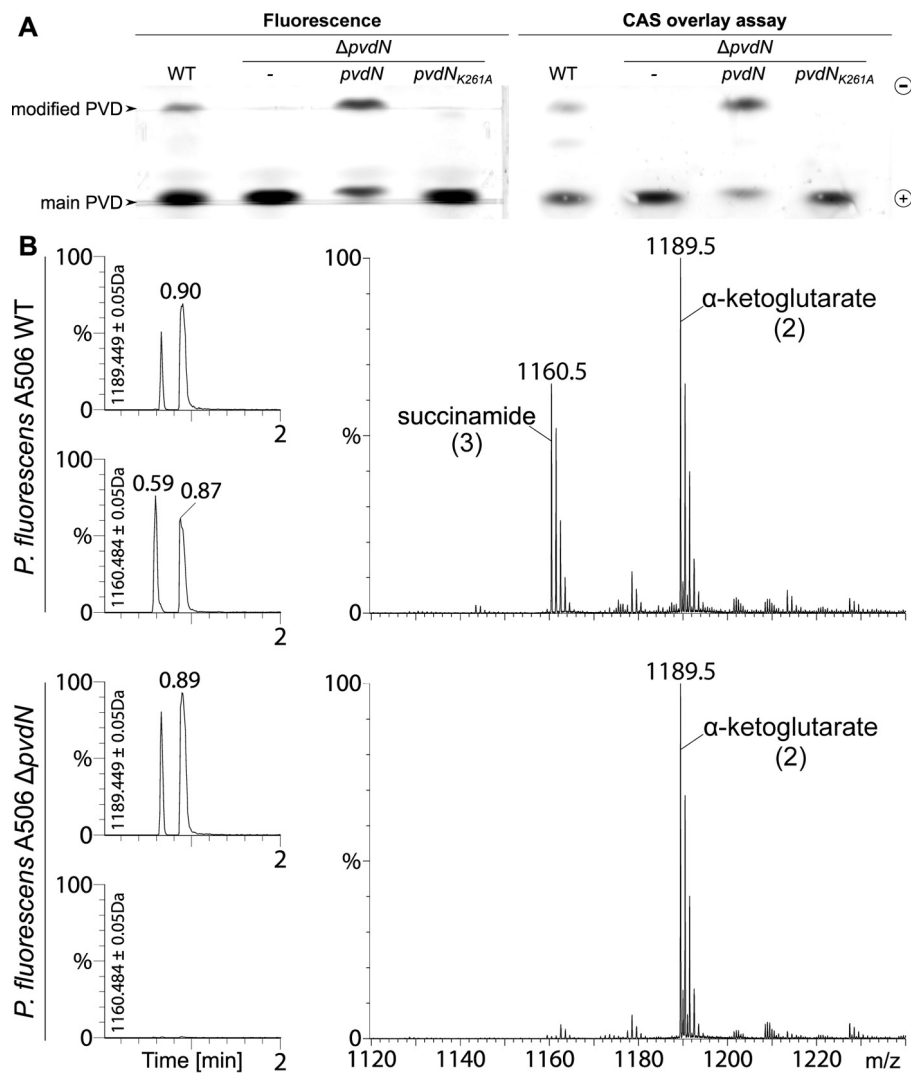


FIGURE 4. PvdN is responsible for a pyoverdine modification. *A*, isoelectric focusing indicates that wild type *P. fluorescens* A506 produces two pyoverdines, whereas the $\Delta pvdN$ mutant strain can only form one pyoverdine species (left gel). Besides the wild type and mutant strains, the IEF gel also shows the pyoverdines of strains with complementation vectors that contain either a wild type *pvdN* gene or a gene encoding the protein with a K261A mutation. Note the functional complementation by the wild type *pvdN* gene, whereas the exchange of the active site lysine completely abolishes the activity. The CAS overlay assay of the same IEF gel demonstrates the iron binding capacity of both pyoverdines (right gel). *B*, analysis of pyoverdine content in wild type *P. fluorescens* A506 and its $\Delta pvdN$ mutant. Left and right, reverse phase chromatography elutions (left) and corresponding mass spectra (right) of the succinamide and α -ketoglutarate forms of the pyoverdine (numbers correspond to structures in Fig. 1A). The elution profiles monitor the respective molecular masses during reverse phase chromatography, indicated beside the y-axes, showing that no succinamide is formed by the $\Delta pvdN$ mutant.

sponds to the α -ketoglutarate. The glutamic acid that is initially formed in the periplasm is therefore virtually completely transformed into the two mentioned variants. In the $\Delta pvdN$ mutant, only the α -ketoglutarate form of pyoverdine was formed, indicating that the transformation to the succinamide was completely abolished.

Having demonstrated the nature of the chemical modification that depends on PvdN, we carried out complementation analyses to exclude that the missing modification in the $\Delta pvdN$ mutant was caused by additional unknown genetic changes. When expressed constitutively from a stable low copy vector, the recombinant *pvdN* gene resulted in full complementation of the phenotype, demonstrating that the phenotype was indeed exclusively caused by the lack of PvdN and no other genomic mutation (Fig. 4A). There were no new intermediates accumulating in the $\Delta pvdN$ mutant, indicating that PvdN most likely transforms the unmodified original glu-

tamic acid residue directly to succinamide at the 3-amino position of the chromophore.

The Modified Pyoverdine Is Not Required for Iron-limited Growth under Specific pH Conditions—PvdN is conserved in all pyoverdine-producing bacteria, and the catalyzed modification must therefore somehow contribute to pyoverdine function. As the major function of pyoverdines is the acquisition of iron under iron limitation, and as we had already observed that the $\Delta pvdN$ mutant was able to grow under such conditions at neutral to slightly basic pH (Fig. 3, B–E), we thought about a potential function of the modification at distinct environmental pH conditions. The modification clearly increases the pI of the siderophore (Fig. 4A), and therefore could contribute to iron uptake under pH conditions near the pI of the non-modified pyoverdine and thereby help to ensure the iron supply in a larger pH range. However, this hypothesis turned out to be wrong. The PvdN-dependent modification was not required for

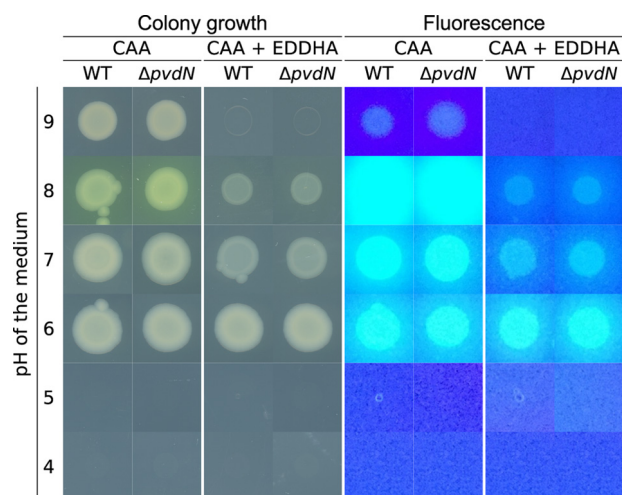


FIGURE 5. The $\Delta pvdN$ mutation does not affect iron acquisition under iron-limiting conditions at pH values that allow growth of strain A506. *P. fluorescens* (WT and $\Delta pvdN$) was grown under iron-limiting (CAA) and iron starvation (CAA + EDDHA) conditions for 36 h at the indicated pH values, colonies were imaged (left), and the pyoverdine fluorescence was detected (right). Note that there is no detectable difference in growth and pyoverdine formation between the two strains.

growth under iron-limiting conditions under any pH condition tested, ranging from pH 6 to 9 (Fig. 5). Below pH 6, *P. fluorescens* A506 did not grow at all, irrespective of the iron content.

PvdN Requires Cytoplasmic Cofactor Assembly for Folding and Tat Transport—As Tat-dependently translocated proteins can be translocated together with bound cofactors, we addressed this question with PvdN, which is believed to contain a PLP cofactor. In related PLP-containing enzymes, a lysine residue is conserved that plays a crucial role in cofactor binding (25). The corresponding residue in PvdN from *P. fluorescens* A506 is Lys-261. In the published *Pseudomonas aeruginosa* PvdN crystal structure, PLP had already formed an external aldimine with some substrate and therefore was non-covalently positioned next to the corresponding lysine residue (12). When we produced *P. fluorescens* A506 PvdN heterologously without its signal peptide in *Escherichia coli*, wild type PvdN could be obtained with a bound PLP cofactor, whereas a PvdN K261A variant was highly unstable and could not be analyzed, indicating that cofactor binding is likely to be highly important for folding (Fig. 6A). Transport was analyzed with the full-length proteins in *P. fluorescens* A506. The enzyme was only detectable in membrane and periplasmic fractions (Fig. 6B). While the wild type PvdN was clearly translocated into the periplasm, the PvdN K261A variant was not translocated anymore, and unprocessed full-length protein was detected exclusively in the membrane fraction instead, indicating that the absence of PLP causes structural characteristics that are no longer compatible with functional Tat transport.

Discussion

The periplasmic maturation of pyoverdines has been a mystery for many years. While significant progress has been made with PvdQ and PvdP (5, 8, 26), the function of any of the proteins encoded by the *pvdMNO* operon has remained unclear. As interposon mutagenesis suggested essential roles of these proteins for pyoverdine production, it was seemingly not pos-

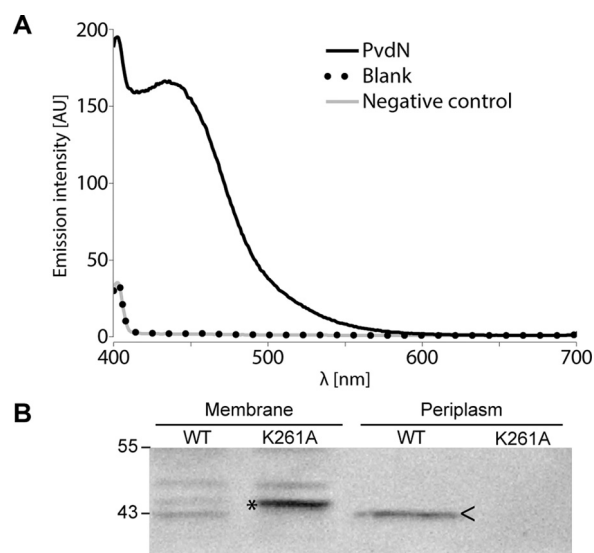


FIGURE 6. PLP binding is required for translocation of PvdN across the cytoplasmic membrane. A, UV-visible absorption-based PLP detection in PvdN as purified after heterologous production in *E. coli* ER2566/pEX-mat-*pvdN-strep* and subsequent transimination with ammonium hydroxide to produce a stable, well detectable PLP oxime (42). AU, arbitrary units. B, *Strep*-Tactin-HRP conjugate-mediated detection of C-terminally *Strep*-tagged PvdN or PvdN K261A in membrane and periplasmic fractions of *P. fluorescens* A506 containing either pME6010-*pvdN-strep* or pME6010-*pvdN*_{K261A}-*strep* by SDS-PAGE/Western blotting. Unprocessed PvdN K261A full-length protein accumulates in membranes and shows abolished translocation, whereas the wild type protein is translocated into the periplasm. >, mature PvdN in the periplasmic fraction; *, full-length PvdN in the membrane fraction. Positions of molecular mass markers (in kDa) are indicated on the left.

sible to address the individual functions of these enzymes (6, 10, 11). Interestingly, we realized that an in-frame deletion of the *pvdN* gene caused a much milder phenotype than the interposon mutation, suggesting that polar effects might disturb the interpretation of the former approaches, which was already considered by the authors of the original deletion study (10). We were surprised to see that the scar-less $\Delta pvdN$ mutation did not reduce the formation and release of fluorescent pyoverdine (Fig. 3, B–E). The only phenotype of the *pvdN* deletion was the absence of one specifically modified pyoverdine, and this phenotype could be complemented by the single *pvdN* gene, proving that PvdN is indeed responsible for the modification (Fig. 4). In a more recent study on PvdP, it was already suggested that PvdN, besides PvdM and PvdO, can only be involved in side-chain modifications, as PvdP promotes all steps of chromophore formation (8). Our study now shows that this suggestion was indeed correct. Moreover, the modification that we can now attribute to PvdN is well known and has been observed in numerous structural studies on pyoverdines (reviewed in Ref. 4). Although α -ketoglutarate, succinamide, and succinate chains have been described as side chains in pyoverdines, the enzymes that catalyze their biogenesis starting from glutamic acid, have never been identified, and this study unravels the first of these conversions.

An open question remains the physiological purpose of this highly conserved modification of pyoverdines. Our experiments indicate that it is not the iron acquisition at any specific pH that requires the PvdN-dependent modification (Fig. 5). The amount of released pyoverdine is unaltered, and the affinity to iron seems to be unaffected as well, because the mutant

Functional Role of PvdN

grows equally well on EDDHA-containing iron-limited minimal medium as the wild type strain. The function of the modification might relate to specific environmental conditions or niches that cannot be mimicked in pure cultures and therefore escape our analyses. One could, for example, imagine that certain interactions with abiotic or biotic surfaces are mediated or enhanced by the modifications that somehow contribute to iron supply. Another potential function may relate to signaling pathways involved in quorum sensing or host interactions. Whatever the reason for the modification, its strong conservation among all pyoverdine-producing pseudomonads implies that it cannot be something dispensable under natural conditions.

A highly interesting side aspect of this study was the analysis of the transport of PvdN to the periplasmic space, as the data for the first time suggest a Tat-mediated cotransport of a PLP cofactor with a periplasmic enzyme. PvdN is known to be a Tat-dependently translocated protein (11), and the crystal structure of *P. aeruginosa* PvdN demonstrated an incorporated PLP cofactor (12). In *Pseudomonas taetrolens*, it has been demonstrated that PLP could be incorporated into a Sec-dependently translocated periplasmic amino acid racemase after translocation (27), and no PLP insertion into Tat-dependently translocated enzymes has been described so far. Why is PvdN transported by the Tat system if the cofactor could in principle also be incorporated after transport? PvdN requires the PLP-binding lysine residue for functional translocation into the periplasm (Fig. 6B), and our data indicate that PvdN is trapped in the membrane if this cofactor binding is affected in PvdN K261A. The speculation may be allowed that cofactor binding is required for correct folding. This is indeed strongly supported by the published crystal structure (12). PvdN forms a dimer, and the deeply buried cofactor that is located close to the subunit interface likely contributes to folding and stable interaction of the to-be-transported protein (12). The observation that the unprocessed form of PvdN K261A is detected in the membrane fraction may relate to the exposure of hydrophobic core regions, which are known to abolish Tat substrate translocation (28). If PvdN is translocated as a folded dimer, it contains two signal peptides that can mediate its translocation. Such homooligomeric Tat substrates are well known, and it is not yet understood how all signal peptides are removed after transport (29, 30).

Mechanistically, it is highly interesting to recognize that PvdN is able to catalyze the production of a succinamide chain at the N terminus of pyoverdines. The substrate of PvdN is likely to be the glutamic acid form of pyoverdine, which is produced by PvdQ after deacylation of the acylated ferribactin (5, 26) immediately after its translocation into the periplasm by PvdE (6). The $\Delta pvdN$ mutant still produces α -ketoglutaric acid, which therefore cannot be the product of a PvdN-catalyzed transamination, and because α -ketoglutaric acid cannot be transformed to succinamide by a PLP cofactor, it neither can be the substrate for PvdN (Fig. 7A). PvdN thus apparently catalyzes the oxidative decarboxylation of the glutamic acid to succinamide, a reaction for which the following mechanism can be proposed. As PvdN solely contains a PLP cofactor and no redox-active cofactors that could be involved (see Ref. 12), the

situation is analogous to the CcbF-catalyzed PLP-dependent decarboxylation-coupled oxidative deamination (31). Unlike CcbF, an oxo group of the peroxo intermediate at the α C atom is retained, which can be readily explained by standard PLP chemistry, including proton abstraction at the α C atom and electron shuffling (Fig. 7B) (25). This would permit the direct formation of the amide of the decarboxylated amino acid, which would be to our knowledge the first description of such a reaction. The known crystal structure of PvdN strongly supports this hypothetical mechanism, as the deeply buried PLP-containing active site is connected to the surface via two channels. One is large enough to allow entering of the side chain, and the other, more narrow tunnel could permit the passage of CO₂ and O₂ (Fig. 7C). Future analyses will hopefully clarify the validity of the proposed mechanism, which might also be used in other biosynthetic pathways.

Experimental Procedures

Strains and Growth Conditions—*P. fluorescens* A506 was used for physiological studies, *E. coli* DH5 α λ pir⁺ was used for cloning, and *E. coli* ER2566 was used for expressions. *P. fluorescens* A506 was grown aerobically at 30 °C, and *E. coli* was grown at 37 °C in LB medium (1% (w/v) Tryptone, 1% (w/v) NaCl, 0.5% (w/v) yeast extract) in the presence of the appropriate antibiotics (100 μ g/ml ampicillin, 50 μ g/ml kanamycin, 20 μ g/ml tetracycline). For subcellular fractionations, the strain was grown in King's B medium (2% (w/v) BD Bacto Proteose Peptone No. 3 (BD Biosciences), 1% (v/v) glycerol, 0.15% (w/v) K₂HPO₄, 0.15% (w/v) MgSO₄).

For the production of pyoverdine, *P. fluorescens* A506 was grown aerobically in Erlenmeyer flasks with baffles in CAA medium (32) at 30 °C (5 g/liter casamino acids, 5 mM K₂HPO₄, 1 mM MgSO₄ and, optionally, 1.5% (w/v) agar noble for plates). For assessment of the pyoverdine phenotype, 0.5 g/liter EDDHA were added to the medium. Growth was assessed after ~36 h at 30 °C. Images of the plates were acquired with the Epson Perfection V850 Pro or the Epson Perfection V700 photo scanner (Epson, Meerbusch, Germany).

To assess the impact of pH on iron acquisition, we used CAA and CAA EDDHA agar supplemented with 100 mM of either of the following buffers: Bicine, pH 9.0, HEPES, pH 8.0, HEPES, pH 7.0, MES, pH 6.0, sodium acetate, pH 5.0 or pH 4.0. All buffers were prepared as 1 M stock solutions from the free acid/base, and the pH was adjusted as needed with HCl or NaOH. The growth was assessed after incubation for ~36 h at 30 °C, and images were acquired as described before. In the above mentioned droplet plate assays, we used LB overnight cultures, which were washed twice with liquid CAA medium and then adjusted to an OD₆₀₀ of 1.0, from which 10 μ l were spotted on a plate.

Genetic Methods and Plasmids—For construction of the scar- and marker-less deletions in *P. fluorescens* A506, the plasmid pK18mobsacB (23) was utilized, according to a published protocol (21) with slight modifications. In particular, we used 3'- and 5'-flanking regions of ~1 kbp in length for plasmid integration, and we employed overlap extension PCR (oePCR (33)) to connect both fragments. Furthermore, we avoided the use of conjugation and instead applied a published quick trans-

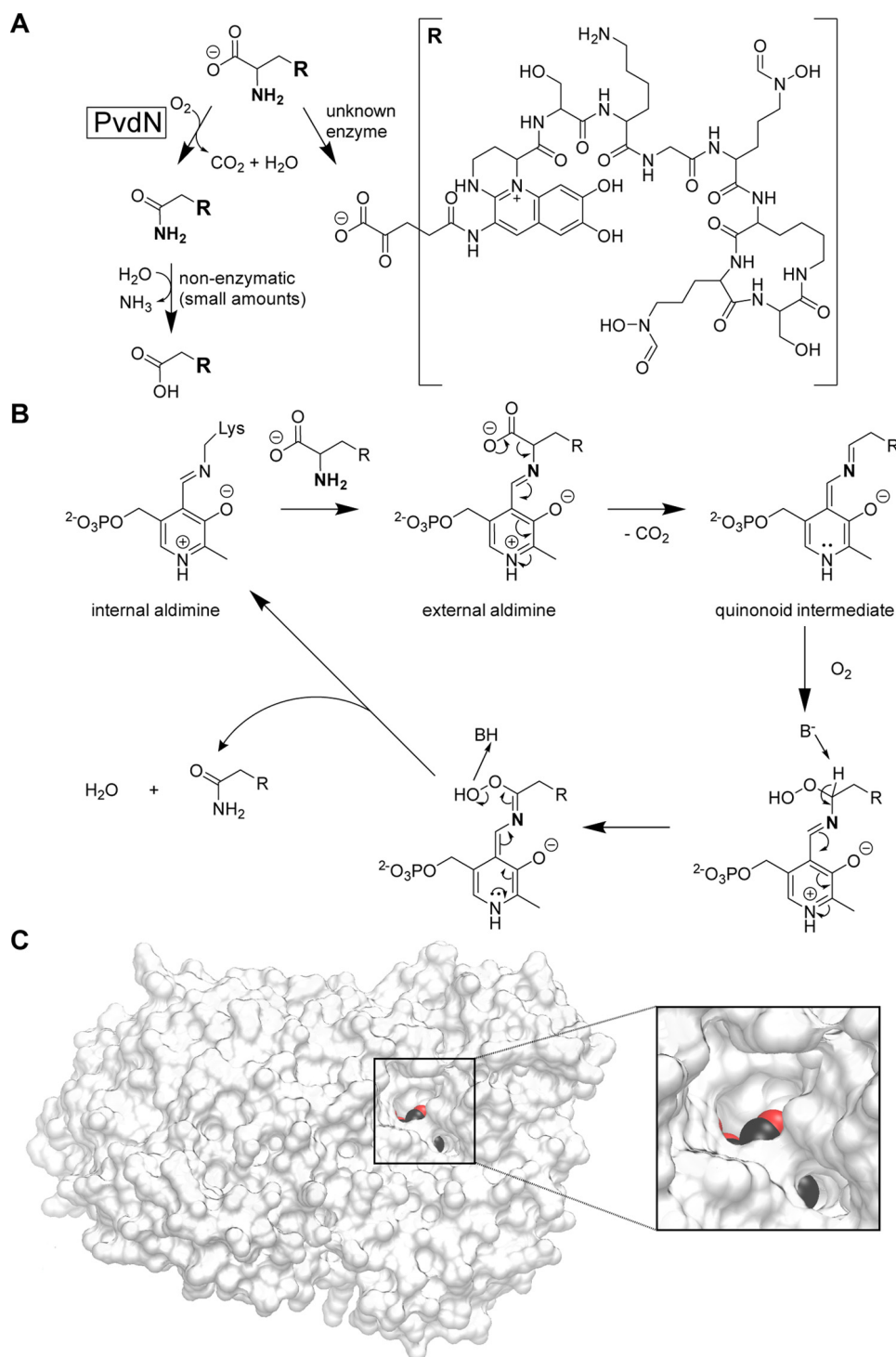


FIGURE 7. **Role and putative mechanism of PvdN catalysis in the biosynthesis of pyoverdines.** *A*, branched modification pathway of the side chains at the N3-position of the pyoverdine fluorophore. *B*, likely mechanism of PvdN-catalyzed PLP-dependent oxidative decarboxylation under retention of the amine nitrogen. See "Results" for details. *C*, as expected for the proposed model, two channels connect the PLP-containing active site cavity with the surface. PLP atoms are colored to visualize the channels, which both lead to the reactive side of the cofactor. For this figure, PvdN of *P. fluorescens* A506 was homology-modeled using the available PvdN structure (PDB5i90; ~62% sequence identity; global model quality estimation (GMQE) 0.79 (44–46)) as template. The image was generated using the VMD software (47).

formation procedure for pseudomonads (22). Additionally, we included an overnight culture step in 5 ml of LB medium after transformant selection on kanamycin plates, which were then diluted 1:1000 before plating 50 μ l on 10% (w/v) sucrose counter-selection plates. All incubation steps were carried out at

30 °C. The deletions were confirmed by colony PCR and sequencing of the PCR product.

For complementation of the deletion strain, *pvdN* was precloned via PCR into the vector pEXH5 (34), adding a *Strep*-tag with the reverse primer. From there, the gene was cloned into

Extraction of pyoverdine was performed with Amberlite XAD-4 resin as described previously (43) with minor modifications. Briefly, the culture was centrifuged at $20,000 \times g$ at 4°C for 30 min and subsequently sterile-filtered through $0.2\text{-}\mu\text{m}$ filters. The pH was adjusted to pH 6.0, and 20 g/liter XAD-4 were added. The mixture was incubated for 3 h at 4°C under constant stirring. Thereafter, the XAD-4 resin was filtered and resuspended in half of the original volume of pure (>18 megahms) water. The mixture was stirred for 1 h at 4°C . Successively, the XAD-4 resin was filtered and resuspended in a fifth of the original volume of 15% (v/v) methanol and incubated at 4°C under constant stirring for 15 min. Consequently, the XAD-4 resin was filtered again, resuspended in 15% of the original volume of 50% (v/v) methanol, and incubated at 4°C under constant stirring for 1 h. Thereafter, the XAD-4 resin was removed by filtration, and the filtrate was reduced to dryness *in vacuo*, never heating the liquid above 25°C . The dried extract was stored at 4°C and then dissolved in pure water for MS or IEF analysis. The dissolved substance was stored at -20°C .

LC-MS analysis was performed using a Q-ToF Premier mass spectrometer (Waters, Eschborn, Germany) equipped with a LockSprayTM unit, an electrospray ionization source (3-kV capillary voltage, 30-V sampling cone voltage, 250°C nitrogen gas at a flow of 650 liters/h), and an ACQUITY UPLC (Waters). Separation was performed on a Waters ACQUITY UPLC HSS T3 column ($1.8\ \mu\text{m}$, 2.1×100 mm) using the following linear gradient of solvent A (double-distilled water with 0.1% (v/v) formic acid) and solvent B (acetonitrile with 0.1% (v/v) formic acid) at a flow of 0.4 ml/min: 10% B (0 min), 90% B (10 min), 90% B (13.00 min), 10% B (13.10 min), 10% B (15 min).

To characterize the produced pyoverdines, we carried out the Csáky assay (16), the Arnow assay (17), and the ferric perchlorate assay as described previously (18). Furthermore, we recorded absorption and emission spectra with the Jasco V-650 spectrophotometer and the Jasco FP-6500 spectrofluorometer (Jasco), respectively, with and without the addition of 1 mM FeCl_3 . To qualitatively estimate the produced amount of pyoverdine, 3 ml of the culture were centrifuged at $16,000 \times g$ for 2 min. 2 ml of the supernatant were adjusted to pH 8.0 by adding 50 mM HEPES, pH 8.0, from a 1 M stock solution. Thereafter, absorption spectra were recorded with the Jasco V-650 spectrophotometer (Jasco). All previously mentioned assays were performed on culture supernatant without further workup. To further characterize the pyoverdines, the XAD-4-extracted samples were subjected to IEF electrophoresis with subsequent chrome azurol S overlay detection as described previously (13) with minor modifications. Briefly, the sample amount was normalized to an absorption at 400 nm of ~ 0.1 , utilizing the NanoDrop 2000 spectrophotometer (Thermo Scientific). For IEF electrophoresis, we employed vertical precast SERVAGelTM IEF 3-10 gels with 12 wells (SERVA Electrophoresis, Heidelberg, Germany) together with an SE260 Mighty Small II Deluxe Mini vertical electrophoresis unit (Hofer, Holliston, MA), an EPS 601 electrophoresis power supply (GE Healthcare), and a MultiTemp III cooling system (GE Healthcare). For IEF analysis, we used $35\ \mu\text{l}$ of sample premixed with the appropriate loading buffer. The IEF gels were run with the cooling set to 4°C with voltage settings according to the man-

ufacturer's instructions, except that the electrophoresis time at 200 V was extended to 3 h. The gels were imaged immediately after running with the MF-ChemiBIS 4.2 imaging system (DNR Bio-Imaging Systems) with top UV lamps turned on. The CAS overlay solution was always prepared fresh from stock solutions, and 30 ml were poured into a $10 \times 10\text{-cm}$ Petri dish (Sarstedt, Nümbrecht, Germany). When the CAS overlay solution had solidified, the IEF gels were wetted with pure water and placed on top of the cast gel. The incubation time was adjusted until bands were visible in the CAS overlay solution (~ 5 min). The CAS assay was imaged with the same lamp settings as the IEF gels.

Author Contributions—M. T. R. performed the experiments, contributed to the preparation of the figures, and analyzed the data together with T. B. G. D. performed the MS analyses. T. B. conceived and coordinated the study, and T. B. and M. T. R. wrote the paper. All authors reviewed the results and approved the final version of the manuscript.

Acknowledgments—We thank Joyce E. Loper for kindly providing the strain *P. fluorescens* A506, Jens Boch for the kind gift of the plasmid *pK18mobsacB*, Guido V. Bloemberg for kindly providing the plasmid *pME6010*, and Andreas Kirschning for fruitful discussions. We thank Sybille Traupe for technical support.

References

- Gessard, M. C. (1892) Sur la fonction fluorescigène des microbes. *Ann. Inst. Pasteur* **4**, 88–102
- Turfit, G. E. (1937) Bacteriological and biochemical relationships in the *pyocyaneus-fluorescens* group: Investigations on the green fluorescent pigment. *Biochem. J.* **31**, 212–218
- Turfit, G. E. (1936) Bacteriological and biochemical relationships in the *pyocyaneus-fluorescens* group: The chromogenic function in relation to classification. *Biochem. J.* **30**, 1323–1328
- Cézard, C., Farvacques, N., and Sonnet, P. (2015) Chemistry and biology of pyoverdines, *Pseudomonas* primary siderophores. *Curr. Med. Chem.* **22**, 165–186
- Drake, E. J., and Gulick, A. M. (2011) Structural characterization and high-throughput screening of inhibitors of PvdQ, an NTN hydrolase involved in pyoverdine synthesis. *ACS Chem. Biol.* **6**, 1277–1286
- Yeterian, E., Martin, L. W., Guillon, L., Journet, L., Lamont, I. L., and Schalk, I. J. (2010) Synthesis of the siderophore pyoverdine in *Pseudomonas aeruginosa* involves a periplasmic maturation. *Amino Acids* **38**, 1447–1459
- Hannauer, M., Schäfer, M., Hoegy, F., Gizzi, P., Wehrung, P., Mislin, G. L. A., Budzikiewicz, H., and Schalk, I. J. (2012) Biosynthesis of the pyoverdine siderophore of *Pseudomonas aeruginosa* involves precursors with a myristic or a myristoleic acid chain. *FEBS Lett.* **586**, 96–101
- Nadal-Jimenez, P., Koch, G., Reis, C. R., Muntendam, R., Raj, H., Jeronimus-Stratingh, C. M., Cool, R. H., and Quax, W. J. (2014) PvdP is a tyrosinase that drives maturation of the pyoverdine chromophore in *Pseudomonas aeruginosa*. *J. Bacteriol.* **196**, 2681–2690
- Ochsner, U. A., Wilderman, P. J., Vasil, A. I., and Vasil, M. L. (2002) GeneChip[®] expression analysis of the iron starvation response in *Pseudomonas aeruginosa*: identification of novel pyoverdine biosynthesis genes. *Mol. Microbiol.* **45**, 1277–1287
- Lamont, I. L., and Martin, L. W. (2003) Identification and characterization of novel pyoverdine synthesis genes in *Pseudomonas aeruginosa*. *Microbiology* **149**, 833–842
- Voulhoux, R., Filloux, A., and Schalk, I. J. (2006) Pyoverdine-mediated iron uptake in *Pseudomonas aeruginosa*: the Tat system is required for PvdN but not for FpvA transport. *J. Bacteriol.* **188**, 3317–3323

12. Drake, E. J., and Gulick, A. M. (2016) 1.2 Å resolution crystal structure of the periplasmic aminotransferase PvdN from *Pseudomonas aeruginosa*. *Acta Crystallogr. F Struct. Biol. Commun.* **72**, 403–408
13. Koedam, N., Wittouck, E., Gaballa, A., Gillis, A., Höfte, M., and Cornelis, P. (1994) Detection and differentiation of microbial siderophores by isoelectric focusing and chrome azurol S overlay. *Biometals* **7**, 287–291
14. Meyer, J. M. (2000) Pyoverdines: pigments, siderophores and potential taxonomic markers of fluorescent *Pseudomonas* species. *Arch. Microbiol.* **174**, 135–142
15. Schäfer, H., Taraz, K., and Budzikiewicz, H. (1991) [On the genesis of the dicarboxylic acids bound amidically to the chromophore of the pyoverdins] *Z. Naturforsch. C* **46**, 398–406
16. Csáky, T. Z., Hassel, O., Rosenberg, T., Lång, S., Turunen, E., and Tuhkanen, A. (1948) On the estimation of bound hydroxylamine in biological materials. *Acta Chem. Scand.* **2**, 450–454
17. Arnow, L. E. (1937) Colorimetric determination of the components of 3,4-dihydroxyphenylalanine-tyrosine mixtures. *J. Biol. Chem.* **118**, 531–537
18. Payne, S. M. (1994) Detection, isolation, and characterization of siderophores. *Methods Enzymol.* **235**, 329–344
19. Meyer, J. M., and Abdallah, M. A. (1978) The fluorescent pigment of *Pseudomonas fluorescens*: biosynthesis, purification and physicochemical properties. *J. Gen. Microbiol.* **107**, 319–328
20. Cox, C. D., and Adams, P. (1985) Siderophore activity of pyoverdine from *Pseudomonas aeruginosa*. *Infect. Immun.* **48**, 130–138
21. Kvitko, B. H., and Collmer, A. (2011) Construction of *Pseudomonas syringae* pv. tomato DC3000 mutant and polymutant strains. *Methods Mol. Biol.* **712**, 109–128
22. Choi, K.-H., Kumar, A., and Schweizer, H. P. (2006) A 10-min method for preparation of highly electrocompetent *Pseudomonas aeruginosa* cells: application for DNA fragment transfer between chromosomes and plasmid transformation. *J. Microbiol. Methods* **64**, 391–397
23. Schäfer, A., Tauch, A., Jäger, W., Kalinowski, J., Thierbach, G., and Pühler, A. (1994) Small mobilizable multi-purpose cloning vectors derived from the *Escherichia coli* plasmids pK18 and pK19: selection of defined deletions in the chromosome of *Corynebacterium glutamicum*. *Gene* **145**, 69–73
24. Hartney, S. L., Mazurier, S., Girard, M. K., Mehnaz, S., Davis, E. W., 2nd, Gross, H., Lemanceau, P., and Loper, J. E. (2013) Ferric-pyoverdine recognition by Fpv outer membrane proteins of *Pseudomonas protegens* Pf-5. *J. Bacteriol.* **195**, 765–776
25. Jansonius, J. N. (1998) Structure, evolution and action of vitamin B₆-dependent enzymes. *Curr. Opin. Struct. Biol.* **8**, 759–769
26. Nadal Jimenez, P., Koch, G., Papaioannou, E., Wahjudi, M., Krzeslak, J., Coenye, T., Cool, R. H., and Quax, W. J. (2010) Role of PvdQ in *Pseudomonas aeruginosa* virulence under iron-limiting conditions. *Microbiology* **156**, 49–59
27. Matsui, D., Oikawa, T., Arakawa, N., Osumi, S., Lausberg, F., Stäbler, N., Freudl, R., and Eggeling, L. (2009) A periplasmic, pyridoxal-5'-phosphate-dependent amino acid racemase in *Pseudomonas taetrolens*. *Appl. Microbiol. Biotechnol.* **83**, 1045–1054
28. Richter, S., Lindenstrauss, U., Lücke, C., Bayliss, R., and Brüser, T. (2007) Functional Tat transport of unstructured, small, hydrophilic proteins. *J. Biol. Chem.* **282**, 33257–33264
29. Nurizzo, D., Halbig, D., Sprenger, G. A., and Baker, E. N. (2001) Crystal structures of the precursor form of glucose-fructose oxidoreductase from *Zymomonas mobilis* and its complexes with bound ligands. *Biochemistry* **40**, 13857–13867
30. Ma, X., and Cline, K. (2010) Multiple precursor proteins bind individual Tat receptor complexes and are collectively transported. *EMBO J.* **29**, 1477–1488
31. Wang, M., Zhao, Q., Zhang, Q., and Liu, W. (2016) Differences in PLP-dependent cysteinyl processing lead to diverse S-functionalization of lincosamide antibiotics. *J. Am. Chem. Soc.* **138**, 6348–6351
32. Ochser, U. A., Snyder, A., Vasil, A. I., and Vasil, M. L. (2002) Effects of the twin-arginine translocase on secretion of virulence factors, stress response, and pathogenesis. *Proc. Natl. Acad. Sci. U.S.A.* **99**, 8312–8317
33. Higuchi, R., Krummel, B., and Saiki, R. (1988) A general method of *in vitro* preparation and specific mutagenesis of DNA fragments: study of protein and DNA interactions. *Nucleic Acids Res.* **16**, 7351–7367
34. Brüser, T., Deutzmann, R., and Dahl, C. (1998) Evidence against the double-arginine motif as the only determinant for protein translocation by a novel Sec-independent pathway in *Escherichia coli*. *FEMS Microbiol. Lett.* **164**, 329–336
35. Heeb, S., Itoh, Y., Nishijyo, T., Schneider, U., Keel, C., Wade, J., Walsh, U., O'Gara, F., and Haas, D. (2000) Small, stable shuttle vectors based on the minimal pVS1 replicon for use in gram-negative, plant-associated bacteria. *Mol. Plant Microbe Interact.* **13**, 232–237
36. Petersen, T. N., Brunak, S., von Heijne, G., and Nielsen, H. (2011) SignalP 4.0: discriminating signal peptides from transmembrane regions. *Nat. Methods* **8**, 785–786
37. Laemmli, U. K. (1970) Cleavage of structural proteins during the assembly of the head of bacteriophage T4. *Nature* **227**, 680–685
38. Burnette, W. (1981) "Western Blotting": electrophoretic transfer of proteins from sodium dodecyl sulfate-polyacrylamide gels to unmodified nitrocellulose and radiographic detection with antibody and radioiodinated protein A. *Anal. Biochem.* **112**, 195–203
39. Towbin, H., Staehelin, T., and Gordon, J. (1979) Electrophoretic transfer of proteins from polyacrylamide gels to nitrocellulose sheets: procedure and some applications. *Proc. Natl. Acad. Sci. U.S.A.* **76**, 4350–4354
40. Neuhoff, V., Arold, N., Taube, D., and Ehrhardt, W. (1988) Improved staining of proteins in polyacrylamide gels including isoelectric focusing gels with clear background at nanogram sensitivity using Coomassie Brilliant Blue G-250 and R-250. *Electrophoresis* **9**, 255–262
41. Ize, B., Viarre, V., and Voulhoux, R. (2014) Cell fractionation. *Methods Mol. Biol.* **1149**, 185–191
42. Ojha, S., Wu, J., LoBrutto, R., and Banerjee, R. (2002) Effects of heme ligand mutations including a pathogenic variant, H65R, on the properties of human cystathionine β-synthase. *Biochemistry* **41**, 4649–4654
43. Meyer, J. M., Stintzi, A., De Vos, D., Cornelis, P., Tappe, R., Taraz, K., and Budzikiewicz, H. (1997) Use of siderophores to type pseudomonads: the three *Pseudomonas aeruginosa* pyoverdine systems. *Microbiology* **143**, 35–43
44. Benkert, P., Biasini, M., and Schwede, T. (2011) Toward the estimation of the absolute quality of individual protein structure models. *Bioinformatics* **27**, 343–350
45. Biasini, M., Bienert, S., Waterhouse, A., Arnold, K., Studer, G., Schmidt, T., Kiefer, F., Gallo Cassarino, T., Bertoni, M., Bordoli, L., and Schwede, T. (2014) SWISS-MODEL: modelling protein tertiary and quaternary structure using evolutionary information. *Nucleic Acids Res.* **42**, W252–W258
46. Arnold, K., Bordoli, L., Kopp, J., and Schwede, T. (2006) The SWISS-MODEL workspace: a web-based environment for protein structure homology modelling. *Bioinformatics* **22**, 195–201
47. Humphrey, W., Dalke, A., and Schulten, K. (1996) VMD: visual molecular dynamics. *J. Mol. Graph.* **14**, 33–38, 27–28

3.2. The periplasmic transaminase PtaA of *Pseudomonas fluorescens* converts the glutamic acid residue at the pyoverdine fluorophore to α -ketoglutaric acid

Authors: Michael T. Ringel¹, Gerald Dräger², and Thomas Brüser¹

Affiliations: ¹Institute of Microbiology, Leibniz Universität Hannover, Herrenhäuser Straße 2, 30419 Hannover
²Institute of Organic Chemistry, Leibniz Universität Hannover, Schneiderberg 1 B, 30167 Hannover, Germany

Type of authorship: First author

Type of article: Original research article

Share of work: 90 %

Contribution: MTR performed the experiments, prepared the figures, and analyzed the data together with TB. GD performed the MS analyses. TB conceived and coordinated the study and TB and MTR wrote the paper.

Journal: Journal of Biological Chemistry

Impact factor (2016): 4.125

Date of publication: September 14th, 2017

Number of citations
(05.04.2018): 1

DOI: 10.1074/jbc.M117.812545

PMID: 28912270

The periplasmic transaminase PtaA of *Pseudomonas fluorescens* converts the glutamic acid residue at the pyoverdine fluorophore to α -ketoglutaric acid

Received for publication, August 15, 2017, and in revised form, September 13, 2017. Published, Papers in Press, September 14, 2017, DOI 10.1074/jbc.M117.812545

Michael T. Ringel[†], Gerald Dräger[§], and Thomas Brüser^{†,1}

From the [†]Institute of Microbiology, Leibniz Universität Hannover, Herrenhäuser Strasse 2, 30419 Hannover, Germany and the

[§]Institute of Organic Chemistry, Leibniz Universität Hannover, Schneiderberg 1 B, 30167 Hannover, Germany

Edited by F. Peter Guengerich

The periplasmic conversion of ferribactin to pyoverdine is essential for siderophore biogenesis in fluorescent pseudomonads, such as pathogenic *Pseudomonas aeruginosa* or plant growth-promoting *Pseudomonas fluorescens*. The non-ribosomal peptide ferribactin undergoes cyclizations and oxidations that result in the fluorophore, and a strictly conserved fluorophore-bound glutamic acid residue is converted to a range of variants, including succinamide, succinic acid, and α -ketoglutaric acid residues. We recently discovered that the pyridoxal phosphate-containing enzyme PvdN is responsible for the generation of the succinamide, which can be hydrolyzed to succinic acid. Based on this, a distinct unknown enzyme was postulated to be responsible for the conversion of the glutamic acid to α -ketoglutaric acid. Here we report the identification and characterization of this enzyme in *P. fluorescens* strain A506. *In silico* analyses indicated a periplasmic transaminase in fluorescent pseudomonads and other proteobacteria that we termed PtaA for “periplasmic transaminase A.” An in-frame-deleted *ptaA* mutant selectively lacked the α -ketoglutaric acid form of pyoverdine, and recombinant PtaA complemented this phenotype. The *ptaA/pvdN* double mutant produced exclusively the glutamic acid form of pyoverdine. PtaA is homodimeric and contains a pyridoxal phosphate cofactor. Mutation of the active-site lysine abolished PtaA activity and affected folding as well as Tat-dependent transport of the enzyme. In pseudomonads, the occurrence of *ptaA* correlates with the occurrence of α -ketoglutaric acid forms of pyoverdines. As this enzyme is not restricted to pyoverdine-producing bacteria, its catalysis of periplasmic transaminations is most likely a general tool for specific biosynthetic pathways.

Iron ions play important roles in all living organisms, but in many habitats their availability is limited due to low solubility of Fe(III) oxide hydrates (1). Pyoverdines are siderophores that permit growth of many pseudomonads under iron limitation. Examples include pathogenic *Pseudomonas aeruginosa* as well

as non-pathogenic or even plant-growth promoting *Pseudomonas fluorescens* strains (2). All pyoverdines originate from non-ribosomally synthesized peptides that are translocated into the periplasm where a quinoline fluorophore is formed (3, 4). The many known “fluorescent pseudomonads” produce a multitude of distinct pyoverdine variants that differ generally in the sequence of the peptide chain and the nature of a fluorophore-attached residue that is synthesized as a glutamic acid and usually converted to succinamide, succinic acid, or α -ketoglutaric acid and in rare cases to malamide and malic acid (4). While the formation of the fluorophore is known to depend on the activity of the periplasmic enzyme PvdP (5), the chemical modification of the glutamic acid that is amide-bonded to the fluorophore via its γ -carboxylic acid has long been puzzling.

We recently revealed that the periplasmic enzyme PvdN is responsible for the direct conversion of the glutamic acid to succinamide by a novel PLP²-catalyzed reaction (6). From these findings, it was concluded that there had to exist a yet unknown transaminase in the periplasm that should, in competition with the PvdN-catalyzed succinamide formation, convert the glutamic acid residue to α -ketoglutaric acid (6). Here we demonstrate that this enzyme indeed exists. Initially, we identified *in silico* a unique candidate that was predicted to possess all required characteristics. The cofactor content, transport, and quaternary structure of this enzyme were experimentally confirmed. We inactivated the corresponding gene by scarless in-frame deletion and showed that the α -ketoglutaric acid variant was indeed absent in the mutant strain, a phenotype that was fully complemented in *trans*. Further analyses indicate that in pseudomonads the occurrence of this transaminase correlates with α -ketoglutaric acid-containing pyoverdines. However, there is strong evidence for additional functions of this transaminase in the periplasm, which is why we term this enzyme “periplasmic transaminase A” (PtaA).

This work was supported by the German Science Foundation (Deutsche Forschungsgemeinschaft) GRK1798 “Signaling at the Plant-Soil Interface” and Project BR 2285/7-1. The authors declare that they have no conflicts of interest with the contents of this article.

This article contains supplemental Figs. S1 and S2.

¹ To whom correspondence should be addressed. Tel.: 49-511-762-5945; Fax: 49-511-762-5287; E-mail: brueser@ifmb.uni-hannover.de.

² The abbreviations used are: PLP, pyridoxal phosphate; CAS, chrome azurol S; EDDHA, ethylenediamine di(o-hydroxy)phenylacetic acid; IEF, isoelectric focusing; ONC, overnight culture; Tat, twin-arginine translocation; UPLC, ultra-performance liquid chromatography; PVD, pyoverdine; DSC, differential scanning calorimetry; SEC, size-exclusion chromatography; MALS-RI, multiangle light scattering/refractive index; CAA, casamino acid; a.m.u., atomic mass units.

Table 1**Potential Tat substrates in *P. fluorescens* A506**

Potential Tat substrates were identified with TATFIND v.1.4 (7) and classified using the InterPro web service (8, 9). ABC, ATP-binding cassette.

Locus tag	Classification
PflA506_0002 ^a	DNA polymerase III, β -chain
PflA506_0050	Gluconate 2-dehydrogenase subunit 3
PflA506_0159	Pectin lyase/hemagglutinin
PflA506_0418	Flavin-dependent halogenase
PflA506_0574	Leu/Ile/Val-binding protein/urea ABC transporter, substrate-binding protein UrtA-like
PflA506_0673	Acid phosphatase, AcpA
PflA506_0796	Alkaline phosphatase D-related/metallo-dependent phosphatase-like
PflA506_0832	Rieske iron--sulphur protein
PflA506_0959	Mannose-1-phosphate guanylyltransferase/mannose-6-phosphate isomerase
PflA506_1047	Multicopper oxidase (CumA)
PflA506_1182	Glucan biosynthesis, MdoD
PflA506_1897	Alkaline phosphatase D-related/metallo-dependent phosphatase-like
PflA506_2032 ^a	Hypothetical protein/no classification possible
PflA506_2213	Oxidoreductase molybdopterin-binding subunit, LorB-related
PflA506_2582	Deferrochelate/peroxidase EfeB
PflA506_2836	Periplasmic binding protein-like II/Aliphatic sulfonate-binding protein-related
PflA506_2902	Dienelactone hydrolase
PflA506_3071	Copper chaperone SCO1/SenC
PflA506_3083	PvdP (uncharacterized domain, dicopper center, tyrosinase family protein)
PflA506_3085	PvdN (aminotransferase class V domain)
PflA506_3359	Leucine-binding protein domain
PflA506_3490	Aldehyde oxidase/xanthine dehydrogenase, molybdopterin-binding
PflA506_3831	Copper-resistance protein CopA
PflA506_4010 ^a	3-Oxoacyl-[acyl-carrier-protein] synthase 2
PflA506_4424	Aminotransferase, class I/class II
PflA506_4509	Oxidoreductase, molybdopterin-binding domain (YedY)
PflA506_4922	Six-bladed β -propeller, TolB-like/protein of unknown function, DUF839
PflA506_5086	Hypothetical protein/no classification possible
PflA506_5390	N-Acetylmuramoyl-L-alanine amidase

^a This hit might represent a false positive in the opinion of the authors.

Results***In silico* prediction of a pyoverdine-modifying periplasmic transaminase in *P. fluorescens* A506**

Recent genetic and biochemical analyses of our model strain *P. fluorescens* A506 indicated the existence of a yet unknown periplasmic enzyme that converts the fluorophore-attached glutamic acid residue of its pyoverdine (PVD_{A506}) into α -keto-glutaric acid (6). We approached the identification of this enzyme initially by combining *in silico* tools, anticipating that the conversion should be carried out by a PLP-containing transaminase, and like the PLP-containing PvdN (6), this enzyme should be Tat-dependently transported into the periplasm.

A TATFIND v.1.4 analysis (7) predicted the presence of 29 putative Tat substrates in the proteome of *P. fluorescens* A506 of which three are most likely false positives. The functional annotation based on the InterPro web service (8, 9) indicated that two of these predicted Tat substrates were sequence-related to transaminases, namely PvdN and PflA506_4424 (Table 1). PvdN has been structurally and functionally characterized (6, 10). It contains a PLP cofactor and catalyzes the unusual amine-retaining oxidative decarboxylation of the fluorophore-attached glutamic acid residue of pyoverdine to succinamide. PvdN thus has already been demonstrated not to be involved in the searched-for transamination reaction. Therefore, the only remaining candidate was PflA506_4424, which we will hereafter term PtaA to avoid confusion and to facilitate reading.

To gain a better understanding of PtaA's properties, we searched all genomes contained in the *Pseudomonas* Genome Database (11) for homologs of PtaA. To reduce the bias by over-represented sequences within the identified homologs, we performed a redundancy reduction with an identity threshold of

0.95 utilizing the CD-HIT web service (12). Thereafter, the sequences were aligned using the T-Coffee web service (13), and the multiple sequence alignment was visualized as sequence logo with WebLogo 3 (14). From the results of these analyses, it can be inferred that Tat signal peptides are common in PtaA homologs (Fig. 1A). Additionally, the initial classification of PtaA by the InterPro web service (8, 9) allowed us to identify the active-site lysine residue Lys-224 in a highly conserved sequence pattern (TFSK(I/L)YG(M/L)AGAR), which is highlighted in the sequence logo (Fig. 1B). Furthermore, the InterPro predictions suggested that PtaA likely forms a homodimer.

PtaA is a periplasmic homodimeric enzyme that requires cytoplasmic cofactor assembly for folding and transport

To identify the predicted PLP cofactor, PtaA was overproduced in its mature form in *Escherichia coli* and purified as described under "Experimental procedures." By means of a PLP binding assay, we removed the PLP cofactor from PtaA and detected the PLP oxime via its fluorescence (Fig. 2). The predicted periplasmic localization was addressed in complemented *P. fluorescens* mutant strains that were constructed for subsequent functional analyses (described below). We carried out an in-frame deletion of the gene encoding PtaA in the wild-type *P. fluorescens* A506 strain as well as in a Δ pvdN deletion strain that was generated previously (6). In *P. fluorescens* A506, the *ptaA* gene is flanked by genes encoding a predicted DNA-binding protein upstream in the opposite direction and a putative autoinducer-binding transcriptional regulator downstream in the same direction. The in-frame deletion removed the sequence from codons 5 to 357 of the coding region to avoid any potential polar effects.

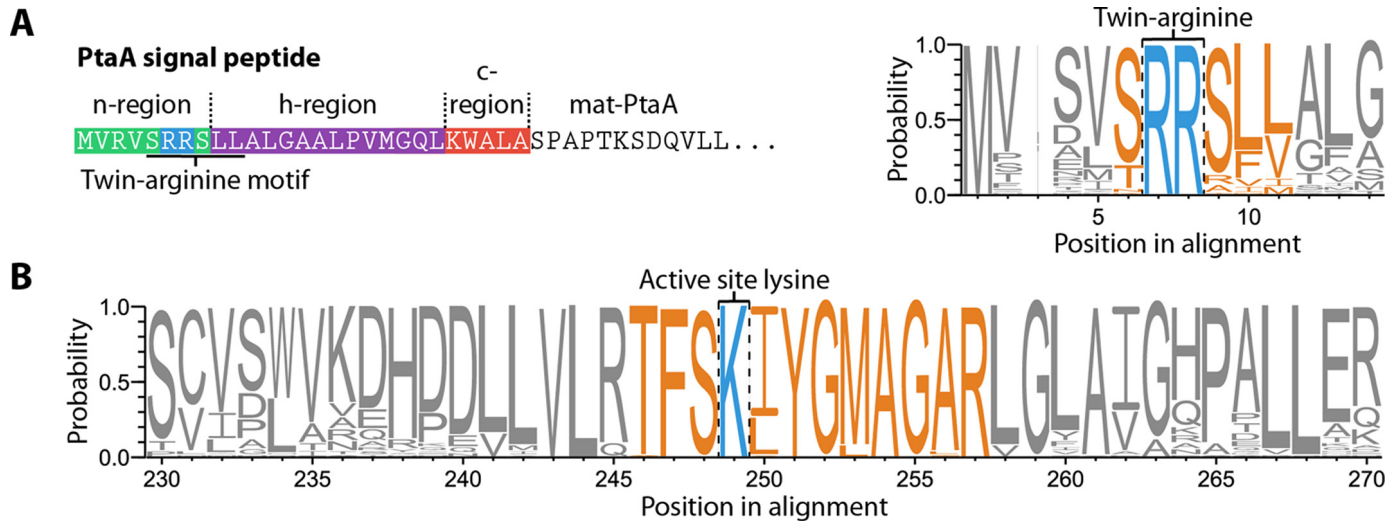


Figure 1. Analysis of the N-terminal Tat signal peptide of PtaA and its conserved PLP-binding site, the lysine residue Lys-224. A, depiction of the N-terminal Tat signal peptide of PtaA containing the eponymous twin-arginine motif (ZRRXΦΦ; Z denotes a polar amino acid, R is an L-arginine residue, X is any amino acid, and Φ is a hydrophobic amino acid; Ref. 30). Furthermore, a subsection of the sequence logo of the signal peptide region demonstrates the conserved twin-arginine motif. B, sequence logo of the active-site lysine, Lys-224, and the sequence in its vicinity. The process to generate the sequence logo is detailed under “Experimental procedures.”

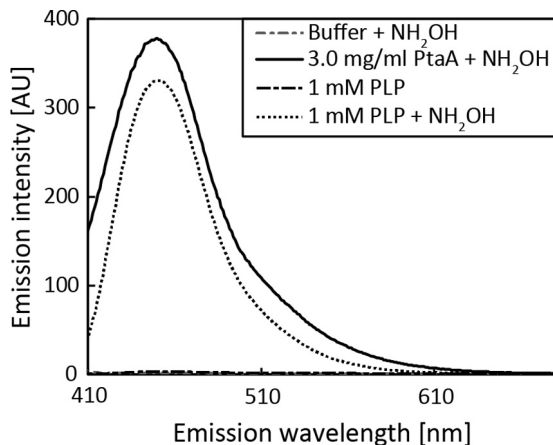


Figure 2. PLP binding assay. Shown are the fluorescence spectrum of the PLP oxime as generated by transimination with hydroxylamine with mature PtaA purified from *E. coli* (continuous line), the reference spectrum of the PLP oxime (dotted line), and buffer as well as PLP negative control spectra (dashed lines), indicating that PtaA binds PLP. Due to different sensitivity modes, spectra are to be qualitatively compared. AU, arbitrary units.

With the $\Delta ptaA$, $\Delta pvdN$, and $\Delta ptaA/\Delta pvdN$ strains in our hands, we constructed complementation vectors for recombinant production of functional PtaA or a PtaA(K224A) variant that is expected to abolish the PLP-dependent activity. The constructs were C-terminally tagged with a Strep-tag II to facilitate detection and purification.

Western blot detection in subcellular fractions proved that PtaA is indeed localized in the periplasmic fraction. Interestingly, the PtaA(K224A) variant accumulated in the membrane fraction, suggesting folding defects that are known to influence the efficiency and accuracy of Tat-dependent translocation (Ref. 15 and Fig. 3A). The precursor form still carrying the N-terminal signal peptide could be distinguished from the mature form in which the signal peptide was cleaved off. These observations were made with both the single- and the double-mutant strains. To examine whether folding defects were caused by the K224A exchange that could influence transport,

the protein was analyzed by differential scanning calorimetry (DSC) (Fig. 3C). The proteins used for this study were purified via affinity chromatography and subsequent size-exclusion chromatography (SEC). A Coomassie-stained SDS-PAGE gel of the purified proteins is depicted in Fig. 3B. The DSC data indicated that covalent PLP binding stabilized the overall protein structure to some extent since the unfolding transition temperature of the PtaA(K224A) variant was lowered from 70.8 to 69.0 °C in comparison with the wild-type PtaA. More importantly, a folded subdomain that gives rise to a minor peak at approximately 60 °C was almost absent in the PtaA(K224A) variant, which can be explained by a stabilization of the binding pocket in wild-type PtaA by the covalently attached PLP cofactor. To assess whether PtaA forms a homodimer, we analyzed the molecular size via SEC coupled with static multiangle light scattering/refractive index (MALS-RI) detectors as detailed under “Experimental procedures.” The experiment allowed us to calculate the approximate molecular mass from the data obtained (Fig. 3D). Since the size of mature monomeric PtaA and PtaA(K224A) (with the Strep-tag II) amounts to 37.3 and 37.2 kDa, respectively, the measured molecular masses of 73.2 ± 1.0 kDa for PtaA and 71.4 ± 1.1 kDa for PtaA(K224A) correlate well with the calculated molecular masses of the dimers when the influence of protein shape on MALS-derived values is considered. From these data, it can be concluded that both the wild-type PtaA and the PtaA(K224A) variant form homodimeric structures.

PtaA is not essential for the overall pyoverdine production and physiological function

The influence of the $\Delta ptaA$ deletion on formation/export of PVD_{A506} was assessed by means of a semiquantitative pyoverdine production assay (Fig. 4A). Furthermore, in the same assay, we included the analysis of $\Delta pvdN$ single- and $\Delta ptaA/\Delta pvdN$ double-deletion strains and the above mentioned in *trans* complementation systems in the analyses. The results obtained (Fig. 4A) demonstrate that the deletions do not affect

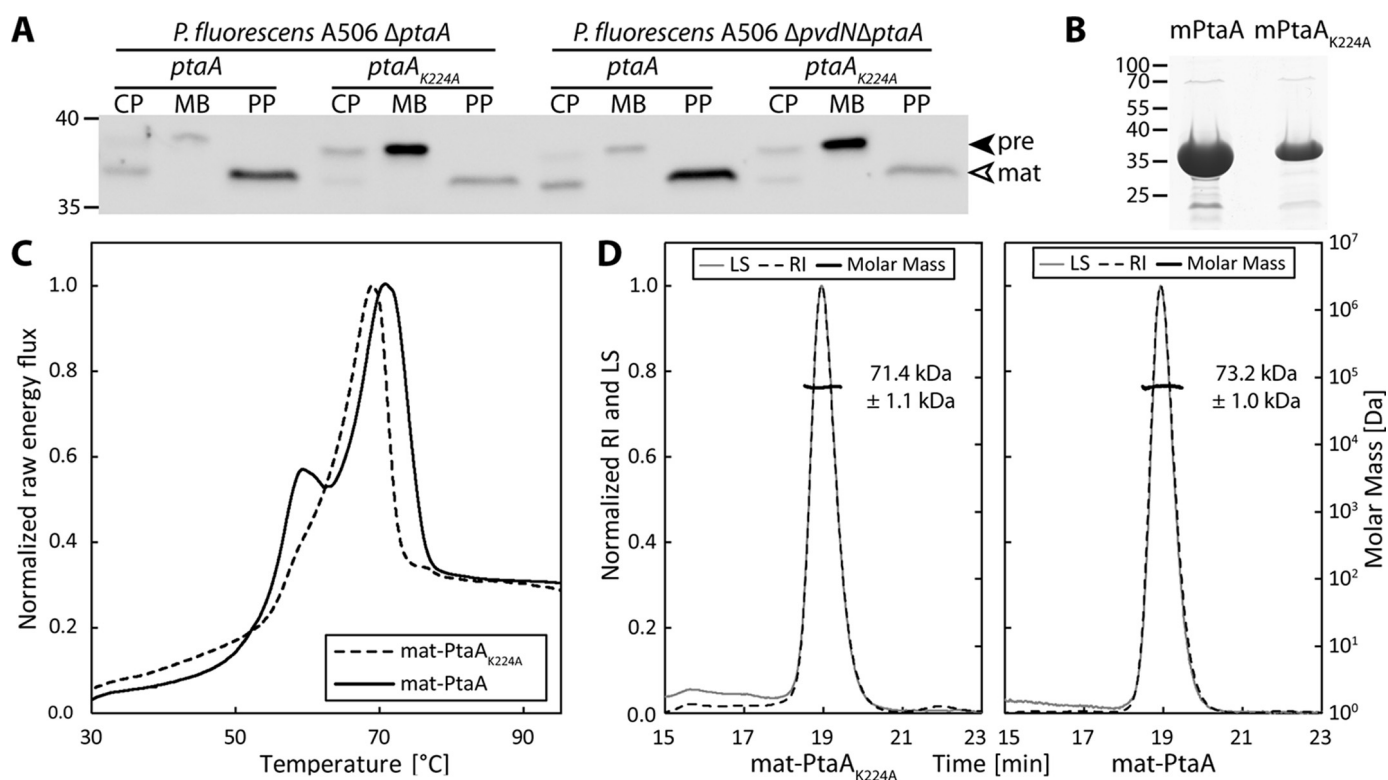


Figure 3. PtaA is periplasmically localized and forms a homodimer that is stabilized by covalent PLP binding. A, SDS-PAGE/Western blot analysis of subcellular fractions of *P. fluorescens* A506 deletion strains carrying plasmids for the production of the indicated C-terminally Strep-tagged PtaA variants. PtaA was detected using tag-specific antibodies. CP, cytoplasm; MB, membrane; PP, periplasm; pre, PtaA precursor; mat, mature PtaA. B, Coomassie stained SDS-PAGE gel of the purified mature PtaA (mPtaA) variants used for the DSC experiment depicted in C. C, DSC analysis of PtaA and PtaA(K224A). D, SEC-MALS-RI molecular mass determination of the indicated PtaA variants, indicating the dimeric structure of the enzyme. LS, light scattering; RI, refractive index. Data in C and D are normalized to the global maximum of the respective data set. In A and B, masses (in kDa) of standard proteins are indicated on the left.

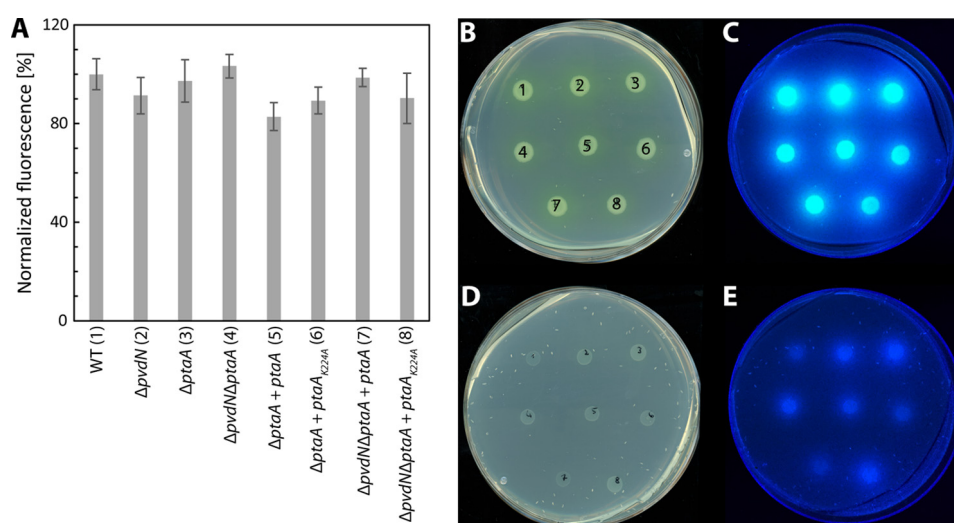


Figure 4. Semiquantitative pyoverdine production and iron binding assay for all *P. fluorescens* A506 strains used in this study. A, relative quantification of pyoverdine production in liquid culture, normalized to *P. fluorescens* A506 (WT) levels. The error bars indicate the standard deviation calculated from triplicates. B–E, droplet assays of all *P. fluorescens* A506 strains used in this study as indicated by numeric notation (1–8) in A. The incubation was performed either in the absence (B and C) or presence of EDDHA (D and E). The same plates were scanned (B and D), or fluorescence was detected on a UV table (C and E).

the overall pyoverdine production. Certainly, this type of assay did not differentiate between predicted differences in the side chain at the chromophore. To exclude that potential side-chain modifications impair iron affinity or pyoverdine import, iron binding and import were examined qualitatively by growth experiments (Fig. 4, B–E). In agreement with the

formation of functional siderophores, the mutant strains were able to grow similarly well on pyoverdine-inducing casamino acid (CAA) medium (Fig. 4, B and C), and even in the presence of 0.5 g/liter iron-depleting chelator ethylenediamine di(o-hydroxy)phenylacetic acid (EDDHA) (Fig. 4, D and E), growth was normal, indicating physiological sidero-

Periplasmic transamination of pyoverdines

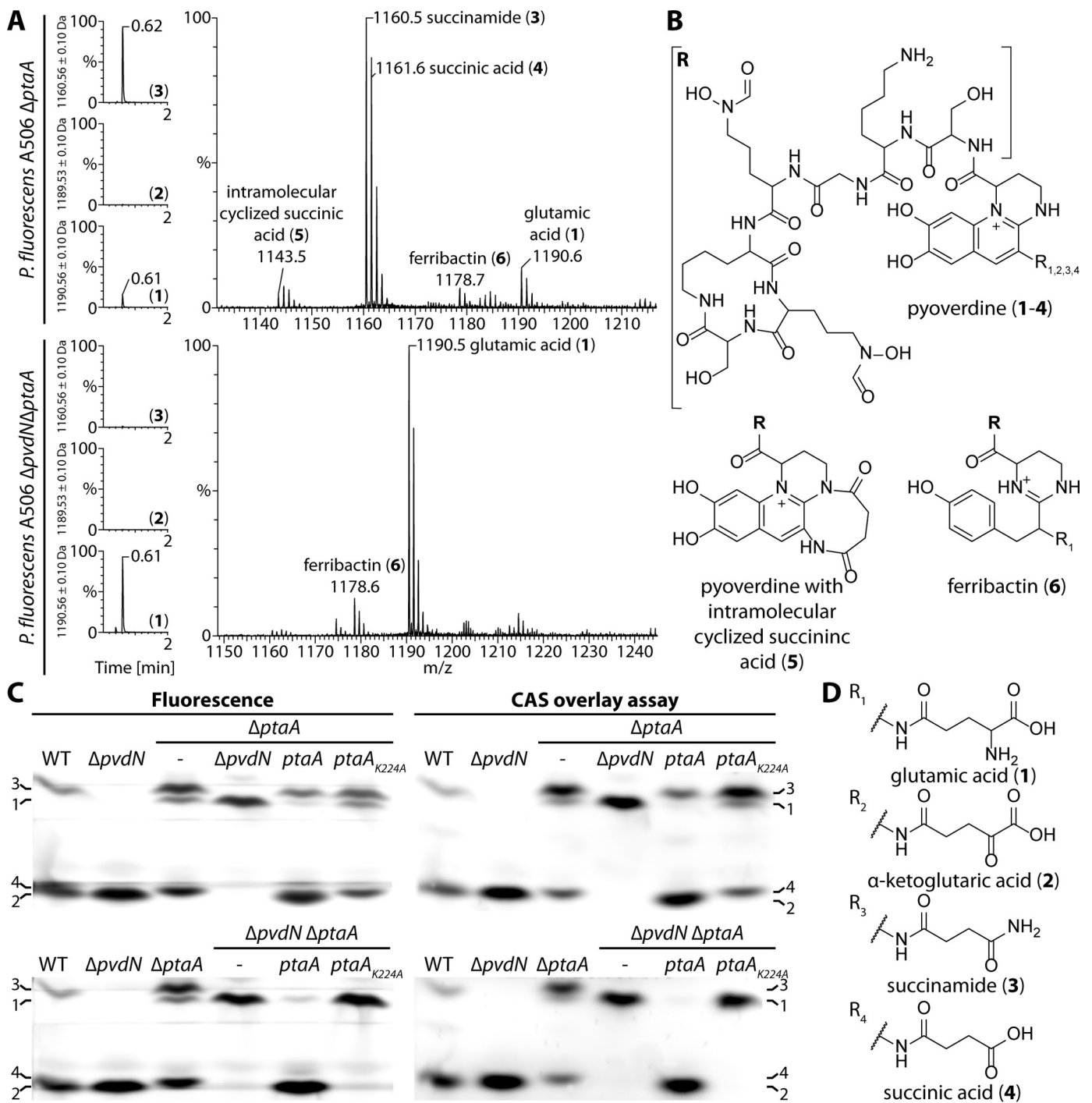


Figure 5. The enzyme PtaA is the periplasmic transaminase that converts the glutamic acid side chain of pyoverdine into the α -ketoglutaric acid variant. A, mass spectrometry results showing the UPLC chromatograms filtered for the masses of the succinamide, α -ketoglutaric acid, and glutamic acid variants on the left. On the right, the corresponding mass spectra of the peak at 0.6 min are depicted. The mass peaks were assigned to the structures shown in B and D. B, structure of the pyoverdine backbone, the intramolecular cyclized succinic acid variant, and the non-cyclized pyoverdine precursor ferribactin. The residues R_{1-4} correspond to the substructures shown in D. C, IEF gels visualized by pyoverdine fluorescence (left) and a CAS overlay assay (right). Numbers denote the identified pyoverdine variants, whose structures are represented in B in conjunction with D.

phore functionality of the pyoverdines produced in the mutant strains.

PtaA is the searched-for transaminase

To examine whether PtaA is responsible for the predicted side-chain modification, we isolated the pyoverdines from all strains and analyzed the molecular composition via ultraperfor-

mance liquid chromatography (UPLC)-coupled high-resolution mass spectrometry (HR-MS) and isoelectric focusing (IEF) gels in combination with the chrome azurol S (CAS) overlay assay. The results verified our hypothesis about the nature of the modification (Fig. 5, A–D). For convenience, the structures of all pyoverdine variants identified in this study are denoted in Fig. 5, B and D, and the assigned numbers 1–6 will be used to

unambiguously attribute the compounds discussed. The masses of compounds 1–6 were determined by HR-MS and compared with the calculated molecular masses (denoted in parentheses) of the respective molecules: 1, 1190.544 atomic mass units (a.m.u.) (1190.544 a.m.u.); 2, 1189.510 a.m.u. (1189.513 a.m.u.); 3, 1160.534 a.m.u. (1160.534 a.m.u.); 4, 1161.520 a.m.u. (1161.518 a.m.u.); 5, 1143.507 a.m.u. (1143.507 a.m.u.); 6, 1178.581 a.m.u. (1178.581 a.m.u.).

To analyze whether the identified structures were truly distinct molecules and not artifacts of MS (e.g. dehydrations), we used a shallower gradient for elution and could thereby prove that all compounds have a distinct elution profile (supplemental Fig. S1). From the MS results, it was obvious that, in the absence of PtaA, no α -ketoglutaric acid variant (2) of PVD_{A506} was produced (Fig. 5A). The equilibrium between the side-chain modifications was clearly shifted in favor of the succinamide variant (3) of PVD_{A506}. Additionally, the unmodified glutamic acid precursor (1) of PVD_{A506} was detectable, indicating an incomplete turnover by PvdN. It should be noted that further pyoverdine species could be detected by MS, including the hydrolysis product of the succinamide variant, namely the succinic acid variant (4); traces of the intramolecular cyclization product thereof (5); and the non-cyclized pyoverdine precursor ferribactin (6). As expected from our previously published analysis of PvdN (6), the Δ *ptaA*/ Δ *pvdN* double-deletion strain produced neither the succinamide variant (3) or further derivatives thereof nor the α -ketoglutaric acid variant (2) of PVD_{A506}. Consequently, the only detectable variants were the fluorophore-containing precursor with the original glutamic acid residue (1) and its non-cyclized precursor ferribactin (6). To examine the validity of our MS data interpretation by an independent method, we performed IEF experiments in combination with the CAS overlay assay (Fig. 5C). The assignments of the bands are denoted on the sides of the images using the definitions given in Fig. 5D. The results obtained by IEF correlate well with the data obtained by MS. Noticeably, the wild-type strain produced an excess of the α -ketoglutaric acid variant (2), whereas the succinamide variant (3) was a minor side product. The Δ *pvdN* deletion strain did not produce the succinamide variant (3) anymore, and all pyoverdine was converted into the α -ketoglutaric acid variant (2) by PtaA. The Δ *ptaA* deletion strain in turn produced at least three variants of pyoverdine, namely the unmodified glutamic acid precursor (1), the succinamide variant (3), and the hydrolysis product thereof, the succinic acid variant (4). It should be noted that the lower band in the Δ *ptaA* strain could easily be mistaken for the α -ketoglutaric acid variant (2) due to its nearly identical pI, but the succinic acid variant (4) migrated slightly higher. Furthermore, in the Δ *ptaA*/ Δ *pvdN* double-deletion strain, no succinic acid variant (4) was present due to the lack of its precursor, the succinamide variant (3). This lane unambiguously clarifies the assignment of the closely migrating α -ketoglutaric acid (2) and succinic acid variants (4) of PVD_{A506}.

The Δ *ptaA* phenotype was entirely complemented in *trans* by the *ptaA* complementation strain, whereas the PtaA(K224A) variant did not complement the phenotype and was therefore inactive. This conclusion can be deduced from the comparison of the IEF pyoverdine band patterns of these strains with the

patterns obtained for the wild-type and the Δ *ptaA* deletion strains. The same holds true for the complementation of the Δ *ptaA*/ Δ *pvdN* double-deletion strains as the *in trans* complementation with *ptaA* resulted in the quantitative turnover of the glutamic acid precursor (1) to the α -ketoglutaric acid variant (2), whereas the strain with PtaA(K224A) produced only the unmodified glutamic acid precursor (1). Moreover, the CAS overlay assay indicated that the side-chain modifications did not alter the iron affinity of the pyoverdine variants as can be inferred from the identical band patterns in comparison with fluorescence imaging of the IEF gels (Fig. 4C).

Discussion

More than 30 years ago, an α -ketoglutaric acid was identified for the first time as an amide-bonded residue at the fluorophore of a pyoverdine in strains of *P. aeruginosa* and *P. fluorescens* (16, 17). Also the at that time already known succinamide (18) and succinic acid residues were detected at this position in those studies. Interestingly, pyoverdines of *P. aeruginosa* strains greatly differ in their peptide moiety but generally have the three above mentioned residues in common that are amidically attached to their fluorophore (19). Also a glutamic acid residue bound to the fluorophore via its γ -carboxylic acid was discovered at this position (20) as well as malamide (21), malic acid (22), and an intramolecular cyclized succinate (23). These variations of the pyoverdine are made in a species- and strain-specific manner (24). Based on the large variability of amino acid sequences and fluorophore-attached side chains, IEF-based siderotyping methods have been developed that use the strain-specific characteristics for systematic purposes (25).

The glutamic acid residue is always the first residue in ferribactins, initially discovered by Hohlneicher *et al.* (26). This glutamic acid residue is myristoylated for transport into the periplasm where it is deacylated by PvdQ (27–29). After formation of the fluorophore, it thus must be the glutamic acid residue that is initially present at this position, and the found succinamide, succinic acid, α -ketoglutaric acid, malamide, and malic acid residues must result from glutamic acid modifications.

Biochemistry of PtaA

It was clear from our recent study on PvdN (6) that an unknown enzyme had to be responsible for the formation of the α -ketoglutaric acid. Using *P. fluorescens* A506 as model organism, we have now identified PtaA as the periplasmic transaminase responsible for the formation of the α -ketoglutaric acid residue in PVD_{A506} (2). PtaA is a PLP-containing enzyme (Fig. 2) that is transported together with its covalently bound cofactor via the Tat pathway in a folded conformation (Fig. 3). The folded state is influenced by cofactor binding to position Lys-224 (Fig. 3C), which is most likely the reason for a partial mislocalization of the mutated protein in the membrane (Fig. 3A). A similar effect had been already observed with PvdN, which also requires PLP binding for Tat-dependent transport (6). In the case of PvdN, the exchange of the active-site Lys resulted even in a complete mislocalization of the enzyme in the mem-

Periplasmic transamination of pyoverdines

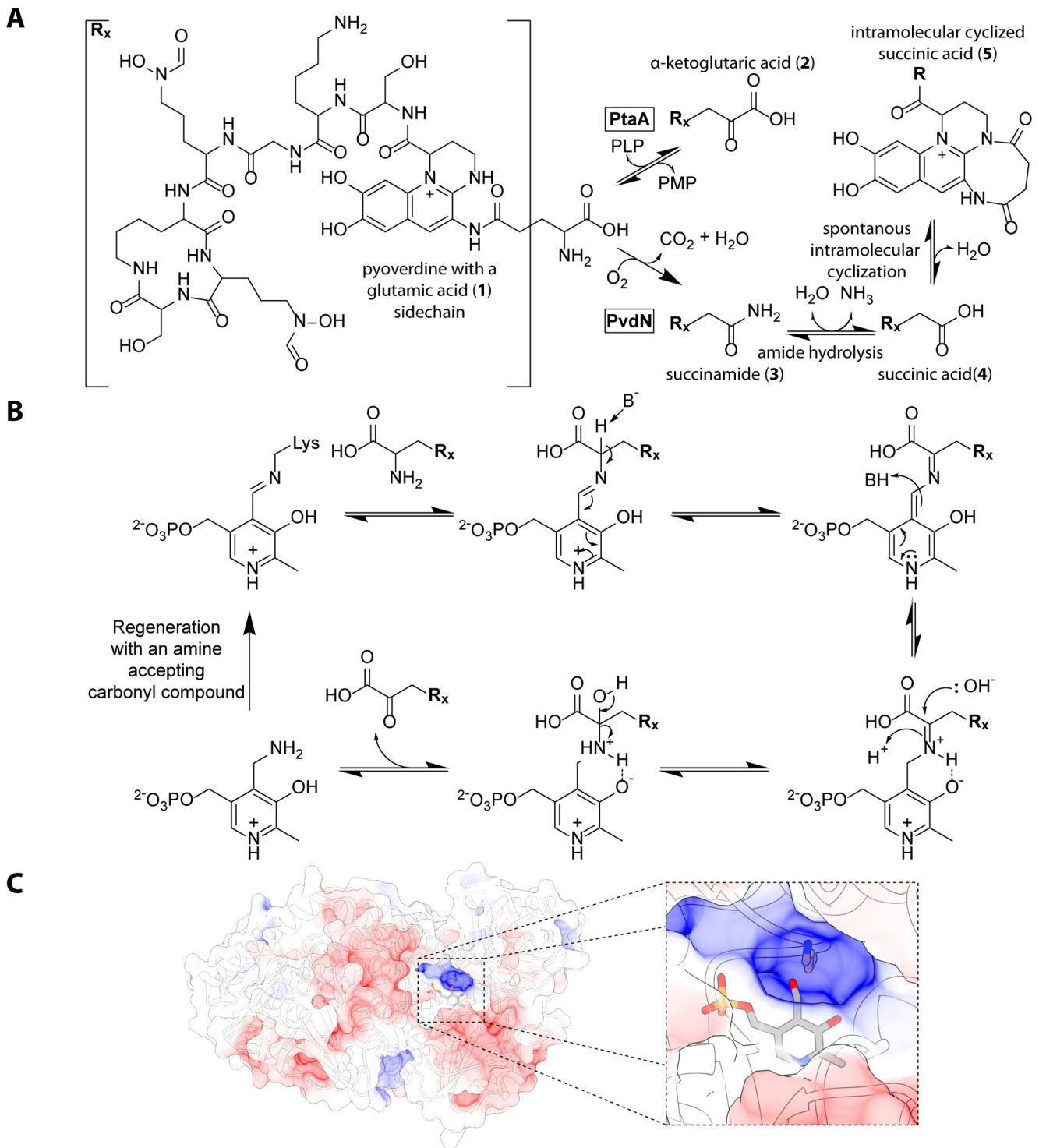


Figure 6. Role and mechanism of PtaA in periplasmic pyoverdine tailoring. A, beginning from the glutamic acid variant (1) of PVD_{A506r}, two competing tailoring pathways are present. Transamination by PtaA results in the α -ketoglutaric acid variant (2) PVD_{A506r}, whereas the PvdN modification results in the succinamide variant (3), which can be partially hydrolyzed to the succinic acid (4) and then intramolecularly cyclized (6). B, proposed mechanism of transamination as catalyzed by PtaA in the periplasm, postulating a carbonyl compound for regeneration of PLP. C, structure of PtaA as calculated by homology modeling, highlighting the Lys-224 residue and the PLP cofactor. The model was visualized with UCSF Chimera.

brane fraction (6). PvdN and PtaA are both homodimeric enzymes (Ref. 6 and Fig. 3D) with their PLP most likely bound close to the dimer interface (Ref. 6 and Fig. 6C). This class of enzymes includes therefore good examples for typical Tat substrates that need to be folded prior to translocation (30). They possess twin-arginine signal peptides that can be used for iden-

tification purposes in addition to transaminase sequence specifications (Fig. 1).

Fig. 6A summarizes the now established modifications of the fluorophore-attached glutamic acid residue of pyoverdines. The transamination probably proceeds via a standard transaminase mechanism, which is interesting to exist in the periplasm

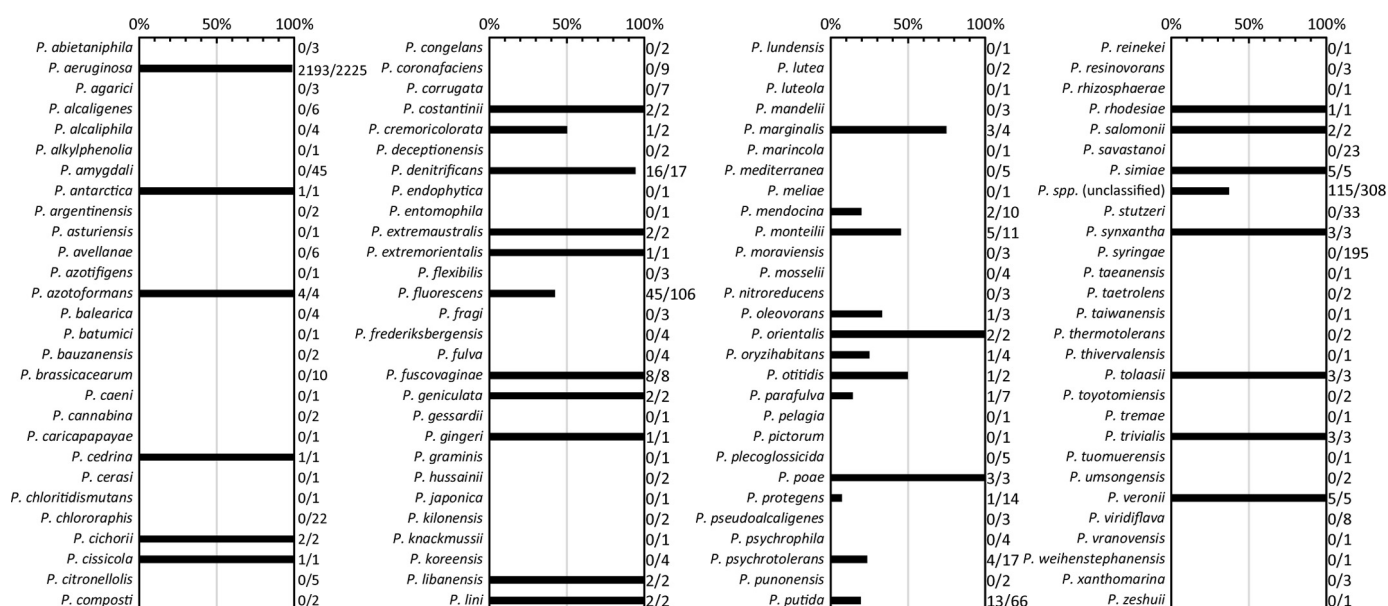


Figure 7. Distribution of PtaA homologs within the genus *Pseudomonas*. Shown is an evaluation of the distribution of PtaA within the genus *Pseudomonas*. Numbers to the right of the bar graph indicate the ratio between genomes positive for the presence of PtaA and the total number of analyzed genomes of the respective species.

as it requires a yet unknown periplasmic carbonyl compound that we postulate to exist (Fig. 6B). As the Tat transport and its PLP requirement indicate that PtaA assembles PLP inside the cytoplasm to fold to an active enzyme, PLP must be regenerated from PtaA-bound pyridoxamine inside the periplasm. The enzymes PvdN and PtaA are responsible for the initial conversions of the glutamic acid pyoverdine variant. The existence of these competing enzyme reactions explains the reported regulatory differences for the formation of succinamide and α -ketoglutaric acid forms of pyoverdine (31). As a side aspect, the glutamic acid variant of pyoverdine that is produced by the $\Delta ptaA/\Delta pvdN$ double mutant can be very helpful for drug delivery by “Trojan horse” antibiotics (32) because bulky side chains may be attached to this residue without affecting uptake (33). Malamide is likely formed by a hydroxylating enzyme acting on succinamide. The acids succinic acid and malic acid are hydrolysis products of their respective amides. A non-enzymatic hydrolysis has been observed and postulated to be responsible for the formation of these acids in cultures (34). It certainly might be that amidases contribute to the rates of these reactions.

PtaA, a transaminase for pyoverdines and other periplasmic compounds

In *P. aeruginosa* PAO1, the homolog of PtaA (53% sequence identity) is encoded by the locus PA2531, which is PvdS-dependently up-regulated in response to iron (35); hence this gene belongs to the regulon of PvdS, the σ factor that mediates pyoverdine production (36). An “iron starvation box” for PvdS binding (37) has been identified in the promoter region of PA2531 (35). We found the consensus box as described for *P. aeruginosa* PAO1 by Ochsner *et al.* (35) also in the *ptaA* promoter region of *P. fluorescens* A506, namely “TAAATN₁₆CGT.” However, the genetic context of *ptaA* is not conserved between *P. aeruginosa* PAO1 and *P. fluorescens*

A506. While the iron-responsive regulation of *ptaA* correlates with its function in pyoverdine modification, its usually *pvd*-unrelated genomic environment is suggestive for additional functions. This interpretation is further strengthened by a previous study on chorismate mutases that included the detection of transaminase activity in the periplasm of *P. aeruginosa* PAO1 (38). In that study, the periplasmic transaminase activity could be assigned to PA2531, the above mentioned PtaA homolog. PA2531 is dimeric just like PtaA from *P. fluorescens* in our study (Fig. 3D). At that time, the authors could not know about its role in pyoverdine modification, which is now clarified by our study. They used α -ketoglutaric acid and phenylalanine as substrates for the transaminase assay. Therefore, PtaA homologs cannot be highly specific for pyoverdine substrates and are likely to be involved in other conversions as well. In support of this conclusion, *ptaA* homologs are also present in some acidobacteria and α -proteobacteria, such as *Zymomonas mobilis* (supplemental Fig. S2), that do not produce any pyoverdines. Therefore, this periplasmic transaminase must be able to exert its function for distinct physiological purposes, possibly in conjunction with the generation of distinct secondary metabolites.

Distribution of PtaA among pseudomonads

As summarized in Fig. 7, we searched for *ptaA* homologs in all *Pseudomonas* genomes available in the *Pseudomonas* Genome Database (11) (see “Experimental procedures” for details). In agreement with the known occurrence of α -ketoglutaric acid forms of pyoverdines, we found this gene in almost all sequenced *P. aeruginosa* strains (2193 out of 2225 genomes; ~99%). The absence of hits in the ~1% of strains without this gene might be due to the inclusion of draft genomes in the analysis.

In the more diverse groups of *P. fluorescens* and *Pseudomonas putida* strains, only 45 out of 106 genomes and 13 out of 66 genomes, respectively, encode PtaA, suggesting that the presence of the α -ketoglutaric acid variant of pyoverdine is not

Periplasmic transamination of pyoverdines

Table 2

Primers used in this study

oePCR, overlap extension PCR.

Name	Sequence	Restriction site	Purpose
PfA506-4424-F1-MR PfA506-4424-R1-MR	ATAGCCGGATCC TAGACAGGTAGCGCCAAATCAGC AGGAGTAGTCACCATGGTGC GTGCACGCAAGTGGTCTGA TCAGGCGGCGCTATAGCTG	BamHI	Forward primer for <i>ptaA</i> left flanking region Reverse primer for <i>ptaA</i> left flanking region
PfA506-4424-F2-MR PfA506-4424-R2-MR PfA506-4424-DF-MR PfA506-4424-DR-MR PfA506-4424-F-MR	GACACGCACCATGGT GACTACTCCTTTG GGCCGCGAATTC TTTGTACAGATTCTTGATTTCCATCTTG TTTGAGTGTGCGCCTATTG CGCGCAATGCTGGTGAAGATATAG TCATCGCATATGGTGC GTGTCAGTCGTCGATCC	EcoRI NdeI	Forward primer for <i>ptaA</i> right flanking region Reverse primer for <i>ptaA</i> right flanking region <i>ptaA</i> genomic deletion control primer <i>ptaA</i> genomic deletion control primer Forward primer for cloning PtaA-coding region into pEXH5
PfA506-4424-strep-R-MR	GGCCGCAAGCTTTTACTTTTCGAACTGCGGGTGGCTCCAG ACCACCTGCGTCGCAAAGGCCCTCGC	HindIII	Reverse primer for cloning PtaA-coding region into pEXH5
PfA506-4424_K224A-F-MR PfA506-4424_K224A-R-MR PfA506-mat4424-F-MR	CTGGTGTGCGCACCTTCTCCGCCATCTAC CCGGCCATGCCGTAGATGGCCGAGAGGGTG GATATACATATGAGCCAGCCGACAAAATCTGACC	NdeI	Primer for K224A exchange by oePCR Primer for K224A exchange by oePCR Forward primer for cloning mature PtaA-coding region into pEXH5
pEXH5-RBS-F-MR	GGCGCGGGATCCGTTTAACTTTAAGAAGGAGATATAC	BamHI	Forward primer for subcloning from pEXH5 into pME6010
pEXH5-strep-term-HindIII-R-MR	CCCCTTAAGCTTAAAAAAAACCCCGCCCTGTCAGGGGGCGG GGTTTTTTTTTTTACTTTTCGAACTGCGGGTGGCTCC	HindIII	Reverse primer for subcloning from pEXH5 into pME6010

strictly conserved in these species. In agreement with this prediction, *P. fluorescens* Pf0-1 has no PtaA and, as expected, has been shown not to contain the α -ketoglutaric acid (24). On the contrary, there are strains that form α -ketoglutaric acid pyoverdine variants but not any succinamide/succinate variants (24), such as the genome-sequenced *P. putida* strain H8234. We found that this strain has a *pvdMO-ptaA* operon instead of the commonly found *pvdMNO* operon. Therefore, in the rarely found strains that do not possess the succinamide/succinic acid modification pathway, *ptaA* can be associated with the *pvd* gene cluster that encodes the periplasmic pyoverdine maturation enzymes. In conclusion, some *Pseudomonas* species with at least the exception of *P. aeruginosa* show the interesting characteristic of containing either only the PtaA pathway or only the PvdN pathway (39). Strains with both pathways acting in parallel also exist. We did not find a strain that produces pyoverdine without modifying its glutamic acid. The reason for the apparent requirement for such modifications is unknown and must be unrelated to iron affinity and uptake (Ref. 40 and Fig. 4). Future studies will have to clarify the exact functions of these modifications as well as the additional roles that PtaA can have in the periplasm of proteobacteria.

Experimental procedures

Strains and growth conditions

For physiological studies, *P. fluorescens* A506 was used. For cloning *E. coli* DH5 α λ *pir*⁺ and for expression *E. coli* Rosetta 2 (DE3) pLysSRARE2 were utilized. *P. fluorescens* A506 was cultivated at 30 °C, whereas *E. coli* strains were cultivated at 37 °C unless noted otherwise. The standard cultivation medium was LB (1% (w/v) tryptone, 1% (w/v) NaCl, 0.5% (w/v) yeast extract). If necessary, the appropriate antibiotics were added to the cultivation media at the following final concentrations: 100 μ g/ml ampicillin, 25 μ g/ml chloramphenicol, 50 μ g/ml kanamycin, and 20 μ g/ml tetracycline.

The production of pyoverdine and the pyoverdine plate assay, pertaining to *P. fluorescens* A506, were carried out as described previously (6). For relative pyoverdine quantification, 5-ml LB overnight cultures (ONCs) of *P. fluorescens* A506 were inoculated from cryocultures and incubated at 30 °C at 180 rpm

overnight. Thereafter, 50 of ml CAA medium (41) (5 g/liter casamino acids, 5 mM K₂HPO₄, 1 mM MgSO₄) precultures in 100-ml Erlenmeyer flasks with one baffle were inoculated with 50 μ l of the respective ONC and incubated for ~16 h at 30 °C and 180 rpm. 2 ml of the respective preculture were sedimented at 16,000 \times g for 2 min at room temperature and subsequently washed twice with 1.5 ml of CAA medium. Afterward, the OD₆₀₀ of the cell suspensions was adjusted to 1.0 with CAA medium, and for each sample three 4.5-ml CAA cultures (without antibiotics) were inoculated with 0.5 ml of the respective adjusted cell suspension. The cultures were then incubated overnight at 30 °C and 180 rpm. These cultures were sedimented by centrifugation at 3,260 \times g and 4 °C for 10 min in 15-ml screw-top plastic tubes. 2.7 ml of the supernatant were mixed with 300 μ l of a 1 M HEPES buffer, pH 8.0, and transferred into 1-cm acrylic cuvettes. The samples were measured with a Jasco FP-6500 spectrofluorometer using the following settings for acquisition: excitation at 405 nm, emission at 460 nm, bandwidth of 3 nm for both excitation and emission, and 0.5 s response time in “low-sensitivity” mode.

Genetic methods and plasmids

The construction of all scarless and markerless deletions in *P. fluorescens* A506 were performed as described previously (6). Furthermore, complementation and production vectors as well as constructs with single-point mutations (pME6010 and pEXH5 derivatives) were generated according to our previously published procedure (6). All primers used for cloning are listed in Table 2. Constructs were verified by restriction analysis and sequencing. *E. coli* DH5 α λ *pir*⁺ cells were rendered competent and transformed as described previously (42).

Biochemical methods

For analysis of subcellular fractionations and protein overexpression by SDS-PAGE, successive Western blotting, or in-gel colloidal Coomassie staining, standard protocols were used (43–46). Western blots were developed according to the manufacturer’s instructions using StrepMAB-Classic (IBA, Göttingen, Germany) as primary antibody and anti-mouse-HRP con-

jugate (Carl Roth, Karlsruhe, Germany) as secondary antibody. Images were acquired with the MF-ChemiBIS 4.2 imaging system (DNR Bio-Imaging Systems, Jerusalem, Israel).

The overproduction of mature PtaA and mature PtaA(K224A) was performed using *E. coli* Rosetta 2 (DE3) pLysSRARE2 as described previously (47) with minor modifications. Briefly, the respective construct was transformed into *E. coli* Rosetta 2 (DE3) pLysSRARE2 by the transformation and storage solution method (48). After recovery, the cells were spread on MDAG-11 plates (47) and incubated at 37 °C overnight. A 5-ml MDAG-135 (47) ONC was then inoculated with a single colony and incubated at 180 rpm and 37 °C. For overproduction, two 0.5-liter ZYM-5052 preheated (37 °C) autoinducer medium cultures (47) in 3-liter Erlenmeyer flasks with four baffles were each inoculated with 0.5 ml of the ONC. The cultures were incubated for 3 h at 200 rpm and 37 °C. Subsequently, the temperature was decreased to 30 °C, and the cultures were incubated for approximately 19 h at 200 rpm. The cells were harvested, and the respective protein was purified by means of four 1.5-ml gravity-flow Strep-Tactin[®]-Sephacrose columns (IBA) as described previously (6). The purified proteins were concentrated using Vivaspin[®] 6 concentrators with a cutoff of 10 kDa (Sartorius, Göttingen, Germany). For molecular weight determination, a Pharmacia FPLC (LKB Pump P-500, V-7 valve, 50- μ l sample loop) was connected to a size-exclusion chromatography column (Superdex 200 Increase 10/300 GL, GE Healthcare) coupled to MALS (miniDAWN TREOS, Wyatt Technology Europe GmbH, Dernbach, Germany) and refractive index detectors (Shodex RI-101, Showa Denko Europe GmbH, Munich, Germany). The flow rate of the mobile phase (PBS; 10 mM phosphate buffer, pH 7.4, 140 mM NaCl) was set to 0.75 ml/min. The chromatograms were recorded and analyzed with ASTRA 6.1 software (Wyatt Technology). For DSC, a NANO DSC in conjunction with a degassing station from TA Instruments (Lindon, UT) was used. For preparation of DSC samples, the protein elution peak (19-min retention time) from the SEC-MALS-RI system was collected by hand and subsequently concentrated with Vivaspin 6 concentrators (cutoff, 10 kDa). The protein concentration was determined using Roti[®]-Nanoquant according to the instruction manual (Carl Roth) using a SpectraMax M3 spectrophotometer (Molecular Devices, Biberach an der Riss, Germany). The protein of interest was diluted with degassed PBS to a concentration of \sim 1.5 mg/ml prior to analysis. The DSC reference cell was filled with degassed PBS. Analyses covered the temperature range from 20 to 110 °C at a heating rate of 1 °C/min with a 900-s pre-equilibration time at a constant pressure of 3 atm.

The subcellular fractionation of *P. fluorescens* A506 cultures was performed as described previously (49) with slight modifications. 50-ml cultures were grown to an OD₆₀₀ of 1 and fractionated into 1-ml fractions that were further analyzed without precipitation.

For PLP cofactor detection, a method modified from that of Ojha *et al.* (50) was used. The purified mature PtaA enzyme in 100 mM potassium phosphate buffer, pH 7.2, was treated with 5 mM hydroxylamine and incubated for \sim 72 h at 4 °C. The sample was loaded onto a Vivaspin 6 concentrator with 5-kDa cutoff, and the PLP oxime in the flow-through was detected at

446-nm emission (scan from 400 to 700 nm) with an excitation of 353 nm, 3-nm bandwidth for both excitation and emission, 0.2-s response time, and three accumulations in “high-sensitivity” mode using a Jasco FP-6500 spectrofluorometer. Reference solutions with the buffer only or with 1 mM PLP in the same buffer were treated identically. PLP- or PLP oxime-containing reference spectra were recorded with the same settings but in “medium-sensitivity” mode.

The extraction of pyoverdine, IEF analysis in conjunction with the CAS overlay assay, and UPLC-MS analysis were performed as described previously (6). To prove that the identified compounds are not artifacts of the MS, an adjusted linear gradient profile was utilized as follows: solvent A (double-distilled water with 0.1% (v/v) formic acid) and solvent B (acetonitrile with 0.1% (v/v) formic acid) at a flow rate of 0.6 ml/min; 2% B (0.0 min), 10% B (10.0 min), 90% B (10.5 min), 90% B (13.0 min), 2% B (13.5 min), and 2% B (20.0 min). The electrospray ionization voltage was set to 100 V, and the injection volume was 5 μ l. All other instrument parameters and all instrument hardware were identical to the method described previously (6) except that an ACQUITY UPLC Column Manager (Waters) was additionally installed on the instrument.

Bioinformatics methods

To perform an initial distribution analysis of PtaA within the genus *Pseudomonas*, we downloaded all amino acid sequences of all complete and draft genomic sequences from the *Pseudomonas* Genome Database (11) and used TATFIND v.1.4 (7) to search for potential Tat substrates. Subsequently, phmmer v3.1b (51) was used to search for PtaA homologs (cutoff, $1e-45$) within all potential Tat substrates. Then a taxonomy table reduced to species level was constructed by means of in-house developed software. Thereafter, the ratio between the total number of genomes of one species and the number of genomes of the same species carrying a potential PtaA homolog was calculated.

To construct the sequence logos, the sequence redundancy of all PtaA homologs was reduced by means of the CD-HIT algorithm contained in the CD-HIT Suite (12) using a similarity threshold of 0.95. Then the resulting sequences were aligned with the T-Coffee web server (13). The sequence alignment was subsequently visualized with WebLogo 3 (14) by plotting the probability of each amino acid at each alignment position. For further investigations into the distribution of PtaA homologs across other bacterial species, a profile hidden Markov model (pHMM) was generated from the multiple sequence alignment with hmmbuild v.3.1b (51). Then all available reference sequences were searched with the generated model (E-value cutoff, $1e-100$) using the HMMER web server (52, 53). The resulting sequences were then analyzed regarding their phylogenetic relationship using the Phylogeny.fr³ web service (54) in conjunction with the ETE toolkit (55) for visualization.

To initially predict the enzyme class and active-site lysine residue, Lys-224, the InterPro web service (8, 9) was used. The SWISS-MODEL web service (56) was used to model the struc-

³ Please note that the JBC is not responsible for the long-term archiving and maintenance of this site or any other third party-hosted site.

Periplasmic transamination of pyoverdines

ture of PtaA (template, Protein Data Bank code 3LY1), and UCSF Chimera (57) in conjunction with APBS (58) was used to visualize the structure of PtaA.

Author contributions—M. T. R. performed the experiments, prepared the figures, and analyzed the data together with T. B. G. D. performed the MS analyses. T. B. conceived and coordinated the study. T. B. and M. T. R. wrote the paper. All authors reviewed the results and approved the final version of the manuscript.

Acknowledgment—We thank Sybille Traupe for technical support.

References

- Andrews, S. C., Robinson, A. K., and Rodríguez-Quinones, F. (2003) Bacterial iron homeostasis. *FEMS Microbiol. Rev.* **27**, 215–237
- Cézard, C., Farvacques, N., and Sonnet, P. (2015) Chemistry and biology of pyoverdines, *Pseudomonas* primary siderophores. *Curr. Med. Chem.* **22**, 165–186
- Gulick, A. M. (2017) Nonribosomal peptide synthetase biosynthetic clusters of ESKAPE pathogens. *Nat. Prod. Rep.* **34**, 981–1009
- Schalk, I. J., and Guillon, L. (2013) Pyoverdine biosynthesis and secretion in *Pseudomonas aeruginosa*: implications for metal homeostasis. *Environ. Microbiol.* **15**, 1661–1673
- Nadal-Jimenez, P., Koch, G., Reis, C. R., Muntendam, R., Raj, H., Jeronimus-Stratingh, C. M., Cool, R. H., and Quax, W. J. (2014) PvdP is a tyrosinase that drives maturation of the pyoverdine chromophore in *Pseudomonas aeruginosa*. *J. Bacteriol.* **196**, 2681–2690
- Ringel, M. T., Dräger, G., and Brüser, T. (2016) PvdN enzyme catalyzes a periplasmic pyoverdine modification. *J. Biol. Chem.* **291**, 23929–23938
- Rose, R. W., Brüser, T., Kissinger, J. C., and Pohlschröder, M. (2002) Adaptation of protein secretion to extremely high-salt conditions by extensive use of the twin-arginine translocation pathway. *Mol. Microbiol.* **45**, 943–950
- Jones, P., Binns, D., Chang, H.-Y., Fraser, M., Li, W., McAnulla, C., McWilliam, H., Maslen, J., Mitchell, A., Nuka, G., Pesseat, S., Quinn, A. F., Sangrador-Vegas, A., Scheremetjew, M., Yong, S.-Y., et al. (2014) InterProScan 5: genome-scale protein function classification. *Bioinformatics* **30**, 1236–1240
- Finn, R. D., Attwood, T. K., Babbitt, P. C., Bateman, A., Bork, P., Bridge, A. J., Chang, H.-Y., Dosztányi, Z., El-Gebali, S., Fraser, M., Gough, J., Haft, D., Holliday, G. L., Huang, H., Huang, X., et al. (2017) InterPro in 2017—beyond protein family and domain annotations. *Nucleic Acids Res.* **45**, D190–D199
- Drake, E. J., and Gulick, A. M. (2016) 1.2 Å resolution crystal structure of the periplasmic aminotransferase PvdN from *Pseudomonas aeruginosa*. *Acta Crystallogr. F Struct. Biol. Commun.* **72**, 403–408
- Winsor, G. L., Griffiths, E. J., Lo, R., Dhillon, B. K., Shay, J. A., and Brinkman, F. S. (2016) Enhanced annotations and features for comparing thousands of *Pseudomonas* genomes in the *Pseudomonas* genome database. *Nucleic Acids Res.* **44**, D646–D653
- Huang, Y., Niu, B., Gao, Y., Fu, L., and Li, W. (2010) CD-HIT Suite: a web server for clustering and comparing biological sequences. *Bioinformatics* **26**, 680–682
- Di Tommaso, P., Moretti, S., Xenarios, I., Orobítz, M., Montanyola, A., Chang, J.-M., Taly, J.-F., and Notredame, C. (2011) T-Coffee: a web server for the multiple sequence alignment of protein and RNA sequences using structural information and homology extension. *Nucleic Acids Res.* **39**, W13–W17
- Crooks, G. E., Hon, G., Chandonia, J.-M., and Brenner, S. E. (2004) WebLogo: a sequence logo generator. *Genome Res.* **14**, 1188–1190
- Halbig, D., Wiegert, T., Blaudeck, N., Freudl, R., and Sprenger, G. A. (1999) The efficient export of NADP-containing glucose-fructose oxidoreductase to the periplasm of *Zymomonas mobilis* depends both on an intact twin-arginine motif in the signal peptide and on the generation of a structural export signal induced by cofactor binding. *Eur. J. Biochem.* **263**, 543–551
- Briskot, G., Taraz, K., and Budzikiewicz, H. (1986) Pyoverdine type siderophores from *Pseudomonas aeruginosa*. *Z. Naturforsch. C* **41**, 497–506
- Poppe, K., Taraz, K., and Budzikiewicz, H. (1987) Pyoverdine type siderophores from *Pseudomonas fluorescens*. *Tetrahedron* **43**, 2261–2272
- Teintze, M., Hossain, M. B., Barnes, C. L., Leong, J., and van der Helm, D. (1981) Structure of ferric pseudobactin: a siderophore from a plant growth promoting *Pseudomonas*. *Biochemistry* **20**, 6446–6457
- Meyer, J. M., Stintzi, A., De Vos D., Cornelis, P., Tappe, R., Taraz, K., and Budzikiewicz, H. (1997) Use of siderophores to type pseudomonads: the three *Pseudomonas aeruginosa* pyoverdine systems. *Microbiology* **143**, 35–43
- Geisen, K., Taraz, K., and Budzikiewicz, H. (1992) New pyoverdin type siderophores from *Pseudomonas fluorescens*. *Monatsh. Chem.* **123**, 151–178
- Yang, C. C., and Leong, J. (1984) Structure of pseudobactin 7SR1, a siderophore from a plant-deleterious *Pseudomonas*. *Biochemistry* **23**, 3534–3540
- Demange, P., Bateman, A., Mertz, C., Dell, A., Piémont, Y., and Abdallah, M. A. (1990) Bacterial siderophores: structures of pyoverdins Pt, siderophores of *Pseudomonas tolaasii* NCPPB 2192, and pyoverdins Pf, siderophores of *Pseudomonas fluorescens* CCM 2798. Identification of an unusual natural amino acid. *Biochemistry* **29**, 11041–11051
- Lenz, C., Amann, C., Briskot, G., Taraz, K., and Budzikiewicz, H. (2000) Succinopyoverdins—a new variety of the pyoverdin chromophore. *Z. Naturforsch. C* **55**, 146–152
- Meyer, J.-M., Gruffaz, C., Raharinosy, V., Bezverbnaya, I., Schäfer, M., and Budzikiewicz, H. (2008) Siderotyping of fluorescent *Pseudomonas*: molecular mass determination by mass spectrometry as a powerful pyoverdine siderotyping method. *Biomaterials* **21**, 259–271
- Koedam, N., Wittouck, E., Gaballa, A., Gillis, A., Höfte, M., and Cornelis, P. (1994) Detection and differentiation of microbial siderophores by isoelectric focusing and chrome azurol S overlay. *Biomaterials* **7**, 287–291
- Hohlneicher, U., Hartmann, R., Taraz, K., and Budzikiewicz, H. (1992) The structure of ferribactin from *Pseudomonas fluorescens* ATCC 13525. *Z. Naturforsch. B* **47**, 1633–1638
- Yeterian, E., Martin, L. W., Guillon, L., Journet, L., Lamont, I. L., and Schalk, I. J. (2010) Synthesis of the siderophore pyoverdine in *Pseudomonas aeruginosa* involves a periplasmic maturation. *Amino Acids* **38**, 1447–1459
- Drake, E. J., and Gulick, A. M. (2011) Structural characterization and high-throughput screening of inhibitors of PvdQ, an NTN hydrolase involved in pyoverdine synthesis. *ACS Chem. Biol.* **6**, 1277–1286
- Hannauer, M., Schäfer, M., Hoegy, F., Gizzi, P., Wehrung, P., Mislin, G. L., Budzikiewicz, H., and Schalk, I. J. (2012) Biosynthesis of the pyoverdine siderophore of *Pseudomonas aeruginosa* involves precursors with a myristoleic or a myristoleic acid chain. *FEBS Lett.* **586**, 96–101
- Hou, B., and Brüser, T. (2011) The Tat-dependent protein translocation pathway. *Biomol. Concepts* **2**, 507–523
- Schäfer, H., Taraz, K., and Budzikiewicz, H. (1991) On the genesis of the dicarboxylic acids bound amidically to the chromophore of the pyoverdins. *Z. Naturforsch. C* **46**, 398–406
- Schalk, I. J., and Mislin, G. L. A. (2017) Bacterial iron uptake pathways: gates for the import of bactericide compounds. *J. Med. Chem.* **60**, 4573–4576
- Schons, V., Atkinson, R. A., Dugave, C., Graff, R., Mislin, G. L., Rochet, L., Hennard, C., Kieffer, B., Abdallah, M. A., and Schalk, I. J. (2005) The structure-activity relationship of ferric pyoverdine bound to its outer membrane transporter: implications for the mechanism of iron uptake. *Biochemistry* **44**, 14069–14079
- Budzikiewicz, H. (2004) Siderophores of the Pseudomonadaceae *sensu stricto* (fluorescent and non-fluorescent *Pseudomonas* spp.), in *Progress in the Chemistry of Organic Natural Products* (Falk, H., and Kirby, G. W., eds), pp. 81–237, Springer, Vienna, Austria
- Ochsner, U. A., Wilderman, P. J., Vasil, A. I., and Vasil, M. L. (2002) GeneChip® expression analysis of the iron starvation response in *Pseudomonas aeruginosa*: identification of novel pyoverdine biosynthesis genes. *Mol. Microbiol.* **45**, 1277–1287

36. Cunliffe, H. E., Merriman, T. R., and Lamont, I. L. (1995) Cloning and characterization of *pvdS*, a gene required for pyoverdine synthesis in *Pseudomonas aeruginosa*: PvdS is probably an alternative σ factor. *J. Bacteriol.* **177**, 2744–2750
37. Wilson, M. J., McMorran, B. J., and Lamont, I. L. (2001) Analysis of promoters recognized by PvdS, an extracytoplasmic-function σ factor protein from *Pseudomonas aeruginosa*. *J. Bacteriol.* **183**, 2151–2155
38. Calhoun, D. H., Bonner, C. A., Gu, W., Xie, G., and Jensen, R. A. (2001) The emerging periplasm-localized subclass of AroQ chorismate mutases, exemplified by those from *Salmonella typhimurium* and *Pseudomonas aeruginosa*. *Genome Biol.* **2**, RESEARCH0030
39. Gwose, I., and Taraz, K. (1992) Pyoverdine from *Pseudomonas putida*. *Z. Naturforsch. B* **47**, 487–502
40. Meyer, J. M. (2000) Pyoverdines: pigments, siderophores and potential taxonomic markers of fluorescent *Pseudomonas* species. *Arch. Microbiol.* **174**, 135–142
41. Ochsner, U. A., Snyder, A., Vasil, A. I., and Vasil, M. L. (2002) Effects of the twin-arginine translocase on secretion of virulence factors, stress response, and pathogenesis. *Proc. Natl. Acad. Sci. U.S.A.* **99**, 8312–8317
42. Inoue, H., Nojima, H., and Okayama, H. (1990) High efficiency transformation of *Escherichia coli* with plasmids. *Gene*. **96**, 23–28
43. Laemmli, U. K. (1970) Cleavage of structural proteins during the assembly of the head of bacteriophage T4. *Nature* **227**, 680–685
44. Burnette, W. N. (1981) “Western blotting”: electrophoretic transfer of proteins from sodium dodecyl sulfate-polyacrylamide gels to unmodified nitrocellulose and radiographic detection with antibody and radioiodinated protein A. *Anal. Biochem.* **112**, 195–203
45. Towbin, H., Staehelin, T., and Gordon, J. (1979) Electrophoretic transfer of proteins from polyacrylamide gels to nitrocellulose sheets: procedure and some applications. *Proc. Natl. Acad. Sci. U.S.A.* **76**, 4350–4354
46. Neuhoff, V., Arold, N., Taube, D., and Ehrhardt, W. (1988) Improved staining of proteins in polyacrylamide gels including isoelectric focusing gels with clear background at nanogram sensitivity using Coomassie Brilliant Blue G-250 and R-250. *Electrophoresis* **9**, 255–262
47. Studier, F. W. (2014) Stable expression clones and auto-induction for protein production in *E. coli*. *Methods Mol. Biol.* **1091**, 17–32
48. Chung, C. T., Niemela, S. L., and Miller, R. H. (1989) One-step preparation of competent *Escherichia coli*: transformation and storage of bacterial cells in the same solution. *Proc. Natl. Acad. Sci. U.S.A.* **86**, 2172–2175
49. Ize, B., Viarre, V., and Voulhoux, R. (2014) Cell fractionation. *Methods Mol. Biol.* **1149**, 185–191
50. Ojha, S., Wu, J., LoBrutto, R., and Banerjee, R. (2002) Effects of heme ligand mutations including a pathogenic variant, H65R, on the properties of human cystathionine β -synthase. *Biochemistry* **41**, 4649–4654
51. Eddy, S. R. (2011) Accelerated profile HMM searches. *PLoS Comput. Biol.* **7**, e1002195
52. Finn, R. D., Clements, J., and Eddy, S. R. (2011) HMMER web server: interactive sequence similarity searching. *Nucleic Acids Res.* **39**, W29–W37
53. Finn, R. D., Clements, J., Arndt, W., Miller, B. L., Wheeler, T. J., Schreiber, F., Bateman, A., and Eddy, S. R. (2015) HMMER web server: 2015 update. *Nucleic Acids Res.* **43**, W30–W38
54. Dereeper, A., Guignon, V., Blanc, G., Audic, S., Buffet, S., Chevenet, F., Dufayard, J.-F., Guindon, S., Lefort, V., Lescot, M., Claverie, J.-M., and Gascuel, O. (2008) Phylogeny.fr: robust phylogenetic analysis for the non-specialist. *Nucleic Acids Res.* **36**, W465–W469
55. Huerta-Cepas, J., Serra, F., and Bork, P. (2016) ETE 3: reconstruction, analysis, and visualization of phylogenomic data. *Mol. Biol. Evol.* **33**, 1635–1638
56. Biasini, M., Bienert, S., Waterhouse, A., Arnold, K., Studer, G., Schmidt, T., Kiefer, F., Gallo Cassarino, T., Bertoni, M., Bordoli, L., and Schwede, T. (2014) SWISS-MODEL: modelling protein tertiary and quaternary structure using evolutionary information. *Nucleic Acids Res.* **42**, W252–W258
57. Pettersen, E. F., Goddard, T. D., Huang, C. C., Couch, G. S., Greenblatt, D. M., Meng, E. C., and Ferrin, T. E. (2004) UCSF Chimera—a visualization system for exploratory research and analysis. *J. Comput. Chem.* **25**, 1605–1612
58. Baker, N. A., Sept, D., Joseph, S., Holst, M. J., and McCammon, J. A. (2001) Electrostatics of nanosystems: application to microtubules and the ribosome. *Proc. Natl. Acad. Sci. U.S.A.* **98**, 10037–10041

Supplementary Information

The periplasmic transaminase PtaA of *Pseudomonas fluorescens* converts the glutamic acid residue at the pyoverdine fluorophore to its α -ketoglutaric acid form

Michael T. Ringel¹, Gerald Dräger², and Thomas Brüser^{1,3}

From the ¹Institute of Microbiology, Leibniz Universität Hannover, Herrenhäuser Str. 2, 30419 Hannover, Germany, the ²Institute of Organic Chemistry, Leibniz Universität Hannover, Schneiderberg 1 B, 30167 Hannover, Germany

Figure S1: UPLC-MS chromatograms filtered for identified compound masses.

Figure S2: Distribution of PtaA homologs.

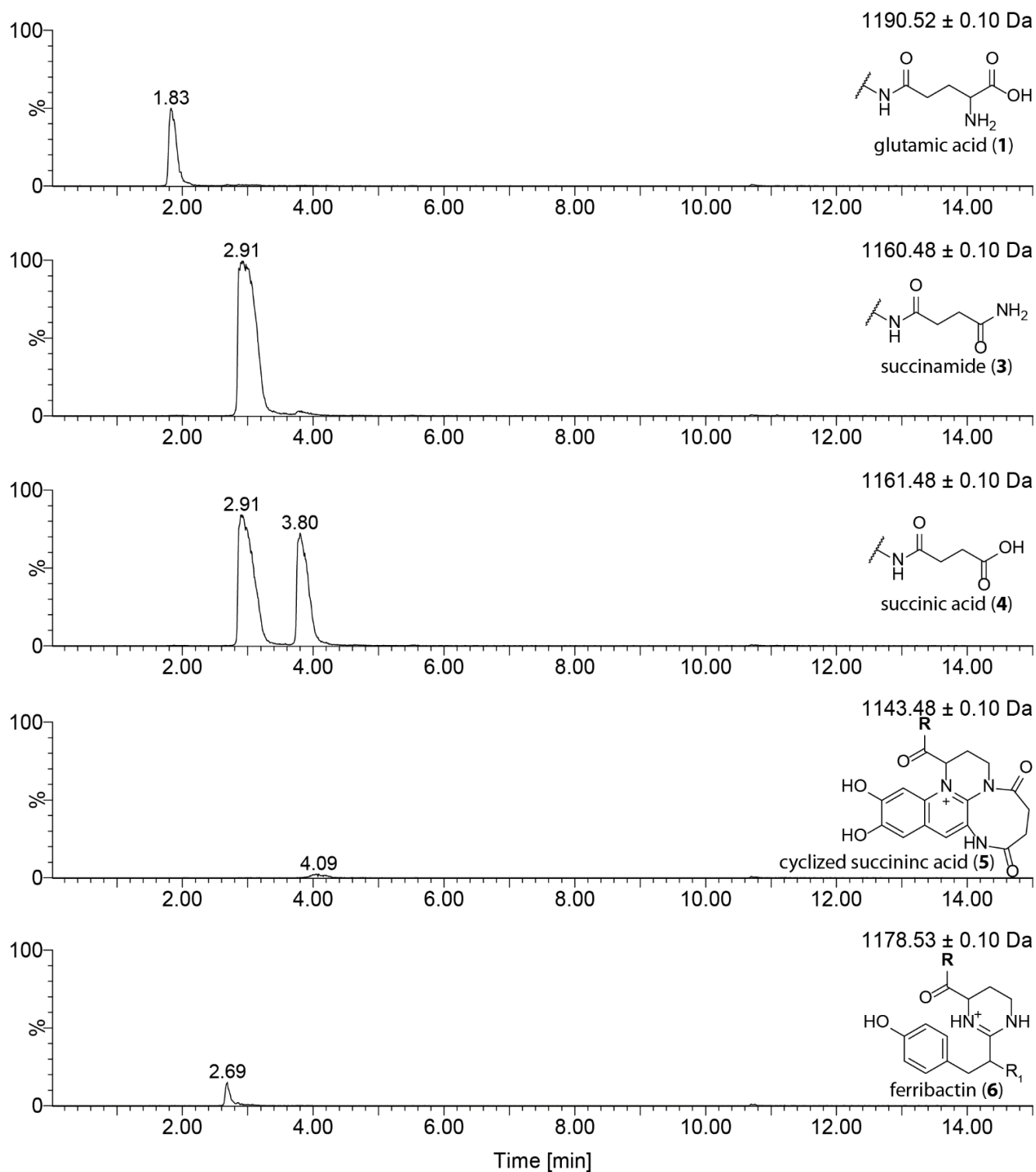


Figure S1: UPLC-MS chromatograms filtered for identified compound masses. The identified compounds (1) and (3)-(6) could be separated employing a shallower gradient for separation. The Peak at 2.91 min in the chromatogram of compound (4) is due to superposition of the isotope-peak of compound (3). The data indicates, that all identified compounds are genuine and not artifacts of MS.

3.3. PvdO is required for the oxidation of dihydropyoverdine as the last step of fluorophore formation in *Pseudomonas fluorescens*.

Authors: Michael T. Ringel¹, Gerald Dräger², and Thomas Brüser¹

Affiliations: ¹Institute of Microbiology, Leibniz Universität Hannover, Herrenhäuser Straße 2, 30419 Hannover
²Institute of Organic Chemistry, Leibniz Universität Hannover, Schneiderberg 1 B, 30167 Hannover, Germany

Type of authorship: First author

Type of article: Original research article

Share of work: 90 %

Contribution: MTR performed the experiments, prepared the figures, and analyzed the data together with TB. GD performed the MS analyses. TB conceived and coordinated the study and TB and MTR wrote the paper.

Journal: Journal of Biological Chemistry

Impact factor (2016): 4.125

Date of publication: February 16th, 2018

Number of citations
(05.04.2018): 0

DOI: 10.1074/jbc.RA117.000121

PMID: 29208656

PvdO is required for the oxidation of dihydropyoverdine as the last step of fluorophore formation in *Pseudomonas fluorescens*

Received for publication, September 26, 2017, and in revised form, November 30, 2017. Published, Papers in Press, December 5, 2017. DOI 10.1074/jbc.RA117.000121

Michael T. Ringel[†], Gerald Dräger[§], and Thomas Brüser^{†1}

From the [†]Institute of Microbiology, Leibniz Universität Hannover, Herrenhäuser Strasse 2, 30419 Hannover, Germany and the [§]Institute of Organic Chemistry, Leibniz Universität Hannover, Schneiderberg 1 B, 30167 Hannover, Germany

Edited by F. Peter Guengerich

Pyoverdines are important siderophores that guarantee iron supply to important pathogenic and non-pathogenic pseudomonads in host habitats. A key characteristic of all pyoverdines is the fluorescent dihydroxyquinoline group that contributes two ligands to the iron complexes. Pyoverdines are derived from the non-ribosomally synthesized peptide ferribactin, and their fluorophore is generated by periplasmic oxidation and cyclization reactions of D-tyrosine and L-diaminobutyric acid. The formation of the fluorophore is known to be driven by the periplasmic tyrosinase PvdP. Here we report that the putative periplasmic oxidoreductase PvdO of *Pseudomonas fluorescens* A506 is required for the final oxidation of dihydropyoverdine to pyoverdine, which completes the fluorophore. The *pvdO* deletion mutant accumulates dihydropyoverdine, and this phenotype is fully complemented by recombinant PvdO. The autoxidation of dihydropyoverdine at alkaline pH and the presence of high copper concentrations can mask this phenotype. Mutagenesis of conserved residues with potential catalytic function identified Glu-260 as an essential residue whose mutation abolished function without affecting stability or transport. Glu-260 of PvdO is at the exact position of the active-site cysteine in the structurally related formylglycine-generating enzyme. Evolution thus used the same protein fold for two distinct functionalities. As purified PvdO was inactive, additional factors are required for catalysis.

The acquisition of iron is often a limiting factor for bacteria that live in host habitats, including pathogenic as well as mutualistic species (1). Fluorescent pseudomonads warrant their iron supply by pyoverdines, fluorescent siderophores that are derived from non-ribosomally synthesized peptides that are called ferribactins (2) (Fig. 1). Ferribactins are transported into the periplasm in acylated form and deacylated thereafter by PvdQ (3–5). In the periplasm, a 5,6-dihydroxyquinoline fluorophore is generated from ferribactin, and the conserved glutamic

acid residue at the first position of the peptide is modified (6–8). Iron can then be chelated by the two hydroxyl groups of the fluorophore and four further ligands from side chains of the peptide moiety (9, 10). Only one enzyme, PvdP, is currently believed to catalyze the complete oxidation of the fluorophore (6). However, the often found dihydropyoverdine had been postulated in the past to be an obligate intermediate in fluorophore biogenesis (11, 12), and a mutant strain was known that produced dihydropyoverdine (13), suggesting two successive oxidation steps for fluorophore biogenesis. The *pvdP* gene is usually encoded adjacent to the *pvdMNO* operon, which encodes three further periplasmic proteins that might act as enzymes (Fig. 2). We recently have shown that PvdN is responsible for one of the glutamic acid modifications, the conversion of this residue to succinamide (7). The functions of PvdM and PvdO have not been resolved yet, but based on interposon mutagenesis, both proteins are postulated to be essential for pyoverdine formation (14, 15). The structure of PvdO has been solved recently (16). It has been shown to be structurally related to the formylglycine-generating enzyme (FGE),² but because the catalytic residues of FGE are not conserved in PvdO (16), no function could be assigned to this important protein so far. Being a periplasmic protein, PvdO can be expected to play a role in periplasmic pyoverdine maturation processes, which are fluorophore formation and pyoverdine modification (Fig. 1).

Here we describe that PvdO from *Pseudomonas fluorescens* A506 is required for the last oxidation step during fluorophore formation. We found that the dihydro-form of the fluorophore was the final product of a mutant strain with a scar-less in-frame *pvdO* deletion, and this phenotype was fully complemented in *trans* by *pvdO*. The requirement of PvdO can be masked by a PvdO-independent oxidation under non-physiological conditions. Purified PvdO from the periplasmic fraction did not contain potentially catalytic metal ions. However, the protein as purified was inactive, and catalysis therefore requires additional factors that are absent in the *in vitro* system.

This work was supported by German Science Foundation (DFG) Grant GRK1798 "Signaling at the Plant-Soil Interface" and Project BR 2285/7-1. The authors declare that they have no conflicts of interest with the contents of this article.

This article contains Video S1 and Fig. S1.

¹ To whom correspondence should be addressed: Institute of Microbiology, Leibniz Universität Hannover, Herrenhäuser Str. 2, 30419 Hannover, Germany. Tel.: 49-511-762-5945; Fax: 49-511-762-5287; E-mail: brueser@ifmb.uni-hannover.de.

² The abbreviations used are: FGE, formylglycine-generating enzyme; CAS, chrome azurol S; CHES, N-cyclohexyl-2-aminoethanesulfonic acid; EDDHA, ethylenediamine di(o-hydroxy)phenylacetic acid; ICP-MS, inductively coupled plasma mass spectrometry; PVD, pyoverdine; PDB, Protein Data Bank; CAA, casamino acid; a.m.u., atomic mass units; oePCR, overlap extension PCR.

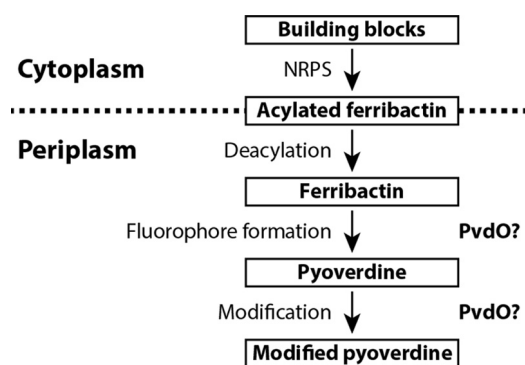


Figure 1. Schematic overview of pyoverdine biosynthesis stages. PvdO is a putative oxidoreductase and, being a periplasmic protein, could be involved in fluorophore formation or pyoverdine modification. NRPS, non-ribosomal peptide synthetase.

Results

A *pvdO* deletion strain produces a non-fluorescent but active siderophore

In the course of our functional analyses of the periplasmic enzymes that are involved in pyoverdine maturation, we deleted the gene encoding PvdO in our model strain *P. fluorescens* A506. Because *pvdO* is organized with two other genes in the *pvdMNO* operon, we applied scar-less in-frame deletion to avoid polar effects. An essential phenotype was previously postulated for all three genes in the operon, but we could recently demonstrate that this is not the case for *pvdN* (7). In-frame deletions of the other two genes of the operon, *pvdM* and *pvdO*, resulted in differential phenotypes; the $\Delta pvdM$ strain could not grow under iron limitation as induced by EDDHA, but the $\Delta pvdO$ strain was indeed able to grow under this condition, indicating that PvdO might be dispensable for functional pyoverdine formation (Fig. 3, top). However, we noted that the *pvdO* deletion strain did not secrete the fluorescent pyoverdine into the medium (Fig. 3, bottom). These initial observations already suggested that PvdO might be somehow involved in a late step of pyoverdine maturation, as apparently an active siderophore was formed that did not show fluorescence. In addition, *pvdM* was found to be indeed essential for the formation of an active siderophore, and this explains the former polar effects of the interposon mutagenesis of *pvdN* as well as of *pvdO* (14).

PvdO oxidizes dihydropyoverdine and thereby completes the formation of the pyoverdine fluorophore

We extracted pyoverdines from culture supernatant of wildtype *P. fluorescens* A506 and the corresponding *pvdO* deletion strain and examined them by mass spectrometry (Fig. 4A). Elution profiles of the respective masses are shown on the left, and the corresponding mass spectra are depicted on the right. The assigned structures are illustrated in Fig. 4 (B and D). While the wildtype strain produced the well-known pyoverdines PVD- α -ketoglutaric acid (2), PVD-succinamide (3), and PVD-succinic acid (4), the data clearly showed that the pyoverdines of the *pvdO* deletion mutant were the known dihydro-intermediates of the pyoverdines with the different modifications known for the first residue, namely glutamic acid (5), α -ketoglutaric acid (6), succinamide (7), and succinic acid (8). The succinic acid form (8) was very low-abundant, and some ferribactin (9)

was detected in both preparations, especially in the *pvdO* deletion strain. The glutamic acid variant (1) was not detected in the wildtype strain, which is due to the known quantitative conversion of 1 to 2 and 3 by PvdN and PtaA (7, 8). The identity of the dihydropyoverdine compounds was verified by high-resolution mass spectrometry (calculated exact masses are denoted in parentheses; see Ref. 8 for the other pyoverdine masses): 5, 1192.560 atomic mass units (a.m.u.) (1192.560 a.m.u.); 6, 1191.528 a.m.u. (1191.528 a.m.u.); 7, 1162.550 a.m.u. (1162.549 a.m.u.). The data demonstrated not only that PvdO is responsible for the final oxidation of dihydropyoverdine, but also that the side chain-modifying enzymes accept the dihydro-substrate.

The pyoverdines of the wildtype and the $\Delta pvdO$ -, $\Delta pvdN$ / $\Delta pvdO$ -, and *pvdO*-complemented $\Delta pvdO$ strains were analyzed by isoelectric focusing, followed by fluorescence detection (Fig. 4C, left) or the CAS overlay assay (Fig. 4C, right). The fluorescence detection confirmed the pyoverdines detected by mass spectrometry, with the succinic acid and α -ketoglutaric acid forms migrating at the lower part of the gel and the succinamide and glutamic acid forms migrating at the upper part. Note that the epifluorescence was recorded without a filter, as the dihydropyoverdines (middle two lanes) exhibit only a rather weak blue fluorescence that can be thereby detected. The CAS overlay assay demonstrated iron binding of all identified siderophores, including the dihydropyoverdines, which agrees with former reports about a complementation of pyoverdine deficiency by dihydropyoverdine as well as with affinity measurements (13).

Non-enzymatic oxidation of dihydropyoverdine masks PvdO activity

The finding that PvdO was required for the final oxidation of dihydropyoverdine in the described cultivations raised the question of why PvdO was not required for the reported PvdP-dependent fluorophore formation from ferribactin in previous *in vitro* experiments (6). In that study, it had been clearly shown that the mature fluorophore was generated in assays that contained PvdP as the only enzyme (6). It thus was very likely that the previously applied *in vitro* conditions had somehow triggered a PvdO-independent completion of fluorophore oxidation. Obvious unusual conditions that had been used in these assays were (i) the alkaline pH 9.0, which is non-physiological as the periplasmic compartment is slightly acidic, and (ii) the inclusion of 250 μM CuSO_4 , which is a copper stress condition. These conditions had been found to be the optimum conditions for the PvdP-catalyzed reaction (6). As fluorescence is quenched by copper ions, we used the oxidation-dependent increase of chromophore absorbance at 405 nm to examine the potential influence of pH and copper on dihydropyoverdine oxidation (Fig. 5A). Non-catalytic oxidation was very rapid at pH 9.0, and this was significantly slowed down by the addition of 250 μM CuSO_4 . At pH 8, there was essentially the same effect of copper, but autoxidation proceeded at a much slower rate. At pH 7, there was hardly any autoxidation observed. In conclusion, alkaline autoxidation occurs rapidly without involvement of copper as catalyst. The alkaline autoxidation had already been recognized in early studies on the structure of dihydropyoverdine (17). In that study, it was also shown that chelation of

Dihydropyoverdine oxidation by PvdO

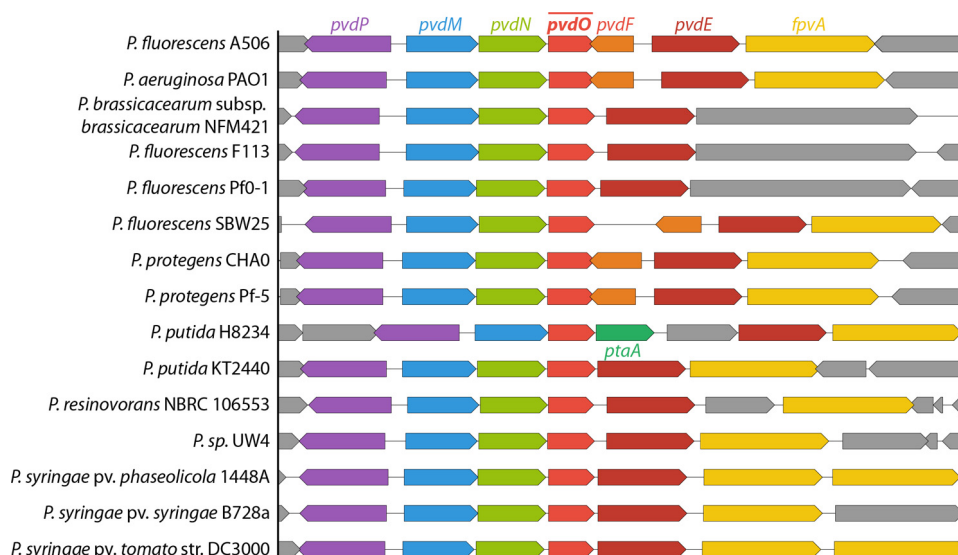


Figure 2. Comparison of genomic environments of *pvdO* in representative *Pseudomonas* genomes.

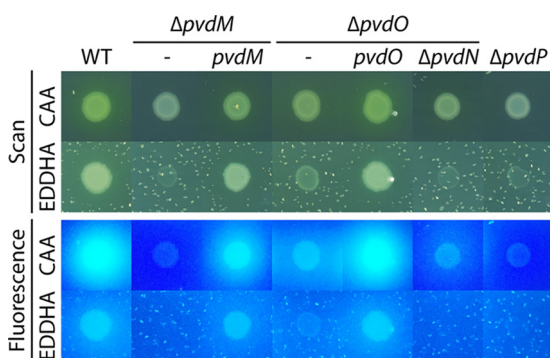


Figure 3. Evidence for a non-fluorescent pyoverdine generated in the *pvdO* deletion strain. Shown is the growth of strain A506 (WT) and its derivatives deleted in *pvdM* ($\Delta pvdM$), *pvdO* ($\Delta pvdO$), *pvdP* ($\Delta pvdP$), or *pvdN* and *pvdO* ($\Delta pvdNO$) on pyoverdine-inducing solid casamino acid (CAA) medium without or with EDDHA for additional iron depletion. Indicated complementation strains are included in the analysis. Growth on EDDHA-containing plates correlates with the formation of pyoverdines and (in case of the $\Delta pvdO$ strain) with dihydropyoverdine, as monitored by fluorescence (bottom).

iron inhibits the autoxidation (17), and our data indicate that chelation of copper has the same effect.

The assay system for the PvdP-dependent formation of completely oxidized pyoverdine from ferribactin did not monitor the potential formation of a dihydropyoverdine intermediate (6). The rapid autoxidation of this intermediate at the applied non-physiological pH 9 masked the PvdO requirement in these assays.

However, the effect of copper is more complex. When we analyzed the impact of copper on the formation of fluorescent pyoverdines in growing cultures, we noted differential effects (Fig. 5B, top). As expected, in the absence of copper, the wild-type strain produced fluorescent pyoverdine, and the medium of the *pvdO* deletion strain contained only very little fluorescence due to the formation of dihydropyoverdine. However, abundant copper in the bacterial cultures promoted the oxidation of dihydropyoverdine in the $\Delta pvdO$ background, and fluorescence reached the level of the wildtype strain at $\sim 300 \mu\text{M}$ copper. At higher copper concentrations, fluorescence was gradually quenched by copper. The positive influence of copper on dihydropyoverdine oxidation thus had a maximum effect in

the range of 200–500 μM copper, which coincides with the reported optimum of PvdP activity at 250 μM copper (6). Therefore, although copper binding to dihydropyoverdine partially inhibits alkaline autoxidation (Fig. 5A), the same high copper concentrations can artificially trigger a dihydropyoverdine-oxidizing activity in the presence of whole cells (see “Discussion”). In control experiments, strains lacking PvdM or PvdP did not produce any fluorescent pyoverdine in the presence of added copper even after prolonged incubations, excluding alternative explanations for fluorescence increase (Fig. 5B, bottom).

PvdO and *PvdP* generally co-occur in fluorescent *pseudomonads*

As shown above, PvdO is required for the oxidation of dihydropyoverdine under physiological conditions in *P. fluorescens* A506. It can therefore be expected that PvdO must always co-occur with PvdP, because PvdP is essential for the preceding ring formation. We thus examined the presence of *pvdO* and *pvdP* in all genomes of *Pseudomonas* strains available in the *Pseudomonas* Genome Database (18) in August 2017. In full agreement with the prediction, these analyses demonstrated a complete co-occurrence of the two genes (Fig. 6). Individual mismatches (in 13 of 3347 analyzed genomes) could all be traced back to unfinished genome assemblies or gaps.

Mutational analysis of *PvdO*

As PvdO is somehow required for the oxidation of dihydropyoverdine in living cells under physiological conditions, it was interesting to investigate its structural and biochemical properties.

We homology-modeled the structure of PvdO from *P. fluorescens* A506 (PvdO_{A506}) to the known structures of PvdO from *Pseudomonas aeruginosa* PAO1 (PvdO_{PAO1}; 73% identity; PDB 5HHA) and the structurally related FGE (25% identity; PDB 2Q17) from *Streptomyces coelicolor*. Neither PvdO_{PAO1} nor FGE contain a redox active cofactor associated with the purified proteins used in crystallographic analyses. However, FGE is suggested to employ a copper cofactor to oxidize cys-

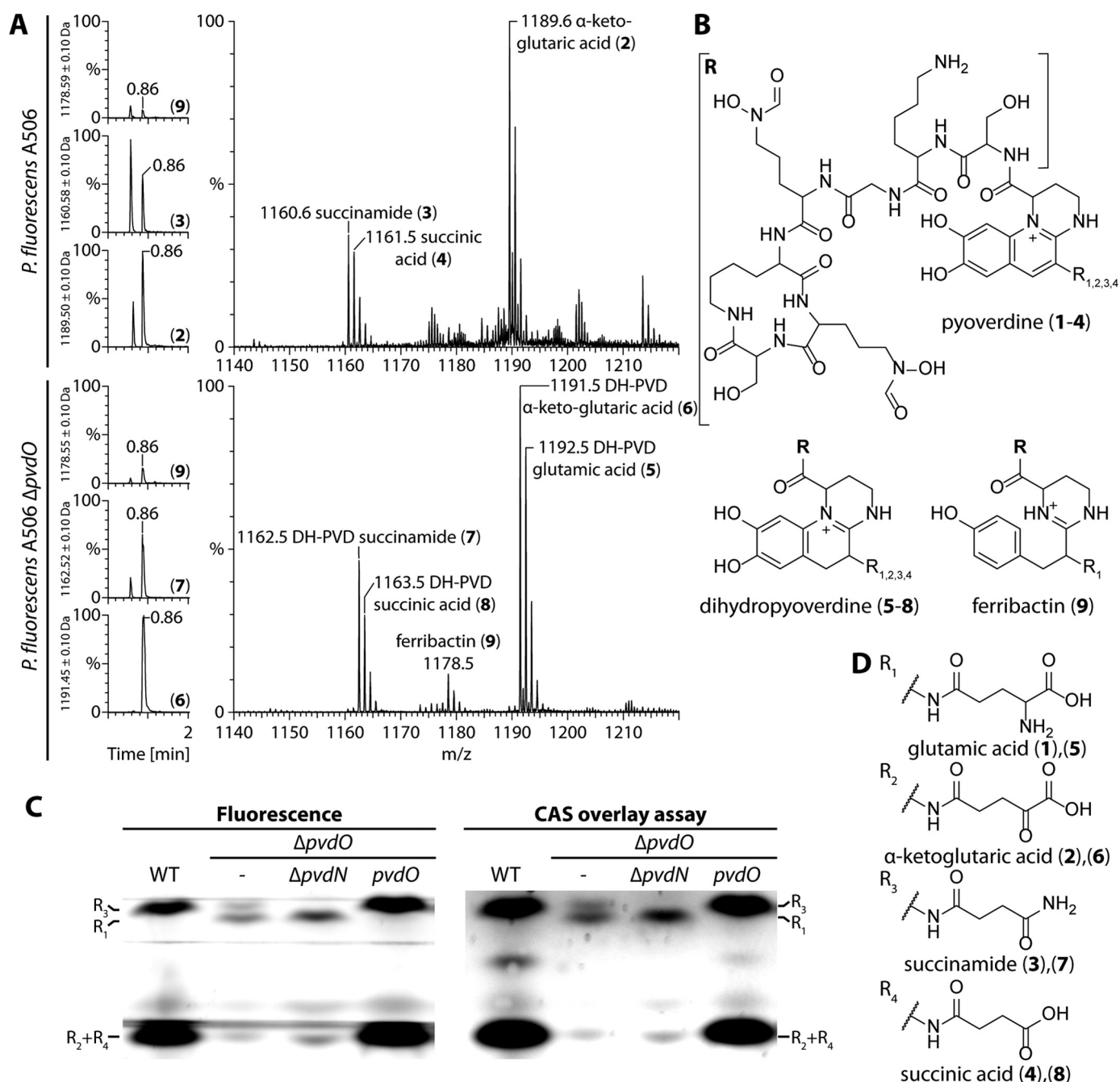


Figure 4. PvdO catalyzes the oxidation of dihydropyoverdine. A, analysis of pyoverdines produced by wildtype *P. fluorescens* A506 (top) and the corresponding dihydropyoverdines (DH-PVD) produced by the *pvdO* deletion strain (bottom). Chromatograms on the left depict the elution profiles of the numbered compounds that are assigned in B and D. C, detection of fluorescence (left) or iron-binding capacity in a CAS overlay assay (right) after isoelectric focusing of the pyoverdines of indicated strains. WT, wildtype A506; $\Delta pvdO$, strains with *pvdO* deletion; $\Delta pvdO/\Delta pvdN$, strain with an additional *pvdN* deletion; $\Delta pvdO/pvdO$, *pvdO*-complemented *pvdO* deletion strain.

teine to formylglycine (19), and according to a structural analysis study on PvdO_{PAO1}, FGE is the only so-far known protein that is structurally related to PvdO, although active-site cysteines of FGE are not conserved in PvdO (16). The PvdO_{PAO1} and FGE-based structural models of PvdO_{A506} are in most parts highly similar with respect to the backbone structure and differ mainly in the conformation of surface loop structures (Video S1). The FGE-derived model was suggestive of a potential His/His/Glu non-heme iron-binding site that resembled known sites (20, 21). These residues (His-188, His-218, and Glu-260)

are highly conserved (Fig. 7D), as are several other potentially important candidate residues (Glu-179, Asn-210, Tyr-215, Asp-216, Met-217, and Asp-257) that were included in a mutational analysis. Also, several non-conserved residues with potential metal-chelating propensity were included as negative controls (Gln-187 and Met-214). As in the case of PvdO from *P. aeruginosa* (16), all six cysteines of *P. fluorescens* A506 PvdO form disulfides and thus are unlikely to be involved in metal binding. Exchanged residues are indicated in the sequence of Fig. 7D as well as in the structural model in Fig. 7E.

Dihydropyoverdine oxidation by PvdO

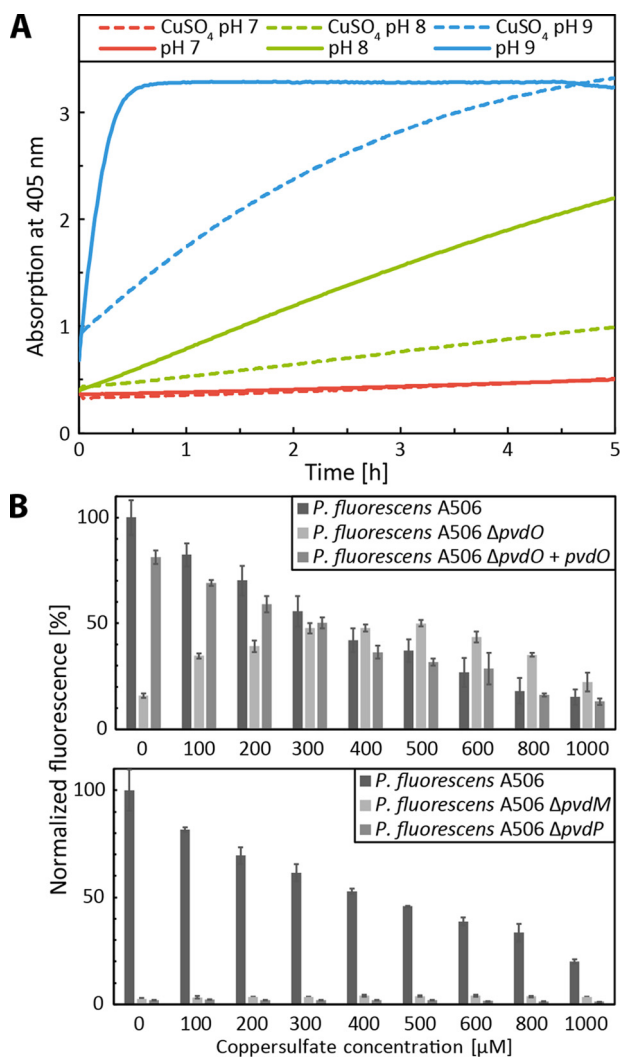


Figure 5. Non-physiological oxidation of dihydropyoverdines by alkaline autoxidation *in vitro* and copper-induced oxidation in growing cultures. A, pH-dependent autoxidation of dihydropyoverdine as monitored by absorbance increase at 405 nm. Kinetics of assays containing 250 μM CuSO_4 (dashed lines) are directly compared with kinetics in the absence of copper. Copper was added after 1 min of incubation. The data of the copper-containing assays were corrected for copper absorption. See “Experimental procedures” for details. B, pyoverdine fluorescence of culture supernatants of wildtype A506, its $\Delta pvdO$ derivative, and the *pvdO*-complemented $\Delta pvdO$ strain after 24 h of growth in CAS medium supplemented with the indicated CuSO_4 concentrations (top). Control measurements are shown, indicating the absence of fluorescence with strains deleted in *pvdM* ($\Delta pvdM$) or *pvdP* ($\Delta pvdP$) after a 48-h incubation (bottom). Error bars are derived from triplicate assays of independent cultures. Fluorescence was normalized to the wildtype levels in the absence of copper. The decrease of fluorescence at higher copper concentrations is due to the quenching of pyoverdine fluorescence by copper ions.

Using our functional complementation system described above, we examined for all of these individual PvdO variants their ability to complement the $\Delta pvdO$ phenotype in terms of pyoverdine production (Fig. 7A, top), their stability (Fig. 7A, bottom), and their transport into the periplasm (Fig. 7B). Fortunately, while a number of exchanges caused an instability of the protein and consequently a loss of functionality, several of the exchanges, namely PvdO(D257A) and PvdO(E260A), abolished complementation of the mutant phenotype without compromising protein stability. The transport of these variants into the periplasm was unaffected, indicating that the non-functionality

was not caused by a mislocalization. As expected from the stability analysis shown in Fig. 7A, the other PvdO variants were not detected in any subcellular fraction (Fig. 7B), indicating degradation to non-detectable levels. From all of these biochemical data, it can be concluded that the residues Asp-257 and Glu-260 are essential for dihydropyoverdine oxidation in living *P. fluorescens* A506 cells, without being required for protein integrity or subcellular targeting.

As a complementary analysis, we also evaluated pyoverdine formation during growth on iron-depleted or iron-limited solid media (Fig. 8). As expected, *pvdO*-deleted strains or strains containing inactivated or destabilized PvdO variants grew with reduced rate under iron-depleted conditions (*i.e.* in the presence of the chelator EDDHA; Fig. 8, A and C) and could not form fluorescent pyoverdine halos (Fig. 8, C and D). Some fluorescence surrounding the strain with the D257A variant indicates a residual activity that had not been detected with planktonic growth. In all other cases, the results of this assay were only confirmative. Together, the *in vivo* data described above indicated that the two acidic residues Asp-257 and Glu-260 of PvdO were important for the oxidation of dihydropyoverdine in living cells.

Based on this knowledge, we then carried out analyses *in vitro*. We purified wildtype PvdO and the E260A variant from the periplasmic fraction of *E. coli* harboring a *pvdO* expression system (Fig. 7C). The protein migrated near 35 kDa, which is slightly above the calculated mass of 30 kDa for the Strep-tagged protein. Using ICP-MS, we did not detect any potentially redox-active iron, copper, cobalt, or manganese ions or zinc ions as constituents of the purified proteins. Therefore, as discussed in more detail below, either a cofactor was not stably assembled or catalysis does not depend on metal ions. The activity of purified PvdO and its variant PvdO(E260A) was not detectable *in vitro* (Fig. S1), which can be due to various reasons (see “Discussion”).

Discussion

PvdO is required for dihydropyoverdine oxidation

The functional role of PvdO has been matter of speculation since its importance had been recognized by Ochsner *et al.* in 2002 (15). It was known that no fluorescent pyoverdine could be formed in a *pvdO* mutant strain that had been generated by interposon mutagenesis (15, 14). However, the deletion strains were not complemented, and the fact that *pvdO* is organized in the *pvdMNO* operon made the interpretations difficult due to possible polar effects. PvdN, which is encoded by the same operon and had also been believed to be essential for pyoverdine formation, is in fact not essential and catalyzes the conversion of the fluorophore-attached glutamic acid to succinamide (7). To clarify this issue for PvdM and PvdO, we carried out in-frame scar-less deletions of these two genes, analyzed their phenotypes, and successfully complemented them. While PvdM turned out to be indeed essential for pyoverdine formation, the $\Delta pvdO$ phenotype was more complex; there was still some growth possible on iron-depleted medium, albeit the typical yellow-greenish pyoverdine fluorescence was absent from this mutant (Fig. 3). This prompted us to investigate the spectrum of potential pyoverdine precursors produced by that strain, and we discovered that PvdO is required for the oxida-

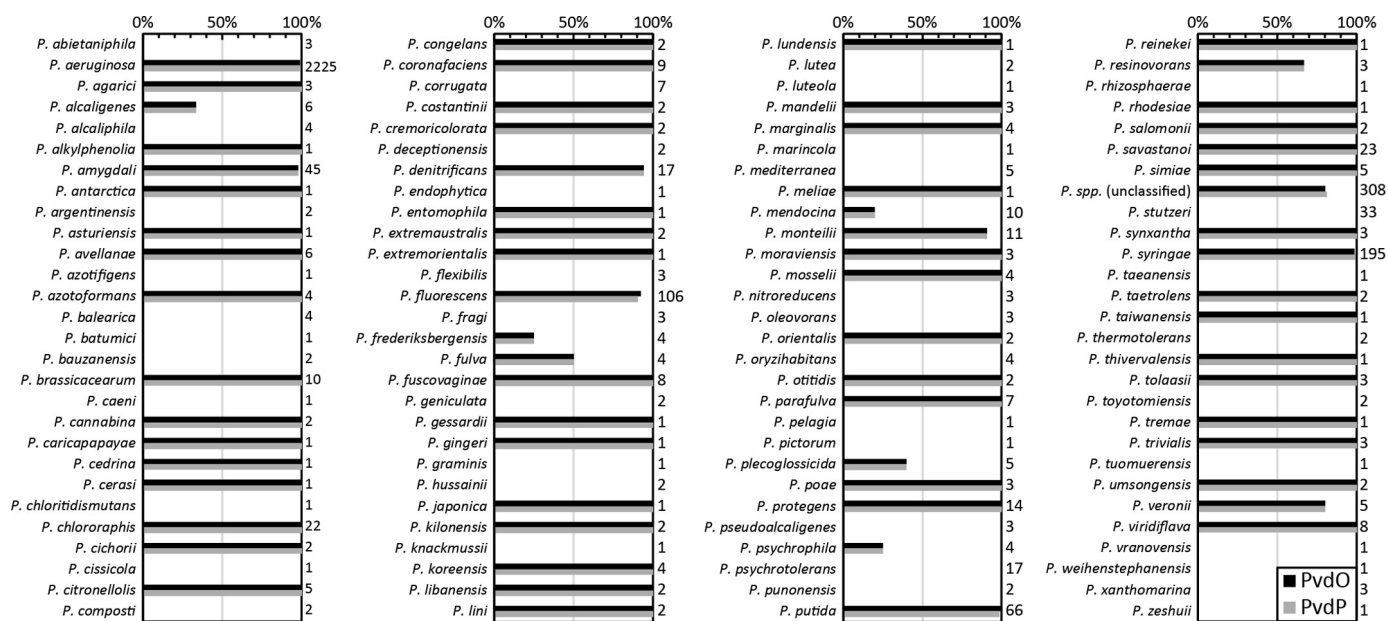


Figure 6. Co-occurrence of PvdO and PvdP homologs within the genus *Pseudomonas*. Numbers to the right of the bar graph indicate the total number of genomes analyzed for the respective species. Note that the two genes co-occurred in 3334 of 3347 genomes, and the 13 exceptions were attributed to unfinished genomes.

tion of dihydropyoverdine *in vivo* under physiological conditions (Fig. 4). The *pvdO* gene fully complemented the $\Delta pvdO$ phenotype and produced wildtype levels of the oxidized pyoverdine fluorophore. Thus, no secondary mutations had caused the phenotype of the gene deletion. The role in fluorophore biogenesis was unexpected, because the early postulated dihydropyoverdine intermediate (11, 12) had not been considered as relevant anymore when PvdP had been shown to catalyze the complete conversion of ferribactin to fluorescent pyoverdine (6). In that *in vitro* study, however, the full oxidation had been demonstrated in assays that contained $250 \mu\text{M}$ CuSO_4 at pH 9.0. As we observed that dihydropyoverdine is rapidly oxidized at pH 9.0 even in the presence of $250 \mu\text{M}$ copper (Fig. 5A), and as PvdO is responsible for the oxidation of dihydropyoverdine under physiological conditions, it is likely that dihydropyoverdine rather than pyoverdine is the product of PvdP. However, it is noteworthy that a growing $\Delta pvdO$ strain could generate fluorescent pyoverdine in the presence of $200\text{--}500 \mu\text{M}$ CuSO_4 . This copper effect most likely relates to living cell constituents, and it is intriguing that the optimal concentration in the published PvdP assays is the same as in our *in vivo* assays (Fig. 5B). It thus might be speculated that an occupancy of low-affinity copper sites on cellular proteins such as PvdP can contribute, besides alkaline autoxidation, to an artificial full oxidation to pyoverdine under these conditions. As PvdO strictly co-occurs with PvdP in fluorescent pseudomonads (Fig. 6), it is clear that the oxidation of dihydropyoverdine must generally be catalyzed in a PvdO-dependent manner under physiological conditions not only in *P. fluorescens* but also in the other species.

Although required, the exact mode by which PvdO contributes to the oxidation of dihydropyoverdine remains unclear

We initially expected a transition metal cofactor as a constituent of PvdO and thus homology-modeled the structure with the related *S. coelicolor* FGE structure and later also with the

recently published *P. aeruginosa* PvdO structure as templates to identify potential metal-binding sites. Several residues were possibly involved in an iron-binding site, but there was no good evidence for any copper site. The mutational analysis therefore included residues with potential metal-binding properties in the environment of the suspected iron site, and we examined the influence of the mutations on fluorescent pyoverdine formation as well as on stability (Figs. 7 and 8). The exchange of the presumed histidine ligands strongly affected PvdO stability, which argued against a primarily catalytic function. Only the mutation of two acidic residues, Asp-257 and Glu-260, resulted in complete (E260A) or strongly reduced (D257A) functionality without any significant effect on protein stability. We had analyzed not only wildtype PvdO but also the E260A variant, as we suspected Glu-260 to be an essential ligand for the supposed metal ion. To our surprise, neither the wildtype nor the mutated protein contained any detectable metal ions, although PvdO had been purified under mild conditions by affinity chromatography. The absence of metals pointed to a mechanism similar to the metal-independent alkaline autoxidation (17) in which the deprotonation of the catechol is the initializing step for the oxidation. It is proposed that unpaired electrons that are generated during the oxidation are stabilized between the neighboring catechol hydroxylates, which promotes the oxidation (17). To this mechanism fits the essential role of Glu-260, and also the significant contribution of a second carboxylic acid, Asp-257. If PvdO directly catalyzes the oxidation of dihydropyoverdine, it probably enables the deprotonations at pH 6.5 in the periplasm, stabilizes the oxyanions, and catalyzes the electron transfer to an unknown electron acceptor (Fig. 9A). Once the ring system is oxidized, tautomerizations would readily generate the 5,6-dihydroxyquinoline fluorophore. However, because we could not reconstitute the activity *in vitro*, PvdO most likely needs to interact with another component in the

Dihydropyoverdine oxidation by PvdO

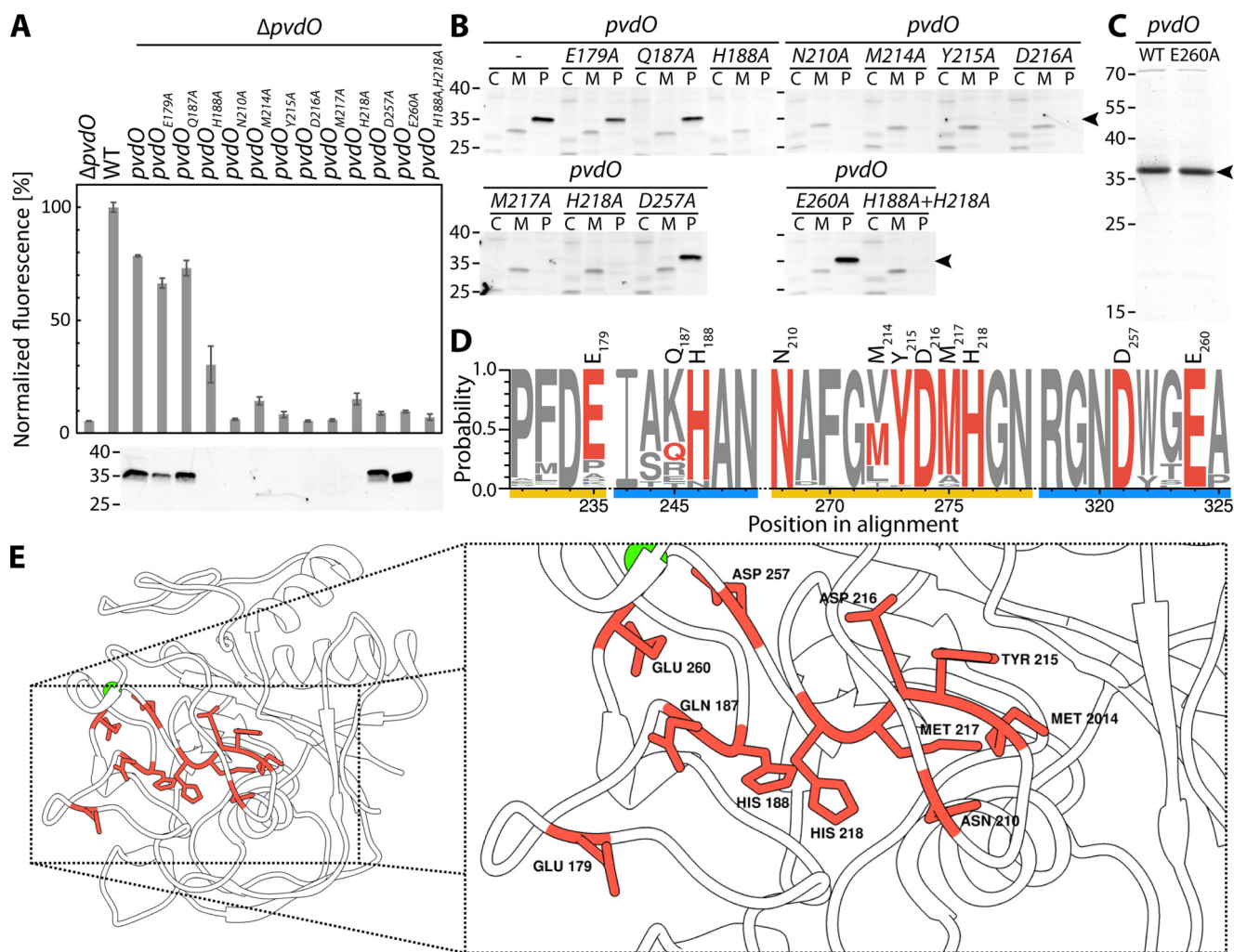


Figure 7. Effects of alanine exchanges of residues with potential catalytic function. *A*, effect of the indicated single-alanine exchanges on the formation of fluorescent pyoverdine and control of the presence of the respective PvdO variants in the periplasm by SDS-PAGE/Western blotting. *B*, subcellular fractionation of all analyzed PvdO variants. Cytoplasmic (C), membrane (M), and periplasmic (P) fractions were analyzed for the presence of PvdO by SDS-PAGE/Western blotting. Note that in case of stable PvdO variants, the protein is exclusively detectable in the periplasm, as expected for Sec transport. *C*, Coomassie-stained PvdO preparations that had been used for metal detections. *D*, sequence logo of the mutated regions (see “Experimental procedures” for details). Exchanged residues in PvdO_{A506} are colored red, and distinct regions are highlighted in yellow and blue. The residue numbers on top of the sequence logo indicate the residue position in PvdO_{A506}. *E*, homology model of the PvdO_{A506} structure based on the known structure of PvdO from *P. aeruginosa* (PDB code 5HHA). Exchanged residues are highlighted in red. *Left*, overview of the structure; *right*, close-up view. The model was visualized using Chimera (36). Masses of marker proteins (in kDa) are indicated on the left side of blots.

periplasm to perform its function. Obviously, this could be a specific electron acceptor that channels the electrons into the respiratory electron transport chain. The inactivity of purified PvdO can be taken as an argument against a more direct electron transfer to oxygen, as implied by an autoxidation-like mechanism. The possibility certainly also cannot be excluded that an unknown cofactor is required that is lost during purification or that PvdO is a protein that enables another enzyme to oxidize dihydropyoverdine, although the active-site conservation argues for a direct enzymatic involvement (see below).

The active-site cavity appears to be conserved between FGE and PvdO

When we examined the position of the identified key acidic residues Glu-260 and Asp-257 in the homology-modeled protein, we readily recognized that these residues were located in a pocket-like cavity that was likely to represent the substrate-binding site (Fig. 9, *B* and *C*). Interestingly, we found that the

supposed binding pocket was exactly at the position reported to be the active site of the structurally related FGEs (PDB code 2Q17). One of the two active-site cysteines in FGE is in fact superimposable with Glu-260, which we had identified as an essential residue of PvdO (Fig. 9C). Glu-254 of PvdO_{PAO1}, which corresponds to Glu-260 of PvdO_{A506}, had already been recognized to be at the position of the active-site cysteine in human FGE (16). Although no function had been assigned to this residue in that study, the corresponding surface cleft was proposed to represent a binding site for an unknown substrate. Therefore, nature apparently used the same protein fold and the same active-site region to generate two distinct functionalities for distinct subcellular compartments. While the cytoplasmic FGEs can use cysteines for active-site metal coordination (22), periplasmic PvdO does not have this cysteine and therefore does not bind copper at that position. Instead, PvdO function requires a glutamic acid that has been placed at the exact position of the copper ligands in FGEs. This finding strongly

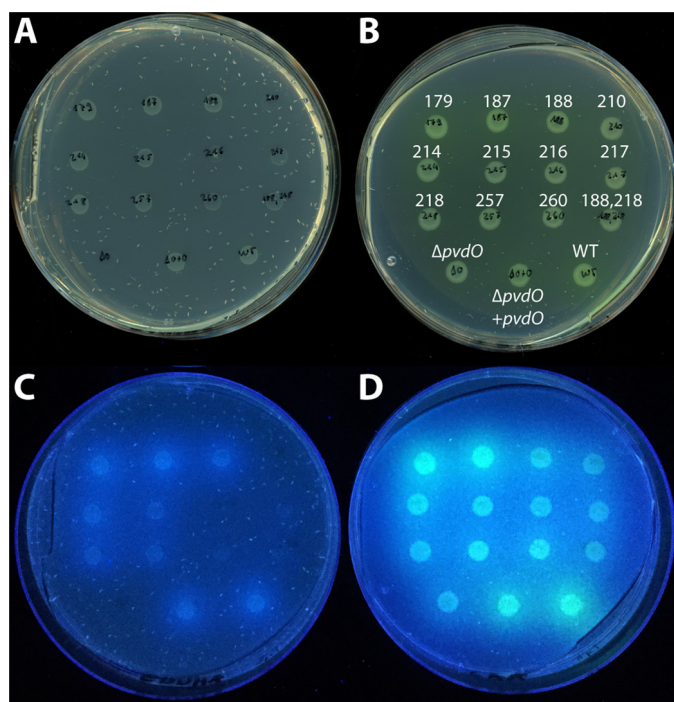


Figure 8. Analysis of physiological functionality of PvdO variants with single-amino acid exchanges. A and C, CAA plates containing iron-depleting EDDHA; B and D, CAA plates without EDDHA. A and B show the growth of spotted cultures on the respective media, whereas B and D show the fluorescence caused by produced pyoverdines. The amino acid exchanges and control strains are denoted in B. All plates contain the same organization of spotted strains.

argues for a direct enzymatic function of PvdO, which remains to be demonstrated in the future. This will help to ultimately clarify the mechanism by which dihydropyoverdine is oxidized.

Experimental procedures

Strains and growth conditions

The strain *P. fluorescens* A506 was utilized for all physiological assays. *Escherichia coli* DH5 α λ *pir*⁺ was employed for cloning and *E. coli* Rosetta 2 (DE3) pLysSRARE2 for protein production. The *E. coli* strains were cultivated at 37 °C and *P. fluorescens* strains at 30 °C unless noted otherwise. LB-Medium (1% (w/v) tryptone, 1% (w/v) NaCl, 0.5% (w/v) yeast extract) was used for standard cultivations. Appropriate antibiotics were supplemented at the following final concentrations: 100 μ g/ml ampicillin, 25 μ g/ml chloramphenicol, 50 μ g/ml kanamycin, 20 μ g/ml tetracycline. The pyoverdine-plate assay and the relative pyoverdine quantification assay were performed as described previously (7, 8).

Genetic methods and plasmids

Construction of all plasmids and scar- and marker-less deletions were performed as described previously (7, 8). All primers used for this study are listed in Table 1.

Biochemical methods

SDS-PAGE, successive Western blotting, and in-gel colloidal Coomassie staining for protein analysis were performed according to standard protocols (23–26). Development of Western blots was performed according to the manufacturer's instructions using a StrepMAB-Classic monoclonal antibody

(IBA, Göttingen, Germany) for detection of Strep-tagged proteins. As secondary antibody, anti-mouse-horseradish peroxidase conjugate (Carl Roth, Karlsruhe, Germany) was employed. Images were recorded using the MF-ChemiBIS version 4.2 imaging system (DNR Bio-Imaging Systems, Jerusalem, Israel).

Subcellular fractionation of *P. fluorescens* A506 was performed as reported previously (27) with minor modifications; cultures (50 ml) were grown to OD₆₀₀ of 1, and a 1-ml fraction volume was used throughout. The samples were not further concentrated by precipitation for further analysis.

The subcellular fractionation of *E. coli* was carried out as described earlier, with minor modifications (28). Briefly, 10 100-ml cultures in 0.5-liter Erlenmeyer flasks with four baffles each were inoculated with 4 ml of the appropriate overnight culture and incubated at 30 °C and ~180 rpm until the OD₆₀₀ reached 0.6. Then the expression was induced with 1 mM isopropyl β -D-1-thiogalactopyranoside for 3 h, maintaining the incubation conditions. Subsequently, cells were sedimented in 250-ml centrifugation buckets for 10 min at 3857 \times g and 4 °C. The pellets were resuspended in 40 ml of TES buffer (20% (w/v) sucrose, 10 mM Tris buffer, pH 8.0, 1 mM EDTA) and incubated at room temperature for 10 min. The cells were transferred to 45-ml centrifugation buckets and sedimented for 10 min at 2990 \times g and 4 °C. Pellets were then resuspended in 1.5 ml of ice-cold 5 mM MgSO₄ each and transferred to 2-ml plastic tubes. Resuspended cells were then incubated for 20 min on ice and subsequently centrifuged for 10 min at 4 °C and 16,060 \times g. The supernatants (periplasmic fraction) were collected and immediately sterile filtered through a 0.2- μ m PES filter. The protein was purified utilizing one 1.5-ml Strep-Tactin® Superflow® column (IBA) according to the manufacturer's instructions using 100 mM Tris-HCl buffer, pH 8.0, with 150 mM NaCl as running buffer. After elution, the elution fractions E3 and E4 were combined and diluted with 100 mM Tris-HCl, pH 8.0, to lower the NaCl concentration to 50 mM for subsequent ICP-MS analysis. The protein was then concentrated using a Vivaspin® 6 concentrator (cutoff 10 kDa; Sartorius, Göttingen, Germany). The protein concentration was estimated via absorption at 280 nm using a NanoDrop 2000 spectrophotometer (Thermo Fisher Scientific). Samples were subsequently analyzed by ICP-MS (Spurenanalytisches Laboratorium Dr. Baumann; Pirkensee, Germany).

A Jasco V-650 spectrophotometer (Jasco, Gross-Umstadt, Germany) was used for *in vitro* dihydropyoverdine oxidation assays with the following settings: wavelength, 405 nm; bandwidth, 2 nm; measurement interval, 1 min; total measurement time, 5 h; temperature, 20 °C; stirrer, 800 rpm. As buffers for the assay, 50 mM HEPES, pH 7, 50 mM HEPES, pH 8, and 50 mM CHES, pH 9, were used. The assays started with the addition of 10 μ l of freshly thawed dihydropyoverdine stock solution to a final assay volume of 2 ml in the respective buffer. After 1 min of incubation time, CuSO₄ was added from a 100 mM stock solution to a final concentration of 250 μ M. The absorptivity caused by CuSO₄ was subtracted from the respective kinetics measurement from the time point of the addition on.

In vitro activity assays were carried out in 50 mM PIPES, pH 6.5, in a final total volume of 2 ml. For each measurement, 10 μ l of the dihydropyoverdine stock solution were mixed with reaction buffer, and the assay was started after 1 min of pre-equili-

Dihydropyoverdine oxidation by PvdO

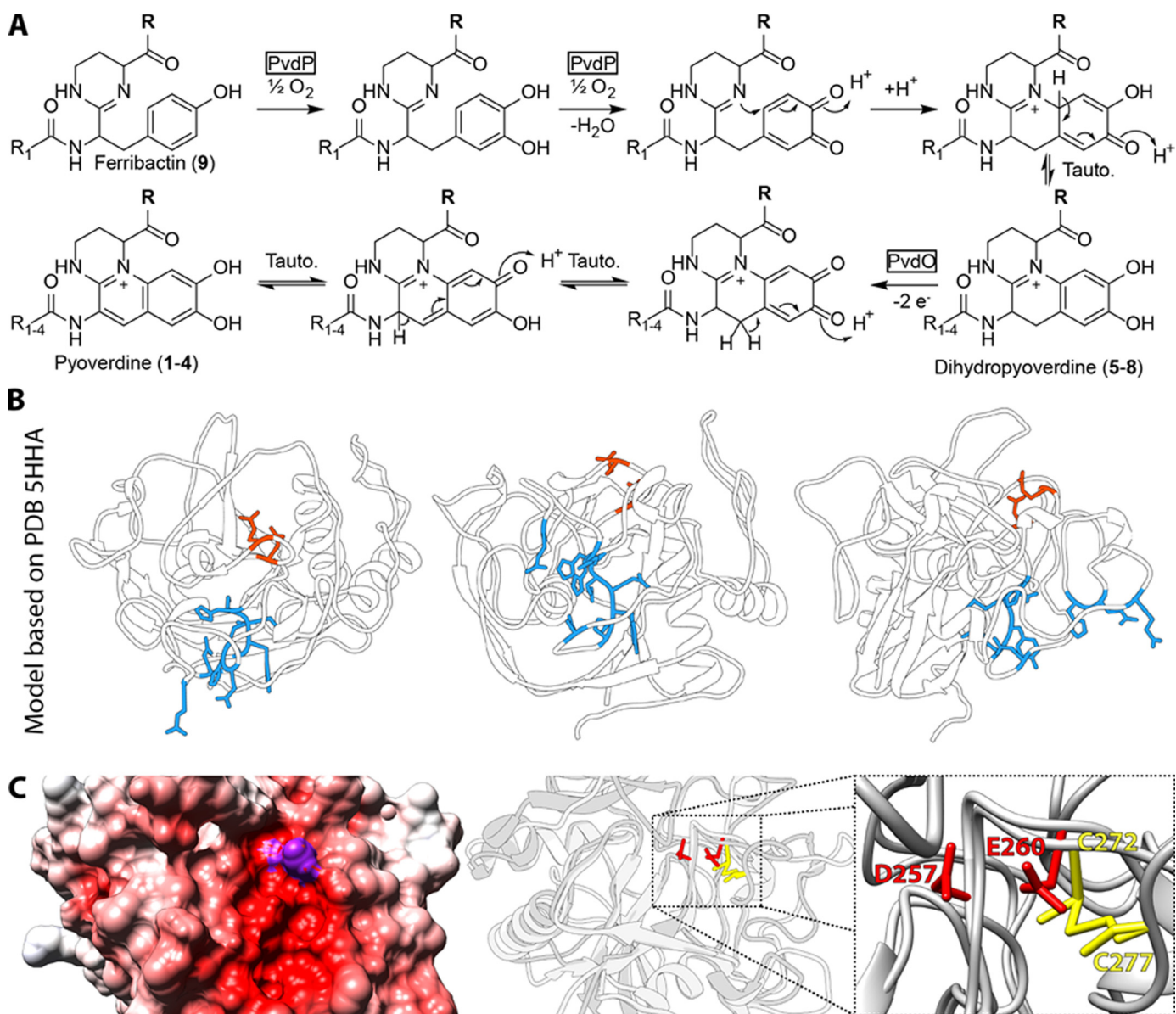


Figure 9. Role of PvdO in fluorophore formation of pyoverdines and identification of functionally important residues in a potential active-site cavity of PvdO. A, biosynthetic reactions leading from ferribactin to pyoverdine via the intermediate dihydropyoverdine. PvdP is required for the initial oxidative cyclization reaction that results in the catechol system. PvdO is required for the final oxidation, resulting in the mature fluorophore. B, the two active-site residues Asp-257 and Glu-260 (red) and their position on the surface of PvdO relative to the other residues mutated in this study (blue). C (left), active-site cavity shown by the APBS (37)-calculated electrostatic potential-colored surface (scale from -10 (red) through 0 (white) to $+10$ (blue)). Surface-exposed side-chain regions of Asp-257 and Glu-260 are colored purple. Middle and right, superposition of the structure from FGE and PvdO_{A506} structural model, highlighting the respective active-site residues at overlapping positions. The active-site Cys-272 of FGE is at exactly the same position as Glu-260 in PvdO.

bration time by adding 100 μ l of the protein (0.4 mg/ml in elution buffer) to a final concentration of 20 μ g/ml. As blank, the same volume of elution buffer was used, and blank data were subtracted. The settings for the Jasco V-650 spectrophotometer were the same as for the above-described dihydropyoverdine oxidation assays.

Pyoverdine isolation, the isoelectric focusing assay in conjunction with the chrome azurolS overlay assay, and the ultraperformance liquid chromatography–high-resolution MS analysis were carried out as reported previously (7, 8).

Bioinformatic methods

The initial classification of PvdO was performed employing the InterPro web service (29, 30). To generate the sequence

logo, PvdO homologs were identified by searching through all amino acid sequences of all complete and draft genomic sequences deposited in the Pseudomonas Genome Database (18) with phmmer version 3.1b (31). The redundancy was subsequently reduced by using the CD-HIT algorithm from the CD-HIT Suite (32), utilizing a similarity threshold of 0.95. Sequences were aligned with MAFFT version 7.310 (33) using the G-INS-i setting. The resulting sequence alignment was visualized using WebLogo 3 (34), plotting the probability of the occurrence of each amino acid at each position.

The distribution analysis was performed by searching the already downloaded sequences from the Pseudomonas Genome Database (18) with phmmer version 3.1b (31). Utilizing an in-house developed software, a taxonomy table reduced to species

Table 1
Primers used in this study

Name	Sequence	Restriction site	Purpose
pEXH5-RBS-F-MR	GGCGGGATCCGTTTAACTTTAAGAAGGAGATATAC	BamHI	Forward primer for subcloning from pEXH5 into pME6010
pEXH5-strep-term-R-MR	CCCTTTGAAATTCAAAAAACCCTCCCTGTCAGGGGGGGGTTTTTTTTTTTAC	EcoRI	Reverse primer for subcloning from pEXH5 into pME6010
pEXPT7-HA-term-R-MR	CCCTTTGAAATTCAAAAAACCCTCCCTGTCAGGGGGGGGTTTTTTTTTTTATAG	EcoRI	Reverse primer for subcloning from pEXH5 into pME6010 with HA-tag
PfA506-dpvdNO-F2-MR	GGCTAGTCCGGCACGTCGTACGGG	HindIII	Forward primer for <i>pvdMNO</i> right flanking region
PfA506-matpvdO-strep-R-MR	CGGAAACCAATCCAATC	HindIII	Reverse primer for cloning PvdO-coding region into pEXH5
PfA506-PvdM-DF-MR	ACCGTGTGGTTGTCGAAAGTAC		<i>pvdM</i> genomic deletion control primer
PfA506-PvdM-DR-MR	GGCCAGCAGTTGGTCTTGGAGTTC		<i>pvdM</i> genomic deletion control primer
PfA506-PvdM-F1-MR	CGCCTTAAGCTTTATGGCGGTGCATGAAGAAGAAGTCC	HindIII	Forward primer for <i>pvdM</i> left flanking region
PfA506-PvdM-F2-MR	CCTCAACTGACTGAGATGGCAATGACAAACCCTAAACCACCCAGAAAGTAC		Forward primer for <i>pvdM</i> right flanking region
PfA506-PvdM-F-MR	TCAGCGCATATGACAAAATCAGCGTTCGAAAAAGGCGCTGTATATC	NdeI	Forward primer for cloning PvdM-coding region into pEXH5
PfA506-PvdM-HA-R-MR	GGCTAAAAGCTTTAGCGGTAGTCCGGCACGTCGTACGGGTAGCGGTTGGCCCAAG	HindIII	Reverse primer for cloning PvdM-coding region into pEXH5
PfA506-PvdM-R1-MR	GGTTTTGGCGGTTTTTTTGGAC		Reverse primer for <i>pvdM</i> left flanking region
PfA506-PvdM-R2-MR	TGTCATTTGCCATCTCAGTTCAGTTGAGG		Reverse primer for <i>pvdM</i> right flanking region
PfA506-pvdO_D216A-F-MR	ATCTGGGATCCTTTGAGGTGCACTTGAAGGCTTCCG	BamHI	Primer for D216A exchange by oelPCR
PfA506-pvdO_D216A-R-MR	CTTTTGGCATGTATGCCATGACACGGCAATGT		Primer for D216A exchange by oelPCR
PfA506-pvdO_D257A-F-MR	CCGTCATGGCATACATGCCAAAAGGCAATTC		Primer for D257A exchange by oelPCR
PfA506-pvdO_D257A-R-MR	GCAATGCCTTGGGCGAGCGCCGGTGTGTTTT		Primer for D257A exchange by oelPCR
PfA506-pvdO_E179A-F-MR	CGCCCAAGGCAATTTGCCGCAATCTGTGTAG		Primer for E179A exchange by oelPCR
PfA506-pvdO_E179A-R-MR	CCCTTTGCAGCCGCGCAAGGCTACAGCAT		Primer for E179A exchange by oelPCR
PfA506-pvdO_E260A-F-MR	CCCTTTGGCGGCTGCAACGGGAAGGGGAAC		Primer for E260A exchange by oelPCR
PfA506-pvdO_E260A-R-MR	GCAATGACTTGGGGCGCCCGCCGCTGTGTTTT		Primer for E260A exchange by oelPCR
PfA506-pvdO_H188A-F-MR	GAAAACCGCGCGCGCCCGCCCACTGATTC		Primer for E260A exchange by oelPCR
PfA506-pvdO_H188A-R-MR	ACAGATCGCCAGGCGCCCAACACCTACG		Primer for H188A exchange by oelPCR
PfA506-pvdO_H218A-F-MR	TGAGTGTTTGGCGGCTGGCGGATGCTGTA		Primer for H218A exchange by oelPCR
PfA506-pvdO_H218A-R-MR	ATACACATTCGGCCATCATATACATGCCAAAGGCATTC		Primer for H218A exchange by oelPCR
PfA506-pvdO_M214A-F-MR	TACCCACCGAATGCTTTGGCGCTATGAC		Primer for M214A exchange by oelPCR
PfA506-pvdO_M214A-R-MR	GTGCATGTCATAGGCGCCAAAGGCATTCGG		Primer for M214A exchange by oelPCR
PfA506-pvdO_M217A-F-MR	CTTTGGCATGTATGACGCCCCACCGCAATGT		Primer for M217A exchange by oelPCR
PfA506-pvdO_M217A-R-MR	GCCGTGGCGTATACATGCAAAAGGCATTC		Primer for M217A exchange by oelPCR
PfA506-pvdO_N210A-F-MR	AGCTACCACCGCGCCCTTTGGCATGTAT		Primer for N210A exchange by oelPCR
PfA506-pvdO_N210A-R2-MR	TCATACATGCCAAAAGGCGCCCGGTGGGTAG		Primer for N210A exchange by oelPCR
PfA506-pvdO_Q187A-F-MR	ACAGCATCGCCCGCCACCCCAACACCTACG		Primer for Q187A exchange by oelPCR
PfA506-pvdO_Q187A-R-MR	GTAGGTGTTGGCGTGGCGGCGGATGCTGTA		Primer for Q187A exchange by oelPCR
PfA506-pvdO_Y215A-F-MR	TGGCATGCGCCGACATGCACGGCAATGTGTA		Primer for Y215A exchange by oelPCR
PfA506-pvdO_Y215A-R-MR	GTGCATGTCGGCATGCCAAAAGGCATTCGG		Primer for Y215A exchange by oelPCR
PfA506-PvdO-DF-MR	CTGCAGGAAACCTGGAAGCGGTGAG		<i>pvdO</i> genomic deletion control primer
PfA506-PvdO-DR-MR	CATGCAAAACGAAGTGTGGCGGTGAC		<i>pvdO</i> genomic deletion control primer
PfA506-PvdO-F1-MR	TTTAGCCGATCCCGAAGGCGTGGCATGATCTATG	BamHI	Forward primer for <i>pvdO</i> left flanking region
PfA506-PvdO-F2-MR	TCCCTTTGAAACGAGACGCTCCATGCGGCACTCTAATATCTTTGTAGG		Forward primer for cloning PvdO-coding region into pEXH5
PfA506-PvdO-F-MR	TTACCGCATATGACGCCATCCCGACTCAAACCGCTCAC	NdeI	Reverse primer for <i>pvdO</i> left flanking region
PfA506-PvdO-R1-MR	CATGAGGCGTCTCGTTTCAAAGGG		Reverse primer for <i>pvdO</i> left flanking region
PfA506-PvdO-R2-MR	GCAGCAAGCTTCCTGGTTCTTCTTGTCTGTAGG	HindIII	Reverse primer for <i>pvdO</i> right flanking region
PfA506-PvdP-DF-MR	GTTCAGTTCCTTGTCTGCTAGGTTG		<i>pvdP</i> genomic deletion control primer
PfA506-PvdP-DR-MR	CCGCGCAGATTTTCTGCTATTC		<i>pvdP</i> genomic deletion control primer
PfA506-PvdP-F1-MR	TGCTCTAAGCTTTTGGTTCGACATTCGGACACGTCGATGATCAC	HindIII	Forward primer for <i>pvdP</i> left flanking region
PfA506-PvdP-F2-MR	ACGCTTTAAAACGTTTTCAGGCGCTCTAGG		Forward primer for <i>pvdP</i> right flanking region
PfA506-PvdP-R1-MR	CGCGCTGCAACACGTTTTAAAGCGTTCATGCGCTTACCTTAGGAAACGGC		Reverse primer for <i>pvdP</i> left flanking region
PfA506-PvdP-R2-MR	TTAAACCCGGGAGGTACTGGGTAGCCTGTCCAGGCGTATCCGACGAG	XmaI	Reverse primer for <i>pvdP</i> right flanking region

Dihydropyoverdine oxidation by PvdO

level was constructed, and the identified homologs were classified accordingly. Subsequently, the number of found homologs in one species was divided by the total number of organisms attributed to the same species, giving the percentage of occurrence. To model the structure of PvdO, the SWISS-MODEL web service (35) was used and in conjunction with UCSF Chimera (36) and APBS (37), and the models were visualized. Sequence identities were calculated from alignments generated using Clustal Ω (38).

To visualize the genomic contexts of *pvdO* in multiple organisms, the MGcV web service (39) was used.

Author contributions—M. T. R. performed the experiments, prepared the figures, and analyzed the data together with T. B., and G. D. performed the MS analyses. T. B. conceived and coordinated the study. T. B. and M. T. R. wrote the paper. All authors reviewed the results and approved the final version of the manuscript.

Acknowledgment—We thank Sybille Traupe for technical support.

References

1. Ellermann, M., and Arthur, J. C. (2017) Siderophore-mediated iron acquisition and modulation of host-bacterial interactions. *Free Radic. Biol. Med.* **105**, 68–78 [CrossRef Medline](#)
2. Cézard, C., Farvacques, N., and Sonnet, P. (2015) Chemistry and biology of pyoverdines, *Pseudomonas* primary siderophores. *Curr. Med. Chem.* **22**, 165–186 [Medline](#)
3. Yeterian, E., Martin, L. W., Guillon, L., Journet, L., Lamont, I. L., and Schalk, I. J. (2010) Synthesis of the siderophore pyoverdine in *Pseudomonas aeruginosa* involves a periplasmic maturation. *Amino Acids* **38**, 1447–1459 [CrossRef Medline](#)
4. Drake, E. J., and Gulick, A. M. (2011) Structural characterization and high-throughput screening of inhibitors of PvdQ, an NTN hydrolase involved in pyoverdine synthesis. *ACS Chem. Biol.* **6**, 1277–1286 [CrossRef Medline](#)
5. Hannauer, M., Schäfer, M., Hoegy, F., Gizzi, P., Wehrung, P., Mislin, G. L. A., Budzikiewicz, H., and Schalk, I. J. (2012) Biosynthesis of the pyoverdine siderophore of *Pseudomonas aeruginosa* involves precursors with a myristic or a myristoleic acid chain. *FEBS Lett.* **586**, 96–101 [CrossRef Medline](#)
6. Nadal-Jimenez, P., Koch, G., Reis, C. R., Muntendam, R., Raj, H., Jeronimus-Stratingh, C. M., Cool, R. H., and Quax, W. J. (2014) PvdP is a tyrosinase that drives maturation of the pyoverdine chromophore in *Pseudomonas aeruginosa*. *J. Bacteriol.* **196**, 2681–2690 [CrossRef Medline](#)
7. Ringel, M. T., Dräger, G., and Brüser, T. (2016) PvdN enzyme catalyzes a periplasmic pyoverdine modification. *J. Biol. Chem.* **291**, 23929–23938 [CrossRef Medline](#)
8. Ringel, M. T., Dräger, G., and Brüser, T. (2017) The periplasmic transaminase PtaA of *Pseudomonas fluorescens* converts the glutamic acid residue at the pyoverdine fluorophore to α -ketoglutaric acid. *J. Biol. Chem.* **292**, 18660–18671 [CrossRef Medline](#)
9. Albrecht-Gary, A.-M., Blanc, S., Rochel, N., Ocaktan, A. Z., and Abdallah, M. A. (1994) Bacterial iron transport: coordination properties of pyoverdine PaA, a peptidic siderophore of *Pseudomonas aeruginosa*. *Inorg. Chem.* **33**, 6391–6402 [CrossRef](#)
10. Teintze, M., Hossain, M. B., Barnes, C. L., Leong, J., and van der Helm, D. (1981) Structure of ferric pseudobactin: a siderophore from a plant growth promoting *Pseudomonas*. *Biochemistry* **20**, 6446–6457 [CrossRef Medline](#)
11. Baysse, C., Budzikiewicz, H., Uría Fernández, D., and Cornelis, P. (2002) Impaired maturation of the siderophore pyoverdine chromophore in *Pseudomonas fluorescens* ATCC 17400 deficient for the cytochrome *c* biogenesis protein CcmC. *FEBS Lett.* **523**, 23–28 [CrossRef Medline](#)
12. Jacques, P., Ongena, M., Bernard, F., Fuchs, R., Budzikiewicz, H., and Thonart, P. (2003) Fluorescent *Pseudomonas* mainly produce the dihydroform of pyoverdine at low specific growth rate. *Let. Appl. Microbiol.* **36**, 259–262 [CrossRef Medline](#)
13. Bultreys, A., Gheysen, I., Maraite, H., and de Hoffmann, E. (2001) Characterization of fluorescent and nonfluorescent peptide siderophores produced by *Pseudomonas syringae* strains and their potential use in strain identification. *Appl. Environ. Microbiol.* **67**, 1718–1727 [CrossRef Medline](#)
14. Lamont, I. L., and Martin, L. W. (2003) Identification and characterization of novel pyoverdine synthesis genes in *Pseudomonas aeruginosa*. *Microbiology* **149**, 833–842 [CrossRef Medline](#)
15. Ochsner, U. A., Wilderman, P. J., Vasil, A. I., and Vasil, M. L. (2002) GeneChip[®] expression analysis of the iron starvation response in *Pseudomonas aeruginosa*: identification of novel pyoverdine biosynthesis genes. *Mol. Microbiol.* **45**, 1277–1287 [CrossRef Medline](#)
16. Yuan, Z., Gao, F., Bai, G., Xia, H., Gu, L., and Xu, S. (2017) Crystal structure of PvdO from *Pseudomonas aeruginosa*. *Biochem. Biophys. Res. Commun.* **484**, 195–201 [CrossRef Medline](#)
17. Teintze, M., and Leong, J. (1981) Structure of pseudobactin A, a second siderophore from plant growth promoting *Pseudomonas* B10. *Biochemistry* **20**, 6457–6462 [CrossRef Medline](#)
18. Winsor, G. L., Griffiths, E. J., Lo, R., Dhillon, B. K., Shay, J. A., and Brinkman, F. S. L. (2016) Enhanced annotations and features for comparing thousands of *Pseudomonas* genomes in the Pseudomonas Genome Database. *Nucleic Acids Res.* **44**, D646–D653 [CrossRef Medline](#)
19. Meury, M., Knop, M., and Seebeck, F. P. (2017) Structural basis for copper-oxygen mediated C–H bond activation by the formylglycine-generating enzyme. *Angew. Chem. Int. Ed. Engl.* **56**, 8115–8119 [CrossRef Medline](#)
20. Buongiorno, D., and Straganz, G. D. (2013) Structure and function of atypically coordinated enzymatic mononuclear non-heme-Fe(II) centers. *Coord. Chem. Rev.* **257**, 541–563 [CrossRef Medline](#)
21. Kovaleva, E. G., and Lipscomb, J. D. (2008) Versatility of biological non-heme Fe(II) centers in oxygen activation reactions. *Nat. Chem. Biol.* **4**, 186–193 [CrossRef Medline](#)
22. Holder, P. G., Jones, L. C., Drake, P. M., Barfield, R. M., Bañas, S., de Hart, G. W., Baker, J., and Rabuka, D. (2015) Reconstitution of formylglycine-generating enzyme with copper(II) for aldehyde tag conversion. *J. Biol. Chem.* **290**, 15730–15745 [CrossRef Medline](#)
23. Laemmli, U. K. (1970) Cleavage of structural proteins during the assembly of the head of bacteriophage T4. *Nature* **227**, 680–685 [CrossRef Medline](#)
24. Burnette, W. N. (1981) “Western Blotting”: electrophoretic transfer of proteins from sodium dodecyl sulfate-polyacrylamide gels to unmodified nitrocellulose and radiographic detection with antibody and radioiodinated protein A. *Anal. Biochem.* **112**, 195–203 [CrossRef Medline](#)
25. Towbin, H., Staehelin, T., and Gordon, J. (1979) Electrophoretic transfer of proteins from polyacrylamide gels to nitrocellulose sheets: procedure and some applications. *Proc. Natl. Acad. Sci. U.S.A.* **76**, 4350–4354 [CrossRef Medline](#)
26. Neuhoff, V., Arold, N., Taube, D., and Ehrhardt, W. (1988) Improved staining of proteins in polyacrylamide gels including isoelectric focusing gels with clear background at nanogram sensitivity using Coomassie Brilliant Blue G-250 and R-250. *Electrophoresis* **9**, 255–262 [CrossRef Medline](#)
27. Ize, B., Viarre, V., and Voulhoux, R. (2014) Cell fractionation. *Methods Mol. Biol.* **1149**, 185–191 [CrossRef Medline](#)
28. Taubert, J., Hou, B., Risselada, H. J., Mehner, D., Lünsdorf, H., Grubmüller, H., and Brüser, T. (2015) TatBC-independent Tata/Tat substrate interactions contribute to transport efficiency. *PLoS One* **10**, e0119761 [CrossRef Medline](#)
29. Jones, P., Binns, D., Chang, H.-Y., Fraser, M., Li, W., McAnulla, C., McWilliam, H., Maslen, J., Mitchell, A., Nuka, G., Pesseat, S., Quinn, A. F., Sangrador-Vegas, A., Scheremetjew, M., Yong, S.-Y., Lopez, R., and Hunter, S. (2014) InterProScan 5: genome-scale protein function classification. *Bioinformatics* **30**, 1236–1240 [CrossRef Medline](#)
30. Finn, R. D., Attwood, T. K., Babbitt, P. C., Bateman, A., Bork, P., Bridge, A. J., Chang, H.-Y., Dosztányi, Z., El-Gebali, S., Fraser, M., Gough, J., Haft, D., Holliday, G. L., Huang, H., Huang, X., et al. (2017) InterPro in 2017: beyond protein family and domain annotations. *Nucleic Acids Res.* **45**, D190–D199 [CrossRef Medline](#)
31. Eddy, S. R. (2011) Accelerated profile HMM searches. *PLoS Comput. Biol.* **7**, e1002195 [CrossRef Medline](#)

32. Huang, Y., Niu, B., Gao, Y., Fu, L., and Li, W. (2010) CD-HIT Suite: a web server for clustering and comparing biological sequences. *Bioinformatics* **26**, 680–682 [CrossRef Medline](#)
33. Katoh, K., and Standley, D. M. (2013) MAFFT multiple sequence alignment software version 7: improvements in performance and usability. *Mol. Biol. Evol.* **30**, 772–780 [CrossRef Medline](#)
34. Crooks, G. E., Hon, G., Chandonia, J.-M., and Brenner, S. E. (2004) WebLogo: a sequence logo generator. *Genome Res.* **14**, 1188–1190 [CrossRef Medline](#)
35. Biasini, M., Bienert, S., Waterhouse, A., Arnold, K., Studer, G., Schmidt, T., Kiefer, F., Gallo Cassarino, T., Bertoni, M., Bordoli, L., and Schwede, T. (2014) SWISS-MODEL: modelling protein tertiary and quaternary structure using evolutionary information. *Nucleic Acids Res.* **42**, W252–W258 [CrossRef Medline](#)
36. Pettersen, E. F., Goddard, T. D., Huang, C. C., Couch, G. S., Greenblatt, D. M., Meng, E. C., and Ferrin, T. E. (2004) UCSF Chimera: a visualization system for exploratory research and analysis. *J. Comput. Chem.* **25**, 1605–1612 [CrossRef Medline](#)
37. Baker, N. A., Sept, D., Joseph, S., Holst, M. J., and McCammon, J. A. (2001) Electrostatics of nanosystems: application to microtubules and the ribosome. *Proc. Natl. Acad. Sci. U.S.A.* **98**, 10037–10041 [CrossRef Medline](#)
38. Sievers, F., Wilm, A., Dineen, D., Gibson, T. J., Karplus, K., Li, W., Lopez, R., McWilliam, H., Remmert, M., Söding, J., Thompson, J. D., and Higgins, D. G. (2011) Fast, scalable generation of high-quality protein multiple sequence alignments using Clustal Omega. *Mol. Syst. Biol.* **7**, 539 [Medline](#)
39. Overmars, L., Kerkhoven, R., Siezen, R. J., and Francke, C. (2013) MGcV: the microbial genomic context viewer for comparative genome analysis. *BMC Genomics* **14**, 209 [CrossRef Medline](#)

Supplementary Information

PvdO is required for the oxidation of dihydropyoverdine as last step of fluorophore formation in *Pseudomonas fluorescens* *Michael T. Ringel¹, Gerald Dräger², and Thomas Brüser^{1,3}

From the ¹Institute of Microbiology, Leibniz Universität Hannover, Herrenhäuser Str. 2, 30419 Hannover, Germany, the ²Institute of Organic Chemistry, Leibniz Universität Hannover, Schneiderberg 1 B, 30167 Hannover, Germany

*Running title: *Dihydropyoverdine oxidation by PvdO*

List of supplementary material:

Video S1: Morphing animation of the two homology-modelled structures of PvdO using either formylglycine generating enzyme (FGE) from *Streptomyces coelicolor* (PDB 2Q17) or PvdO from *Pseudomonas aeruginosa* (PDB 5HHA) as template. Residues that have been exchanged for alanine's in this study are highlighted in blue.

Figure S1: Activity measurement of PvdO and the PvdO_{E260A} proteins in comparison to chemical autoxidation

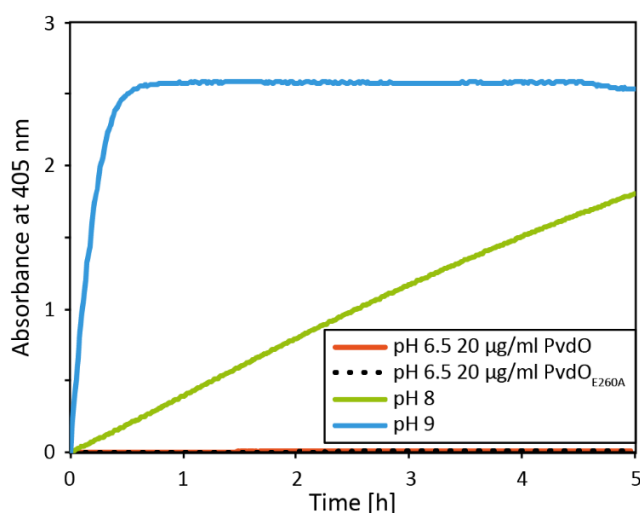


Figure S1: Activity measurement of PvdO and the PvdO_{E260A} proteins in comparison to chemical autoxidation. The purified PvdO and PvdO_{E260A}-proteins were tested for activity *in vitro* at pH 6.5 (as described in the methods section), under the same measurement conditions used for the chemical autoxidation that is shown for comparison (pH 8 and pH 9). Note that at pH 6.5 no autoxidation occurs and that there is no detectable *in vitro* activity of PvdO as purified. All values are corrected for blank measurements and the first measurement point was set to 0.

3.4. Additional data – Studies on the functional role of PvdN, PtaA and PvdM

To address a number of unresolved questions concerning the function of side-chain modifications of pyoverdines and the exact role of PvdM in pyoverdine biosynthesis, a number of additional assays were performed. The data obtained will be elaborated upon in the following sections.

3.4.1. Pyoverdine side-chain modifications and their implication in export

Since, as detailed in sections 3.1 and 3.2, the deletion-mutant strains lacking either PvdN or PtaA or even both, had no obvious defect in pyoverdine uptake, recycling or signaling even under a wide range of different environmental pH conditions, a key question remained to be answered, specifically: Which biological function do the side-chain modifications fulfill? One reasonable explanation for the necessity of side-chain modifications could be that one exporter of pyoverdine imposes a specificity on export. Since it is known that multiple exporters must be involved in pyoverdine export but only the PvdRT-OpmQ exporter has been directly (see section 1.4) implicated therein, we set out to test this hypothesis with a $\Delta pvdT$ - and a $\Delta pvdN\Delta pvdT$ double deletion mutant. Qualitatively, as estimated with a pyoverdine production plate assay, no obvious defect in pyoverdine export or growth on EDDHA could be

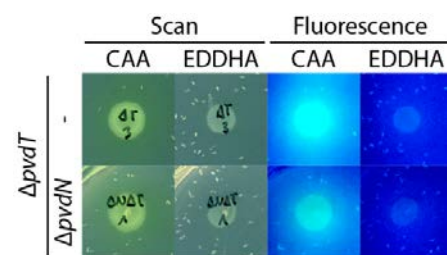


Figure 6: Pyoverdine export by the $\Delta pvdT$ - and the $\Delta pvdN\Delta pvdT$ double deletion mutants. Both the $\Delta pvdT$ - and the $\Delta pvdN\Delta pvdT$ double deletion mutant produce and export similar quantities of pyoverdine as evidenced by the green and the fluorescent halo around colonies grown on pyoverdine inducing casamino acid (CAA) medium. Furthermore, the strains are not impaired in iron acquisition demonstrated by growth on iron-depleted ethylenediamine di(*o*-hydroxy)phenylacetic acid (EDDHA) containing CAA medium.

observed for either of the two mutant strains (Figure 6). Although these data were unexpected in regard to our hypothesis, a mass-spectrometric and IEF analyses with chrome azurol S (CAS) overlay assay were carried out to investigate the exact chemical composition of the produced pyoverdines (Figure 7). Interestingly, the mass spectrometry (MS) results revealed that the ratio between C_5 (α -ketoglutaric- [2] and glutamic acid [1]) and C_4 (succinamide [3] and succinic acid [4]) side-chain variants (Figure 7A; upper panel) was inverted compared to wild-type pyoverdine produced and isolated under the same conditions (section 3.1; Figure 4B). Usually, the C_5 side-

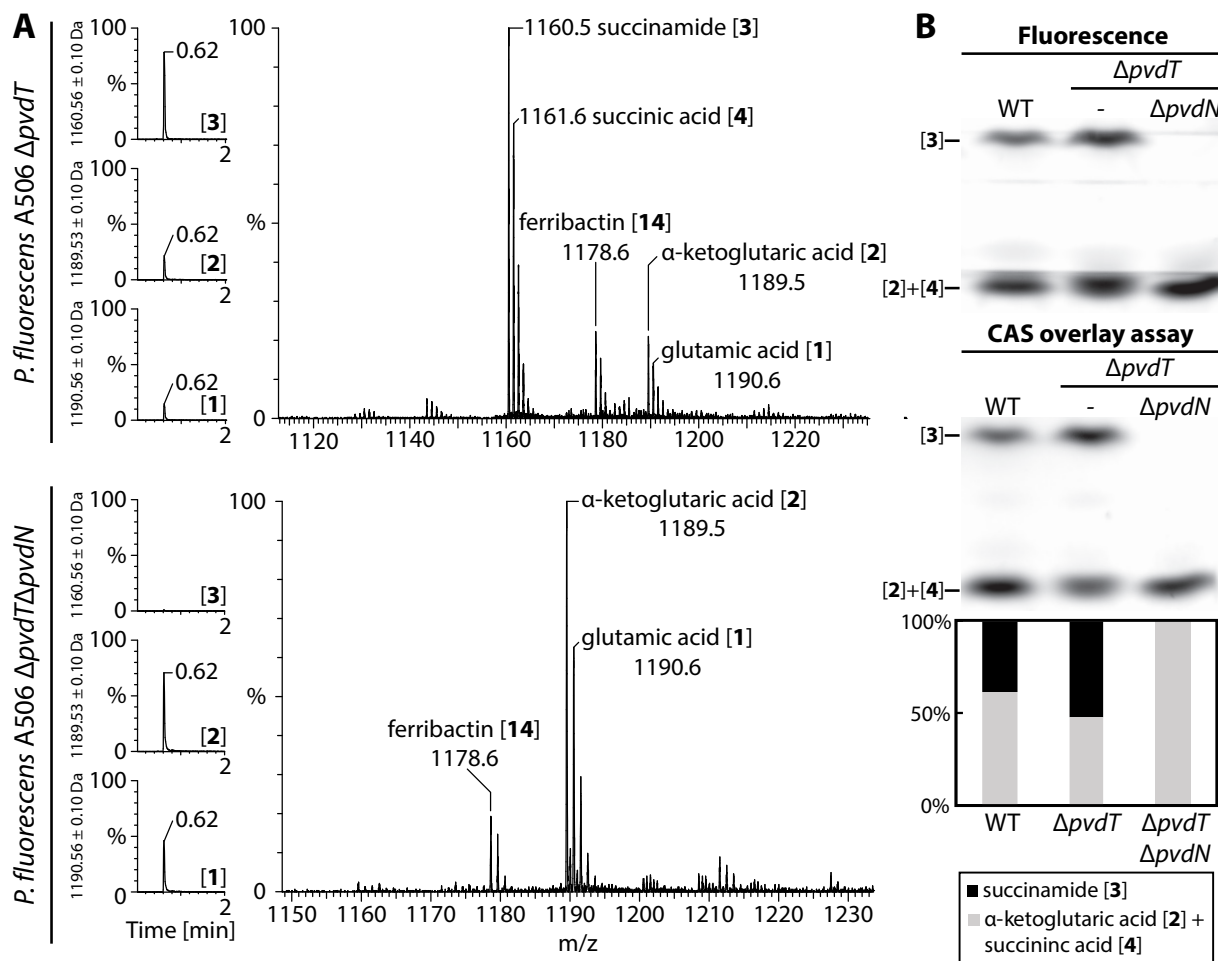


Figure 7: The $\Delta pvdT$ mutant strain is impaired in the export of C_5 pyoverdine side-chain variants. (A) Mass spectrometry results, depicting the mass-filtered UHPLC chromatograms for the glutamic acid- [1], the α -ketoglutaric acid- [2] and the succinamide [3] variants on the left. On the right, the corresponding mass-spectra of the peak at 0.62 min are shown. The mass peaks were assigned and numbered according to the structures depicted in Figure 4. (B) IEF gels detected by fluorescens (top) and by the CAS overlay assay (middle). Numbers to the left of the gels indicate the identified pyoverdine variants as depicted in Figure 4. By integration of the bands obtained from the lanes of the CAS overlay assay, the ratio between C_4 and C_5 variants could be approximated (bottom). Because the succinic acid [3] variant could not be completely separated from the α -ketoglutaric acid [2] variant, it contributes to the intensity thereof.

chain variants are the predominant form under the conditions used for production, which is obviously not the case in a $\Delta pvdT$ mutant strain. As expected, the $\Delta pvdN\Delta pvdT$ double deletion mutant did not produce any C_4 pyoverdine variants anymore (Figure 7A; lower panel).

However, to verify the obtained results with an independent method, the isolated pyoverdines were analyzed via IEF in conjunction with the CAS overlay assay (Figure 7B). When comparing the ratio of C_4 - to C_5 variants between the wildtype and the $\Delta pvdT$ deletion mutant, the data suggests a similar tendency as obtained with MS, although it is not as pronounced (Figure 7B; lower panel). Since both fluorescence and iron-affinity of pyoverdines are pH-dependent, the obtained intensities cannot be easily compared more quantitatively, thus a more accurate

quantification of all pyoverdine variants for future experiments *via* MS would be preferable. Furthermore, a quantitative pyoverdine-formation assay needs to be performed to investigate any defects in export of the $\Delta pvdT$ - and a $\Delta pvdN\Delta pvdT$ double deletion mutants.

3.4.2. Towards understanding the function of PvdM

The data obtained in section 3.3 indicated that PvdM is required for pyoverdine formation, since a $\Delta pvdM$ deletion mutant could neither produce pyoverdine, nor could it grow on iron-depleted EDDHA supplemented CAA medium, which could be fully complemented *in trans* by a HA-tagged variant of PvdM (section 3.3; Figure 3). However, it was not clear in which process, in regard to pyoverdine biogenesis, PvdM was involved. To examine whether PvdM is generally relevant for pyoverdine biogenesis, a co-occurrence analysis with PvdP for all available genomes from the pseudomonas genome database (281) was performed. Since it is known that PvdP is required for pyoverdine formation, the strict co-occurrence of PvdM with PvdP (Figure 8) indicates that PvdM may also be indispensable for pyoverdine biogenesis, recycling or signaling in other *Pseudomonas* strains. Furthermore, PvdM does not occur in strains that cannot produce pyoverdine, which can be concluded from the absence of PvdM from strains that do not contain PvdP. However, to obtain a better understanding of the potential function of PvdM, a more

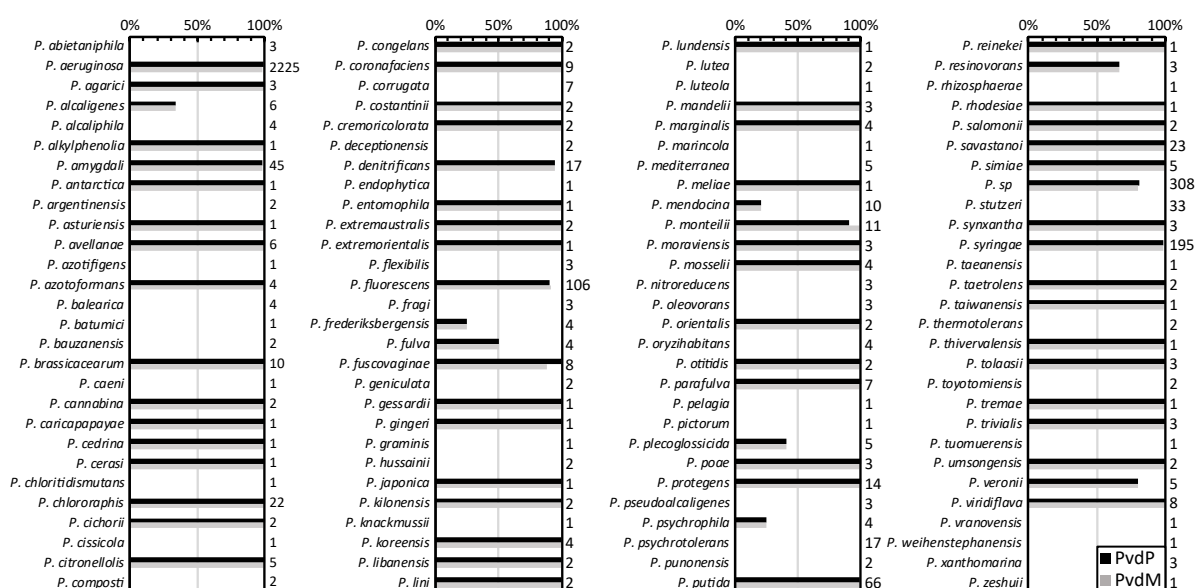


Figure 8: Co-occurrence analysis of PvdM and PvdP homologs within the genus *Pseudomonas*. The numbers behind the bar-graphs indicate the aggregate number of genomes analyzed for the respective species.

into the periplasm. To evaluate possible enzymatic functions of PvdM, it was classified using the InterPro webservice (282, 283). The classification predicted that PvdM belonged to the family of M19 peptidases, but according to the MEROPS database (284), it belonged to the non-peptidase homologs (identifier: MER0471750), since it lacked a conserved active site residue. The extended analysis using the NCBI CDD classification system (285) confirmed the classification by InterPro, showing that PvdM belongs to membrane associated renal dipeptidases (identifier: cd01301). The potential active site residues were mostly conserved, although an otherwise highly conserved glutamic acid residue was replaced by a leucine (L₁₇₉) and a glutamine (Q₂₅₄) substitutes a typical histidine residue. To evaluate whether these exchanges are characteristic for PvdM homologs, the sequences of all identified homologs of PvdM were redundancy reduced employing an identity threshold of 0.95 using the CD-Hit algorithm contained in the CD-HIT Suite (286). The resulting sequences were aligned using the T-Coffee webservice (287). The alignment was visualized as sequence logo with WebLogo 3 (288; Figure 9D). Interestingly, the analysis revealed that the L₁₇₉ exchange is present in all aligned PvdM homologs and the Q₂₅₃ substitution is also rather conserved, although some sequences have retained the original H₂₅₃ residue. To evaluate the structural similarity of the active site, PvdM was homology-modeled with SWISS-MODEL (289) using the known crystal structure of the PvdM ortholog from *P. aeruginosa* PAO1 (PDB 3B40; 290) as template, which has a sequence identity of 77% as calculated with ClustalΩ (291). Subsequently, the structure was visualized with UCSF Chimera (292) in conjunction with APBS (293) to calculate the electrostatic surface potential (Figure 9E). The structure shows a negatively charged region surrounding the active site. The putative dimerization interface is located on the outside of the protein and the back of the enzyme has a neutral electrostatic surface potential, which may be in contact with the membrane. The superposition of the active site residues with those of the human renal dipeptidase (hrDP; PDB 1ITQ; 26% sequence identity) illustrate how conserved the active site geometry surrounding the binuclear Zn²⁺ center is. However, two major differences are directly apparent: 1) the glutamic acid residue from hrDP is substituted by a leucine residue L₁₇₀ and 2) an additional amino acid D₃₉₄ is possibly involved in the coordination

of zinc. Since it is reasonable to assume from these results that PvdM is a membrane associated peptidase, one possible involvement would be the maturation of PvdQ, if the autoproteolytic activity needed support *in vivo*. To test this hypothesis, both a $\Delta pvdQ$ and a $\Delta pvdM\Delta pvdQ$ strain, *in trans* complemented with a C-terminally *Strep*-tagged PvdQ-variant were subject to a

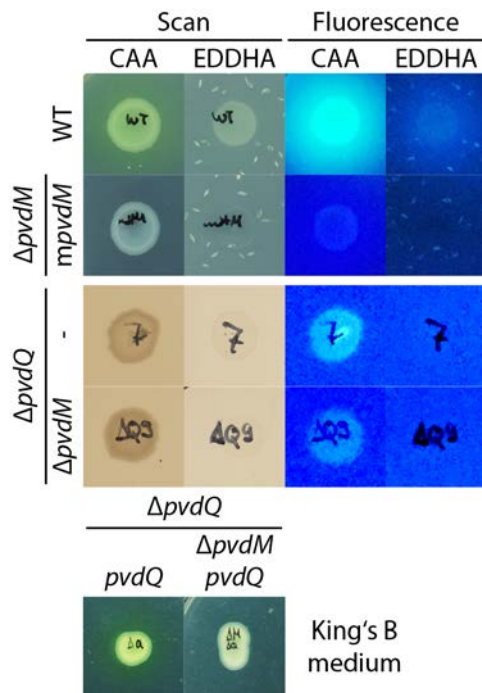


Figure 10: Comparison of pyoverdine production of various mutant strains. The phenotype of the $\Delta pvdM$ deletion strain complemented *in trans* with a PvdM variant lacking the membrane anchor region (mpvdM) does not produce pyoverdine and cannot grow on iron-depleted (EDDHA) medium (top panel). Neither the $\Delta pvdQ$ nor the $\Delta pvdM\Delta pvdQ$ strain can grow on iron-depleted (EDDHA) medium (middle) but the colony of the $\Delta pvdQ$ strains shows slightly more residual fluorescence than the $\Delta pvdM\Delta pvdQ$ double deletion strain. The $\Delta pvdQ$ strain complemented *in trans* with a *Strep*-tagged variant of PvdQ can produce pyoverdine again as evidenced by the greenish halo around the colony when grown on pyoverdine inducing King's B medium (bottom). On the other hand, the $\Delta pvdM\Delta pvdQ$ complemented with the same construct cannot produce pyoverdine.

subcellular fractionation with subsequent SDS-PAGE/Western blotting (Figure 9C). The C-terminal β -fragment after autoproteolytic cleavage of PvdQ (~60 kDa) could be detected in the periplasmic fraction of both strains, therefore, the maturation of PvdQ is independent of PvdM. Since the $\Delta pvdQ$ and the $\Delta pvdM\Delta pvdQ$ strain are both not able to grow on iron-depleted media and do not secrete pyoverdine into the medium (Figure 10, middle), both strains were complemented *in trans* with a C-terminally *Strep*-tagged variant of PvdQ and tested for the ability to produce pyoverdine (Figure 10, bottom). The complemented $\Delta pvdQ$ strain produced and excreted pyoverdine into the medium, whilst the complemented $\Delta pvdM\Delta pvdQ$ double deletion strain did not. Interestingly, the $\Delta pvdQ$ colony shows a slightly more intense residual fluorescence in comparison to the $\Delta pvdM\Delta pvdQ$ double deletion strain, which suggests that the pyoverdine chromophore can be formed in the $\Delta pvdQ$ strain.

As a membrane anchored protein can either face into the cytoplasm or into the periplasm, a residual activity may be expected when the enzyme is produced without the membrane anchor in case it would face towards the cytoplasm. To test this hypothesis, a variant of PvdM was

constructed that did not contain the signal-peptide/membrane anchor referred to as mPvdM, which was tested for its qualities regarding *in trans* complementation of a $\Delta pvdM$ mutant strain. However, mPvdM could not complement the $\Delta pvdM$ phenotype (Figure 10, top) indicating that the putative enzyme faces towards the periplasm, which agrees with the bioinformatic results, although this needs further investigation by alternative methods. Nevertheless, it could be proven that the membrane anchor is required for PvdM function.

3.4.3. Experimental procedures

The experimental procedures described here only refer to the section 3.4.

Strains and growth conditions- For physiological studies, the strain *P. fluorescence* A506 was employed, whilst *Escherichia coli* DH5 α λ *pir*⁺ was used for cloning. *E. coli* was cultivated at 37 °C and *P. fluorescence* at 30 °C. For standard cultivations, LB-medium (1% (w/v) tryptone, 1% (w/v) NaCl, 0.5% (w/v) yeast extract) was used. Antibiotics were supplanted at the following final concentrations when appropriate: 100 μ g/ml ampicillin, 50 μ g/ml kanamycin, 20 μ g/ml tetracycline. Pyoverdine plate assays on CAA and EDDHA supplemented CAA medium were performed as described previously (294, 295). King's B medium was prepared as described by King *et al.* (296), and may be used in the same way as CAA medium to monitor pyoverdine formation as described above.

Genetic methods and plasmids- The construction of plasmids and scar- and marker-less deletion strains were carried out as previously described (294, 295). However, the arabinose inducible construct for the *in trans* expression of *pvdQ* shown in Figure 9C was assembled starting at the pEXH5-*pvdQ*-strep intermediate. The *pvdQ*-sequence was amplified with the primers pEXPT7-RBS-SacI-F-MR and pEXPT7-XmaI-R-MR and was cut with SacI and XmaI. A shuttle plasmid carrying an arabinose-inducible promotor system was constructed starting from pUC19. The pUC19 plasmid was cut with BspHI, which removed the ampicillin resistance cassette. A kanamycin resistance cassette was amplified from the plasmid pAH120 (297) using the primers pAH120-Kan-PciI-F-MR and pAH120-Kan-PciI-R-MR and was cut with PciI. The obtained fragment was ligated into the pUC19 (298) fragment and transformed into *E. coli* DH5 α λ *pir*⁺ via

the transformation procedure described by Inoue *et al.* (299). The resulting clones were screened for plasmids carrying insertions that pointed into the same direction as the original kanamycin resistance cassette. The resulting plasmid was termed pUCK19F, which was subsequently cut with NdeI and XbaI. Using the primers araRed-F-MR and araRed-R-MR, the region containing an arabinose inducible λ Red system (consisting of the components γ , β and *exo* as well as *araC*) from plasmid pKD46 (300) was amplified and cut with NdeI and XbaI. After ligation of the obtained fragments, the resulting plasmid pUCK19F-araRed was cut with HindIII and SbfI. The minimal origin of replication (for replication in *Pseudomonas*), as described by Janson *et al.* (301) of the plasmid pUCP18-RedS (302) was amplified with the primers Pori-F-MR and Pori-R-MR, then cut with SbfI and HindII and ligated into the plasmid backbone, resulting in the shuttle plasmid pUCKP19F-araRed. This plasmid was then cut with SacI and XmaI, excising most of the λ Red system from the plasmid, but retained the *araC* and P_{bad} regions. The sequence fragment amplified from pEXH5-*pvdQ*-strep and cut with SacI and XmaI was then ligated into the cut plasmid, yielding the arabinose inducible plasmid pUCKP19F- P_{bad} -*pvdQ*-strep. All constructs were verified by restriction analysis and sequencing. All primers used in this study are listed in Table 1:

Table 1: Primers used in this study. Restr. site, restriction site.

Name	Sequence	Restr. site	Purpose
araRed-F-MR	CGCGGCTCTAGATTAT GACAACCTTGACGGCTA C	XbaI	Forward primer for cloning the arabinose inducible λ Red system from pKD46
araRed-R-MR	GCCCGCCATATGCTAC TGGTATTGGCACAAC CTG	NdeI	Reverse primer for cloning the arabinose inducible λ Red system from pKD46
pAH120-Kan-PciI-F-MR	CACTTAACATGTGGGA AATGTGCGCGGAACCC	PciI	Forward primer for cloning the kanamycin resistance cassette
pAH120-Kan-PciI-R-MR	ACATCCACATGTATCG TGGCCGGATCTTGCG	PciI	Reverse primer for cloning the kanamycin resistance cassette
pEXH5-RBS-F-MR	GGCGCGGGATCCGTTT AACTTTAAGAAGGAGA TATAC	BamHI	Forward primer for subcloning from pEXH5 into pME6010
pEXH5-strep-term-R-MR	CCCCTTGAATTCAAAA AAAACCCCGCCCTGTC AGGGGCGGGTTTTTTT TTTTTACTTTTTCGAAC TGCGGGTGGCTCC	EcoRI	Reverse primer for subcloning from pEXH5 into pME6010
pEXH5-RBS-SacI-F-MR	GGCGCGGAGCTCGTTT AACTTTAAGAAGGAGA TATAC	SacI	Forward primer for subcloning from pEXH5 into pUCKP19F

Name	Sequence	Restr. site	Purpose
pEXH5-XmaI-R-MR	TTTGC GCCCGGTTT ACTTTTCGA ACTGCGG GTGGCTCC	XmaI	Reverse primer for subcloning from pEXH5 into pUCKP19F
PfA506-matPvdM-F-MR	ATACGGCATATGGGCT TGCTGGTCTGGGATCA GTGGTTCAAGG	NdeI	Forward primer for cloning the PvdM-coding region into pEXH5
PfA506-matPvdM-strep-R-MR	CCGATTAAGCTTTTAC TTTTTCGA ACTGCGGGT GGCTCCAGCGGTTGGC CAAGGGTTTGGCGGCT TTTTGGAC	HindIII	Reverse primer for cloning the PvdM-coding region into pEXH5, adding a <i>Strep</i> -tag
PfA506-pvdQ-DF-MR	GCGTTCGTAAATTCGG CCGCCATCATCGTG	-	<i>pvdQ</i> genomic deletion control primer
PfA506-pvdQ-DR-MR	GTTC AATACTCACACC GCTCGCCACCAAG	-	<i>pvdQ</i> genomic deletion control primer
PfA506-pvdQ-F1-MR	GCGCCAAAGCTTGGGC TTCAAAGGTCTGTCAG GCGTAG	HindIII	Forward primer for <i>pvdQ</i> left flanking region
PfA506-pvdQ-F2-MR	GTGAAGGAGTAGGGCA GACGCGCAACCCCTTG ATGC	-	Forward primer for <i>pvdQ</i> right flanking region
PfA506-pvdQ-F-MR	TTCCCCTCTAGAAATA ATTTTGTTTAACTTTA AGAAGGAGATATACAT GTGATTATTTCCAACG GGTTGTCCAGAGTGGG C	XbaI	Forward primer for cloning the PvdQ-coding region into pEXH5
PfA506-pvdQ-R1-MR	GGGTTGCGCGTCTGCC CTACTCCTTCACCACG CCGACTCCACAGTCAA ATTGAACAC	-	Reverse primer for <i>pvdQ</i> left flanking region
PfA506-pvdQ-R2-MR	TTAGCGGGATCCGGTC CACGGCGCAGAATCGT TTTGCCAAAG	BamHI	Reverse primer for <i>pvdQ</i> right flanking region
PfA506-PvdQ-strep-R-MR	GGCCGCAAGCTTTTAC TTTTTCGA ACTGCGGGT GGCTCCACTCCTTCAC TGTTTGGATTTGGTAG TGC	HindIII	Reverse primer for cloning the PvdQ-coding region into pEXH5, adding a <i>Strep</i> -tag
PfA506-pvdT-DF-MR	GTTGCCGCCAGGTCGA GATAGCTTG	-	<i>pvdT</i> genomic deletion control primer
PfA506-pvdT-DR-MR	CACGGTAGGTTTGCAG CAGTTCATC	-	<i>pvdT</i> genomic deletion control primer
PfA506-pvdT-F1(2)-MR	AGACAGGGATCCGGAC AGATCCGCAAGATCCA TGTCGAG	BamHI	Forward primer for <i>pvdT</i> left flanking region
PfA506-pvdT-F2-MR	GGGTTGATGTGACCAC GCCACTGTTCCGGCTTC ATGCCGGCCCCGTAAAG C	-	Forward primer for <i>pvdT</i> right flanking region
PfA506-pvdT-F-MR	TTCCCCTCTAGAAATA ATTTTGTTTAACTTTA AGAAGGAGATATACAT	XbaI	Forward primer for cloning the PvdT-coding region into pEXH5

Name	Sequence	Restr. site	Purpose
	GTGACCACGCCACTGA TCGAACTCAAGAAC		
PfA506-pvdT-R1-MR	CAGTGGCGTGGTCACA TCAACCC	-	Reverse primer for <i>pvdT</i> left flanking region
PfA506-pvdT-R2(2)-MR	ATCAGCAAGCTTATCA GGCCCGAAGTCAGGGT GTAGAAGG	HindIII	Reverse primer for <i>pvdT</i> right flanking region
PfA506-pvdT-strep-R-MR	GGCCGCAAGCTTTTAC TTTTCGAACTGCGGGT GGCTCCATTCACTGGT CAACGCCTTAACCG	HindIII	Reverse primer for cloning the PvdT-coding region into pEXH5, adding a <i>Strep</i> -tag
Pori-F-MR	AATTTACCTGCAGGGA AAGGCAGGCCGGGCCG TGGTG	SbfI	Forward primer for cloning the minimal <i>ori</i> from pUCP18-RedS
Pori-R-MR	AATATTAAGCTTCCTC TCAGGCGCCGCTGGTG CCG	HindIII	Reverse primer for cloning the minimal <i>ori</i> from pUCP18-RedS

Biochemical methods- The standard methods for SDS-PAGE and successive Western blotting were carried out according to established protocols (303–305). Western blots were developed according to the manufacturer's instructions using either *Strep*-Tactin-HRP conjugate (IBA, Göttingen, Germany) for *Strep*-tagged proteins, or a HA-tag polyclonal antibody (TaKaRa Clontech, CA, USA) in conjunction with anti-mouse-HRP conjugate (Carl Roth, Karlsruhe, Germany) for HA-tagged proteins. The blots were imaged with the MF-ChemiBIS 4.2 imaging system (DNR Bio-Imaging Systems, Jerusalem, Israel).

The subcellular fractionation of *P. fluorescens* A506 was carried out as described previously (306) with minor modifications to the original procedure as reported in (295). For the arabinose inducible system, the expression was induced after 1 h of cultivation with a final concentration of 0.1% (w/v) L-arabinose and the cultivation was continued until cells reached the required OD₆₀₀.

The isolation of pyoverdine, the IEF analysis in conjunction with the CAS overlay assay and the UPLC-HR-MS-analysis were carried out as previously described (294, 295).

Bioinformatic methods- To classify PvdM, the InterPro webservice (282, 283) in conjunction with the NCBI CDD webservice (285) was used. To evaluate the potential function of PvdM as peptidase, the MEROPS webservice was employed (284). The structure of PvdM was homology modelled using the SWISS-MODEL webservice (289), which was visualized using UCSF Chimera (292) in

conjunction with APBS (293) and PDB2PQR (307, 308). Relevant crystal structures and sequences were obtained from the protein data bank (PDB) (290) and the UniProt database (309) respectively. The sequence logo of PvdM was generated by identifying PvdM homologs within all amino acid sequences of all complete- and draft genomic sequences deposited at the pseudomonas database (281) using phmmer v 3.1b (310) with a cutoff of 2.5×10^{-56} . Sequences were redundancy reduced employing the CD-HIT algorithm from the CD-HIT Suite (286), using a cutoff of 0.95 to facilitate the sequence alignment performed with the T-Coffee webservice (287). The sequence alignment was visualized with WebLogo 3 (288), plotting the probability of occurrence for each amino acid. Sequence identities were calculated with Clustal Ω (291). The co-occurrence analysis of PvdP and PvdM was performed using the same approach described for identifying PvdM homologs, which was extended by assigning found homologs to a taxonomy table reduced to species-level with an in-house developed software. The semi-quantitative pyoverdine quantification of C₅ and C₄ variants of pyoverdine was performed using Fiji (311).

4. Concluding discussion and outlook

At the beginning of this thesis, we sought to extend our knowledge about the involvement of the putative periplasmic enzymes PvdM, PvdN and PvdO in pyoverdine biosynthesis, uptake, recycling and regulation to explain yet unresolved enigmas of pyoverdine research. The data obtained during this endeavor allows for the formulation of a more detailed model of pyoverdine biogenesis (Figure 11), which extends the current model in two major points:

- 1) The previously reported and well known side-chain modifications of pyoverdine can now be accounted for in the extended biosynthetic scheme.
- 2) The oxidative cyclization of ferribactin generating the mature chromophore proceeds *via* two distinct steps.

These two findings and the hypothetical involvement of PvdM will be discussed in greater detail in the following sections, elaborating which conclusions can be drawn from the extended model.

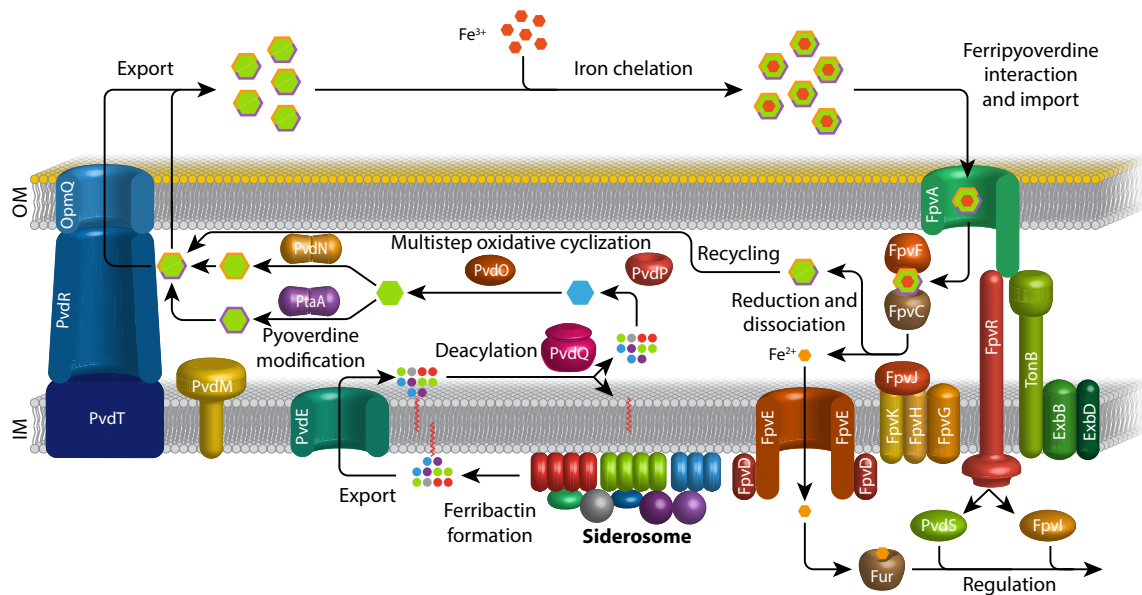


Figure 11: Extended model of pyoverdine biosynthesis, export, recycling and signaling in *P. fluorescence* A506. The acylated ferribactin precursor is synthesized in the periplasm by the NRPSs PvdL, PvdI and PvdD in conjunction with the auxiliary enzymes PvdH, PvdF and PvdA, which are required for the synthesis of L-Dab and L-fOHOrn. Furthermore, the putative adenylation-domain activating protein Mbth may support NRPS-dependent synthesis, while the soluble thioesterase PvdG may facilitate inter-NRPS transfer of peptide building blocks (see section 1.6 for details). The cytoplasmic enzymes form membrane associated complexes referred to as “siderosomes”, probably to avoid adverse effects by cytoplasmic toxicity and to implement an efficient biosynthetic machinery. The acylated ferribactin is exported into the periplasm *via* PvdE, where it is deacylated by the NTN-type hydrolase PvdQ. Subsequently, the copper dependent tyrosinase like enzyme PvdP catalyzes the oxidative cyclization, resulting in dihydropyoverdine. Consequently, PvdO, possibly in conjunction with PvdP or other yet unidentified proteins, facilitates the final oxidative step, yielding the characteristic pyoverdine chromophore. Thereafter, a branched side-chain modification-pathway transforms the original L-glutamic acid side chain either to the succinamide, catalyzed by PvdN, or the α -ketoglutaric acid, catalyzed by PtaA. The modified pyoverdines are then exported into the extracellular compartment, where they fulfill their natural function (see sections 1.4 and 1.5 for details).

4.1. Pyoverdine side-chain modifications

Although a number of side-chain modifications of pyoverdines have been known for many years (14, 236–240), their biosynthetic origin as well as their biosignificance have remained a mystery. Nevertheless, the inherent physicochemical properties of these variants were exploited by the widely used method of siderotyping, which produces a characteristic siderophore band-pattern by making use of the changes in the isoelectric points (pI) by IEF and subsequent visualization by in-gel fluorescence detection or by the chrome azurol S (CAS) overlay assay (242). In an early study on the biogenesis of the side-chain modifications by Schäfer *et al.* in 1991 (241), a systematic examination revealed that the ratios between the glutamic acid-, the α -ketoglutaric acid-, the succinamide and the succinic acid variants of pyoverdine were influenced significantly by the incubation time of the bacterial culture and also somewhat by pH and iron-content of the cultivation medium. From their observations, Schäfer *et al.* concluded that the glutamic acid variant must be produced by reductive transamination from the α -ketoglutaric acid variant but that both variants must be in a chemical equilibrium, possibly catalyzed by an enzyme. Furthermore, it was suggested that both the α -ketoglutaric acid- and the succinamide variant were the true primary products, since both were present from the beginning of pyoverdine production and therefore, the succinic acid variant must be an artifact of alkaline amide hydrolysis. Moreover, the iron-concentration in the cultivation medium correlated inversely with the ratio between C₄ and C₅ variants but no explanation for this phenomenon could be given. Based on the observation that all known modifications were intermediates of the citric acid cycle, a possible involvement was implied (241). Later, also dihydropyoverdine- and dihydropyoverdine-7-sulfonic acid variants carrying various side-chains could be identified (312). However, only after the realization that ferribactin is a precursor in pyoverdine biosynthesis (223, 224, 220, 225–227), in conjunction with the observation that ferribactin usually contains only the glutamic acid side-chain², it was concluded that glutamic acid could be the precursor of all observed side-chain variants (15). Nevertheless, a biological function could not be assigned to the pyoverdine variants and the sequence of modifying reactions could not be experimentally established.

Based on the assumption that glutamic acid is truly the precursor of all pyoverdine variants, our investigations began with the analysis of PvdN. After classification of PvdN with the InterPro webservice (282, 283), which suggested that the enzyme belonged to the pyridoxal phosphate (PLP) containing class-V amino-transferases, we originally thought that PvdN might catalyze the transamination reaction leading towards the α -ketoglutaric acid variant. This was based on the fact that transaminations belong to the well-known repertoire of PLP catalyzed reactions (reviewed in 315, 316). However, to our surprise, the UPLC-HR-MS analysis of pyoverdine variants produced by the $\Delta pvdN$ mutant suggested a completely different role. Obviously, the conversion of glutamic acid to the succinamide is catalyzed by the unusual PLP containing enzyme PvdN, which was hypothesized to proceed *via* a novel PLP catalyzed oxidative decarboxylation under retention of the amine (section 3.1; Figure 7B; 294). PLP is a well-known and versatile cofactor, involved in the catalysis of transaminations, decarboxylations, racemizations, β -eliminations, β -substitutions, retro-aldol reactions, γ -eliminations, γ -substitutions, Claisen- and retro-Claisen condensations (315, 316). However, a reaction identical to the one described for PvdN, involving a PLP cofactor, was unprecedented. Therefore, the reaction catalyzed by PvdN is mechanistically highly interesting, since it probably proceeds *via* a radical intermediate involving molecular oxygen. The only so far known similar reaction mechanism is catalyzed by the enzyme CcbF, which is involved in the biosynthesis of the lincosamide antibiotic celesticetin (317) produced by *Streptomyces caelestis*. Unlike PvdN, CcbF catalyzes the oxidative decarboxylation and deamination, which yields the carboxylic acid instead of the amide. However, PvdN is not only unusual because of its novel reaction mechanism but also in respect to the subcellular compartment where the reaction proceeds. Whilst CcbF is a cytoplasmic enzyme, PvdN is a twin-arginine translocation (Tat) substrate that is translocated into the periplasm after folding and acquisition of the cofactor PLP. It could be demonstrated that a PvdN_{K216A} variant, which is

² There are only two known exceptions to this rule: 1) It was observed that *P. fluorescence* G173 produces a ferribactin-derivative under some cultivation conditions that carries a glutamic acid side chain either partially or fully converted to a hydroxamic acid (313) and 2) the strain *P. fluorescence* ATCC 17400 produces a ferribactin with a succinamide side-chain (314).

impaired in PLP binding, is not translocated into the periplasm but instead trapped in the membrane (section 3.1; Figure 6B). This is remarkable in two ways: 1) PvdN is the first Tat-substrate known to carry a PLP cofactor and 2) it is known that other periplasmic PLP containing enzymes, such as the amino acid racemase produced by *P. taetrolens*, can be exported *via* the general secretion system (Sec) (318), which exports proteins in an unfolded state, being prohibitive to cofactor acquisition in the cytoplasm. Since PvdN forms a dimer (319) it may be speculated that a defect in binding of the PLP cofactor may disturb the subunit interaction, supported by the fact that PLP binding occurs in close proximity to the dimerization interface. The disturbed dimerization may thus cause the observed defect in translocation. This inevitably leads to the question, whether PvdN is translocated and processed as a dimer, which would fit the data obtained for other Tat substrates (320, 321), or as a monomer, but the exact mechanism remains to be elucidated. It will be interesting to investigate the mechanistic details of the catalyzed reaction and translocation. Also, it will be important to understand which structural features of PvdN determine its mode of action, which will help to gain insights into the details of the reaction mechanism but also facilitate bioinformatic predictions. Possible approaches to validate the proposed reaction mechanism will be discussed together with PtaA at the end of this section.

The enzyme PtaA was postulated to exist after realizing that the PLP containing enzyme PvdN did not catalyze the transamination reaction converting the glutamic acid- into the α -keto glutaric acid variant as initially anticipated (section 3.1; Figure 7A; 294). From the experiences gained during the investigation of the enzyme PvdN it was hypothesized that the sought-after transaminase could also be a Tat substrate. Therefore, a targeted *in silico* analysis was performed, first predicting all putative Tat substrates from *P. fluorescence* A506 and then classifying all putative substrates to assess their PLP binding potential (section 3.2; Table 1; 295). This analysis indicated two proteins possibly possessing the specified properties, specifically PvdN, which was expected, and an uncharacterized protein PflA506_4424. A thorough literature research in combination with further bioinformatic characterizations revealed that a homolog of PflA506_4424 existed in *P. aeruginosa* PA01, namely PA2531, which is PvdS-dependently

upregulated in response to iron starvation (164) and had indeed been proven to be a periplasmic transaminase (322). Remarkably, the latter aspect reported by Calhoun *et al.* in 2001 (322) had been neglected in previous studies, although it should be stated here that the authors could not assign any involvement of the observed activity to pyoverdine maturation, since the study investigated periplasmic chorismate mutases. However, taken together, the data supported the assumption that PflA506_4424 may be involved in pyoverdine maturation, which could be proven by the UPLC-HR-MS analysis of pyoverdine variants produced by a Δ *ptaA* mutant (section 3.2; Figure 5; 295). A more detailed biochemical characterization revealed that PtaA forms a homodimer (section 3.2; Figure 3D), and that a PtaA_{K224A} variant impaired in PLP binding is trapped in the membrane, resembling the data obtained for PvdN. Furthermore, to assess the impact of the K224A exchange that abolished PLP-binding, the protein stability was investigated employing differential scanning calorimetry, which revealed that PLP-binding does indeed stabilize the overall protein structure. This may explain the observed defect in translocation of the PtaA_{K224A} variant, consistent with our model that PLP binding supports correct folding and thereby may influence a stable dimerization. However, the distribution analysis of PtaA homologs within the genus *Pseudomonas* revealed that PtaA is not strictly conserved in all pyoverdine producing fluorescent pseudomonads, not even within the same species (section 3.2; Figure 7; 295), which is consistent with the observed non-essentiality of PtaA for pyoverdine production. This prompted us to investigate whether PtaA might have a more general function, which was approached by identifying putative homologs in all available reference proteomes with the hmmsearch webservice (323). The analysis revealed that homologs could be identified even within distantly related bacteria such as the α -proteobacterium *Zymomonas mobilis* and some acidobacteria (section 3.2; Figure S2; 295). The study conducted by Calhoun *et al.* (322) included an evaluation of possible substrates, using phenylalanine and α -ketoglutaric acid for their activity assay, suggesting that the substrate specificity of PtaA may be rather broad. Together with the fact, that the genetic neighborhood of PtaA is neither conserved between *P. aeruginosa* PAO1 and *P. fluorescence* A506, nor is *ptaA* associated with genes involved in pyoverdine biosynthesis, it

may be concluded that PtaA has a more general function, other than pyoverdine modifications. This is also the reason for terming the enzyme PtaA, which stands for “periplasmic transaminase A”.

The data presented in sections 3.1 and 3.2 reveal that the observed side-chain modifications

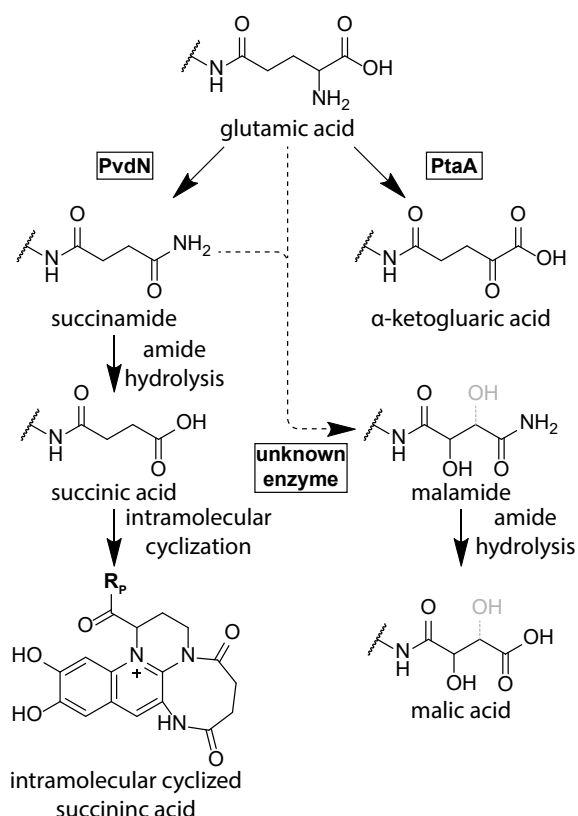


Figure 12: Biosynthetic scheme for side-chain modifications encountered in pyoverdines. Beginning with the glutamic acid variant, two possible but mutually exclusive routes can be taken. Either PvdN catalyzes the oxidative decarboxylation under retention of the amine, leading to the succinamide variant, or PtaA transforms the glutamic acid into the α-ketoglutaric acid by transamination. However, both products cannot be interconverted and the oxidative decarboxylation under retention of the amine is not reversible for obvious reasons. The succinamide can hydrolyze, which is accelerated under alkaline conditions, yielding the succinic acid variant. Subsequently, the succinic acid can form the intramolecularly cyclized succinic acid variant that is stabilized under slightly acidic conditions. Nevertheless, the enzymes involved in malamide formation have not been identified yet, thus the precursor of malamide is not known and can either be glutamic acid or the succinamide (indicated by the dotted lines). As with succinic acid, malamide can hydrolyze under alkaline conditions yielding malic acid. However, the orientation of the attachment of malamide and malic acid is currently under discussion (indicated by the dotted gray hydroxy-groups), although the orientation facing the hydroxy-group towards the amine is currently preferred, as elaborated by Budzikiewicz *et al.* 2007. Please refer to the text for details.

are attributable to the periplasmic enzymes PvdN and PtaA. Summarizing the obtained results for the various mutants of PtaA and PvdN, a general biosynthetic scheme can be postulated (Figure 12). Evidently, the side-chain variants are not derived from the citric acid cycle as implied by Schäfer *et al.* (241) but are instead generated in the periplasmic compartment by an enzyme catalyzed divergent pathway. This can be concluded from the observations that the $\Delta pvdN$ strain cannot produce any C₄ variants of pyoverdine anymore, whilst the $\Delta ptaA$ mutant in turn is impaired in the generation of the α-ketoglutaric acid variant. Furthermore, in pyoverdine isolated from the $\Delta ptaA$ mutant the succinamide-variant is predominant, not the glutamic acid variant, which suggests a divergent pathway, that is shifted into one direction by the absence of the enzyme catalyzing the alternative reaction. Also, resulting from the higher relative amounts of the succinamide form, the hydrolysis product

thereof, namely the succinic acid variant and the intramolecularly cyclized succinic acid variant are more abundant. Finally, a $\Delta pvdN\Delta ptaA$ double deletion mutant produces only the glutamic acid variant, arguing for the biosynthetic scheme presented in Figure 12. This also resolves the question, whether the α -ketoglutaric acid is the predecessor of the glutamic acid variant, as originally hypothesized by Schäfer *et al.* (241), since obviously glutamic acid is the precursor to all other observed variants. Furthermore, it is evident from the data, that both pathways are mutually exclusive, since the α -ketoglutaric acid variant cannot be directly converted to the succinamide variant and *vice versa*. However, since our model strain *P. fluorescence* A506 does not produce the malamide- or malic acid variants, it was impossible to determine the biosynthetic precursor for these. It may be hypothesized that the succinamide variant is hydroxylated by an unknown enzyme. Another possibility would be that the hydroxylation is produced in one step with the decarboxylation under retention of the amine, although such a reaction is not easily envisaged. Considering the reasonings by Budzikiewicz *et al.* from 2007 (314) concerning the malamide side-chain orientation, a hydroxylating enzyme oxidizing the succinamide side-chain would be preferable. This is based on the observation of a McLaferty rearrangement within the malamide side-chain during mass-spectrometry, suggesting an inverse orientation thereof (314), which would complicate the conception of a reaction scheme based on PLP-chemistry alone even further. Another alternative would be a two-step reaction, proceeding *via* a γ -hydroxyglutamic acid intermediate that is subsequently decarboxylated under retention of the amine by PvdN. However, no such intermediates have yet been identified. Interestingly, a $\Delta ccmC$ mutant of *P. fluorescence* ATCC 17400 not only produces a wide variety of chromophore intermediates but also side-chain modifications not common to the wildtype strain (232). The authors suggested that, in the $\Delta ccmC$ mutant, the periplasm is more reducing compared to the wildtype, which was explicitly correlated with the impaired maturation of the pyoverdine chromophore (232). Nevertheless, it could not be deduced, how the mutation could have affected side-chain modifications. It will be

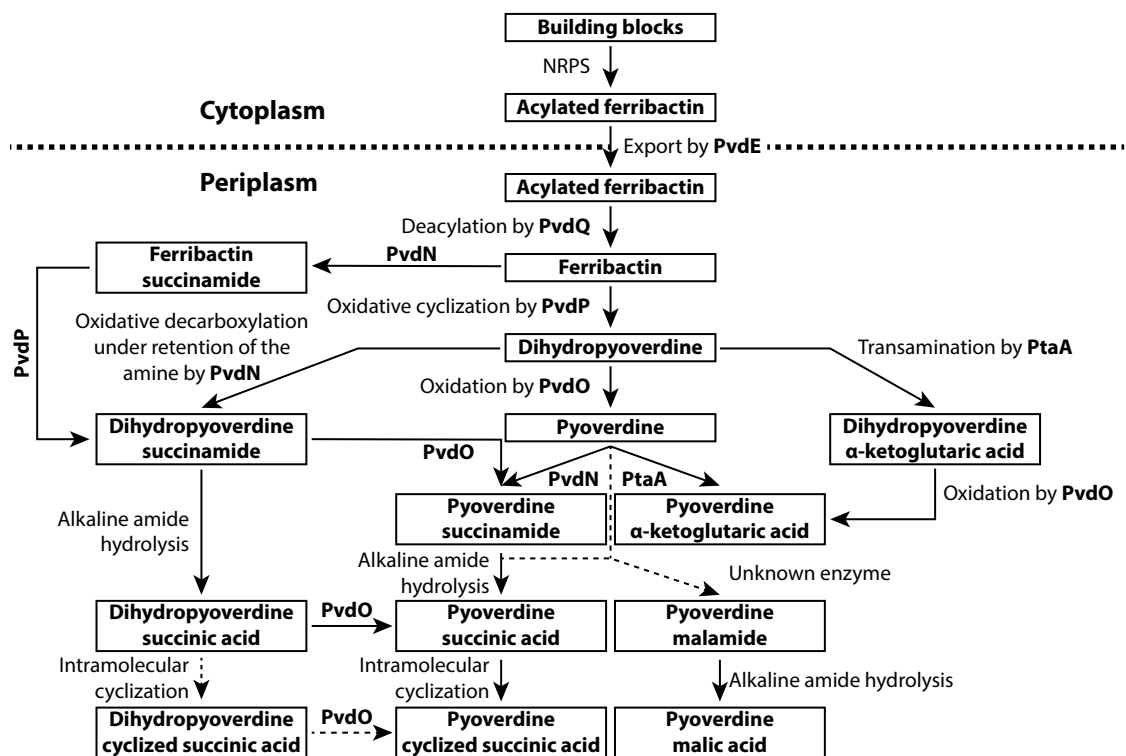


Figure 13: Integrative scheme of the chronological order of pyoverdine biosynthesis steps, including all studied reactions in the periplasmic space. The chronological order of observed side-chain modifications illustrates a broad substrate specificity of the enzymes PvdN and PtaA. Beginning with the acylated ferribactin precursor, synthesized in the cytoplasm and subsequently exported into the periplasm *via* PvdE, the periplasmic modifications ensue. The first step is the deacylation catalyzed by PvdQ. As observed by Budzikiewicz *et al.* 2007, ferribactin can already be converted to its succinamide form, implying that PvdP can catalyze the oxidative cyclization from both precursors. The already cyclized intermediate dihydropyoverdine has been detected with both side-chain modifications (section 3.3; Figure 4), indicating that both PtaA and PvdN accept dihydropyoverdine as substrate, which can then be oxidized by PvdO. Finally, Pyoverdine can also be modified by PvdN and PtaA. Malamide derivatives of earlier intermediates have not been observed yet. Dotted lines indicate hypothetical steps.

interesting to explore the relation of CcmC to pyoverdine formation. Despite the formulation of a hierarchical biosynthetic scheme regarding the generation of side-chain modifications, it is tempting to formulate an equivalently hierarchical and thereby chronological periplasmic maturation pathway as depicted in Figure 11. In that scheme, for the sake of simplicity, the side-chain modifications occur after maturation of the chromophore. However, it should not be assumed that these reactions occur in such a strict chronological order, as the MS-data indicate that the side-chain modifications introduced by PvdN and PtaA can already occur in the non-oxidized intermediate dihydropyoverdine (section 3.3; Figure 4). Furthermore, Budzikiewicz *et al.* (314) observed a ferribactin intermediate with a succinamide side-chain, indicating that PvdN also accepts ferribactin as substrate. However, no malamide variants of ferribactin or dihydropyoverdine have yet been observed, indicating a later maturation. This is in support of the

hypothesis, that additional enzymatic steps may be necessary to generate the malamide derivative, such as oxidations. Nevertheless, with the ongoing improvement of mass-spectrometric equipment, further intermediates will surely be discovered, as it seems that the enzymes PvdN and PtaA accept non-oxidized or cyclized precursors of pyoverdine albeit their reaction may proceed with a slower reaction kinetics, illustrating that the side-chain modifications occur simultaneously and are in competition with one another. The preferred substrate may be the fully oxidized pyoverdine, thus proceeding with the fastest kinetics. The observed intermediates are summarized in Figure 13.

Yet, even after understanding how the side-chain modifications are accomplished in the periplasm, their biological function remains a mystery. The observation that the side-chain modifications had a large influence on the pI of pyoverdine led to the hypothesis that the overall charge of pyoverdines under different environmental pH-conditions may be favorable for uptake or recycling. However, no difference in growth on iron-depleted media of a $\Delta pvdN$ mutant strain in comparison to the wildtype strain could be observed over a wide range of strongly buffered pH-conditions (section 3.1; Figure 5; 294). Nevertheless, these assays cannot account for other environmental influences encountered in a rhizosphere environment, such as adsorption. It could be that pyoverdines may be stored in the periplasm by adhering to the inner membrane, since the periplasmic space has a pH of approx. 6.5 and the α -ketoglutaric acid variant of pyoverdine would have a negligible overall charge under these conditions. This would also enhance the efficiency of the membrane-efflux pump PvdRT-OpmQ because pyoverdine would not freely float around in the periplasm. Therefore, a $\Delta pvdT$ mutant would need to export less of the α -ketoglutaric acid pyoverdine variant compared to the wildtype. To test this hypothesis, a $\Delta pvdT$ and a $\Delta pvdT\Delta pvdN$ strain were constructed and their produced pyoverdine variants were subject to UPLC-HR-MS and IEF analysis (section 3.4.1; Figure 7). Indeed, the $\Delta pvdT$ mutant seemed to be impaired in export of the α -ketoglutaric acid variant. However, the export of the succinamide variant was not impaired, which may be explained by the involvement of an alternative, not yet identified exporter. Nevertheless, considering that the $\Delta pvdT$ mutant strain seems to be specifically

compromised in the export of the α -ketoglutaric acid variant, it is remarkable that a $\Delta pvdN\Delta pvdT$ double deletion mutant, which cannot produce the succinamide variant, is at least qualitatively not impaired in pyoverdine export in comparison to the $\Delta pvdT$ mutant strain (Figure 6). If the hypothesis concerning the biased export *via* PvdRT-OpmQ is correct, how can this observation be reconciled? One possibility is that an excess of pyoverdine accumulates in the periplasm of the $\Delta pvdN\Delta pvdT$ double deletion mutant, which leaks across the outer membrane at some point. This hypothesis could be tested by microscopy, as the periplasmic pyoverdine is fluorescent and can thus be visualized with a fluorescence microscope (137). However, the unknown pyoverdine exporter may have a bias towards exporting the succinamide variant but maybe it also allows for a limited export of the α -ketoglutaric acid variant. To examine these differences, quantitative pyoverdine formation assays need to be performed for the evaluation of the amount of exported pyoverdine for each mutant.

Although the overall understanding of pyoverdine side-chain modifications has been advanced by the presented data (Figure 13), some questions regarding PvdN and PtaA remain. Of prominent importance is the validation of the proposed reaction mechanism for PvdN. To investigate this question, a fully ^{15}N labeled glutamic acid pyoverdine variant could be produced in the $\Delta pvdN\Delta ptaA$ strain. Then a pyoverdine deficient mutant will need to be constructed that does not carry the enzymes for periplasmic modifications, for instance by creating a $\Delta pvdL\Delta pvdN\Delta ptaA$ triple knockout strain, which can then be complemented with either *ptaA* or *pvdN* *in trans*. The complemented strains could then be fed with the ^{15}N labeled pyoverdine and subsequently analyzed by UPLC-HR-MS. If the proposed mechanism for PvdN is valid, then the ^{15}N label will be retained in the succinamide form after being transformed by PvdN. However, the ^{15}N labeled glutamic acid pyoverdine variant may also be used as substrate for *in vitro* assays, if the enzyme PvdN can be produced and isolated in an active state in sufficient quantities. In that case, the reaction may be allowed to proceed in an $^{18}\text{O}_2$ atmosphere, which would then result in an ^{18}O labeled amide, proving the incorporation of molecular oxygen. Furthermore, the amine-accepting carbonyl compound for the regeneration of PLP in the PtaA reaction mechanism is unknown,

which could be investigated by tracing the ^{15}N through the metabolome of the complemented triple-mutant. Furthermore, the role of PtaA in other organisms, such as *Z. mobilis* should be investigated. Knowledge gained thereby may complete the picture in regard to the true function of PtaA in pseudomonads. Finally, the glutamic acid variant produced by $\Delta pvdN\Delta ptaA$ strains may facilitate the generation of novel “trojan horse” antibiotics, by providing a simple access to a free amine group for modification at a position within the molecule that is not prone to sterical hindrance during import (275).

4.2. Chromophore maturation

Initially, three different chromophore cyclization reactions have been proposed on the basis of discovered intermediates or other chemical/biochemical evidences (see section 1.6 for details). However, the now most widely accepted variant is the one proposed by Dorrestein *et al.* (228, 229), which is depicted in Figure 4E. Nevertheless, it should be noted that one of the major breakthroughs in the field was the realization, that ferribactin is a precursor to pyoverdine/dihydropyoverdine, which was based on two main observations: 1) Ferribactins, dihydropyoverdines and pyoverdines produced by one organism always shared the same peptide backbone and 2) isopyoverdines could elegantly be explained by the rotation of the D-tyrosine residue around its bond connected to the L-Dab residue (Figure 4D; 222–224, 220, 225–227). However, the alternative cyclization based on the observation of trihydroxylated “pseudoverdin-” and dihydropyoverdine-7-sulfonic acid intermediates suggested a different mechanism for the oxidative cyclization reaction based on a modified intramolecular Bucherer reaction, mostly promoted by Budzikiewicz *et al.* (Figure 4F; 230, 225, 231, 226, 232, 233). Both proposed reaction mechanisms were based on scientifically sound biochemical data, thus a decision between both pathways would need an unequivocal and conclusive chemical demonstration of the proposed intermediates and enzymatic functions. In a study regarding the uncharacterized periplasmic protein PvdP and its involvement in pyoverdine biogenesis by Nadal-Jimenez *et al.* in 2014 (266), the authors could prove that this enzyme converted ferribactin into mature pyoverdine *in vitro*. Since the enzyme seemed to resemble a tyrosinase with a dinuclear copper center, the authors

avored the oxidative cyclization mechanism as proposed by Dorrestein *et al.* and furthermore justifiably claimed that the other until then uncharacterized enzymes PvdM, PvdN and PvdO must be involved in the observed side-chain modifications, which now turns out to be partially true. However, in an effort to determine the function of the uncharacterized protein PvdO in the periplasmic maturation pathway, we discovered that a $\Delta pvdO$ strain could still grow on iron depleted media but that no fluorescent pyoverdine was formed (section 3.3; Figure 3). This observation unexpectedly challenged the role of PvdP in the maturation of the pyoverdine chromophore. Nevertheless, it was also clear from the data that, unlike the $\Delta pvdO$ strain, a $\Delta pvdP$ deletion mutant could not grow on iron-depleted media. This posed a new question, specifically, which pyoverdine intermediate would allow growth on iron-depleted media and at the same time display no characteristic yellow-green fluorescence? The answer to this question reached back to the initial observation of dihydropyoverdine in 1981 by Teintze & Leong (223), at that time better known as “pseudobactin A”. Dihydropyoverdine obviously exhibits the observed characteristics, particularly, it displays no yellow-green fluorescence and is able to promote growth on iron-depleted media (324). The analysis of the extracted pyoverdine-precursors by UPLC-HR-MS substantiated this conclusion (section 3.3; Figure 4), proving that the $\Delta pvdO$ strain produced dihydropyoverdine instead of pyoverdine. How could this observation be reconciled with the explicit formulation that PvdP alone is responsible for the oxidative cyclization of the chromophore? The data presented in section 3.3 (Figure 5AB) suggest that dihydropyoverdine is the true product of PvdP and that the *in vitro* conditions, specifically the alkaline reaction-buffer, may have led to an artificial autoxidation. Surprisingly, in *in vivo* experiments increased copper-concentrations could also complement the $\Delta pvdO$ phenotype. The explanation for this phenomenon is purely speculative but it may be envisaged that PvdP, when overloaded with copper, may catalyze both oxidative steps required for maturation. A possibly preferable hypothesis is that copper leads to oxidative stress, which thus results in the formation of highly reactive hydroxy- and peroxy-radicals (325) that may artificially complete the oxidative cascade in the periplasm.

However, nothing is known about the reaction mechanism of PvdO, although two important residues could be identified (section 3.3; Figure 7), specifically D₂₅₇ and E₂₆₀. According to our original hypothesis, at least one of these residues may have been involved in metal chelation. As potential metal cofactor, an Fe²⁺ center was proposed, based on the putative His-His-Glu binding site. Such mononuclear non-heme iron binding sites, referred to as 2-His-1-carboxylate facial triad (although there exist variations on this theme) are well-known and enzymes containing these catalyze a wide variety of oxidation reactions, including desaturations (reviewed in 326–332). Nevertheless, no metal cofactor could be detected in the purified enzyme *via* ICP-MS, therefore it remains speculative whether the cofactor was lost during purification or whether such a metal cofactor even exists. It is clear from the data that PvdO is required *in vivo* to perform the last oxidative step but a hypothetical mechanism could not be proposed, especially since the attempted *in vitro* reactions did not succeed. Reasons for the inactivity may have been the loss of a cofactor or absence of a co-substrate, the absence of a functional electron transport chain or maybe PvdO acts as auxiliary protein by activating or enhancing the function of another enzyme. The observation that a $\Delta ccmC$ mutant impaired in hemoprotein biogenesis is also impaired in the oxidative cyclization reactions required to form functional pyoverdine (333, 334, 232, 335, 336) suggests that a functional electron-transport chain or potentially a yet unidentified hemoprotein is important for the correct electron flux. All these aspects need to be investigated further, necessitating a fully functional *in vitro* assay. A first step towards the optimization of the *in vitro* system may be the addition of artificial electron acceptors to imitate a functional electron transport chain. On the other hand, it will be important to find potential interaction partners of PvdO considering that hypothetically hemoproteins may be involved in catalysis.

In regard to the proposed oxidative cyclization reactions it may be noted that the data prove that dihydropyoverdine is a true intermediate in pyoverdine biogenesis as its oxidation requires the protein PvdO. Taken together with the recent observation of a dihydroxylated ferribactin precursor termed hydroxyferribactin in *Azotobacter vinelandii* (337), the oxidative cyclization reaction postulated by Dorrestein *et al.* (228, 229) seems to be preferable to all other alternatives.

4.3. Putative role of PvdM in pyoverdine biogenesis, recycling and signaling

In our analysis of PvdM, PvdN and PvdO, only the function of PvdM remains enigmatic. The putative enzyme PvdM is required for pyoverdine production and a $\Delta pvdM$ mutant cannot grow on iron-depleted media (section 3.3; Figure 3), which could be complemented *in trans* by an HA-tagged PvdM variant. However, the role of PvdM remained obscure, especially when considering that all essential steps of pyoverdine biosynthesis can be explained satisfactorily. Furthermore, a classification of PvdM revealed that it belongs to the class of membrane-bound M19 dipeptidases although potentially lacking an essential residue involved in zinc-chelation (see section 3.4.2 for details). No step directly involved in pyoverdine biosynthesis requires a potential peptidolytic activity. This leads to the assumption that PvdM must be involved either in the processing of important enzymes required for pyoverdine biosynthesis, such as PvdQ, or it may be involved in signaling, uptake or export. The investigation of PvdM activity can therefore not proceed *via* the analysis of exported pyoverdine intermediates, that has proven useful in case of PvdN, PtaA and PvdO. To investigate whether PvdM is generally important for pyoverdine biogenesis in fluorescent pseudomonads, a co-occurrence analysis with PvdP was performed, which revealed a strict conservation of both proteins within all identified fluorescent pseudomonads (Figure 8). To examine the potential role of PvdM within the suggested pathways, the protein subcellular localization was predicted with a number of methods (Figure 9A), which however was not unambiguous, thus the localization was verified by subcellular fractionation (Figure 9B). The results suggest that PvdM is a membrane-associated dipeptidase. In combination with the observation that a PvdM variant lacking the membrane anchor (mPvdM) showed no residual activity, in conjunction with the bioinformatic analysis, it may be speculated that the protein is anchored to the cytoplasmic membrane facing into the periplasm (Figure 10). As it is known that PvdQ needs to be processed to form an active hetero-dimer, a possible involvement of PvdM was suggested, although the processing of PvdQ was observed to be autoproteolytic *in vitro*, which may be different under *in vivo* conditions. The results of the subcellular fractionation obviously showed that PvdQ-maturation proceeds without the involvement of PvdM (Figure 9C). A more

detailed bioinformatic analysis revealed that all PvdM homologs from fluorescent pseudomonads carried a conserved exchange of an important glutamic acid residue (Figure 9D), when compared to other dipeptidases. For the human renal dipeptidase (hrDP), it was shown that the corresponding E₁₂₅ residue retains 11% activity when exchanged against a Gln and that activity is abolished when exchanged against an Asp or a Cys residue (338). These data inevitably suggest that the corresponding conserved L₁₇₀ exchange in PvdM may inactivate the putative dipeptidase activity. However, further important residues have been identified in the hrDP that are at least functionally substituted in the PvdM variant, specifically, H₂₀ (339) is conserved as H₆₀, H₁₅₂ (339) is substituted by Y₁₉₇, H₁₉₈ (339) is substituted by Q₂₄₅, H₂₁₉ (340) is conserved as H₂₆₆ and a recent computational study has demonstrated the importance of D₂₈₈ (341) which is also conserved as D₃₉₁. Furthermore, by homology-modeling of PvdM using the known crystal-structure of the PvdM ortholog from *P. aeruginosa* PAO1 and analysis of the metal-coordination center, an additional amino acid could be implicated in metal binding, namely D₃₉₄ (Figure 9EF), which may thereby provide a stable zinc-binding site. When compared to the known structure of hrDP, resolved in 2002 by Nitanaï *et al.* (342), the potential active-site residues from PvdM show a significant overlap with those of the known active site from hrDP (Figure 9F). The residues implicated in a potential dimerization-site are also conserved. It may thus be speculated that PvdM is an active membrane associated dipeptidase that forms a homodimer. The (h)rDP is renowned for its activity towards β -lactam-, penem-, carbapenem antibiotics and dipeptides (343–347) but has also been suggested to be involved in the conversion of leukotriene D₄ to E₄ and glutathione metabolism (348, 349) and is known to be competitively inhibited by cilastatin (343) and bestatin (347). The structure and enzymatic function of a close homolog of hrDP from *S. coelicolor* (Sco3058) have been elucidated (350), which revealed that the enzyme hydrolyzes a large variety of dipeptides, although the preferred substrate was identified as L-Arg-D-Asp. However, it is complicated to envisage a mechanism in pyoverdine biosynthesis, where a dipeptidase reactivity would be necessary. One of the few unknown steps requiring a membrane-associated peptidolytic activity is found within the regulation cascade, specifically the “site-1-like” peptidase (S1P)

involved in cleavage of FpvR after the pyoverdine has bound to the outer-membrane receptor FpvA (section 1.5; Figure 3). If PvdM were to be this peptidase, then a deletion would abolish pyoverdine production, since the ECF PvdS could not be liberated from the membrane. This would result in a complete abolishment of pyoverdine production due to the strict regulatory mechanisms involved. To prove that PvdM is not directly involved in an essential step of pyoverdine biosynthesis, an elegant approach could be chosen, specifically, a $\Delta fpvR\Delta pvdM$ double knockout strain would have to be constructed. This would result in the lack of the anti-sigma factor FpvR, which usually sequesters PvdS and FpvI to the membrane, thereby inactivating them. In the mutant-strain, the ECFs PvdS and FpvI need not be liberated from the membrane by activating the proteolytic cascade involved in FpvA-FpvR-dependent signaling. However, iron-starvation would still be necessary to induce pyoverdine production, since the formation of PvdS and FpvI is suppressed by Fur in the presence of sufficient iron. Thus, a $\Delta fpvR\Delta pvdM$ double knockout strain would need to be able to form pyoverdine under iron-starvation, otherwise PvdM is essential for a different step in biogenesis, sensing or export. Assuming that PvdM is the searched-for S1P, then this would have important clinical implications. As stated above, there exist known inhibitors for the homolog hrDP, specifically cilastatin (343), which is already in use in combination with hydrolysis sensitive antibiotics for human treatment of infections. It would be plausible that cilastatin or a cilastatin derivative may inhibit PvdM and thereby the pyoverdine signaling cascade, which would be straightforward to test. This in turn would not only downregulate pyoverdine-related genes but also virulence-related genes such as those encoding for the exotoxin A (182–184), the PrpL endopeptidase (185) and possibly also the alkaline protease AprA (186–188).

5. References

1. Gessard, M. C. (1892) Sur la fonction fluorescigène des microbes. In: Institut Pasteur, Ed. *Annales de l'Institut Pasteur*, Paris: Masson, **6**, 801–823
2. Schroeter, J. (1872) Ueber einige durch Bacterien gebildete Pigmente. In: Cohn, F., Ed. *Beiträge zur Biologie der Pflanzen*, Breslau: J. U. Kern's Verlag, **1**, 2. Heft, 109–126
3. Turfitt, G. E. (1936) Bacteriological and biochemical relationships in the *pyocyaneus-fluorescens* group: The chromogenic function in relation to classification. *Biochem. J.* **30**, 1323–1328
4. Turfitt, G. E. (1937) Bacteriological and biochemical relationships in the *pyocyaneus-fluorescens* group: Investigations on the green fluorescent pigment. *Biochem. J.* **31**, 212–218
5. Turfreijer, A. (1941) *Pyoverdinen, de groen fluoresceerende kleurstoffen van pseudomonas fluorescens*, Amsterdam
6. Elliott, R. P. (1958) Some properties of pyoverdine, the water-soluble fluorescent pigment of the pseudomonads. *Appl. Microbiol.* **6**, 241–246
7. Cox, C. D., and Adams, P. (1985) Siderophore activity of pyoverdin for *Pseudomonas aeruginosa*. *Infect. Immun.* **48**, 130–138
8. Kloepper, J. W., Leong, J., Teintze, M., and Schroth, M. N. (1980) *Pseudomonas* siderophores: A mechanism explaining disease-suppressive soils. *Curr. Microbiol.* **4**, 317–320
9. Meyer, J.-M., and Stintzi, A. (1998) Iron metabolism and siderophores in *Pseudomonas* and related species. In: Montie, T. C., Ed. *Pseudomonas*. Biotechnology Handbooks, Boston, MA: Springer, **10**, 201–243
10. Totter, J. R., and Moseley, F. T. (1953) Influence of the concentration of iron on the production of fluorescin by *Pseudomonas aeruginosa*. *J. Bacteriol.* **65**, 45–47
11. Meyer, J. M., and Hornsperger, J. M. (1978) Role of pyoverdine_{Pf}, the iron-binding fluorescent pigment of *Pseudomonas fluorescens*, in iron transport. *J. Gen. Microbiol.* **107**, 329–331
12. Meyer, J. M., and Abdallah, M. A. (1978) The fluorescent pigment of *Pseudomonas fluorescens*: Biosynthesis, purification and physicochemical properties. *J. Gen. Microbiol.* **107**, 319–328

13. Lankford, C. E., and Byers, B. R. (1973) Bacterial assimilation of iron. *CRC Crit. Rev. Microbiol.* **2**, 273–331
14. Teintze, M., Hossain, M. B., Barnes, C. L., Leong, J., and van der Helm, D. (1981) Structure of ferric pseudobactin: A siderophore from a plant growth promoting *Pseudomonas*. *Biochemistry* **20**, 6446–6457
15. Budzikiewicz, H. (2004) Siderophores of the Pseudomonadaceae *sensu stricto* (fluorescent and non-fluorescent *Pseudomonas* spp.). In: Falk, H., Kirby, G. W., Eds. *Progress in the chemistry of organic natural products*, Vienna: Springer, **87**, 81–205
16. Wiberg, N., Fischer, G., Holleman, A. F., and Wiberg, E. (2008) *Lehrbuch der Anorganischen Chemie*, 102nd Ed., De Gruyter, Berlin, Boston
17. C. Hider, R., and Xiaole Kong (2010) Chemistry and biology of siderophores. *Nat. Prod. Rep.* **27**, 637–657
18. Ahmed, E., and Holmström, S. J. M. (2014) Siderophores in environmental research: Roles and applications. *Microb. Biotechnol.* **7**, 196–208
19. Saha, M., Sarkar, S., Sarkar, B., Sharma, B. K., Bhattacharjee, S., and Tribedi, P. (2015) Microbial siderophores and their potential applications: a review. *Environ. Sci. Pollut. Res.*, 1–16
20. O'Brien, I. G., and Gibson, F. (1970) The structure of enterochelin and related 2,3-dihydroxy-N-benzoyne conjugates from *Escherichia coli*. *Biochim. Biophys. Acta.* **215**, 393–402
21. Pollack, J. R., and Neilands, J. B. (1970) Enterobactin, an iron transport compound from *Salmonella typhimurium*. *Biochem. Biophys. Res. Commun.* **38**, 989–992
22. Carrano, C. J., and Raymond, K. N. (1979) Ferric ion sequestering agents. 2. Kinetics and mechanism of iron removal from transferrin by enterobactin and synthetic tricatechols. *J. Am. Chem. Soc.* **101**, 5401–5404
23. Bickel, H., Hall, G. E., Keller-Schierlein, W., Prelog, V., Vischer, E., and Wettstein, A. (1960) Stoffwechselprodukte von Actinomyceten. 27. Mitteilung. Über die Konstitution von Ferrioxamin B. *Helv. Chim. Acta* **43**, 2129–2138

24. Snow, G. A. (1954) Mycobactin. A growth factor for *Mycobacterium johnei*. Part III. Degradation and tentative structure. *J. Chem. Soc.* **0**, 4080–4093
25. Tait, G. H. (1975) The identification and biosynthesis of siderochromes formed by *Micrococcus denitrificans*. *Biochem. J.* **146**, 191–204
26. Harris, W. R., Carrano, C. J., and Raymond, K. N. (1979) Coordination chemistry of microbial iron transport compounds. 16. Isolation, characterization, and formation constants of ferric aerobactin. *J. Am. Chem. Soc.* **101**, 2722–2727
27. Smith, M. J., Shoolery, J. N., Schwyn, B., Holden, I., and Neilands, J. B. (1985) Rhizobactin, a structurally novel siderophore from *Rhizobium meliloti*. *J. Am. Chem. Soc.* **107**, 1739–1743
28. Sugiura, Y., Tanaka, H., Mino, Y., Ishida, T., Ota, N., Inoue, M., Nomoto, K., Yoshioka, H., and Takemoto, T. (1981) Structure, properties, and transport mechanism of iron(III) complex of mugineic acid, a possible phytosiderophore. *J. Am. Chem. Soc.* **103**, 6979–6982
29. Sokol, P. A., Lewis, C. J., and Dennis, J. J. (1992) Isolation of a novel siderophore from *Pseudomonas cepacia*. *J. Med. Microbiol.* **36**, 184–189
30. Anthoni, U., Christophersen, C., Nielsen, P. H., Gram, L., and Petersen, B. O. (1995) Pseudomonine, an isoxazolidone with siderophoric activity from *Pseudomonas fluorescens* AH2 isolated from lake victorian Nile perch. *J. Nat. Prod.* **58**, 1786–1789
31. Meyer, J. M., Azelvandre, P., and Georges, C. (1992) Iron metabolism in *Pseudomonas*: Salicylic acid, a siderophore of *Pseudomonas fluorescens* CHAO. *BioFactors* **4**, 23–27
32. Visca, P., Ciervo, A., Sanfilippo, V., and Orsi, N. (1993) Iron-regulated salicylate synthesis by *Pseudomonas* spp. *J. Gen. Microbiol.* **139**, 1995–2001
33. Cox, C. D., and Graham, R. (1979) Isolation of an iron-binding compound from *Pseudomonas aeruginosa*. *J. Bacteriol.* **137**, 357–364
34. Cox, C. D. (1980) Iron uptake with ferripyochelin and ferric citrate by *Pseudomonas aeruginosa*. *J. Bacteriol.* **142**, 581–587

35. Cox, C. D., Rinehart, K. L., Moore, M. L., and Cook, J. C. (1981) Pyochelin: Novel structure of an iron-chelating growth promoter for *Pseudomonas aeruginosa*. *Proc. Natl. Acad. Sci. U S A* **78**, 4256–4260
36. Cobessi, D., Celia, H., and Pattus, F. (2005) Crystal structure at high resolution of ferric-pyochelin and its membrane receptor FptA from *Pseudomonas aeruginosa*. *J. Mol. Biol.* **352**, 893–904
37. Chipperfield, J. R., and Ratledge, C. (2000) Salicylic acid is not a bacterial siderophore: A theoretical study. *Biometals* **13**, 165–168
38. Winslow, C. E., Broadhurst, J., Buchanan, R. E., Krumwiede, C., Rogers, L. A., and Smith, G. H. (1917) The Families and Genera of the Bacteria: Preliminary Report of the Committee of the Society of American Bacteriologists on Characterization and Classification of Bacterial Types. *J. Bacteriol.* **2**, 505–566
39. Migula, W. (1894) Über ein neues System der Bakterien. *Arb. Bakteriolog. Inst. Karlsruhe* **1**, 235–238
40. Palleroni, N. J. (1981) Introduction to the family pseudomonadaceae: Chapter 58. In: Starr, M. P., Stolp, H., Trüper, H. G., Balows, A., Schlegel, H. G., Eds. *The Prokaryotes: A handbook on habitats, isolation, and identification of bacteria*, Berlin, Heidelberg, New York: Springer, **1**, 655–665
41. Palleroni, N. J., Kunisawa, R., Contopoulou, R., and Doudoroff, M. (1973) Nucleic Acid Homologies in the Genus *Pseudomonas*. *Int. J. Syst. Bacteriol.* **23**, 333–339
42. Lyczak, J. B., Cannon, C. L., and Pier, G. B. (2000) Establishment of *Pseudomonas aeruginosa* infection: Lessons from a versatile opportunist. *Microbes Infect.* **2**, 1051–1060
43. Kerr, K. G., and Snelling, A. M. (2009) *Pseudomonas aeruginosa*: A formidable and ever-present adversary. *J. Hosp. Infect.* **73**, 338–344
44. Kim, S. E., Park, S.-H., Park, H. B., Park, K.-H., Kim, S.-H., Jung, S.-I., Shin, J.-H., Jang, H.-C., and Kang, S. J. (2012) Nosocomial *Pseudomonas putida* bacteremia: High rates of carbapenem resistance and mortality. *Chonnam Med. J.* **48**, 91–95

45. Fernández, M., Porcel, M., La Torre, J. de, Molina-Henares, M. A., Daddaoua, A., Llamas, M. A., Roca, A., Carriel, V., Garzón, I., Ramos, J. L., Alaminos, M., and Duque, E. (2015) Analysis of the pathogenic potential of nosocomial *Pseudomonas putida* strains. *Front. Microbiol.* **6**, 871
46. Höfte, M., and Vos, P. de (2007) Plant pathogenic *Pseudomonas* species. In: Gnanamanickam, S. S., Ed. *Plant-Associated Bacteria*, Dordrecht: Springer, 507–533
47. Morris, C. E., Sands, D. C., Vinatzer, B. A., Glaux, C., Guilbaud, C., Buffière, A., Yan, S., Dominguez, H., and Thompson, B. M. (2008) The life history of the plant pathogen *Pseudomonas syringae* is linked to the water cycle. *ISME J.* **2**, 321–334
48. Xin, X.-F., and He, S. Y. (2013) *Pseudomonas syringae* pv. *tomato* DC3000: A model pathogen for probing disease susceptibility and hormone signaling in plants. *Annu. Rev. Phytopathol.* **51**, 473–498
49. Trantas, E. A., Sarris, P. F., Mpalantinaki, E. E., Pentari, M. G., Ververidis, F. N., and Goumas, D. E. (2013) A new genomovar of *Pseudomonas cichorii*, a causal agent of tomato pith necrosis. *Eur. J. Plant Pathol.* **137**, 477–493
50. Dowling, D. N., and O'Gara, F. (1994) Metabolites of *Pseudomonas* involved in the biocontrol of plant disease. *Trends Biotechnol.* **12**, 133–141
51. Lugtenberg, B., and Kamilova, F. (2009) Plant-growth-promoting rhizobacteria. *Annu. Rev. Microbiol.* **63**, 541–556
52. Santoyo, G., Orozco-Mosqueda, M. d. C., and Govindappa, M. (2012) Mechanisms of biocontrol and plant growth-promoting activity in soil bacterial species of *Bacillus* and *Pseudomonas*: A review. *Biocontrol Sci. Technol.* **22**, 855–872
53. Shen, X., Hu, H., Peng, H., Wang, W., and Zhang, X. (2013) Comparative genomic analysis of four representative plant growth-promoting rhizobacteria in *Pseudomonas*. *BMC Genomics* **14**, 271
54. Ankenbauer, R., Sriyosachati, S., and Cox, C. D. (1985) Effects of siderophores on the growth of *Pseudomonas aeruginosa* in human serum and transferrin. *Infect. Immun.* **49**, 132–140

55. Sriyosachati, S., and Cox, C. D. (1986) Siderophore-mediated iron acquisition from transferrin by *Pseudomonas aeruginosa*. *Infect. Immun.* **52**, 885–891
56. Wolz, C., Hohloch, K., Ocaktan, A., Poole, K., Evans, R. W., Rochel, N., Albrecht-Gary, A. M., Abdallah, M. A., and Döring, G. (1994) Iron release from transferrin by pyoverdinin and elastase from *Pseudomonas aeruginosa*. *Infect. Immun.* **62**, 4021–4027
57. Xiao, R., and Kisaalita, W. S. (1997) Iron acquisition from transferrin and lactoferrin by *Pseudomonas aeruginosa* pyoverdinin. *Microbiology* **143 (Pt 7)**, 2509–2515
58. Meyer, J. M., Neely, A., Stintzi, A., Georges, C., and Holder, I. A. (1996) Pyoverdinin is essential for virulence of *Pseudomonas aeruginosa*. *Infect. Immun.* **64**, 518–523
59. Takase, H., Nitani, H., Hoshino, K., and Otani, T. (2000) Impact of siderophore production on *Pseudomonas aeruginosa* infections in immunosuppressed mice. *Infect. Immun.* **68**, 1834–1839
60. Haas, B., Kraut, J., Marks, J., Zanker, S. C., and Castignetti, D. (1991) Siderophore presence in sputa of cystic fibrosis patients. *Infect. Immun.* **59**, 3997–4000
61. Martin, L. W., Reid, D. W., Sharples, K. J., and Lamont, I. L. (2011) *Pseudomonas* siderophores in the sputum of patients with cystic fibrosis. *Biometals* **24**, 1059–1067
62. Vos, D. de, Chial, M. de, Cochez, C., Jansen, S., Tümmler, B., Meyer, J.-M., and Cornelis, P. (2001) Study of pyoverdinin type and production by *Pseudomonas aeruginosa* isolated from cystic fibrosis patients: Prevalence of type II pyoverdinin isolates and accumulation of pyoverdinin-negative mutations. *Arch. Microbiol.* **175**, 384–388
63. Griffin, A. S., West, S. A., and Buckling, A. (2004) Cooperation and competition in pathogenic bacteria. *Nature* **430**, 1024–1027
64. Harrison, F., and Buckling, A. (2005) Hypermutability impedes cooperation in pathogenic bacteria. *Curr. Biol.* **15**, 1968–1971
65. Bruce, J. B., Cooper, G. A., Chabas, H., West, S. A., and Griffin, A. S. (2017) Cheating and resistance to cheating in natural populations of the bacterium *Pseudomonas fluorescens*. *Evolution* **71**, 2484–2495

66. Butaitė, E., Baumgartner, M., Wyder, S., and Kümmerli, R. (2017) Siderophore cheating and cheating resistance shape competition for iron in soil and freshwater *Pseudomonas* communities. *Nat. Commun.* **8**, 414
67. Granato, E. T., Harrison, F., Kümmerli, R., and Ross-Gillespie, A. (2016) Do bacterial "virulence factors" always increase virulence? A meta-analysis of pyoverdine production in *Pseudomonas aeruginosa* as a test case. *Front. Microbiol.* **7**, 1952
68. Taguchi, F., Suzuki, T., Inagaki, Y., Toyoda, K., Shiraishi, T., and Ichinose, Y. (2010) The siderophore pyoverdine of *Pseudomonas syringae* pv. *tabaci* 6605 is an intrinsic virulence factor in host tobacco infection. *J. Bacteriol.* **192**, 117–126
69. Cody, Y. S., and Gross, D. C. (1987) Outer membrane protein mediating iron uptake via pyoverdin_{pss}, the fluorescent siderophore produced by *Pseudomonas syringae* pv. *syringae*. *J. Bacteriol.* **169**, 2207–2214
70. Jones, A. M., and Wildermuth, M. C. (2011) The phytopathogen *Pseudomonas syringae* pv. *tomato* DC3000 has three high-affinity iron-scavenging systems functional under iron limitation conditions but dispensable for pathogenesis. *J. Bacteriol.* **193**, 2767–2775
71. Kloepper, J. W., and Schroth, M. N. (1978) Plant growth-promoting rhizobacteria in radish. In: Station de pathologic Vegetal et Phytobacteriologic, Ed. *Proceedings of the 4th International Conference on Plant Pathogenic Bacteria*, France: Agners, 879–882
72. Hiltner, L. (1904) Über neuerer Erfahrungen und Probleme auf dem Gebiete der Bodenbakteriologie unter besonderer Berücksichtigung der Gründüngung und Brache. *Arbeiten der Deutschen Landwirtschaftlichen Gesellschaft* **98**, 59–78
73. Hartmann, A., Rothballer, M., and Schmid, M. (2008) Lorenz Hiltner, a pioneer in rhizosphere microbial ecology and soil bacteriology research. *Plant Soil* **312**, 7–14
74. Lugtenberg, B. J.J., Chin-A-Woeng, T. F.C., and Bloemberg, G. V. (2002) Microbe–plant interactions: principles and mechanisms. *Antonie Van Leeuwenhoek* **81**, 373–383
75. Kloepper, J. W., Leong, J., Teintze, M., and Schroth, M. N. (1980) Enhanced plant growth by siderophores produced by plant growth-promoting rhizobacteria. *Nature* **286**, 885–886

76. Misaghi, I. J. (1982) Fungistatic activity of water-soluble fluorescent pigments of fluorescent pseudomonads. *Phytopathology* **72**, 33–36
77. Vandenberg, P. A., Gonzalez, C. F., Wright, A. M., and Kunka, B. S. (1983) Iron-chelating compounds produced by soil pseudomonads: correlation with fungal growth inhibition. *Appl. Environ. Microbiol.* **46**, 128–132
78. Weller, D. M. (1988) Relationship between *in vitro* inhibition of *Gaeumannomyces graminis* var. *tritici* and suppression of take-all of wheat by fluorescent pseudomonads. *Phytopathology* **78**, 1094–1100
79. Loper, J. E. (1988) Role of fluorescent siderophore production in biological control of *Pythium ultimum* by a *Pseudomonas fluorescens* strain. *Phytopathology* **78**, 166–172
80. Buysens, S., Heungens, K., Poppe, J., and Hofte, M. (1996) Involvement of pyochelin and pyoverdine in suppression of *Pythium*-induced damping-off of tomato by *Pseudomonas aeruginosa* 7NSK2. *Appl. Environ. Microbiol.* **62**, 865–871
81. Ran, L. X., Liu, C. Y., Wu, G. J., van Loon, L. C., and Bakker, P.A.H.M. (2005) Suppression of bacterial wilt in *Eucalyptus urophylla* by fluorescent *Pseudomonas* spp. in China. *Biological Control* **32**, 111–120
82. Ran, L. X., Xiang, M. L., Zhou, B., and Bakker, P.A.H.M. (2005) Siderophores are the main determinants of fluorescent *Pseudomonas* strains in suppression of grey mould in *Eucalyptus urophylla*. *Acta phytopathologica sinica* **35**, 6–12
83. Lemanceau, P., Robin, A., Mazurier, S., and Vansuyt, G. (2007) Implication of pyoverdines in the interactions of fluorescent pseudomonads with soil microflora and plant in the rhizosphere. In: Varma, A., Chincholkar, S. B., Eds. *Microbial siderophores*, Berlin, New York: Springer, **12**, 165–192
84. Kloepper, J. W., Tuzun, S., and Kuć, J. A. (1992) Proposed definitions related to induced disease resistance. *Biocontrol Sci. Technol.* **2**, 349–351
85. Maurhofer, M., Hase, C., Meuwly, P., Métraux, J.-P., and Défago, G. (1994) Induction of systemic resistance of tobacco to tobacco necrosis virus by the root-colonizing *Pseudomonas*

- fluorescens* strain CHA0: influence of the *gacA* gene and of pyoverdine production. *Phytopathology* **84**, 139–146
86. Leeman, M., den Ouden, F. M., Dirkx, F. P. M., Steijl, H., Bakker, P. A. H. M., and Schippers, B. (1996) Iron availability affects induction of systemic resistance to fusarium wilt of radish by *Pseudomonas fluorescens*. *Phytopathology* **86**, 149–155
87. Meziane, H., van der Sluis, I., van Loon, L. C., Höfte, M., and Bakker, P. A. H. M. (2005) Determinants of *Pseudomonas putida* WCS358 involved in inducing systemic resistance in plants. *Mol. Plant. Pathol.* **6**, 177–185
88. Ran, L. X., Li, Z. N., Wu, G. J., van Loon, L. C., and Bakker, P. A. H. M. (2005) Induction of systemic resistance against bacterial wilt in *Eucalyptus urophylla* by fluorescent *Pseudomonas* spp. *Eur. J. Plant Pathol.* **113**, 59–70
89. Vleesschauwer, D. de, Djavaheri, M., Bakker, P. A. H. M., and Höfte, M. (2008) *Pseudomonas fluorescens* WCS374r-induced systemic resistance in rice against *Magnaporthe oryzae* is based on pseudobactin-mediated priming for a salicylic acid-repressible multifaceted defense response. *Plant Physiol.* **148**, 1996–2012
90. Bar-Ness, E., Chen, Y., Hadar, Y., Marschner, H., and Römheld, V. (1991) Siderophores of *Pseudomonas putida* as an iron source for dicot and monocot plants. *Plant Soil* **130**, 231–241
91. Vansuyt, G., Robin, A., Briat, J.-F., Curie, C., and Lemanceau, P. (2007) Iron acquisition from Fe-pyoverdine by *Arabidopsis thaliana*. *Mol. Plant Microbe Interact.* **20**, 441–447
92. Shirley, M., Avoscan, L., Bernaud, E., Vansuyt, G., and Lemanceau, P. (2011) Comparison of iron acquisition from Fe-pyoverdine by strategy I and strategy II plants. *Botany* **89**, 731–735
93. Nagata, T., Oobo, T., and Aozasa, O. (2013) Efficacy of a bacterial siderophore, pyoverdine, to supply iron to *Solanum lycopersicum* plants. *J. Biosci. Bioeng.* **115**, 686–690
94. Cornu, J. Y., Elhabiri, M., Ferret, C., Geoffroy, V. A., Jezequel, K., Leva, Y., Lollier, M., Schalk, I. J., and Lebeau, T. (2014) Contrasting effects of pyoverdine on the phytoextraction of Cu and Cd in a calcareous soil. *Chemosphere* **103**, 212–219

95. Singh, P. K., Parsek, M. R., Greenberg, E. P., and Welsh, M. J. (2002) A component of innate immunity prevents bacterial biofilm development. *Nature* **417**, 552–555
96. Banin, E., Vasil, M. L., and Greenberg, E. P. (2005) Iron and *Pseudomonas aeruginosa* biofilm formation. *Proc. Natl. Acad. Sci. U S A* **102**, 11076–11081
97. Yang, L., Nilsson, M., Gjermansen, M., Givskov, M., and Tolker-Nielsen, T. (2009) Pyoverdine and PQS mediated subpopulation interactions involved in *Pseudomonas aeruginosa* biofilm formation. *Mol. Microbiol.* **74**, 1380–1392
98. Musk, D. J., Banko, D. A., and Hergenrother, P. J. (2005) Iron salts perturb biofilm formation and disrupt existing biofilms of *Pseudomonas aeruginosa*. *Chem. Biol.* **12**, 789–796
99. Visca, P., Imperi, F., and Lamont, I. L. (2007) Pyoverdine siderophores: from biogenesis to biosignificance. *Trends Microbiol.* **15**, 22–30
100. Braud, A., Geoffroy, V., Hoegy, F., Mislin, G. L. A., and Schalk, I. J. (2010) Presence of the siderophores pyoverdine and pyochelin in the extracellular medium reduces toxic metal accumulation in *Pseudomonas aeruginosa* and increases bacterial metal tolerance. *Environ. Microbiol. Rep.* **2**, 419–425
101. Schalk, I. J., Hannauer, M., and Braud, A. (2011) New roles for bacterial siderophores in metal transport and tolerance. *Environ. Microbiol.* **13**, 2844–2854
102. Cunrath, O., Geoffroy, V. A., and Schalk, I. J. (2016) Metallome of *Pseudomonas aeruginosa*: a role for siderophores. *Environ. Microbiol.* **18**, 3258–3267
103. Hohnadel, D., and Meyer, J. M. (1988) Specificity of pyoverdine-mediated iron uptake among fluorescent *Pseudomonas* strains. *J. Bacteriol.* **170**, 4865–4873
104. Cornelis, P., Hohnadel, D., and Meyer, J. M. (1989) Evidence for different pyoverdine-mediated iron uptake systems among *Pseudomonas aeruginosa* strains. *Infect. Immun.* **57**, 3491–3497
105. Meyer, J. M., Hohnadel, D., Khan, A., and Cornelis, P. (1990) Pyoverdin-facilitated iron uptake in *Pseudomonas aeruginosa*: immunological characterization of the ferripyoverdin receptor. *Mol. Microbiol.* **4**, 1401–1405

106. Poole, K., Neshat, S., and Heinrichs, D. (1991) Pyoverdine-mediated iron transport in *Pseudomonas aeruginosa*: Involvement of a high-molecular-mass outer membrane protein. *FEMS Microbiol. Lett.* **78**, 1–6
107. Poole, K., Neshat, S., Krebs, K., and Heinrichs, D. E. (1993) Cloning and nucleotide sequence analysis of the ferripyoverdine receptor gene *fpvA* of *Pseudomonas aeruginosa*. *J. Bacteriol.* **175**, 4597–4604
108. Wirth, C., Meyer-Klaucke, W., Pattus, F., and Cobessi, D. (2007) From the periplasmic signaling domain to the extracellular face of an outer membrane signal transducer of *Pseudomonas aeruginosa*: crystal structure of the ferric pyoverdine outer membrane receptor. *J. Mol. Biol.* **368**, 398–406
109. Brillet, K., Journet, L., Célia, H., Paulus, L., Stahl, A., Pattus, F., and Cobessi, D. (2007) A β strand lock exchange for signal transduction in TonB-dependent transducers on the basis of a common structural motif. *Structure* **15**, 1383–1391
110. James, H. E., Beare, P. A., Martin, L. W., and Lamont, I. L. (2005) Mutational analysis of a bifunctional ferrisiderophore receptor and signal-transducing protein from *Pseudomonas aeruginosa*. *J. Bacteriol.* **187**, 4514–4520
111. Shen, J.-S., Geoffroy, V., Neshat, S., Jia, Z., Meldrum, A., Meyer, J.-M., and Poole, K. (2005) FpvA-mediated ferric pyoverdine uptake in *Pseudomonas aeruginosa*: Identification of aromatic residues in FpvA implicated in ferric pyoverdine binding and transport. *J. Bacteriol.* **187**, 8511–8515
112. Nader, M., Dobbelaere, W., Vincent, M., Journet, L., Adams, H., Cobessi, D., Gallay, J., and Schalk, I. J. (2007) Identification of residues of FpvA involved in the different steps of Pvd-Fe uptake in *Pseudomonas aeruginosa*. *Biochemistry* **46**, 11707–11717
113. Greenwald, J., Nader, M., Celia, H., Gruffaz, C., Geoffroy, V., Meyer, J.-M., Schalk, I. J., and Pattus, F. (2009) FpvA bound to non-cognate pyoverdines: Molecular basis of siderophore recognition by an iron transporter. *Mol. Microbiol.* **72**, 1246–1259

114. Adams, H., Zeder-Lutz, G., Schalk, I., Pattus, F., and Celia, H. (2006) Interaction of TonB with the outer membrane receptor FpvA of *Pseudomonas aeruginosa*. *J. Bacteriol.* **188**, 5752–5761
115. Nader, M., Journet, L., Meksem, A., Guillon, L., and Schalk, I. J. (2011) Mechanism of ferripyoverdine uptake by *Pseudomonas aeruginosa* outer membrane transporter FpvA: No diffusion channel formed at any time during ferrisiderophore uptake. *Biochemistry* **50**, 2530–2540
116. Zhao, Q., and Poole, K. (2000) A second *tonB* gene in *Pseudomonas aeruginosa* is linked to the *exbB* and *exbD* genes. *FEMS Microbiol. Lett.* **184**, 127–132
117. Schalk, I. J., Kyslik, P., Prome, D., van Dorsselaer, A., Poole, K., Abdallah, M. A., and Pattus, F. (1999) Copurification of the FpvA ferric pyoverdin receptor of *Pseudomonas aeruginosa* with its iron-free ligand: implications for siderophore-mediated iron transport. *Biochemistry* **38**, 9357–9365
118. Schalk, I. J., Hennard, C., Dugave, C., Poole, K., Abdallah, M. A., and Pattus, F. (2001) Iron-free pyoverdin binds to its outer membrane receptor FpvA in *Pseudomonas aeruginosa*: A new mechanism for membrane iron transport. *Mol. Microbiol.* **39**, 351–361
119. Schalk, I. J., Abdallah, M. A., and Pattus, F. (2002) Recycling of pyoverdin on the FpvA receptor after ferric pyoverdin uptake and dissociation in *Pseudomonas aeruginosa*. *Biochemistry* **41**, 1663–1671
120. Schalk, I. J., Abdallah, M. A., and Pattus, F. (2002) A new mechanism for membrane iron transport in *Pseudomonas aeruginosa*. *Biochem. Soc. Trans.* **30**, 702–705
121. Clément, E., Mesini, P. J., Pattus, F., and Schalk, I. J. (2004) The binding mechanism of pyoverdin with the outer membrane receptor FpvA in *Pseudomonas aeruginosa* is dependent on its iron-loaded status. *Biochemistry* **43**, 7954–7965
122. Greenwald, J., Zeder-Lutz, G., Hagege, A., Celia, H., and Pattus, F. (2008) The metal dependence of pyoverdine interactions with its outer membrane receptor FpvA. *J. Bacteriol.* **190**, 6548–6558

123. Cornelis, P. (2008) Unexpected interaction of a siderophore with aluminum and its receptor. *J. Bacteriol.* **190**, 6541–6543
124. Braud, A., Hoegy, F., Jezequel, K., Lebeau, T., and Schalk, I. J. (2009) New insights into the metal specificity of the *Pseudomonas aeruginosa* pyoverdine–iron uptake pathway. *Environ. Microbiol.* **11**, 1079–1091
125. Hartney, S. L., Mazurier, S., Girard, M. K., Mehnaz, S., Davis, E. W., Gross, H., Lemanceau, P., and Loper, J. E. (2013) Ferric-pyoverdine recognition by Fpv outer membrane proteins of *Pseudomonas protegens* Pf-5. *J. Bacteriol.* **195**, 765–776
126. Liu, P. V., and Shokrani, F. (1978) Biological activities of pyochelins: Iron-chelating agents of *Pseudomonas aeruginosa*. *Infect. Immun.* **22**, 878–890
127. Poole, K., Young, L., and Neshat, S. (1990) Enterobactin-mediated iron transport in *Pseudomonas aeruginosa*. *J. Bacteriol.* **172**, 6991–6996
128. Screen, J., Moya, E., Blagbrough, I. S., and Smith, A. W. (1995) Iron uptake in *Pseudomonas aeruginosa* mediated by *N*-(2,3-dihydroxybenzoyl)-L-serine and 2,3-dihydroxybenzoic acid. *FEMS Microbiol. Lett.* **127**, 145–149
129. Meyer, J. M. (1992) Exogenous siderophore-mediated iron uptake in *Pseudomonas aeruginosa*: Possible involvement of porin OprF in iron translocation. *J. Gen. Microbiol.* **138**, 951–958
130. Meyer, J.-M., and Hohnadel, D. (1992) Use of nitrilotriacetic acid (NTA) by *Pseudomonas* species through iron metabolism. *Appl. Microbiol. Biotechnol.* **37**, 114–118
131. Harding, R. A., and Royt, P. W. (1990) Acquisition of iron from citrate by *Pseudomonas aeruginosa*. *J. Gen. Microbiol.* **136**, 1859–1867
132. Smith, A. W., Poyner, D. R., Hughes, H. K., and Lambert, P. A. (1994) Siderophore activity of myo-inositol hexakisphosphate in *Pseudomonas aeruginosa*. *J. Bacteriol.* **176**, 3455–3459
133. Schalk, I. J., and Guillon, L. (2013) Fate of ferrisiderophores after import across bacterial outer membranes: Different iron release strategies are observed in the cytoplasm or periplasm depending on the siderophore pathways. *Amino Acids* **44**, 1267–1277

134. Greenwood, K. T., and Luke, R. K.J. (1978) Enzymatic hydrolysis of enterochelin and its iron complex in *Escherichia coli* K-12. Properties of enterochelin esterase. *Biochim. Biophys. Acta.* **525**, 209–218
135. Brickman, T. J., and McIntosh, M. A. (1992) Overexpression and purification of ferric enterobactin esterase from *Escherichia coli*. Demonstration of enzymatic hydrolysis of enterobactin and its iron complex. *J. Biol. Chem.* **267**, 12350–12355
136. Greenwald, J., Hoegy, F., Nader, M., Journet, L., Mislin, G. L. A., Graumann, P. L., and Schalk, I. J. (2007) Real time fluorescent resonance energy transfer visualization of ferric pyoverdine uptake in *Pseudomonas aeruginosa*. A role for ferrous iron. *J. Biol. Chem.* **282**, 2987–2995
137. Hannauer, M., Yeterian, E., Martin, L. W., Lamont, I. L., and Schalk, I. J. (2010) An efflux pump is involved in secretion of newly synthesized siderophore by *Pseudomonas aeruginosa*. *FEBS Lett.* **584**, 4751–4755
138. Brillet, K., Ruffenach, F., Adams, H., Journet, L., Gasser, V., Hoegy, F., Guillon, L., Hannauer, M., Page, A., and Schalk, I. J. (2012) An ABC transporter with two periplasmic binding proteins involved in iron acquisition in *Pseudomonas aeruginosa*. *ACS Chem. Biol.* **7**, 2036–2045
139. Ganne, G., Brillet, K., Basta, B., Roche, B., Hoegy, F., Gasser, V., and Schalk, I. J. (2017) Iron release from the siderophore pyoverdine in *Pseudomonas aeruginosa* involves three new actors: FpvC, FpvG, and FpvH. *ACS Chem. Biol.* **12**, 1056–1065
140. Imperi, F., Tiburzi, F., and Visca, P. (2009) Molecular basis of pyoverdine siderophore recycling in *Pseudomonas aeruginosa*. *Proc. Natl. Acad. Sci. U S A* **106**, 20440–20445
141. Yeterian, E., Martin, L. W., Lamont, I. L., and Schalk, I. J. (2010) An efflux pump is required for siderophore recycling by *Pseudomonas aeruginosa*. *Environ. Microbiol. Rep.* **2**, 412–418
142. Chen, W.-J., Kuo, T.-Y., Hsieh, F.-C., Chen, P.-Y., Wang, C.-S., Shih, Y.-L., Lai, Y.-M., Liu, J.-R., Yang, Y.-L., and Shih, M.-C. (2016) Involvement of type VI secretion system in secretion of iron chelator pyoverdine in *Pseudomonas taiwanensis*. *Sci. Rep.* **6**, srep32950

143. Yeterian, E., Martin, L. W., Guillon, L., Journet, L., Lamont, I. L., and Schalk, I. J. (2010) Synthesis of the siderophore pyoverdine in *Pseudomonas aeruginosa* involves a periplasmic maturation. *Amino Acids* **38**, 1447–1459
144. Schalk, I. J., and Guillon, L. (2013) Pyoverdine biosynthesis and secretion in *Pseudomonas aeruginosa*: implications for metal homeostasis. *Environ. Microbiol.* **15**, 1661–1673
145. Braun, V. (1997) Avoidance of iron toxicity through regulation of bacterial iron transport. *Biol. Chem.* **378**, 779–786
146. Escolar, L., Pérez-Martín, J., and Lorenzo, V. d. (1999) Opening the iron box: Transcriptional metalloregulation by the Fur protein. *J. Bacteriol.* **181**, 6223–6229
147. Ernst, J. F., Bennett, R. L., and Rothfield, L. I. (1978) Constitutive expression of the iron-enterochelin and ferrichrome uptake systems in a mutant strain of *Salmonella typhimurium*. *J. Bacteriol.* **135**, 928–934
148. Hantke, K. (1981) Regulation of ferric iron transport in *Escherichia coli* K12: Isolation of a constitutive mutant. *Molec. Gen. Genet.* **182**, 288–292
149. Hantke, K. (1984) Cloning of the repressor protein gene of iron-regulated systems in *Escherichia coli* K12. *Molec. Gen. Genet.* **197**, 337–341
150. Bagg, A., and Neilands, J. B. (1985) Mapping of a mutation affecting regulation of iron uptake systems in *Escherichia coli* K-12. *J. Bacteriol.* **161**, 450–453
151. Schäffer, S., Hantke, K., and Braun, V. (1985) Nucleotide sequence of the iron regulatory gene *fur*. *Molec. Gen. Genet.* **200**, 110–113
152. Wee, S., Neilands, J. B., Bittner, M. L., Hemming, B. C., Haymore, B. L., and Seetharam, R. (1988) Expression, isolation and properties of Fur (ferric uptake regulation) protein of *Escherichia coli* K 12. *Biol. Met.* **1**, 62–68
153. Prince, R. W., Storey, D. G., Vasil, A. I., and Vasil, M. L. (1991) Regulation of *tox*A and *reg*A by the *Escherichia coli fur* gene and identification of a Fur homologue in *Pseudomonas aeruginosa* PA103 and PA01. *Mol. Microbiol.* **5**, 2823–2831

154. Prince, R. W., Cox, C. D., and Vasil, M. L. (1993) Coordinate regulation of siderophore and exotoxin A production: Molecular cloning and sequencing of the *Pseudomonas aeruginosa fur* gene. *J. Bacteriol.* **175**, 2589–2598
155. Pasqua, M., Visaggio, D., Lo Sciuto, A., Genah, S., Banin, E., Visca, P., and Imperi, F. (2017) The ferric uptake regulator Fur is conditionally essential in *Pseudomonas aeruginosa*. *J. Bacteriol.*, (in press)
156. Bagg, A., and Neilands, J. B. (1987) Ferric uptake regulation protein acts as a repressor, employing iron(II) as a cofactor to bind the operator of an iron transport operon in *Escherichia coli*. *Biochemistry* **26**, 5471–5477
157. Lorenzo, V. de, Wee, S., Herrero, M., and Neilands, J. B. (1987) Operator sequences of the aerobactin operon of plasmid ColV-K30 binding the ferric uptake regulation (*fur*) repressor. *J. Bacteriol.* **169**, 2624–2630
158. Escolar, L., Lorenzo, V. d., and Pérez-Martín, J. (1997) Metalloregulation *in vitro* of the aerobactin promoter of *Escherichia coli* by the Fur (ferric uptake regulation) protein. *Mol. Microbiol.* **26**, 799–808
159. Escolar, L., Pérez-Martín, J., and Lorenzo, V. d. (1998) Coordinated repression *in vitro* of the divergent *fepA-fes* promoters of *Escherichia coli* by the iron uptake regulation (Fur) protein. *J. Bacteriol.* **180**, 2579–2582
160. Vassinova, N., and Kozyrev, D. (2000) A method for direct cloning of Fur-regulated genes: Identification of seven new Fur-regulated loci in *Escherichia coli*. *Microbiology* **146**, 3171–3182
161. Massé, E., and Gottesman, S. (2002) A small RNA regulates the expression of genes involved in iron metabolism in *Escherichia coli*. *Proc. Natl. Acad. Sci. U S A* **99**, 4620–4625
162. Troxell, B., and Hassan, H. M. (2013) Transcriptional regulation by Ferric Uptake Regulator (Fur) in pathogenic bacteria. *Front. Cell. Infect. Microbiol.* **3**, 59

163. Ochsner, U. A., and Vasil, M. L. (1996) Gene repression by the ferric uptake regulator in *Pseudomonas aeruginosa*: Cycle selection of iron-regulated genes. *Proc. Natl. Acad. Sci. U S A* **93**, 4409–4414
164. Ochsner, U. A., Wilderman, P. J., Vasil, A. I., and Vasil, M. L. (2002) GeneChip® expression analysis of the iron starvation response in *Pseudomonas aeruginosa*: Identification of novel pyoverdine biosynthesis genes. *Mol. Microbiol.* **45**, 1277–1287
165. Palma, M., Worgall, S., and Quadri, L. E. N. (2003) Transcriptome analysis of the *Pseudomonas aeruginosa* response to iron. *Arch. Microbiol.* **180**, 374–379
166. Cornelis, P., Matthijs, S., and van Oeffelen, L. (2009) Iron uptake regulation in *Pseudomonas aeruginosa*. *Biometals* **22**, 15–22
167. Lamont, I. L., Beare, P. A., Ochsner, U., Vasil, A. I., and Vasil, M. L. (2002) Siderophore-mediated signaling regulates virulence factor production in *Pseudomonas aeruginosa*. *Proc. Natl. Acad. Sci. U S A* **99**, 7072–7077
168. Beare, P. A., For, R. J., Martin, L. W., and Lamont, I. L. (2003) Siderophore-mediated cell signalling in *Pseudomonas aeruginosa*: divergent pathways regulate virulence factor production and siderophore receptor synthesis. *Mol. Microbiol.* **47**, 195–207
169. Schalk, I. J., Lamont, I. L., and Cobessi, D. (2009) Structure-function relationships in the bifunctional ferrisiderophore FpvA receptor from *Pseudomonas aeruginosa*. *Biometals* **22**, 671–678
170. Shirley, M., and Lamont, I. L. (2009) Role of TonB1 in pyoverdine-mediated signaling in *Pseudomonas aeruginosa*. *J. Bacteriol.* **191**, 5634–5640
171. Rédly, G. A., and Poole, K. (2005) FpvIR control of *fpvA* ferric pyoverdine receptor gene expression in *Pseudomonas aeruginosa*: demonstration of an interaction between FpvI and FpvR and identification of mutations in each compromising this interaction. *J. Bacteriol.* **187**, 5648–5657

172. Spencer, M. R., Beare, P. A., and Lamont, I. L. (2008) Role of cell surface signaling in proteolysis of an alternative sigma factor in *Pseudomonas aeruginosa*. *J. Bacteriol.* **190**, 4865–4869
173. Tiburzi, F., Imperi, F., and Visca, P. (2008) Intracellular levels and activity of PvdS, the major iron starvation sigma factor of *Pseudomonas aeruginosa*. *Mol. Microbiol.* **67**, 213–227
174. Draper, R. C., Martin, L. W., Beare, P. A., and Lamont, I. L. (2011) Differential proteolysis of sigma regulators controls cell-surface signalling in *Pseudomonas aeruginosa*. *Mol. Microbiol.* **82**, 1444–1453
175. Bastiaansen, K. C., Otero-Asman, J. R., Luirink, J., Bitter, W., and Llamas, M. A. (2015) Processing of cell-surface signalling anti-sigma factors prior to signal recognition is a conserved autoproteolytic mechanism that produces two functional domains. *Environ. Microbiol.* **17**, 3263–3277
176. Wilson, M. J., and Lamont, I. L. (2000) Characterization of an ECF sigma factor protein from *Pseudomonas aeruginosa*. *Biochem. Biophys. Res. Commun.* **273**, 578–583
177. Wilson, M. J., McMorran, B. J., and Lamont, I. L. (2001) Analysis of promoters recognized by PvdS, an extracytoplasmic-function sigma factor protein from *Pseudomonas aeruginosa*. *J. Bacteriol.* **183**, 2151–2155
178. Wilson, M. J., and Lamont, I. L. (2006) Mutational analysis of an extracytoplasmic-function sigma factor to investigate its interactions with RNA polymerase and DNA. *J. Bacteriol.* **188**, 1935–1942
179. Rédly, G. A., and Poole, K. (2003) Pyoverdine-mediated regulation of FpvA synthesis in *Pseudomonas aeruginosa*: Involvement of a probable extracytoplasmic-function sigma factor, FpvI. *J. Bacteriol.* **185**, 1261–1265
180. Cunliffe, H. E., Merriman, T. R., and Lamont, I. L. (1995) Cloning and characterization of *pvdS*, a gene required for pyoverdine synthesis in *Pseudomonas aeruginosa*: PvdS is probably an alternative sigma factor. *J. Bacteriol.* **177**, 2744–2750

181. Lamont, I. L., and Martin, L. W. (2003) Identification and characterization of novel pyoverdine synthesis genes in *Pseudomonas aeruginosa*. *Microbiology* **149**, 833–842
182. Ochsner, U. A., Johnson, Z., Lamont, I. L., Cunliffe, H. E., and Vasil, M. L. (1996) Exotoxin A production in *Pseudomonas aeruginosa* requires the iron-regulated *pvdS* gene encoding an alternative sigma factor. *Mol. Microbiol.* **21**, 1019–1028
183. Vasil, M. L., Ochsner, U. A., Johnson, Z., Colmer, J. A., and Hamood, A. N. (1998) The Fur-regulated gene encoding the alternative sigma factor PvdS is required for iron-dependent expression of the LysR-type regulator PtxR in *Pseudomonas aeruginosa*. *J. Bacteriol.* **180**, 6784–6788
184. Gaines, J. M., Carty, N. L., Tiburzi, F., Davinic, M., Visca, P., Colmer-Hamood, J. A., and Hamood, A. N. (2007) Regulation of the *Pseudomonas aeruginosa* *toxA*, *regA* and *ptxR* genes by the iron-starvation sigma factor PvdS under reduced levels of oxygen. *Microbiology* **153**, 4219–4233
185. Wilderman, P. J., Vasil, A. I., Johnson, Z., Wilson, M. J., Cunliffe, H. E., Lamont, I. L., and Vasil, M. L. (2001) Characterization of an endoprotease (PrpL) encoded by a PvdS-regulated gene in *Pseudomonas aeruginosa*. *Infect. Immun.* **69**, 5385–5394
186. Sexton, R., Gill, P. R., Callanan, M. J., O'Sullivan, D. J., Dowling, D. N., and O'Gara, F. (1995) Iron-responsive gene expression in *Pseudomonas fluorescens* M114; cloning and characterization of a transcription-activating factor, PbrA. *Mol. Microbiol.* **15**, 297–306
187. Shigematsu, T., Fukushima, J., Oyama, M., Tsuda, M., Kawamoto, S., and Okuda, K. (2001) Iron-mediated regulation of alkaline proteinase production in *Pseudomonas aeruginosa*. *Microbiol. Immunol.* **45**, 579–590
188. Maunsell, B., Adams, C., and O'Gara, F. (2006) Complex regulation of AprA metalloprotease in *Pseudomonas fluorescens* M114: Evidence for the involvement of iron, the ECF sigma factor, PbrA and pseudobactin M114 siderophore. *Microbiology* **152**, 29–42

189. Xiong, Y. Q., Vasil, M. L., Johnson, Z., Ochsner, U. A., and Bayer, A. S. (2000) The oxygen- and iron-dependent sigma factor *pvdS* of *Pseudomonas aeruginosa* is an important virulence factor in experimental infective endocarditis. *J. Infect. Dis.* **181**, 1020–1026
190. Imperi, F., Massai, F., Facchini, M., Frangipani, E., Visaggio, D., Leoni, L., Bragonzi, A., and Visca, P. (2013) Repurposing the antimycotic drug flucytosine for suppression of *Pseudomonas aeruginosa* pathogenicity. *Proc. Natl. Acad. Sci. U S A* **110**, 7458–7463
191. Swingle, B., Thete, D., Moll, M., Myers, C. R., Schneider, D. J., and Cartinhour, S. (2008) Characterization of the PvdS-regulated promoter motif in *Pseudomonas syringae* pv. *tomato* DC3000 reveals regulon members and insights regarding PvdS function in other pseudomonads. *Mol. Microbiol.* **68**, 871–889
192. Edgar, R. J., Hampton, G. E., Garcia, G. P. C., Maher, M. J., Perugini, M. A., Ackerley, D. F., and Lamont, I. L. (2017) Integrated activities of two alternative sigma factors coordinate iron acquisition and uptake by *Pseudomonas aeruginosa*. *Mol. Microbiol.*, (in press)
193. Gaines, J. M., Carty, N. L., Colmer-Hamood, J. A., and Hamood, A. N. (2005) Effect of static growth and different levels of environmental oxygen on *toxA* and *ptxR* expression in the *Pseudomonas aeruginosa* strain PAO1. *Microbiology* **151**, 2263–2275
194. Wei, Q., Le Minh, P. N., Dötsch, A., Hildebrand, F., Panmanee, W., Elfarash, A., Schulz, S., Plaisance, S., Charlier, D., Hassett, D., Häussler, S., and Cornelis, P. (2012) Global regulation of gene expression by OxyR in an important human opportunistic pathogen. *Nucleic Acids Res.* **40**, 4320–4333
195. Reen, F. J., Haynes, J. M., Mooij, M. J., and O’Gara, F. (2013) A non-classical LysR-type transcriptional regulator PA2206 is required for an effective oxidative stress response in *Pseudomonas aeruginosa*. *PLoS One* **8**, e54479
196. Zaborin, A., Romanowski, K., Gerdes, S., Holbrook, C., Lepine, F., Long, J., Poroyko, V., Diggle, S. P., Wilke, A., Righetti, K., Morozova, I., Babrowski, T., Liu, D. C., Zaborina, O., and Alverdy, J. C. (2009) Red death in *Caenorhabditis elegans* caused by *Pseudomonas aeruginosa* PAO1. *Proc. Natl. Acad. Sci. U S A* **106**, 6327–6332

197. Zaborin, A., Gerdes, S., Holbrook, C., Liu, D. C., Zaborina, O. Y., and Alverdy, J. C. (2012) *Pseudomonas aeruginosa* overrides the virulence inducing effect of opioids when it senses an abundance of phosphate. *PLoS One* **7**, e34883
198. Frangipani, E., Slaveykova, V. I., Reimann, C., and Haas, D. (2008) Adaptation of aerobically growing *Pseudomonas aeruginosa* to copper starvation. *J. Bacteriol.* **190**, 6706–6717
199. Imperi, F., Tiburzi, F., Fimia, G. M., and Visca, P. (2010) Transcriptional control of the *pvdS* iron starvation sigma factor gene by the master regulator of sulfur metabolism CysB in *Pseudomonas aeruginosa*. *Environ. Microbiol.* **12**, 1630–1642
200. Stintzi, A., Evans, K., Meyer, J. M., and Poole, K. (1998) Quorum-sensing and siderophore biosynthesis in *Pseudomonas aeruginosa*: *lasR/lasI* mutants exhibit reduced pyoverdine biosynthesis. *FEMS Microbiol. Lett.* **166**, 341–345
201. Pesci, E. C., Milbank, J. B. J., Pearson, J. P., McKnight, S., Kende, A. S., Greenberg, E. P., and Iglewski, B. H. (1999) Quinolone signaling in the cell-to-cell communication system of *Pseudomonas aeruginosa*. *Proc. Natl. Acad. Sci. U S A* **96**, 11229–11234
202. Bredenbruch, F., Geffers, R., Nimtz, M., Buer, J., and Häussler, S. (2006) The *Pseudomonas aeruginosa* quinolone signal (PQS) has an iron-chelating activity. *Environ. Microbiol.* **8**, 1318–1329
203. Diggle, S. P., Matthijs, S., Wright, V. J., Fletcher, M. P., Chhabra, S. R., Lamont, I. L., Kong, X., Hider, R. C., Cornelis, P., Cámara, M., and Williams, P. (2007) The *Pseudomonas aeruginosa* 4-quinolone signal molecules HHQ and PQS play multifunctional roles in quorum sensing and iron entrapment. *Chem. Biol.* **14**, 87–96
204. Balasubramanian, D., Kumari, H., Jaric, M., Fernandez, M., Turner, K. H., Dove, S. L., Narasimhan, G., Lory, S., and Mathee, K. (2014) Deep sequencing analyses expands the *Pseudomonas aeruginosa* AmpR regulon to include small RNA-mediated regulation of iron acquisition, heat shock and oxidative stress response. *Nucleic Acids Res.* **42**, 979–998

205. Lapouge, K., Schubert, M., Allain, F. H.-T., and Haas, D. (2008) Gac/Rsm signal transduction pathway of γ -proteobacteria: From RNA recognition to regulation of social behaviour. *Mol. Microbiol.* **67**, 241–253
206. Moscoso, J. A., Jaeger, T., Valentini, M., Hui, K., Jenal, U., and Filloux, A. (2014) The diguanylate cyclase SadC is a central player in Gac/Rsm-mediated biofilm formation in *Pseudomonas aeruginosa*. *J. Bacteriol.* **196**, 4081–4088
207. Burrowes, E., Baysse, C., Adams, C., and O’Gara, F. (2006) Influence of the regulatory protein RsmA on cellular functions in *Pseudomonas aeruginosa* PAO1, as revealed by transcriptome analysis. *Microbiology* **152**, 405–418
208. Brencic, A., and Lory, S. (2009) Determination of the regulon and identification of novel mRNA targets of *Pseudomonas aeruginosa* RsmA. *Mol. Microbiol.* **72**, 612–632
209. Ryan, R. P., Lucey, J., O’Donovan, K., McCarthy, Y., Yang, L., Tolker-Nielsen, T., and Dow, J. M. (2009) HD-GYP domain proteins regulate biofilm formation and virulence in *Pseudomonas aeruginosa*. *Environ. Microbiol.* **11**, 1126–1136
210. Hassan, K. A., Johnson, A., Shaffer, B. T., Ren, Q., Kidarsa, T. A., Elbourne, L. D. H., Hartney, S., Duboy, R., Goebel, N. C., Zabriskie, T. M., Paulsen, I. T., and Loper, J. E. (2010) Inactivation of the GacA response regulator in *Pseudomonas fluorescens* Pf-5 has far-reaching transcriptomic consequences. *Environ. Microbiol.* **12**, 899–915
211. Malone, J. G., Jaeger, T., Spangler, C., Ritz, D., Spang, A., Arrieumerlou, C., Kaefer, V., Landmann, R., and Jenal, U. (2010) YfiBNR mediates cyclic di-GMP dependent small colony variant formation and persistence in *Pseudomonas aeruginosa*. *PLoS pathogens* **6**, e1000804
212. Kong, H. S., Roberts, D. P., Patterson, C. D., Kuehne, S. A., Heeb, S., Lakshman, D. K., and Lydon, J. (2012) Effect of overexpressing *rsmA* from *Pseudomonas aeruginosa* on virulence of select phytotoxin-producing strains of *P. syringae*. *Phytopathology* **102**, 575–587
213. Frangipani, E., Visaggio, D., Heeb, S., Kaefer, V., Cámara, M., Visca, P., and Imperi, F. (2014) The Gac/Rsm and cyclic-di-GMP signalling networks coordinately regulate iron uptake in *Pseudomonas aeruginosa*. *Environ. Microbiol.* **16**, 676–688

214. Attila, C., Ueda, A., and Wood, T. K. (2008) PA2663 (PpyR) increases biofilm formation in *Pseudomonas aeruginosa* PAO1 through the *psl* operon and stimulates virulence and quorum-sensing phenotypes. *Appl. Microbiol. Biotechnol.* **78**, 293–307
215. Funken, H., Knapp, A., Vasil, M. L., Wilhelm, S., Jaeger, K.-E., and Rosenau, F. (2011) The lipase LipA (PA2862) but not LipC (PA4813) from *Pseudomonas aeruginosa* influences regulation of pyoverdine production and expression of the sigma factor PvdS. *J. Bacteriol.* **193**, 5858–5860
216. Pelzer, A., Polen, T., Funken, H., Rosenau, F., Wilhelm, S., Bott, M., and Jaeger, K.-E. (2014) Subtilase SprP exerts pleiotropic effects in *Pseudomonas aeruginosa*. *MicrobiologyOpen* **3**, 89–103
217. Llamas, M. A., Imperi, F., Visca, P., and Lamont, I. L. (2014) Cell-surface signaling in *Pseudomonas*: Stress responses, iron transport, and pathogenicity. *FEMS Microbiol. Rev.* **38**, 569–597
218. Meyer, J. M. (2000) Pyoverdines: pigments, siderophores and potential taxonomic markers of fluorescent *Pseudomonas* species. *Arch. Microbiol.* **174**, 135–142
219. Cézard, C., Farvacques, N., and Sonnet, P. (2015) Chemistry and biology of pyoverdines, *Pseudomonas* primary siderophores. *Curr. Med. Chem.* **22**, 165–186
220. Jacques, P., Gwose, I., Seinsche, D., Taraz, K., Budzikiewicz, H., Schröder, H., Ongena, M., and Thonart, P. (1993) Isopyoverdin Pp BTP 1, a biogenetically interesting novel siderophore from *Pseudomonas putida*. *Nat. Prod. Lett.* **3**, 213–218
221. Jacques, P., Ongena, M., Gwose, I., Seinsche, D., Schröder, H., Delfosse, P., Thonart, P., Taraz, K., and Budzikiewicz, H. (1995) Structure and characterization of isopyoverdin from *Pseudomonas putida* BTP1 and its relation to the biogenetic pathway leading to pyoverdins. *Z. Naturforsch., C, J. Biosci.* **50**, 622–629
222. Maurer, B., Müller, A., Keller-Schierlein, W., and Zähler, H. (1968) Stoffwechselprodukte von Mikroorganismen: Ferribactin, ein Siderochrom aus *Pseudomonas fluorescens* Migula. *Arch. Microbiol.* **60**, 326–339

223. Teintze, M., and Leong, J. (1981) Structure of pseudobactin A, a second siderophore from plant growth promoting *Pseudomonas* B10. *Biochemistry* **20**, 6457–6462
224. Taraz, K., Tappe, R., Schröder, H., Hohlneicher, U., Gwose, I., Budzikiewicz, H., Mohn, G., and Lefèvre, F. J. (1991) Ferribactins - the biogenetic precursors of pyoverdins. *Z. Naturforsch., C, J. Biosci.* **46**, 527–533
225. Budzikiewicz, H. (1994) The biosynthesis of pyoverdins. *Pure & Appl. Chem.* **66**, 2207–2210
226. Böckmann, M., Taraz, K., and Budzikiewicz, H. (1997) Biogenesis of the pyoverdin chromophore. *Z. Naturforsch., C, J. Biosci.* **52**, 319–324
227. Hohlneicher, U., Schäfer, M., Fuchs, R., and Budzikiewicz, H. (2001) Ferribactins as the biosynthetic precursors of the *Pseudomonas* siderophores pyoverdins. *Z. Naturforsch., C, J. Biosci.* **56**, 308–310
228. Dorrestein, P. C., Poole, K., and Begley, T. P. (2003) Formation of the chromophore of the pyoverdine siderophores by an oxidative cascade. *Org. Lett.* **5**, 2215–2217
229. Dorrestein, P., and Begley, T. P. (2005) Oxidative cascades: A facile biosynthetic strategy for the assembly of complex molecules. *Bioorg. Chem.* **33**, 136–148
230. Longerich, I., Taraz, K., Budzikiewicz, H., Tsai, L., and Meyer, J. M. (1993) Pseudoverdin, a compound related to the pyoverdin chromophore from a *Pseudomonas aeruginosa* strain incapable to produce pyoverdins. *Z. Naturforsch., C, J. Biosci.* **48**, 425–429
231. Schröder, H., Taraz, J. A. K., and Budzikiewicz, H. (1995) Dihydropyoverdinsulfonsäuren - Zwischenstufen bei der Biogenese? *Z. Naturforsch., C, J. Biosci.* **50**, 616–621
232. Baysse, C., Budzikiewicz, H., Uría Fernández, D., and Cornelis, P. (2002) Impaired maturation of the siderophore pyoverdine chromophore in *Pseudomonas fluorescens* ATCC 17400 deficient for the cytochrome *c* biogenesis protein CcmC. *FEBS Lett.* **523**, 23–28
233. Budzikiewicz, H. (2006) Bacterial aromatic sulfonates - A bucherer reaction in nature? *Mini. Rev. Org. Chem.* **3**, 93–97

234. Maksimova, N. P., Blazhevich, O. V., and Fomichev, I. K. (1993) The role of pyrimidines in the biosynthesis of the fluorescing pigment pyoverdin P_m in *Pseudomonas putida* M. *Mol. Gen. Mikrobiol. Virusol.* **5**, 22–26
235. Blazhevich, O. V., and Maksimova, N. P. (1994) Biosynthesis of the fluorescent pigment pyoverdin P_m from the rhizosphere bacterium *Pseudomonas putida* M. *Izv. Acad. Nauk. Ser. Biol.*, 205–210
236. Geisen, K., Taraz, K., and Budzikiewicz, H. (1992) New pyoverdin type siderophores from *Pseudomonas fluorescens*. *Monatsh. Chem.* **123**, 151–178
237. Briskot, G., Taraz, K., and Budzikiewicz, H. (1986) Pyoverdine type siderophores from *Pseudomonas aeruginosa*. *Z. Naturforsch., C, J. Biosci.* **41**, 497–506
238. Demange, P., Bateman, A., Mertz, C., Dell, A., Piemont, Y., and Abdallah, M. A. (1990) Bacterial siderophores: structures of pyoverdins Pt, siderophores of *Pseudomonas tolaasii* NCPPB 2192, and pyoverdins Pf, siderophores of *Pseudomonas fluorescens* CCM 2798. Identification of an unusual natural amino acid. *Biochemistry*, 11041–11051
239. Lenz, C., Amann, C., Briskot, G., Taraz, K., and Budzikiewicz, H. (2000) Succinopyoverdins - a new variety of the pyoverdin chromophore. *Z. Naturforsch., C, J. Biosci.* **55**, 146–152
240. Yang, C. C., and Leong, J. (1984) Structure of pseudobactin 7SR1, a siderophore from a plant-deleterious *Pseudomonas*. *Biochemistry* **23**, 3534–3540
241. Schäfer, H., Taraz, K., and Budzikiewicz, H. (1991) Zur Genese Der Amidisch An Den Chromophor Von Pyoverdinen Gebundenen Dicarbonsäuren. *Z. Naturforsch., C, J. Biosci.* **46**, 398–406
242. Koedam, N., Wittouck, E., Gaballa, A., Gillis, A., Höfte, M., and Cornelis, P. (1994) Detection and differentiation of microbial siderophores by isoelectric focusing and chrome azurol S overlay. *Biometals* **7**, 287–291
243. Mossialos, D., Ochsner, U., Baysse, C., Chablain, P., Pirnay, J.-P., Koedam, N., Budzikiewicz, H., Fernández, D. U., Schäfer, M., Ravel, J., and Cornelis, P. (2002) Identification of new,

- conserved, non-ribosomal peptide synthetases from fluorescent pseudomonads involved in the biosynthesis of the siderophore pyoverdine. *Mol. Microbiol.* **45**, 1673–1685
244. Lehoux, D. E., Sanschagrin, F., and Levesque, R. C. (2000) Genomics of the 35-kb *pvd* locus and analysis of novel *pvdIJK* genes implicated in pyoverdine biosynthesis in *Pseudomonas aeruginosa*. *FEMS Microbiol. Lett.* **190**, 141–146
245. Merriman, T. R., Merriman, M. E., and Lamont, I. L. (1995) Nucleotide sequence of *pvdD*, a pyoverdine biosynthetic gene from *Pseudomonas aeruginosa*: PvdD has similarity to peptide synthetases. *J. Bacteriol.* **177**, 252–258
246. Ackerley, D. F., Caradoc-Davies, T. T., and Lamont, I. L. (2003) Substrate specificity of the nonribosomal peptide synthetase PvdD from *Pseudomonas aeruginosa*. *J. Bacteriol.* **185**, 2848–2855
247. Drake, E. J., and Gulick, A. M. (2011) Structural characterization and high-throughput screening of inhibitors of PvdQ, an NTN hydrolase involved in pyoverdine synthesis. *ACS Chem. Biol.* **6**, 1277–1286
248. Hannauer, M., Schäfer, M., Hoegy, F., Gizzi, P., Wehrung, P., Mislin, G. L. A., Budzikiewicz, H., and Schalk, I. J. (2012) Biosynthesis of the pyoverdine siderophore of *Pseudomonas aeruginosa* involves precursors with a myristic or a myristoleic acid chain. *FEBS Lett.* **586**, 96–101
249. Vandenende, C. S., Vlasschaert, M., and Seah, S. Y. K. (2004) Functional characterization of an aminotransferase required for pyoverdine siderophore biosynthesis in *Pseudomonas aeruginosa* PAO1. *J. Bacteriol.* **186**, 5596–5602
250. Visca, P., Serino, L., and Orsi, N. (1992) Isolation and characterization of *Pseudomonas aeruginosa* mutants blocked in the synthesis of pyoverdin. *J. Bacteriol.* **174**, 5727–5731
251. Visca, P., Ciervo, A., and Orsi, N. (1994) Cloning and nucleotide sequence of the *pvdA* gene encoding the pyoverdin biosynthetic enzyme L-ornithine N^5 -oxygenase in *Pseudomonas aeruginosa*. *J. Bacteriol.* **176**, 1128–1140

252. Ge, L., and Seah, S. Y. K. (2006) Heterologous expression, purification, and characterization of an L-Ornithine N⁵-hydroxylase involved in pyoverdine siderophore biosynthesis in *Pseudomonas aeruginosa*. *J. Bacteriol.* **188**, 7205–7210
253. Meneely, K. M., Barr, E. W., Bollinger, J. M., and Lamb, A. L. (2009) Kinetic mechanism of ornithine hydroxylase (PvdA) from *Pseudomonas aeruginosa*: substrate triggering of O₂ addition but not flavin reduction. *Biochemistry* **48**, 4371–4376
254. McMorran, B. J., Shanta Kumara, H. M., Sullivan, K., and Lamont, I. L. (2001) Involvement of a transformylase enzyme in siderophore synthesis in *Pseudomonas aeruginosa*. *Microbiology* **147**, 1517–1524
255. Imperi, F., and Visca, P. (2013) Subcellular localization of the pyoverdine biogenesis machinery of *Pseudomonas aeruginosa*: a membrane-associated "siderosome". *FEBS Lett.* **587**, 3387–3391
256. Gasser, V., Guillon, L., Cunrath, O., and Schalk, I. J. (2015) Cellular organization of siderophore biosynthesis in *Pseudomonas aeruginosa*: Evidence for siderosomes: 12th European Biological Inorganic Chemistry Conference (EuroBIC 12) in Zurich, Switzerland, August 24-28, 2014. *J. Inorg. Biochem.* **148**, 27–34
257. Drake, E. J., Cao, J., Qu, J., Shah, M. B., Straubinger, R. M., and Gulick, A. M. (2007) The 1.8 Å crystal structure of PA2412, an MbtH-like protein from the pyoverdine cluster of *Pseudomonas aeruginosa*. *J. Biol. Chem.* **282**, 20425–20434
258. Felnagle, E. A., Barkei, J. J., Park, H., Podevels, A. M., McMahon, M. D., Drott, D. W., and Thomas, M. G. (2010) MbtH-like proteins as integral components of bacterial nonribosomal peptide synthetases. *Biochemistry* **49**, 8815–8817
259. Zhang, W., Heemstra, J. R., Walsh, C. T., and Imker, H. J. (2010) Activation of the pacidamycin PaCL adenylation domain by MbtH-like proteins. *Biochemistry* **49**, 9946–9947
260. Ravel, J., and Cornelis, P. (2003) Genomics of pyoverdine-mediated iron uptake in pseudomonads. *Trends Microbiol.* **11**, 195–200

261. Lamont, I. L., Martin, L. W., Sims, T., Scott, A., and Wallace, M. (2006) Characterization of a gene encoding an acetylase required for pyoverdine synthesis in *Pseudomonas aeruginosa*. *J. Bacteriol.* **188**, 3149–3152
262. McMorran, B. J., Merriman, M. E., Rombel, I. T., and Lamont, I. L. (1996) Characterisation of the *pvdE* gene which is required for pyoverdine synthesis in *Pseudomonas aeruginosa*. *Gene* **176**, 55–59
263. Bokhove, M., Nadal Jimenez, P., Quax, W. J., and Dijkstra, B. W. (2010) The quorum-quenching *N*-acyl homoserine lactone acylase PvdQ is an Ntn-hydrolase with an unusual substrate-binding pocket. *Proc. Natl. Acad. Sci. U S A* **107**, 686–691
264. Eberhard, A., Burlingame, A. L., Eberhard, C., Kenyon, G. L., Nealson, K. H., and Oppenheimer, N. J. (1981) Structural identification of autoinducer of *Photobacterium fischeri* luciferase. *Biochemistry* **20**, 2444–2449
265. Pearson, J. P., Passador, L., Iglewski, B. H., and Greenberg, E. P. (1995) A second *N*-acylhomoserine lactone signal produced by *Pseudomonas aeruginosa*. *Proc. Natl. Acad. Sci. U S A* **92**, 1490–1494
266. Nadal-Jimenez, P., Koch, G., Reis, C. R., Muntendam, R., Raj, H., Jeronimus-Stratingh, C. M., Cool, R. H., and Quax, W. J. (2014) PvdP is a tyrosinase that drives maturation of the pyoverdine chromophore in *Pseudomonas aeruginosa*. *J. Bacteriol.* **196**, 2681–2690
267. Voulhoux, R., Filloux, A., and Schalk, I. J. (2006) Pyoverdine-mediated iron uptake in *Pseudomonas aeruginosa*: the Tat system is required for PvdN but not for FpvA transport. *J. Bacteriol.* **188**, 3317–3323
268. Lewenza, S., Gardy, J. L., Brinkman, F. S. L., and Hancock, R. E. W. (2005) Genome-wide identification of *Pseudomonas aeruginosa* exported proteins using a consensus computational strategy combined with a laboratory-based PhoA fusion screen. *Genome Res.* **15**, 321–329
269. Budzikiewicz, H. (2001) Siderophore-antibiotic conjugates used as trojan horses against *Pseudomonas aeruginosa*. *Curr. Top. Med. Chem.* **1**, 73–82

270. Mislin, G. L. A., and Schalk, I. J. (2014) Siderophore-dependent iron uptake systems as gates for antibiotic Trojan horse strategies against *Pseudomonas aeruginosa*. *Metallomics* **6**, 408–420
271. Schalk, I. J., and Mislin, G. L. A. (2017) Bacterial iron uptake pathways: Gates for the import of bactericide compounds. *J. Med. Chem.* **60**, 4573–4576
272. Kinzel, O., Tappe, R., Gerus, I., and Budzikiewicz, H. (1998) The synthesis and antibacterial activity of two pyoverdinin-ampicillin conjugates, entering *Pseudomonas aeruginosa* via the pyoverdinin-mediated iron uptake pathway. *J. Antibiot. (Tokyo)* **51**, 499–507
273. Kinzel, O., and Budzikiewicz, H. (1999) Synthesis and biological evaluation of a pyoverdinin- β -lactam conjugate: A new type of arginine-specific cross-linking in aqueous solution. *J. Pept. Res.* **53**, 618–625
274. Hennard, C., Truong, Q. C., Desnottes, J.-F., Paris, J.-M., Moreau, N. J., and Abdallah, M. A. (2001) Synthesis and activities of pyoverdinin–quinolone adducts: A prospective approach to a specific therapy against *Pseudomonas aeruginosa*. *J. Med. Chem.* **44**, 2139–2151
275. Schons, V., Atkinson, R. A., Dugave, C., Graff, R., Mislin, G. L. A., Rochet, L., Hennard, C., Kieffer, B., Abdallah, M. A., and Schalk, I. J. (2005) The structure-activity relationship of ferric pyoverdinin bound to its outer membrane transporter: implications for the mechanism of iron uptake. *Biochemistry* **44**, 14069–14079
276. Ross-Gillespie, A., Weigert, M., Brown, S. P., and Kümmerli, R. (2014) Gallium-mediated siderophore quenching as an evolutionarily robust antibacterial treatment. *Evol. Med. Public. Health.* **2014**, 18–29
277. Kaneko, Y., Thoendel, M., Olakanmi, O., Britigan, B. E., and Singh, P. K. (2007) The transition metal gallium disrupts *Pseudomonas aeruginosa* iron metabolism and has antimicrobial and antibiofilm activity. *J. Clin. Invest.* **117**, 877–888
278. Clevenger, K. D., Wu, R., Er, J. A. V., Liu, D., and Fast, W. (2013) Rational design of a transition state analogue with picomolar affinity for *Pseudomonas aeruginosa* PvdQ, a siderophore biosynthetic enzyme. *ACS Chem. Biol.* **8**, 2192–2200

279. Wurst, J. M., Drake, E. J., Theriault, J. R., Jewett, I. T., VerPlank, L., Perez, J. R., Dandapani, S., Palmer, M., Moskowitz, S. M., Schreiber, S. L., Munoz, B., and Gulick, A. M. (2014) Identification of inhibitors of PvdQ, an enzyme involved in the synthesis of the siderophore pyoverdine. *ACS Chem. Biol.* **9**, 1536–1544
280. Nadal Jimenez, P., Koch, G., Papaioannou, E., Wahjudi, M., Krzeslak, J., Coenye, T., Cool, R. H., and Quax, W. J. (2010) Role of PvdQ in *Pseudomonas aeruginosa* virulence under iron-limiting conditions. *Microbiology* **156**, 49–59
281. Winsor, G. L., Griffiths, E. J., Lo, R., Dhillon, B. K., Shay, J. A., and Brinkman, F. S. L. (2016) Enhanced annotations and features for comparing thousands of *Pseudomonas* genomes in the *Pseudomonas* genome database. *Nucleic Acids Res.* **44**, D646-53
282. Jones, P., Binns, D., Chang, H.-Y., Fraser, M., Li, W., McAnulla, C., McWilliam, H., Maslen, J., Mitchell, A., Nuka, G., Pesseat, S., Quinn, A. F., Sangrador-Vegas, A., Scheremetjew, M., Yong, S.-Y., Lopez, R., and Hunter, S. (2014) InterProScan 5: genome-scale protein function classification. *Bioinformatics* **30**, 1236–1240
283. Finn, R. D., Attwood, T. K., Babbitt, P. C., Bateman, A., Bork, P., Bridge, A. J., Chang, H.-Y., Dosztányi, Z., El-Gebali, S., Fraser, M., Gough, J., Haft, D., Holliday, G. L., Huang, H., Huang, X., Letunic, I., Lopez, R., Lu, S., Marchler-Bauer, A., Mi, H., Mistry, J., Natale, D. A., Necci, M., Nuka, G., Orengo, C. A., Park, Y., Pesseat, S., Piovesan, D., Potter, S. C., Rawlings, N. D., Redaschi, N., Richardson, L., Rivoire, C., Sangrador-Vegas, A., Sigrist, C., Sillitoe, I., Smithers, B., Squizzato, S., Sutton, G., Thanki, N., Thomas, P. D., Tosatto, S. C. E., Wu, C. H., Xenarios, I., Yeh, L.-S., Young, S.-Y., and Mitchell, A. L. (2017) InterPro in 2017-beyond protein family and domain annotations. *Nucleic Acids Res.* **45**, D190-D199
284. Rawlings, N. D., Barrett, A. J., and Finn, R. (2016) Twenty years of the MEROPS database of proteolytic enzymes, their substrates and inhibitors. *Nucleic Acids Res.* **44**, D343-50
285. Marchler-Bauer, A., Bo, Y., Han, L., He, J., Lanczycki, C. J., Lu, S., Chitsaz, F., Derbyshire, M. K., Geer, R. C., Gonzales, N. R., Gwadz, M., Hurwitz, D. I., Lu, F., Marchler, G. H., Song, J. S., Thanki, N., Wang, Z., Yamashita, R. A., Zhang, D., Zheng, C., Geer, L. Y., and Bryant, S. H. (2017)

CDD/SPARCLE: Functional classification of proteins via subfamily domain architectures.

Nucleic Acids Res. **45**, D200-D203

286. Huang, Y., Niu, B., Gao, Y., Fu, L., and Li, W. (2010) CD-HIT Suite: A web server for clustering and comparing biological sequences. *Bioinformatics* **26**, 680–682
287. Di Tommaso, P., Moretti, S., Xenarios, I., Orobittg, M., Montanyola, A., Chang, J.-M., Taly, J.-F., and Notredame, C. (2011) T-Coffee: A web server for the multiple sequence alignment of protein and RNA sequences using structural information and homology extension. *Nucleic Acids Res.* **39**, W13-W17
288. Crooks, G. E., Hon, G., Chandonia, J.-M., and Brenner, S. E. (2004) WebLogo: a sequence logo generator. *Genome Res.* **14**, 1188–1190
289. Biasini, M., Bienert, S., Waterhouse, A., Arnold, K., Studer, G., Schmidt, T., Kiefer, F., Gallo Cassarino, T., Bertoni, M., Bordoli, L., and Schwede, T. (2014) SWISS-MODEL: modelling protein tertiary and quaternary structure using evolutionary information. *Nucleic Acids Res.* **42**, W252-W258
290. Berman, H. M. (2000) The Protein Data Bank. *Nucleic Acids Res.* **28**, 235–242
291. Sievers, F., Wilm, A., Dineen, D., Gibson, T. J., Karplus, K., Li, W., Lopez, R., McWilliam, H., Remmert, M., Söding, J., Thompson, J. D., and Higgins, D. G. (2011) Fast, scalable generation of high-quality protein multiple sequence alignments using Clustal Omega. *Mol. Syst. Biol.* **7**, 539
292. Pettersen, E. F., Goddard, T. D., Huang, C. C., Couch, G. S., Greenblatt, D. M., Meng, E. C., and Ferrin, T. E. (2004) UCSF Chimera—a visualization system for exploratory research and analysis. *J. Comput. Chem.* **25**, 1605–1612
293. Baker, N. A., Sept, D., Joseph, S., Holst, M. J., and McCammon, J. A. (2001) Electrostatics of nanosystems: application to microtubules and the ribosome. *Proc. Natl. Acad. Sci. U S A* **98**, 10037–10041
294. Ringel, M. T., Dräger, G., and Brüser, T. (2016) PvdN enzyme catalyzes a periplasmic pyoverdine modification. *J. Biol. Chem.* **291**, 23929–23938

295. Ringel, M. T., Draeger, G., and Brueser, T. (2017) The periplasmic transaminase PtaA of *Pseudomonas fluorescens* converts the glutamic acid residue at the pyoverdine fluorophore to α -ketoglutaric acid. *J. Biol. Chem.*, 18660–18671
296. King, E. O., Ward, M. K., and Raney, D. E. (1954) Two simple media for the demonstration of pyocyanin and fluorescin. *J. Lab. Clin. Med.* **44**, 301–307
297. Haldimann, A., and Wanner, B. L. (2001) Conditional-replication, integration, excision, and retrieval plasmid-host systems for gene structure-function studies of bacteria. *J. Bacteriol.* **183**, 6384–6393
298. Yanisch-Perron, C., Vieira, J., and Messing, J. (1985) Improved M13 phage cloning vectors and host strains: Nucleotide sequences of the M13mpl8 and pUC19 vectors. *Gene* **33**, 103–119
299. Inoue, H., Nojima, H., and Okayama, H. (1990) High efficiency transformation of *Escherichia coli* with plasmids. *Gene* **96**, 23–28
300. Datsenko, K. A., and Wanner, B. L. (2000) One-step inactivation of chromosomal genes in *Escherichia coli* K-12 using PCR products. *Proc. Natl. Acad. Sci. U S A* **97**, 6640–6645
301. Jansons, I., Touchie, G., Sharp, R., Almquist, K., Farinha, M. A., Lam, J. S., and Kropinski, A. M. (1994) Deletion and transposon mutagenesis and sequence analysis of the pR01600 OriR region found in the broad-host-range plasmids of the pQF series. *Plasmid* **31**, 265–274
302. Lesic, B., and Rahme, L. G. (2008) Use of the lambda Red recombinase system to rapidly generate mutants in *Pseudomonas aeruginosa*. *BMC Mol. Biol.* **9**, 20
303. Laemmli, U. K. (1970) Cleavage of structural proteins during the assembly of the head of bacteriophage T4. *Nature* **227**, 680–685
304. Burnette, W.N. (1981) “Western Blotting”: Electrophoretic transfer of proteins from sodium dodecyl sulfate-polyacrylamide gels to unmodified nitrocellulose and radiographic detection with antibody and radioiodinated protein A. *Anal. Biochem.* **112**, 195–203

305. Towbin, H., Staehelin, T., and Gordon, J. (1979) Electrophoretic transfer of proteins from polyacrylamide gels to nitrocellulose sheets: procedure and some applications. *Proc. Natl. Acad. Sci. U S A* **76**, 4350–4354
306. Izé, B., Viarre, V., and Voulhoux, R. (2014) Cell fractionation. *Methods Mol. Biol.* **1149**, 185–191
307. Dolinsky, T. J., Nielsen, J. E., McCammon, J. A., and Baker, N. A. (2004) PDB2PQR: An automated pipeline for the setup of Poisson-Boltzmann electrostatics calculations. *Nucleic Acids Res.* **32**, W665-7
308. Dolinsky, T. J., Czodrowski, P., Li, H., Nielsen, J. E., Jensen, J. H., Klebe, G., and Baker, N. A. (2007) PDB2PQR: Expanding and upgrading automated preparation of biomolecular structures for molecular simulations. *Nucleic Acids Res.* **35**, W522-5
309. The UniProt Consortium (2017) UniProt: The universal protein knowledgebase. *Nucleic Acids Res.* **45**, D158-D169
310. Eddy, S. R. (2011) Accelerated Profile HMM Searches. *PLoS Comput. Biol.* **7**, e1002195
311. Schindelin, J., Arganda-Carreras, I., Frise, E., Kaynig, V., Longair, M., Pietzsch, T., Preibisch, S., Rueden, C., Saalfeld, S., Schmid, B., Tinevez, J.-Y., White, D. J., Hartenstein, V., Eliceiri, K., Tomancak, P., and Cardona, A. (2012) Fiji: an open-source platform for biological-image analysis. *Nat. Methods* **9**, 676–682
312. Budzikiewicz, H., Fuchs, R., Taraz, K., Marek-kozaczuk, M., and Skorupska, A. (1998) Dihydropyoverdin-7-sulfonic acids - unusual bacterial metabolites. *Nat. Prod. Lett.* **12**, 125–130
313. Fernández, D. U., Fuchs, R., Schäfer, M., Budzikiewicz, H., and Meyer, J.-M. (2003) The pyoverdin of *Pseudomonas fluorescens* G173, a novel structural type accompanied by unexpected natural derivatives of the corresponding ferribactin. *Z. Naturforsch., C, J. Biosci.* **58**, 1–10

314. Budzikiewicz, H., Schäfer, M., Fernández, D. U., Matthijs, S., and Cornelis, P. (2007) Characterization of the chromophores of pyoverdins and related siderophores by electrospray tandem mass spectrometry. *Biometals* **20**, 135–144
315. Eliot, A. C., and Kirsch, J. F. (2004) Pyridoxal phosphate enzymes: Mechanistic, structural, and evolutionary considerations. *Annu. Rev. Biochem.* **73**, 383–415
316. Phillips, R. S. (2015) Chemistry and diversity of pyridoxal-5'-phosphate dependent enzymes. *Biochim. Biophys. Acta* **1854**, 1167–1174
317. Wang, M., Zhao, Q., Zhang, Q., and Liu, W. (2016) Differences in PLP-dependent cysteinyl processing lead to diverse S-functionalization of lincosamide antibiotics. *J. Am. Chem. Soc.* **138**, 6348–6351
318. Matsui, D., Oikawa, T., Arakawa, N., Osumi, S., Lausberg, F., Stäbler, N., Freudl, R., and Eggeling, L. (2009) A periplasmic, pyridoxal-5'-phosphate-dependent amino acid racemase in *Pseudomonas taetrolens*. *Appl. Microbiol. Biotechnol.* **83**, 1045–1054
319. Drake, E. J., and Gulick, A. M. (2016) 1.2 Å resolution crystal structure of the periplasmic aminotransferase PvdN from *Pseudomonas aeruginosa*. *Acta Crystallogr. F Struct. Biol. Commun.* **72**, 403–408
320. Nurizzo, D., Halbig, D., Sprenger, G. A., and Baker, E. N. (2001) Crystal structures of the precursor form of glucose-fructose oxidoreductase from *Zymomonas mobilis* and its complexes with bound ligands. *Biochemistry* **40**, 13857–13867
321. Ma, X., and Cline, K. (2010) Multiple precursor proteins bind individual Tat receptor complexes and are collectively transported. *EMBO J.* **29**, 1477–1488
322. Calhoun, D. H., Bonner, C. A., Gu, W., Xie, G., and Jensen, R. A. (2001) The emerging periplasm-localized subclass of AroQ chorismate mutases, exemplified by those from *Salmonella typhimurium* and *Pseudomonas aeruginosa*. *Genome Biol.* **2**, 1-16
323. Finn, R. D., Clements, J., Arndt, W., Miller, B. L., Wheeler, T. J., Schreiber, F., Bateman, A., and Eddy, S. R. (2015) HMMER web server: 2015 update. *Nucleic Acids Res.* **43**, W30-W38

324. Bultreys, A., Gheysen, I., Maraite, H., and Hoffmann, E. de (2001) Characterization of fluorescent and nonfluorescent peptide siderophores produced by *Pseudomonas syringae* strains and their potential use in strain identification. *Appl. Environ. Microbiol.* **67**, 1718–1727
325. Teitzel, G. M., Geddie, A., Long, S. K. de, Kirisits, M. J., Whiteley, M., and Parsek, M. R. (2006) Survival and growth in the presence of elevated copper: Transcriptional profiling of copper-stressed *Pseudomonas aeruginosa*. *J. Bacteriol.* **188**, 7242–7256
326. Straganz, G. D., and Nidetzky, B. (2006) Variations of the 2-His-1-carboxylate theme in mononuclear non-heme Fe^{II} oxygenases. *Chembiochem* **7**, 1536–1548
327. A. Bruijninx, P. C., van Koten, G., and Gebbink, Robertus J. M. Klein (2008) Mononuclear non-heme iron enzymes with the 2-His-1-carboxylate facial triad: Recent developments in enzymology and modeling studies. *Chem. Soc. Rev.* **37**, 2716–2744
328. Buongiorno, D., and Straganz, G. D. (2013) Structure and function of atypically coordinated enzymatic mononuclear non-heme-Fe(II) centers. *Coord. Chem. Rev.* **257**, 541–563
329. Martinez, S., and Hausinger, R. P. (2015) Catalytic mechanisms of Fe(II)- and 2-oxoglutarate-dependent oxygenases. *J. Biol. Chem.* **290**, 20702–20711
330. Solomon, E. I., Goudarzi, S., and Sutherlin, K. D. (2016) O₂ activation by non-heme iron enzymes. *Biochemistry* **55**, 6363–6374
331. Kal, S., and Que, L. (2017) Dioxygen activation by nonheme iron enzymes with the 2-His-1-carboxylate facial triad that generate high-valent oxoiron oxidants. *J. Biol. Inorg. Chem.* **22**, 339–365
332. Peck, S. C., and van der Donk, W. A. (2017) Go it alone: Four-electron oxidations by mononuclear non-heme iron enzymes. *J. Biol. Inorg. Chem.* **22**, 381–394
333. Gaballa, A., Koedam, N., and Cornelis, P. (1996) A cytochrome *c* biogenesis gene involved in pyoverdine production in *Pseudomonas fluorescens* ATCC 17400. *Mol. Microbiol.* **21**, 777–785

334. Gaballa, A., Baysse, C., Koedam, N., Muyldermans, S., and Cornelis, P. (1998) Different residues in periplasmic domains of the CcmC inner membrane protein of *Pseudomonas fluorescens* ATCC 17400 are critical for cytochrome *c* biogenesis and pyoverdine-mediated iron uptake. *Mol. Microbiol.* **30**, 547–555
335. Baysse, C., Matthijs, S., Schobert, M., Layer, G., Jahn, D., and Cornelis, P. (2003) Co-ordination of iron acquisition, iron porphyrin chelation and iron-protoporphyrin export via the cytochrome *c* biogenesis protein CcmC in *Pseudomonas fluorescens*. *Microbiology* **149**, 3543–3552
336. Baert, B., Baysse, C., Matthijs, S., and Cornelis, P. (2008) Multiple phenotypic alterations caused by a *c*-type cytochrome maturation *ccmC* gene mutation in *Pseudomonas aeruginosa*. *Microbiology* **154**, 127–138
337. Baars, O., Zhang, X., Morel, F. M. M., and Seyedsayamdost, M. R. (2015) The siderophore metabolome of *Azotobacter vinelandii*. *Appl. Environ. Microbiol.* **82**, 27–39
338. Adachi, H., Katayama, T., Nakazato, H., and Tsujimoto, M. (1993) Importance of Glu-125 in the catalytic activity of human renal dipeptidase. *Biochim. Biophys. Acta.* **1163**, 42–48
339. Keynan, S., Hooper, N. M., and Turner, A. J. (1997) Identification by site-directed mutagenesis of three essential histidine residues in membrane dipeptidase, a novel mammalian zinc peptidase. *Biochem. J.* **326**, 47–51
340. Keynan, S., Hooper, N. M., and Turner, A. J. (1994) Directed mutagenesis of pig renal membrane dipeptidase His 219 is critical but the DHXXH motif is not essential for zinc binding or catalytic activity. *FEBS Lett.* **349**, 50–54
341. Liao, R.-Z., Himo, F., Yu, J.-G., and Liu, R.-Z. (2010) Dipeptide hydrolysis by the dinuclear zinc enzyme human renal dipeptidase: Mechanistic insights from DFT calculations. *J. Inorg. Biochem.* **104**, 37–46
342. Nitnai, Y., Satow, Y., Adachi, H., and Tsujimoto, M. (2002) Crystal structure of human renal dipeptidase involved in β -lactam hydrolysis. *J. Mol. Biol.* **321**, 177–184

343. Kropp, H., Sundelof, J. G., Hajdu, R., and Kahan, F. M. (1982) Metabolism of thienamycin and related carbapenem antibiotics by the renal dipeptidase, dehydropeptidase-I. *Antimicrob. Agents. Chemother.* **22**, 62–70
344. Mikami, H., Ogashiwa, M., Saino, Y., Inoue, M., and Mitsuhashi, S. (1982) Comparative stability of newly introduced β -lactam antibiotics to renal dipeptidase. *Antimicrob. Agents. Chemother.* **22**, 693–695
345. Kim, H. S., and Campbell, B. J. (1982) β -lactamase activity of renal dipeptidase against *N*-formimidoyl-thienamycin. *Biochem. Biophys. Res. Commun.* **108**, 1638–1642
346. Kahan, F. M., Kropp, H., Sundelof, J. G., and Birnbaum, J. (1983) Thienamycin: Development of imipenen-cilastatin. *J. Antimicrob. Chemother.* **12 Suppl D**, 1–35
347. Campbell, B. J., Di Shih, Y., Forrester, L. J., and Zahler, W. L. (1988) Specificity and inhibition studies of human renal dipeptidase. *Biochim. Biophys. Acta* **956**, 110–118
348. Adachi, H., Kubota, I., Okamura, N., Iwata, H., Tsujimoto, M., Nakazato, H., Nishihara, T., and Noguchi, T. (1989) Purification and characterization of human microsomal dipeptidase. *J. Biochem.* **105**, 957–961
349. Habib, G. M., Shi, Z. Z., Cuevas, A. A., Guo, Q., Matzuk, M. M., and Lieberman, M. W. (1998) Leukotriene D₄ and cystinyl-bis-glycine metabolism in membrane-bound dipeptidase-deficient mice. *Proc. Natl. Acad. Sci. USA* **95**, 4859–4863
350. Cummings, J. A., Nguyen, T. T., Fedorov, A. A., Kolb, P., Xu, C., Fedorov, E. V., Shoichet, B. K., Barondeau, D. P., Almo, S. C., and Raushel, F. M. (2010) Structure, mechanism, and substrate profile for Sco3058: The closest bacterial homologue to human renal dipeptidase. *Biochemistry* **49**, 611–622

Acknowledgements

First and foremost, I would like to express my sincere gratitude to my team of supervisors, my direct supervisor Prof. Dr. Thomas Brüser and my co-supervisors Prof. Dr. Hans-Peter Braun and Prof. Dr. Helge Küster for giving me the opportunity to work on this highly interesting research topic within the GRK1798. Furthermore, I would like to thank Prof. Dr. Thomas Brüser for supporting my enthusiasm to establish and employ new methods throughout my entire project.

I am very grateful for the fantastic working atmosphere at the Institute of Microbiology owing to my colleagues. Special thanks go to Heinrich Schäfer and Ingo Hantke for putting up with me during my entire time at the institute, sharing an office with me, and to Dr. Patrick Stolle for always trying to find solutions to any problems regarding practical and bureaucratic difficulties. Additionally, I would like to thank Dr. Denise Mehner, Dr. Claudia Rathmann, Dr. Bo Hou and Eyleen Heidrich for basically rebuilding the laboratory of the Institute of Microbiology with me after moving to our new building.

I am sincerely grateful for my cooperation-partners at the Institute of Organic Chemistry, specifically Prof. Dr. Andreas Kirschning and Prof. Dr. Markus Kalesse. Special thanks go to Dr. Gerald Dräger for the fantastic cooperation and for always finding measurement time on his UPLC-HR-MS for my samples. Moreover, my thanks go to Dr. Jörg Fohrer for his support regarding NMR studies.

I would like to thank Dr. Heinrich Lünsdorf from the ZEIM at the HZI in Braunschweig for his excellent support in conjunction with *in vivo* electron microscopy gold labeling and Dr. Jan Hegermann from the MHH for his continuing support in this matter. Furthermore, I would like to thank Dr. Anja Pöhlein from the Institute of Microbiology and Genetics, Department of Genomic and Applied Microbiology at the Georg-August University of Göttingen for her great support concerning full genome sequencing.

Last but not least I want to thank my parents and my brother Peter, for their continuing, incredible support. This thesis would definitively not have been possible without them.

Curriculum vitae

Persönliches	
Name:	Michael Thomas Ringel
Geburtsdatum:	23.12.1989
Geburtsort:	Portland/ME, USA
Ausbildung	
2005-2008	Abitur, Lore-Lorentz-Schule, Düsseldorf
2005-2008	Staatl. gepr. Umwelttechnischer Assistent, Lore-Lorentz-Schule, Düsseldorf
2008-2011	B. Sc. Life-Science, Leibniz Universität Hannover
2011-2013	M. Sc. Life-Science, Leibniz Universität Hannover
2013 bis 2017	Doktorand am Institut für Mikrobiologie, Leibniz Universität Hannover

List of publications:

1. Ringel, M. T., Dräger, G., and Brüser, T. (2016) PvdN enzyme catalyzes a periplasmic pyoverdine modification. *J. Biol. Chem.* **291**, 23929–23938
2. Ringel, M. T., Dräger, G., and Brüser, T. (2017) The periplasmic transaminase PtaA of *Pseudomonas fluorescens* converts the glutamic acid residue at the pyoverdine fluorophore to α -ketoglutaric acid. *J. Biol. Chem.* **292**, 18660–18671
3. Ringel, M. T., Dräger, G., and Brüser, T. (2018) PvdO is required for the oxidation of dihydropyoverdine as the last step of fluorophore formation in *Pseudomonas fluorescens*. *J. Biol. Chem.* **293**, 2330-2341